NADPH Oxidase-dependent ROS Production and Impaired Ca^{2+} Regulation are Associated with Exercise-induced Cardiac Fatigue in the Rat

by

Christopher Vigna

A thesis

presented to the University of Waterloo

in fulfillment of the

thesis requirement for the degree of

Doctor of Philosophy

in

Kinesiology

Waterloo, Ontario, Canada, 2015

Author's Declaration:

I hereby declare that I am the sole author of this thesis. This is a true copy of the thesis, including any required final revisions, as accepted by my examiners.

I understand that my thesis may be made electronically available to the public.

Abstract

Cardiac fatigue is a phenomenon that is characterized by a transient reduction in left ventricular contractile and/or relaxation function following acute aerobic exercise. Few studies have utilized rodent models to examine possible cellular mechanisms associated with cardiac fatigue given the logistical limitations present in human models of cardiac fatigue. Thus, the overall objective of this thesis was to determine if oxidative stress, impaired regulation of Ca^{2+}, Na^+ and K^+ or increased proteolytic activity contribute to the development of cardiac fatigue using a rat model.

The aim of the first study in this thesis was to develop an exercise protocol that induced cardiac fatigue. Male Sprague-Dawley rats (21-23 weeks) were randomly assigned to either a control group (CTL), an acute exercise group (AC) or a group that performed acute exercise and were allowed to recover for 24 hours (24H). Animals in the AC and 24H groups performed treadmill running (5% grade; 20 m/min) until exhaustion, which occurred after 69 ± 3 and 72 ± 5 minutes in the AC and 24H groups, respectively. Subsequently, the hearts from anaesthetized animals were excised, perfused in a retrograde fashion and instrumented, which permitted the assessment of heart rate, hemodynamics and left ventricular contractile and relaxation properties. The exhaustive exercise protocol induced cardiac fatigue in the basal state as indicated by a respective, 12 and 14% reduction ($p<0.05$) in LVDP in the AC and 24H groups. In addition, there was a trend ($p=0.076$) for a reduction in the maximal rate of pressure decline (-dP/dt) but no significant differences ($p>0.05$) in the maximal rate of pressure development (+dP/dt) were observed. The cardiac fatigue present in the basal state persisted during β-adrenergic stimulation, such that LVDP was significantly lower ($p<0.05$) in the AC and 24H groups and –dP/dt was lower ($p<0.05$) in the AC group during the isoproterenol (ISO) dose response. The cardiac

fatigue observed in the basal state and during β-adrenergic stimulation was not due to changes in coronary flow or heart rate, which suggests that the mechanisms responsible for cardiac fatigue stem from within the cardiomyocyte.

The features of cardiac fatigue were reminiscent of myocardial stunning, which directed the experiments in Chapter 3 to examine reactive oxygen species (ROS) production, Ca^{2+} homeostasis, proteolytic activity and regulation of Na^+ and K^+. Left ventricle (LV) homogenates were collected for *in vitro* experiments. Norepinephrine (NE) and epinephrine (Epi) were extracted from plasma and the concentrations were determined using a HPLC assay. The maximal rates of Ca^{2+}-ATPase activity and Na^+/K^+-ATPase activity were determined using a NADH-enzyme linked spectrophotometric assay. A fluorometric assay and the Ca^{2+} sensitive dye, Indo-1 were used to measure the rates of Ca^{2+} uptake, leak and release. The production of ROS was determined using dihydrodichlorofluorescein-diacetate, which, upon oxidation, yields the highly fluorescent dichlorofluorescein. Lipid peroxidation was determined by measuring the concentration of malondialdehyde (MDA) in LV homogenates. Western blotting and immunoprecipitation were used to assess protein expression and to determine RyR specific oxidative post-translational modification.

Acute exercise resulted in a ~5-fold increase ($p<0.05$) in plasma Epi concentration, which returned to baseline 24 hours post-exercise. There were no differences ($p>0.05$) in plasma NE between the groups. The maximal rates of Ca^{2+}-ATPase activity and Na^+/K^+-ATPase activity were not affected ($p>0.05$) by exhaustive exercise. In addition, the rates of SR Ca^{2+} release were not significantly different between the three groups. A novel finding was that the rate of SR Ca^{2+} leak increased ~40% in the AC group when compared to the CTL group ($p<0.05$). These data suggest that impaired Ca^{2+} regulation may have contributed to the cardiac fatigue observed in

the AC group. The functional alteration to RyR was associated with a ~15% increase ($p<0.05$) in ROS production in the AC group. However, lipid peroxidation and glutathionylation, nitration and carbonylation content on RyR were not significantly different ($p>0.05$) between the three groups. Furthermore, the ratio of phosphorylated RyR (pRyR) to total RyR was not altered by acute exercise despite the rise in plasma Epi. The increased SR Ca^{2+} leak in the AC group likely contributed to the increase ($p<0.05$) in calpain activity observed in the AC group. Taken together, an increased rate of SR Ca^{2+} leak and subsequent calpain activation may contribute mechanistically to the cardiac fatigue observed in the AC and 24H group via reduced SR Ca^{2+} load and excitation contraction uncoupling, respectively.

The purpose of the experiments presented in Chapter 4 were to examine the hypothesis that NADPH oxidase (NOX) inhibition would prevent cardiac fatigue by reducing ROS production, reducing SR Ca^{2+} leak and preventing calpain activation. NOX was inhibited by providing 1.5 mM apocynin (APO) in the drinking water of rats for three days prior to the exhaustive exercise bout. NOX inhibition prevented exercise-induced cardiac fatigue as LVDP and -dP/dt were not significantly different ($p>0.05$) between the three APO treated groups, whether in the basal state or during β-adrenergic stimulation. The production of ROS was similar amongst the APO treated groups ($p>0.05$). The rates of SR Ca^{2+} leak were not significantly different ($p>0.05$) between the APO treated groups. In association with the reduced rates of SR Ca^{2+} leak, the calpain activity was not significantly different ($p>0.05$) between the APO groups, which likely contributed to the prevention of cardiac fatigue in the APO 24H group. These data suggest that improved Ca^{2+} regulation and reduced proteolytic activity likely contributed to the prevention of cardiac fatigue in the APO AC and APO 24H groups.

These studies demonstrate that cardiac fatigue present immediately after exhaustive exercise was associated with increased ROS production and increased SR Ca^{2+} leak and that cardiac fatigue present 24 hours post-exercise was associated with enhanced proteolytic activity. In the presence of NOX inhibition, cardiac fatigue was prevented and ROS production, SR Ca^{2+} leak and calpain activity were maintained at control levels. Although these results demonstrate a strong association between NOX activity and ROS production with SR Ca^{2+} leak and cardiac fatigue, the exact mechanisms that prevent Ca^{2+} leak remain to be determined.

Acknowledgements

This thesis would not have been possible without the support and guidance of Dr. James Rush and Dr. Russ Tupling. I cannot thank you enough for your mentorship and friendship throughout my graduate career at the University of Waterloo. Many years have gone by since I began graduate studies at UW and many lab members that contributed to this thesis have come and gone as well. I thank them for their passion for research and their help. In particular, I would like to thank Drs. Eric Bombardier, Andrew Levy and Elliott McMillan. If it were not for them then I would not have possessed the technical skills to complete this thesis.

Lastly, I would like to thank my wife, Christine whose love, support and patience has never wavered and has pushed me towards the completion of this document. I am forever grateful for the sacrifices that you have made so that I could complete this degree, I love you.

Table of Contents

List of Figures

List of Tables

List of Abbreviations

$[Ca^{2+}]_f$	Cytosolic free Ca^{2+} concentration
˙OH	Hydroxyl radical
+dP/dt	Maximal rate of pressure development
-dP/dt	Maximal rate of pressure decline
24H	24 hours post
2D	Two dimensional
3NY	3-nitrotyrosine
4-CMC	4-chloro-m-cresol
4-HAE	4-hydroxy-alkenal
A	Active left ventricular filling
AC	Acute
ADP	Adenosine diphosphate
AMP	Adenosine monophosphate
APO	Apocynin
ATP	Adenosine triphosphate
AVN	Atrioventricular node
BSA	Bovine serum albumin
Ca^{2+}	Calcium ion
CaMKII	Ca^{2+}/Calmodulin-dependent protein kinase II
cAMP	Cyclic adenosine monophosphate
CICR	Ca^{2+}-induced Ca^{2+}-release
CK	Creatine kinase
CPA	Cyclopiazonic acid
CTL	Control
CVP	Central venous pressure
CVR	Coronary vascular resistance
Cys	Cysteine
DCF	2',7'-dichlorofluorescein
DCFH	2',7'-dichlorodihydrofluorescein
DCFH-DA	2',7'-dichlorodihydrofluorescein-diacetate
DHE	Dihydroethidium
DHPR	Dihydropyridine receptor
DNPH	2,4-dinitrophenylhydrazine
DPI	diphenyliodonium
DTDP	4-4'-dithiopyridine
DTT	Dithiothreitol
E	Passive left ventricular filling
E'	Early diastolic tissue velocity
EC Coupling	Excitation-contraction coupling
ECG	Electrocardiogram

ECL	Enhanced chemiluminescence
EDV	End diastolic volume
EF	Ejection fraction
Epi	Epinephrine
FDAR	Frequency-dependent acceleration of relaxation
FFR	Force-frequency relationship
GSH	Reduced glutathione
GSH:GSSG	Ratio of reduced glutathione to oxidized glutathione
GSSG	Oxidized glutathione
H^+	Hydrogen ion
H_2O	Water
H_2O_2	Hydrogen peroxide
HEK-293	Human embryonic kidney cells
HEPES	4-(2-hydroxyethyl)-1-piperazineethanesulfonic acid
HNO	Nitroxyl
HOCl	Hypochlorus acid
HPLC	High performance liquid chromatography
HR	Heart rate
HRP	Horseradish peroxidase
I_{Ca}	L-type Ca^{2+} current
I_K	Delayed, rectifying K^+ currents
I_{Na}	Inward Na^+ current
ISO	Isoproterenol
I_{to}	Transient outward K^+ currents
IVRT'	Tissue isovolumetric relaxation time
K^+	Potassium ion
KO	Knockout
LA	Left atrium
LDH	Lactate dehydrogenase
LV	Left ventricle
LVDP	Left ventricular developed pressure
LVeDP	Left ventricular end diastolic pressure
MDA	Malondialdehyde
Mg^{2+}	Magnesium ion
MLC	Myosin light chain
MRI	Magnetic resonance imaging
MyBP-C	Myosin binding protein C
Na^+	Sodium ion
NADH	Nicotinamide adenine dinucleotide
NADPH	Nicotinamide adenine dinucleotide phosphate
NCX	Sodium calcium exchanger

NE	Norepinephrine
NKA	Na^+/K^+-ATPase
NO	Nitric oxide
NOX	NADPH oxidase
$O2^{\cdot-}$	Superoxide anion
$ONOO^-$	Peroxynitrite
PEP	Phosphoenol pyruvate
P_i	Inorganic Phosphate
PK	Pyruvate kinase
PKA	Protein kinase A
PLM	Phospholeman
PLN	Phospholamban
PMSF	Phenylmethylsulphonyl fluoride
P_o	Open probability
PO2	Partial pressure of oxygen
PP1/PP2A	Protein phosphatase 1/protein phosphatase 2A
pPLN	Phosphorylated phospholamban
pRyR	Phosphorylated ryanodine receptor
PVDF	Polyvinyldiene difluoride
RA	Right atrium
rac	Ras-related C3 botulinum toxin substrate
REDOX	Reduction/oxidation
RIPA	Radioimmunoprecipitation assay
ROS	Reactive oxygen species
RV	Right ventricle
RyR	Ryanodine receptor
SAN	Sinoatrial node
SBP	Systolic blood pressure
SDS-PAGE	Sodium dodecyl sulphate polyacrylamide gel electrophoresis
SE	Standard error
Ser	Serine
SERCA	Sarco(endo)plasmic reticulum Ca^{2+}-ATPase
SH	Sulfhydryl
SLN	Sarcolipin
SR	Sarcoplasmic reticulum
STI	Speckle tracking imaging
Suc-LLVY-AMC	N-Succinyl-Leu-Leu-Val-Tyr-7-amino-4-methylcoumarin
SV	Stroke volume
TBA	Thiobarbituric acid
TBARS	Thiobarbituric acid reactive substances
TBST	Tris-buffered saline plus Tween

TDI	Tissue Doppler imaging
Tm	Tropomyosin
TnC	Troponin C
TnI	Troponin I
TnT	Troponin T
T-tubules	Transverse tubule
Tyr	Tyrosine
Z-LL-CHO	N-benzyloxycarbonyl-Leu-leucinal

Chapter I: Introduction, review of the literature and statement of problem

Overview

The positive effects of regular endurance exercise on cardiovascular health in the general population are well recognized (King et al., 1989; Dengel et al., 1998; Andersen et al., 1999; Ross et al., 2000). However, prolonged endurance events, such as marathons, triathlons and ultramarathons have been shown to have transient, negative effects on LV function (Shave & Oxborough, 2012). Mechanistically, it has been demonstrated that prolonged exercise may alter ventricular repolarization (Sahlen et al., 2009), LV mechanics (Nottin et al., 2012) and the myocardium's sensitivity to β-adrenergic stimulation (Scott et al., 2007). Animal studies that have subjected rats to prolonged aerobic exercise have demonstrated, transient LV fatigue, which was associated with increased lipid peroxidation (Wonders et al., 2007) and oxidative stress (Vitiello et al., 2011). In addition, rats that swam to exhaustion had significantly lower rates of cardiac SR Ca^{2+}-uptake when compared to a control group (Pierce et al., 1984). However, the study by Piece and co-workers (1984) did not examine LV function following the exhaustive swim bout. Several disease models, which include heart failure, diabetic cardiomyopathy and muscular dystrophy cardiomyopathy present with reduced cardiac function in association with impaired regulation of intracellular Ca^{2+}. It is possible that LV fatigue following prolonged endurance exercise may occur as a result of increased oxidative stress and impaired Ca^{2+} regulation by the sarcoplasmic reticulum, features observed in the stunned myocardium. The studies in this thesis will employ a rat model of exhaustive treadmill exercise to determine the role of oxidative stress and impaired SR function in exercise-induced cardiac fatigue.

Introduction

Exercise-Induced Cardiac Fatigue in Humans

In humans, prolonged endurance events, such as marathons, triathlons and ultramarathons have been shown to have transient, negative effects on left ventricular function (Shave & Oxborough, 2012). It has been nearly 50 years since Saltin and Stenburg (1964) observed a reduction in stroke volume (SV) following three hours of exercise, despite preserved blood volume. Since then numerous human studies have demonstrated a reduction in LV function in the basal state (i.e. at rest) following an acute bout of prolonged or exhaustive exercise. Significant work in this field has been performed by R. Shave's group at Cardiff Metropolitan University, UK (Oxborough et al., 2010a; Shave & Oxborough, 2012)

Early human studies utilized two-dimensional M mode echocardiography to measure LV cavity dimensions, and pulsed-wave Doppler ultrasound to assess passive filling of the LV in early diastole (E) and active filling late in diastole (A), before and after endurance events. Douglas and colleagues (1987) monitored 21 athletes competing in an Ironman® Triathlon and found significant reductions in LV diastolic dimension, fractional shortening and the ratio of early to late (E:A) filling velocities following the race (Douglas et al., 1987). Similarly, George and colleagues (2004) observed a reduction in diastolic function as indicated by a reduced E to A ratio; however, they did not observe any deficits in LV systolic function following a marathon. These authors speculated that the observed changes in diastolic function might be related to a disturbance in Ca^{2+} removal from the cytosol (George et al., 2004). The removal of Ca^{2+} from the cytosol results in myocyte relaxation, which is critical for proper diastolic function (i.e. passive filling of the LV). Several human studies have reported impaired systolic and/or diastolic function following endurance events that were performed under a variety of conditions (i.e.

temperature, humidity, elevation and pace) and did not account for changes in preload (Douglas et al., 1987; Whyte et al., 2000; Shave et al., 2004; Dawson et al., 2005). Preload is a major determinant of LV contractility and thus, by not controlling the environmental conditions and fluid replacement, changes in preload may have contributed to the observed deficits in LV function.

Researchers have attempted to maintain or manipulate preload in an attempt to more accurately compare post-exercise indices of LV function to those recorded pre-exercise. A study by Goodman and co-workers (2001) attempted to maintain preload via *ad libitum* fluid consumption and intravenous saline infusion in participants during 150 min of cycling at 70-74% of HR_{max}. Despite the intervention used to maintain preload, EDV decreased over the course of the 150 minute protocol. Ejection fraction (EF) was not different following the exercise bout; however, there was a significant delay in the time to peak filling of the LV, which may be due to elevate heart rate post-exercise (Goodman et al., 2001). A delay in the time to peak filling of the LV may also be due to lower left atrial pressure, a slower rate of LV pressure decline, incomplete LV relaxation or increased LV stiffness (Lew, 1989). A similar study maintained central venous pressure (CVP), an indicator of preload, during three hours of cycling by infusing saline into the superior vena cava (Dawson et al., 2007). There were no observable changes in systolic function following three hours of cycling. However, despite maintenance of CVP, diastolic function was reduced, as indicated by a lower E:A ratio. Similarly, a small but significant decline in E:A ratio was observed in athletes following an Ironman® triathlon despite maintenance of preload and afterload (Hassan et al., 2006). These studies suggest that even when preload is maintained there are deficits intrinsic to the cardiomyocyte that contributes to a reduction in diastolic function (Hassan et al., 2006).

Advances in imaging techniques and analysis software, namely tissue Doppler imaging (TDI) and speckle tracking imaging (STI), have made it possible to examine LV wall motion, strain and strain rates *in vivo*. In simplistic terms, strain is a regional deformation of LV tissue and typically is measured as longitudinal, radial, circumferential or rotational movement (Gorcsan & Tanaka, 2011). TDI analysis of cardiac function following four consecutive days of cycling (3 hours/day) indicated that early diastolic tissue velocity (E′) was decreased and that tissue isovolumetric relaxation time (IVRT′) was prolonged (Oosthuyse et al., 2012). Two separate studies assessed LV function before and after an 89 km and 160 km race using standard echocardiography and STI. It was observed that ejection fraction (EF), the E:A ratio, peak strain and peak systolic and diastolic strain rates were significantly reduced following the races (George et al., 2009; Scott et al., 2009). Furthermore, Oxborough and colleagues (2010b) utilized STI analysis and observed a significant reduction in LV filling during early diastole following a marathon. These imaging techniques have been described as load-independent (Zhou et al., 2013), which suggests that the existence of diastolic fatigue following endurance exercise is due to intracellular deficits in the cardiomyocyte.

Further development of TDI and STI techniques has provided the unique opportunity to examine the interval between ventricular excitation and peak tissue velocities as well as rotation of the ventricles. A study by Chan-Dewar and co-workers (2010) assessed the time to peak systolic and peak diastolic tissue velocity from the onset of the Q wave (normalized to the R-R interval) following an 89 km marathon. Immediately following exercise there was a reduction in indices of LV function (i.e. reduced EF, E:A and peak tissue velocities), as well as an electro-mechanical delay indicated by the ~44 ms increase in time from QRS to peak systolic tissue velocity. These authors indicated that the electro-mechanical delay was not a result of altered

membrane excitability as QRS duration was not affected by exercise. Rather they suggested that intrinsic deficits in the cardiomyocyte downstream of excitation are likely candidates and could be a combination of either Ca^{2+} mobilization, Ca^{2+} sequestration, energy turnover or myofibrillar ATPase activity (Chan-Dewar et al., 2010).

Left ventricular torsion is the twisting of the ventricle during systole and untwisting prior to diastolic filling. Proper LV torsion is essential for ventricle function during rest and exercise (Buckberg et al., 2011). Nottin and colleagues (Nottin et al., 2009) evaluated LV torsion via 2D ultrasound STI following an Ironman® Triathlon. These authors observed a significant decrease and delay in LV twisting during systole, which contributed to the lower ventricular untwisting during isovolumetric relaxation (Nottin et al., 2009). These changes in ventricular mechanics would likely impact ventricular filling during diastole as the potential energy stored when the ventricles twist during systole, is released during diastole and contributes to the untwisting of the ventricles, which is vital for the rapid drop in LV pressure (Nottin et al., 2009). A more recent study by the same group had participants cycle for two hours, such that their HR was ≥ 150 bpm at all times and compared LV strain and twist before and after cycling (Nottin et al., 2012). Following exercise, there was a reduction in diastolic function (decreased peak E), which was associated with a delay in peak untwisting velocity. Impaired LV untwisting would likely reduce LV filling during diastole, which would decrease EDV and reduce contractility.

The activation of β-adrenergic receptors and subsequent phosphorylation of target proteins by protein kinase A (PKA) is pivotal to the increase in LV contractility observed during exercise (discussed below). A reduction in β-adrenergic sensitivity following exhaustive exercise could in theory reduce contractility of the heart during a subsequent bout of exercise and may represent a form of cardiac fatigue. Indeed, a study by Eysmann and colleagues (1996) had

humans cycle at ~60% VO$_2$max until exhaustion (~95 minutes) and demonstrated that following a 10 minute post-exercise recovery period, subjects had a reduced EF, E:A ratio and EDV. In addition, there was a decrease in the chronotropic (heart rate) response to a given concentration of the β-adrenergic agonist, ISO. The results of this study suggest that submaximal exercise to the point of exhaustion may blunt the positive chronotropic response to β-adrenergic receptor stimulation in pacemaker cells of the sinoatrial (SA) node. Conversely, an acute bout of running at ~70% VO$_2$max for one hour did not alter the chronotropic response to ISO in humans (Martin et al., 1991). These studies suggest that perhaps there is an interaction between exercise intensity and duration with respect to alterations in the heart rate response to β-adrenergic stimulation. Work by Welsh and colleagues (2005) examined the end-systolic elastance and the relationship between fractional area change and wall stress (i.e. indices of LV contractility) during a continuous infusion of the β-adrenergic agonist, dobutamine, following a half-Ironman® Triathlon. The LV contractility, HR and systolic blood pressure (SBP) response to dobutamine infusion was blunted post-exercise when compared to the pre-exercise dose response. Similar findings were observed following four hours of simulated rowing and a half-Ironman Triathlon® (Hart et al., 2006; Scott et al., 2007). These data demonstrate that β-adrenergic responsiveness in humans is depressed following prolonged exercise, which may limit the capacity of the myocardium to attain a desired cardiac output during a subsequent bout of exercise (i.e. cardiac fatigue). The evidence in human research suggests that long duration or high intensity exercise can have a negative effect on cardiac mechanics at the whole organ level. However, the intracellular mechanisms associated with exercise-induced cardiac fatigue remain to be elucidated.

Exercise-Induced Cardiac Fatigue in Animals

The use of animal models has greatly advanced our understanding of cardiac physiology in relation to disease and adaptation to exercise. Surprisingly, there are a limited number of investigations that have utilized animal models to explore the development of, and mechanisms associated with, exercise-induced cardiac fatigue. Grimditch and co-workers (1981) ran instrumented dogs at 70% of their maximum heart rate until exhaustion, which occurred on average after a duration of 77 minutes. These authors compared SV, cardiac output and $\pm$dP/dt at the point of exhaustion to steady state values recorded within the first five minutes of exercise and found that upon exhaustion the cardiovascular parameters examined remained unchanged. In fact there was an increase in both $\pm$dP/dt (Grimditch et al., 1981). More recent work using echocardiography and pressure transducers fed into the LV of anesthetized rats has demonstrated that prolonged aerobic exercise resulted in cardiac fatigue (Vitiello et al., 2011; Olah et al., 2015). Olah and colleagues (2015) assessed EF in anesthetized rats following three hours of swim exercise and found that EF was significantly lower in the exercise group when compared to the control group. In animals that were forced to run for four hours at 60-65% of their maximal heart rate there was approximately a 12% reduction in LVDP (Vitiello et al., 2011). These data suggest that the duration of exercise can impact the function of the myocardium following acute exercise or perhaps there are species differences in relation to cardiac fatigue.

The isolated trabeculae and isolated perfused heart techniques permit the evaluation of cardiac function in a controlled environment with regard to loading conditions, pH, temperature and humoral factors. Early work by Maher and co-workers (1972) measured force production from isolated LV trabecular muscles from control rats and rats run to exhaustion on a motorized treadmill. These researchers observed an approximate 50% reduction in force from trabeculae of

exhausted rats. In a later study, LVDP was assessed using the isolated perfused rat heart following four hours of treadmill exercise at 60-65% of maximal heart rate. When compared to control hearts, prolonged exercise caused a significant reduction in LVDP (Vitiello et al., 2011). A study by Wonders and co-workers (2007) determined the LVDP of isolated rat hearts immediately post-exercise and at 24, 48 and 72 hours post-exercise. These authors demonstrated that one hour of running at 25 m/min resulted in a transient decline in LVDP that peaked (~25% reduction) 48 hours post-exercise and returned to pre-exercise levels at 72 hours post-exercise. However, not all studies that have examined cardiac fatigue in rodents have found equivalent results. Indices of LV function from hearts excised from rats that ran at 18 m/min and 0% grade until exhaustion were not significantly different than hearts from the sedentary control group (Seward et al., 1995). Thus, exercise-induced cardiac fatigue has been demonstrated using some, but not all exercise protocols.

The literature regarding β-adrenergic responsiveness following acute exercise in animals is more contentious than the evidence in humans. Friedman and colleagues (1987) demonstrated a significant desensitization of the β-adrenergic receptors in the canine myocardium following 60 minutes of treadmill running at a speed and grade that elicited 60-80% of their maximal heart rate. Once fully recovered, animals were infused with progressive doses of ISO in order to increase heart rate by 25 beats per minute (bpm). The ISO dose required was 3-fold greater post-exercise when compared to the pre-exercise dose (Friedman et al., 1987). These authors failed to assess cardiac function following exercise so it is not certain whether this β-adrenergic desensitization occurred in conjunction with LV fatigue. In another study, β-adrenergic responsiveness in conjunction with LVDP were assessed using the isolated perfused heart technique following four hours of submaximal treadmill exercise in rats (Vitiello et al., 2011).

These authors did not observe a significant difference in LVDP between control and exercise hearts in response to progressive doses of ISO. These findings are at odds with observations in dogs and in previous work performed on humans (Friedman et al., 1987; Welsh et al., 2005; Hart et al., 2006; Scott et al., 2007), suggesting that there are perhaps species-dependent changes in β-adrenergic signalling following exhaustive exercise.

Cardiac Excitation-Contraction Coupling

In order to discuss potential mechanisms that contribute to the development of exercise-induced cardiac fatigue it is important to be aware of the processes involved with force production and relaxation in the cardiomyocyte. Excitation-contraction (EC) coupling is the term given to the molecular events that start with electrical excitation of the cardiomyocyte and culminate with myocyte contraction. During diastole, the resting membrane potential of a ventricular cardiomyocyte is approximately -90 mV. Slight depolarization of the ventricular sarcolemmal membrane, resulting from cation (Na^+, Ca^{2+}) influx from adjacent cardiomyocytes through gap junctions, activates voltage-gated Na^+ channels, which causes rapid Na^+ influx (inward Na^+ current, I_{Na}) and contributes to the rapid rise of the cardiac action potential (Phase 0, see Figure 1.1 and for a detailed review see (Bers et al., 2003)). The membrane potential peaks at approximately +25 mV followed by rapid inactivation of Na^+ channels that contributes to cessation of depolarization. Repolarization and Na^+ removal from the cytosol of the cardiomyocyte will be discussed below.
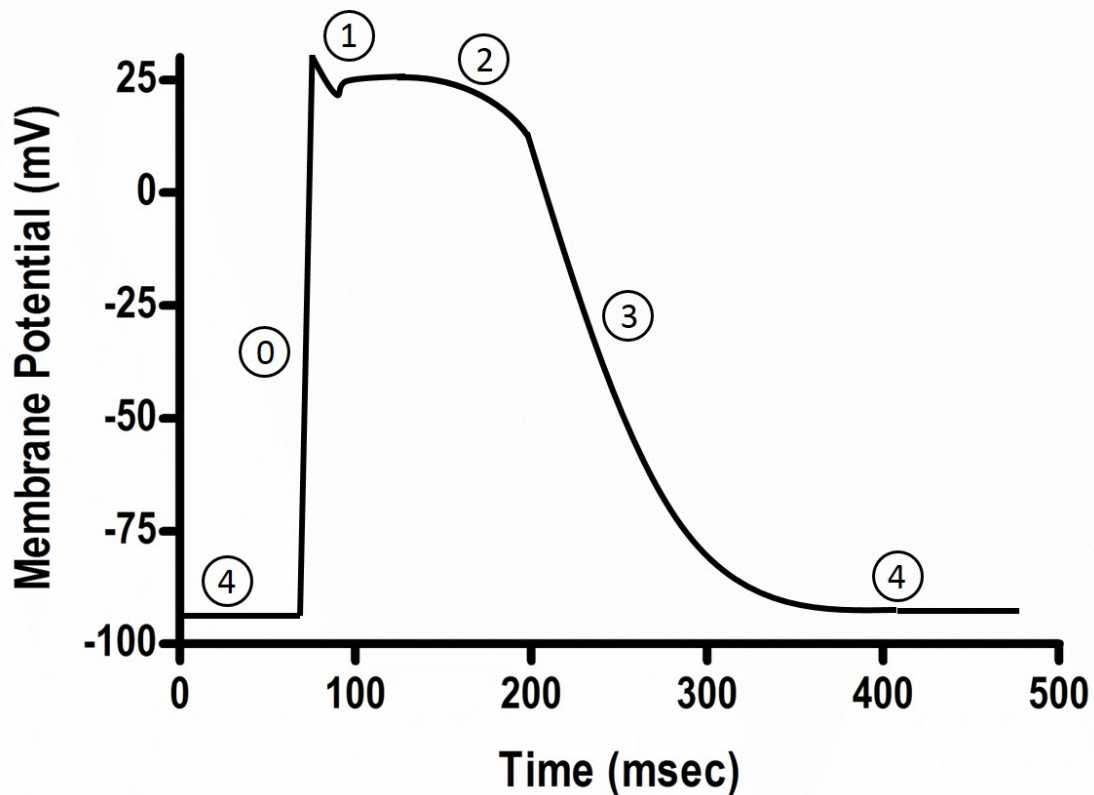
Figure 1.1. An illustration of the ventricular myocyte action potential. Phase 0: The steep rise in membrane potential is due to opening of Na^+ channels and rapid Na^+ influx. Phase 1: The action potential notch occurs as the Na^+ channels are inactivated and the transient outward K^+ channels open. Phase 2: Entry of Ca^{2+} via the DPHR contributes to the action potential plateau. Phase 3: The majority of cardiomyocyte repolarization is due to the delayed, rectifying K^+ current. Phase 4: The Na^+/K^+-ATPase restores the electrochemical gradient of Na^+ and K^+ and contributes to repolarization. Adapted from (Bers, 2002).

The wave of depolarization flows to the interior of the cardiomyocyte via the transverse tubules (T-tubules) where there are a high density of voltage-dependent Ca^{2+} channels, known as dihydropyridine receptors (DHPR) or L-type calcium channels. DHPRs were first purified using skeletal muscle (Curtis & Catterall, 1984) and are heterotetrameric protein complexes comprised of α_1, α_2/δ, β and γ subunits (Hosey et al., 1987; Bodi et al., 2005). Upon depolarization, the α_1 subunit undergoes a conformational change, which results in opening of the pore region and extracellular Ca^{2+} influx. Movement of Ca^{2+} across the sarcolemma creates

an inward current, termed L-type Ca^{2+} current (I_{Ca}). The Ca^{2+} entry via I_{Ca} contributes to the plateau phase of the cardiac action potential (Phase 2, Figure 1.1) and can raise sub-sarcolemmal Ca^{2+} concentration up to 10-20 µM (Figure 1.2) (Bers, 2008). The entry of Ca^{2+} is often referred to as *trigger* Ca^{2+} as it initiates Ca^{2+}-induced Ca^{2+}-release (CICR) from the SR through the Ca^{2+} release channel (Fabiato & Fabiato, 1975a).
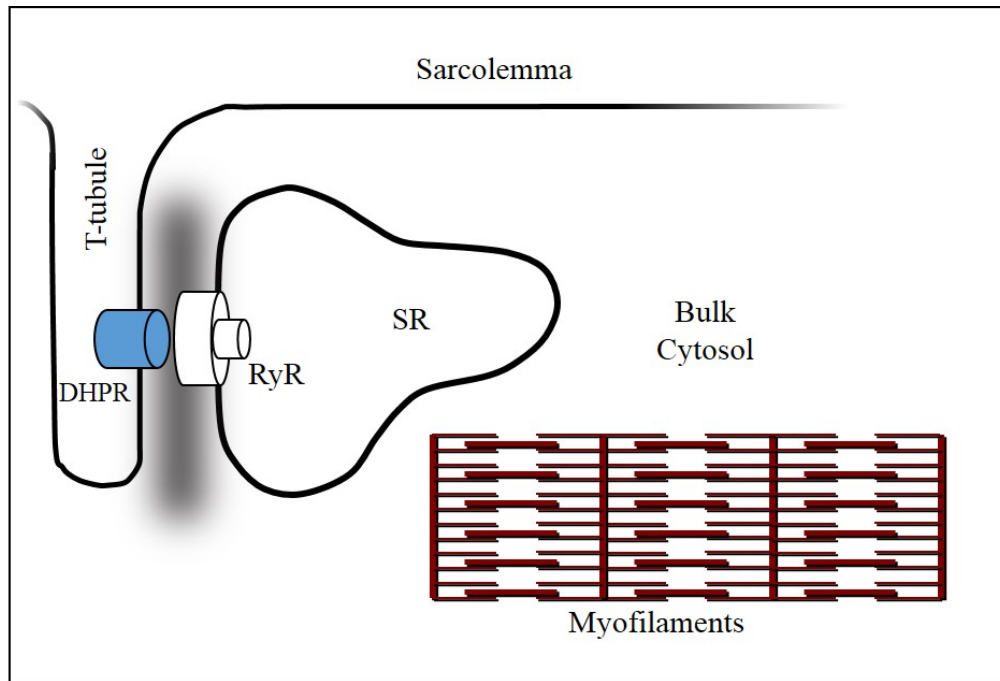
Figure 1.2. An illustration of a ventricular cardiomyocyte. A single t-tubule and the terminal cisterna of the sarcoplasmic reticulum (SR) are in close proximity to each other and form a diad. The shaded area between the t-tubule and the SR terminal cisterna is the *subsarcolemmal cleft region*. The dihydropyridine receptor (DHPR) and the ryanodine receptor (RyR) are included for reference.

The cardiac isoform of the Ca^{2+} release channel (Ryanodine Receptor; RyR2) is a homotetrameric protein complex with a large cytoplasmic N-terminal domain and a C-terminal pore region that spans the SR membrane (Lai et al., 1989; Lehnart et al., 2004a; Ludtke et al., 2005). The cytoplasmic domain acts as a scaffold for regulatory proteins that modulate RyR gating, such as calstabin2 (Brillantes et al., 1994; Timerman et al., 1994), PKA (Marx et al.,

11

2000), protein phosphatase 1 (PP1), protein phosphatase 2A (PP2A) (Marx et al., 2001) and calmodulin (Fruen et al., 2000; Lehnart et al., 2004a). In vivo, RyR2 gating is modulated by Ca^{2+}, Mg^{2+}, ATP (Copello et al., 2002), phosphorylation (Hain et al., 1995) and oxidation (Marengo et al., 1998). Entry of trigger Ca^{2+} raises the subsarcolemmal cleft Ca^{2+} concentration, such that Ca^{2+} occupies the Ca^{2+} binding sites on each of the 4 RyR2 subunits. Occupation of the Ca^{2+} binding sites causes a rotation in the RyR2 complex that aligns the central pore and permits Ca^{2+} release from the lumen of the SR (Serysheva et al., 1999).

The Ca^{2+} that is released from the SR rapidly diffuses throughout the cytosol and binds to the N-terminal, low affinity Ca^{2+} binding site on troponin C (TnC). TnC is the 3rd member in the troponin complex, which is comprised of troponin I (TnI), the inhibitory subunit, and troponin T (TnT), the isoform that anchors the troponin complex to tropomyosin (Fuchs & Smith, 2001). Tropomyosin (Tm) lies in the groove between actin filaments and regulates the actin-myosin interaction. When Ca^{2+} binds to TnC the protein undergoes a conformational change that is transmitted through the Tn complex and causes Tm to move to the outer domain of the actin filament, which exposes the myosin binding sites on actin (Craig & Lehman, 2001; Kobayashi et al., 2008). Thin filament activation permits transition of weakly bound cross-bridges to strongly bound cross-bridges and results in shortening of the sarcomere and the development of force (McKillop & Geeves, 1993).

The degree of developed tension in ventricular myocytes is highly dependent on the concentration of cytosolic free calcium ($[Ca^{2+}]_f$). The first recordings of Ca^{2+} transients in cardiac tissue were carried out in atrial trabeculae from frogs using the calcium-sensitive bioluminescent protein aequorin (Allen & Blinks, 1978). These experiments demonstrated that the classical inotropic effects of increased stimulation frequency (i.e. increased heart rate), increased

extracellular Ca^{2+} concentration or β-adrenergic stimulation were due to a greater Ca^{2+} transient amplitude. Using aequorin, Yue and co-workers (1986) measured the $[Ca^{2+}]_f$ in tetanized papillary muscles from ferrets and calculated that maximal Ca^{2+}-activated force occurred at ~1.0 μM. The evolution of fluorescent Ca^{2+} indicators improved the resolution of measuring intracellular Ca^{2+} transients. Using fura-2 several groups confirmed the finding of Yue and co-workers (1986) that maximal Ca^{2+}-activated force occurred at ~1.0 μM (Gao et al., 1994; Backx et al., 1995). The relationship between intracellular free Ca^{2+} concentration ($[Ca^{2+}]_f$) and force production is sigmoidal in nature and has a steep linear portion of the curve (Gao et al., 1994; Backx et al., 1995) (Figure 1.3). Accordingly, a small change in the $[Ca^{2+}]_f$ anywhere along the linear portion of the force-Ca^{2+} curve will result in relatively large changes in force.
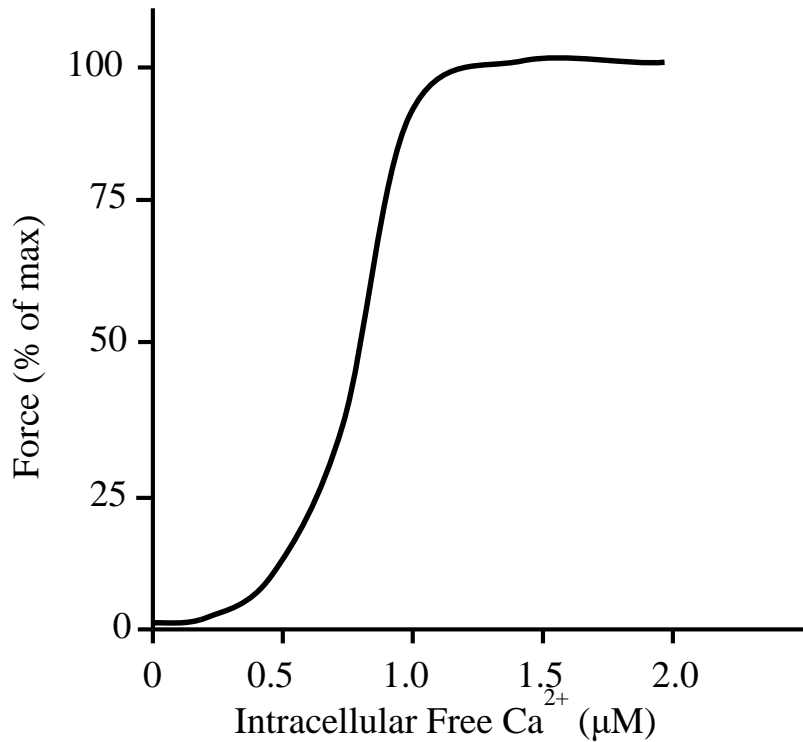
Figure 1.3. The relationship between intracellular free Ca^{2+} concentration and force. The sigmoidal nature of this curve dictates that small changes in the physiologically relevant range of intracellular free Ca^{2+} (0.1-1.0 µM) results in significant changes in force production. Adapted from (Gao et al., 1994).

Repolarization and Restoration of Electrochemical Ion Gradients

Repolarization of the membrane potential is accomplished primarily by opening of K^+ channels. In the heart, there are numerous types of K^+ channels that have been classified based on the duration of their open state, the timing of channel opening and the molecules that activate or inactivate the channel (for a comprehensive review see (Nerbonne & Kass, 2005)). As with Na^+ and Ca^{2+} channels, flow of K^+ through a K^+ channel and out of the cell generates an ionic current. Transient outward K^+ currents (I_{to}) and delayed, rectifying K^+ currents (I_K) are the two general classes of currents that contribute to cardiomyocyte repolarization (Josephson et al., 1984; Matsuura et al., 1987). Activation of I_{to} occurs early in the cardiac action potential as Na^+ channels are inactivated and contributes to the action potential notch (Figure 1.1). I_K currents

14

activate early in the cardiac action potential as well, however, K^+ conductance remains prominent for the bulk of the action potential duration and provides the majority of the repolarizing current (Nerbonne & Kass, 2005).

Restoration of diastolic extracellular and intracellular concentrations of Na^+ and K^+ is mediated primarily by the Na^+/K^+-ATPase (NKA). The NKA transitions between two conformations (E1 & E2) and transports Na^+ out of the cell and K^+ into the cell against a strong concentration gradient using energy derived from ATP hydrolysis (Bers et al., 2003). The α subunit of the NKA contains one ATP, three Na^+ and two K^+ binding sites and is modulated by several smaller accessory proteins, namely the β subunit and phospholeman (PLM) (Shinoda et al., 2009). Based on the stoichiometry of Na^+ and K^+ transport by the NKA, the NKA also contributes to the restoration of sarcolemmal membrane potential. Regulation of NKA activity by PLM is analogous to that of SERCA2a regulation by phospholamban (PLN; discussed below). PLM appears to modulate NKA activity by decreasing the affinity of NKA for Na^+ and K^+ (Bossuyt et al., 2009; Han et al., 2009). Repolarization of the cardiomyocyte and restoration of ion gradients across the sarcolemma permits myocyte relaxation and subsequent depolarizations.

Cardiomyocyte Relaxation

In order for relaxation of the cardiomyocyte to occur, the $[Ca^{2+}]_f$ must be lowered to ~100 nM (Lattanzio & Pressman, 1986; Marban et al., 1987). Equally important, the same amount of Ca^{2+} that entered the cell via I_{Ca} and amount released from the SR must be extruded to the extracellular space or sequestered in the lumen of the SR, respectively. In humans, the relative contribution of I_{Ca} and SR Ca^{2+} release to the total rise in $[Ca^{2+}]_f$ is approximately 30% and 70%, respectively (Bers, 2002). However, in rodents this ratio is shifted in favour of SR Ca^{2+} release and sequestration with ~90% of activating Ca^{2+} originating from the SR. The primary protein

responsible for Ca^{2+} extrusion is the sodium-calcium exchanger (NCX) and the protein responsible for pumping Ca^{2+} into the lumen of the SR is SERCA.

The NCX is a unique antiporter, in that it is driven by the concentration gradient of Ca^{2+} and Na^+ across the sarcolemma as well as the prevailing membrane potential (Matsuoka & Hilgemann, 1992). The NCX is also electrogenic because it transports 3 Na^+ for every Ca^{2+} (Bridge & Bassingthwaighte, 1983). Early in the cardiac action potential, subsarcolemmal Na^+ is high and membrane potential is positive, which drives Na^+ extrusion and Ca^{2+} entry via the NCX (reverse mode). Late in the action potential, as repolarization of the ventricular myocyte proceeds, the membrane potential is negative and the $[Ca^{2+}]_f$ is high, which drives the NCX to extrude Ca^{2+} from the cytosol. During diastole, extracellular Na^+ concentration is high, $[Ca^{2+}]_f$ is low and the membrane potential is negative, which favours Na^+ influx and Ca^{2+} efflux (forward mode).

SERCA2a is the primary SERCA isoform present in ventricular myocytes and is responsible for maintaining low diastolic $[Ca^{2+}]_f$ and pumping Ca^{2+} back into the lumen of the SR following systole. Based on the number of Ca^{2+} and ATP binding sites, the stoichiometry of Ca^{2+} transport via SERCA2a is 2 moles of Ca^{2+} per mole of ATP hydrolysed (Inesi et al., 1973). Activation of SERCA2a can occur directly in a $[Ca^{2+}]_f$ dependent manner as Ca^{2+} interaction with binding sites on SERCA2a is a prerequisite for catalytic turnover. Although controversial (Odermatt et al., 1996; Rodriguez et al., 2004), SERCA2a may be activated by Ca^{2+}/calmodulin-dependent protein kinase (CaMKII) phosphorylation at serine 38 (Hawkins et al., 1994; Xu & Narayanan, 1999). SERCA2a activity can be augmented by ROS-dependent glutathionylation of cysteine 674 (Lancel et al., 2009). Lastly, SERCA2a is regulated by the small integral SR membrane protein, phospholamban (PLN). PLN physically interacts with SERCA2a and

modulates its activity by lowering the apparent affinity of SERCA2a to Ca^{2+} (Cantilina et al., 1993). Acting in unison, NCX and SERCA2a effectively lower $[Ca^{2+}]_f$, which facilitates cardiomyocyte relaxation.

Enhanced Cardiac Contractility during Exercise

During exercise, perfusion of the skeletal muscles must increase several fold in order to meet metabolic demand. The heart is finely tuned to match the demand placed upon it during exercise by increasing cardiac output. The force-frequency relationship (FFR), frequency-dependent acceleration of relaxation (FDAR) and the Frank-Starling Law of the heart are phenomena intrinsic to the cardiomyocyte that enhance the kinetics and strength of ventricular contraction, thus increasing the volume of blood ejected per beat. These phenomena can occur independent of β-adrenergic stimulation. A brief outline of the FFR, FDAR and the Frank-Starling Law is given below. A more in-depth examination of β-adrenergic-induced changes in the phosphorylation state of key EC coupling proteins is discussed as these changes can augment each of these three phenomena.

The Force-Frequency Relationship and Frequency-Dependent Acceleration of Relaxation

In 1871, Bowditch described the force-frequency relationship, which states that as the stimulation frequency of cardiac muscle increases, so too does the strength of contraction (Janssen, 2010). It is now recognized that not only does the absolute force of contraction increase when stimulation frequency increases, but the rate of contraction and the rate of relaxation increase as well (Janssen & Periasamy, 2007). It has been demonstrated that the augmented force of contraction observed in the FFR is primarily due to an increase in the Ca^{2+} transient amplitude (Gwathmey et al., 1990; Layland & Kentish, 1999; Miyamoto et al., 1999; Monasky & Janssen, 2009). The frequency-dependent increase in the Ca^{2+} transient is due to the temporal effects of

increased HR and increased Ca^{2+} influx via I_{Ca}. In a finite period, the cardiomyocyte spends more time in the depolarized state, which means that the concentration of Ca^{2+} entering the cardiomyocyte is augmented. Consequently, there is an increased rate of Ca^{2+} transport into the SR lumen via SERCA2a and thus SR Ca^{2+} load is increased. Greater SR Ca^{2+} load leads to augmented Ca^{2+} release from the SR, which would result in enhanced force production (Layland & Kentish, 1999; Janssen, 2010). Transgenic studies have demonstrated that the FFR was blunted in hearts from PLN knockout mice, which implicates PLN as a contributor to the augmented SERCA2a activity and thus the FFR (Brittsan et al., 1999; Bluhm et al., 2000). It would seem logical that SERCA2a-PLN would also contribute to the FDAR. However, using PLN KO mice and CaMKII inhibitors, it was demonstrated that FDAR was not dependent on PLN but rather phosphorylation of CaMKII target proteins (DeSantiago et al., 2002; Wu et al., 2012). CaMKII phosphorylation of sarcomeric proteins, namely, TnI, myosin binding protein-C (MyBP-C) and myosin light chain (MLC2) has been demonstrated to enhance the rate of relaxation as frequency is increased (Tong et al., 2004; Varian & Janssen, 2007). Interestingly, phosphorylation of MyBP-C and TnI enhanced the rate of contraction as well as the rate of relaxation, which would support more effective ventricular filling and ejection, given the abbreviated cardiac cycle (Tong et al., 2004). Taken together the FFR and FDAR are associated with altered SERCA2a-PLN interaction that increase the rate of Ca^{2+} transport and SR Ca^{2+} load and CaMKII phosphorylation of sarcomeric proteins that augment contraction and relaxation kinetics.

The Frank-Starling Law of the Heart

Over a century ago, Otto Frank and Ernest Starling observed that a relationship existed between the degree of ventricular filling and the strength of ventricular contraction such that as

EDV (i.e. preload) increased so too did the strength of the subsequent heart beat and a greater volume of blood was ejected. This is a fundamental property of cardiac muscle and is a result of an increase in sarcomere length, which increases the myofilament sensitivity to the $[Ca^{2+}]_f$ (de Tombe et al., 2010). Early experiments conducted by Fabiato and Fabiato suggested that the fraction of Ca^{2+} released from the SR varied with sarcomere length (Fabiato & Fabiato, 1975b). However, this line of evidence has since been disproved using permeabilized fibres (Hibberd & Jewell, 1982; Dobesh et al., 2002) and fluorescent dyes sensitive to Ca^{2+} (Claflin et al., 1998). X-ray diffraction experiments demonstrated that an increase in sarcomere length caused a decrease in the myofilament lattice spacing, which effectively brings the myosin heads closer to actin increasing the probability of strong cross-bridge formation at a given $[Ca^{2+}]_f$ (Irving et al., 2000). Recent experiments using osmotic compression to alter myofilament lattice spacing suggests that changes in lattice spacing may not be the primary mechanism responsible for myofilament length-dependent activation (Konhilas et al., 2002). Studies that employed transgenic mouse models, protein digestion or protein substitution suggest that the cardiac isoforms of titin and TnI participate in length-dependent thin filament activation and are critical for the classical changes in myofilament Ca^{2+} sensitivity as a result of increased sarcomere length (Cazorla et al., 2001; Konhilas et al., 2003; Tachampa et al., 2007).

Exercise-Induced Phosphorylation of EC Coupling Proteins

During exercise NE is released from sympathetic neurons and binds to β_1 adrenergic receptors on ventricular cardiomyocytes, which activates a cAMP-dependent signalling cascade that increases phosphorylation activity of PKA. PKA phosphorylates several EC coupling proteins, which results in enhanced lusitropy (relaxation) and inotropy (contractility).

Ca²⁺ Trigger and Ca²⁺ Release

Dihydropyridine receptors are targets of PKA mediated phosphorylation during exercise. The use of phospho-specific antibodies suggests that PKA phosphorylates serine 1928 on the α_1 subunit of the DHPR in rat ventricular myocytes (De Jongh et al., 1996; Hulme et al., 2006). Phosphorylation of DHPR increases the open probability of the channel, which results in enhanced I_{Ca} during depolarization (Reuter, 1983; Tsien et al., 1986; Bannister & Ohrtman, 2009). Therefore, over several beats, more Ca^{2+} enters the cardiomyocyte and is retained within the SR, thus phosphorylation of DHPR is critical to the progressive increase in SR Ca^{2+} load and enhanced inotropy observed during exercise.

Sarcoplasmic reticulum Ca^{2+} release through the RyR is augmented by PKA mediated phosphorylation at serine 2809 (Marx et al., 2000; Wehrens et al., 2004). The current understanding of the functional effects of serine 2809 phosphorylation of RyR has been well documented by Andrew Marks' group (for review see (Lehnart et al., 2004b)); however, these findings are controversial (Kranias & Bers, 2007). The working hypothesis states that in the basal state, a small regulatory protein called calstabin is bound to RyR, which stabilizes the tetramer and reduces the open probability of the channel. PKA mediated phosphorylation of RyR causes calstabin to dissociate from the RyR complex, which destabilizes the complex and increases the open probability of the channel. The functional consequence of RyR phosphorylation is an increase in the maximal rate of release and faster "turning off" of release (Ginsburg & Bers, 2004). The importance of exercise-induced phosphorylation of RyR at serine 2808 (PKA target in mice) has recently been documented in a study by Shan and colleagues (Shan et al., 2010). These authors developed a mouse line that possessed cardiac RyR that could not be phosphorylated at serine 2808. In response to ISO, these mice had reduced Ca^{2+} transients and

reduced inotropy as well as impaired exercise tolerance when compared to wild type mice. It appears that at least in murine cardiomyocytes, PKA mediated phosphorylation of RyR is required for the exercise-induced β-adrenergic response.

Phosphorylation of Myofibrillar Proteins

Phosphorylation of specific myofibrillar proteins can influence force production by altering cross-bridge kinetics and/or the sensitivity of the myofilaments to Ca^{2+}. TnI contains 2 tandem PKA phosphorylation sites at serine 23 and serine 24 (Swiderek et al., 1990). Phosphorylation of TnI results in a reduction in the sensitivity of the myofilaments to Ca^{2+} (Mope et al., 1980; Stelzer et al., 2007), which would decrease force on its own; however, the enhanced I_{Ca}, SR Ca^{2+} load and SR Ca^{2+} release offsets the decreased myofibrillar Ca^{2+} sensitivity during β-adrenergic stimulation (Bers, 2002). Transgenic experiments involving substitution of the cardiac TnI isoform with the non-phosphorylatable slow-twitch skeletal TnI isoform suggests that TnI phosphorylation results in an enhanced rate of relaxation (Kentish et al., 2001). Functionally, the effects of TnI phosphorylation would enhance the decline in ventricular tension during diastole, which could facilitate ventricular filling.

Myosin binding protein C is an ~140 kDa sarcomeric protein that forms transverse fibres that connect adjacent thick filaments. MyBP-C binds to both myosin and titin and through this interaction is believed to modulate the orientation of myosin heads relative to actin (Colson et al., 2010). Phosphorylation of MyBP-C by PKA creates a charge repulsion that drives the myosin head away from the thick filament backbone towards actin, thus increasing the probability of cross-bridge formation and force generation (Stelzer et al., 2007; Colson et al., 2010). Consequently, MyBP-C phosphorylation accelerates the rate of force development (Stelzer et al., 2007). Together, phosphorylation of MyBP-C and TnI results in faster rates of contraction

and relaxation, respectively, which facilitates ejection during systole and filling during diastole when HR is accelerated (Stelzer et al., 2007).

Ca^{2+} Removal

Phosphorylation of PLN is unique in that it directly increases lusitropy and indirectly enhances inotropy (for a comprehensive review see (MacLennan & Kranias, 2003)). As previously stated, under resting conditions PLN physically interacts with SERCA2a and lowers the apparent affinity of SERCA2a for Ca^{2+}, which reduces SERCA2a activity in the physiologically relevant range of 0.1-1.0 µM $[Ca^{2+}]_f$ (James et al., 1989; Cantilina et al., 1993). Phosphorylation of PLN by PKA at serine 16 causes PLN to dissociate from SERCA2a, thus relieving PLN's inhibitory effect, which increases SERCA2a activity (Lindemann et al., 1983; Simmerman et al., 1986; Wegener et al., 1989). The increase in SERCA2a activity results in a greater percentage of total $[Ca^{2+}]_f$ being sequestered to the SR versus being extruded by the NCX. Thus, there is an overall net gain of Ca^{2+} in the SR, which augments the open probability of RyRs and enhances the fraction of Ca^{2+} released during a subsequent beat.

In contrast to the well-defined effects of PLN phosphorylation, there is limited and conflicting data regarding β-adrenergic regulation of NCX activity (for a recent review see (Zhang & Hancox, 2009)). Studies in mammalian cardiomyocytes have demonstrated that β-adrenergic mediated activation of PKA significantly increased NCX activity (Perchenet et al., 2000; Wei et al., 2003). However, Ginsburg and Bers (Ginsburg & Bers, 2005) failed to observe any change in NCX activity following ISO treatment in rabbit cardiomyocytes. These conflicting reports likely arise due to the complexity of measuring NCX activity and the experimental techniques employed. Given the numerous PKA targets associated with EC coupling in the mammalian myocardium, it seems plausible that NCX activity may be regulated in some

capacity by PKA. The physiological consequence of increased NCX activity due to phosphorylation would be an increase in Ca^{2+} entry early in the cardiac action potential, which would amplify the amount of trigger Ca^{2+}. During repolarization, the rate of Ca^{2+} extrusion would be greater if NCX was phosphorylated, which would increase the decay rate of the Ca^{2+} transient and enhance relaxation of the myocyte (Zhang & Hancox, 2009).

PLM Phosphorylation and NKA Activity

NKA activity is dependent on intracellular Na^+ and extracellular K^+ concentrations. The acceleration of heart rate during exercise increases NKA activity due to Na^+ accumulation in the subsarcolemmal space, which is due to the more frequent opening of Na^+ channels in a finite period of time (Bers et al., 2003). Activation of the NKA can also be mediated by PKA phosphorylation of PLM at serine 68 (Silverman et al., 2005; Cheung et al., 2010). Work by Bers' group using cardiomyocytes isolated from wild type and PLM knock-out mice demonstrated that ISO treatment increased PLM phosphorylation in wild type myocytes, which enhanced NKA activity by increasing the apparent affinity of NKA to intracellular Na^+ without effecting the maximal activity of the pump (Despa et al., 2005). Physiologically, an increase in NKA activity is important to restore Na^+ and K^+ gradients because as heart rate increases, the number of depolarization events in a finite period of time also increases, which would result in an electrochemical imbalance if coordinated augmentation of NKA activity did not occur.

The cumulative effects of phosphorylation of key EC coupling proteins during exercise results in a myocardium that is able to generate more force, at a faster rate and to relax at a faster rate. Given the dynamic interplay between the activities of several key EC coupling proteins, a deficit in the activity of one or more proteins may contribute to exercise-induced cardiac fatigue.

Potential Mechanisms of Exercise-Induced Cardiac Fatigue

Despite the evidence of exercise-induced cardiac fatigue in humans and rodents, few studies have attempted to examine potential mechanisms that contributed to cardiac fatigue. Biochemical analysis of ventricular tissue in humans is problematic logistically; however, two studies have examined electrophysiological variables following prolonged exercise to determine if altered depolarization-repolarization is associated with exercise-induced cardiac fatigue. A study by Whyte and co-workers (2000) monitored 12-lead ECG before and after a half and full Ironman® Triathlon. These authors found that there were no significant changes in ST segment or T-wave form when compared to pre-race ECG recordings. In a more recent study, vectorcardiography was utilized to evaluate ventricular repolarization in seasoned runners (≥55 yrs) following a 30 km cross-country race (Sahlen et al., 2009). The QT interval normalized to heart rate was prolonged immediately after the 30 km race and at 24 hours post-competition. A prolonged QT interval is indicative of a delay and/or slowing of ventricular repolarization and in pathological circumstances can lead to arrhythmias such as delayed after depolarizations (van Noord et al., 2010). Functionally, a slowing of cardiac repolarization would delay ventricular relaxation, which may impair ventricular filling during periods when the cardiac cycle is shortened (i.e. during exercise).

There is substantial evidence that the production of ROS are increased during exercise in skeletal muscle and may contribute to the generation of fatigue (Davies et al., 1982; Jackson et al., 1985; Diaz et al., 1993; Kobzik et al., 1994). A model of tension versus cellular reduction/oxidation (REDOX) state was presented by Reid (2001), which states that in skeletal muscle, under basal conditions, small amounts of ROS are constitutively produced and that under basal conditions a muscle will generate a given amount of tension (Figure 1.4). An increase in exogenous (i.e. *in vitro)* or endogenous (i.e. during exercise) ROS may act as signalling

molecules and modify proteins in a manner that augments force production. During diseased states or periods of prolonged exercise, ROS production is exacerbated (i.e. oxidative stress) and may have a negative impact on the ability of the muscle to develop tension (Reid, 2001).
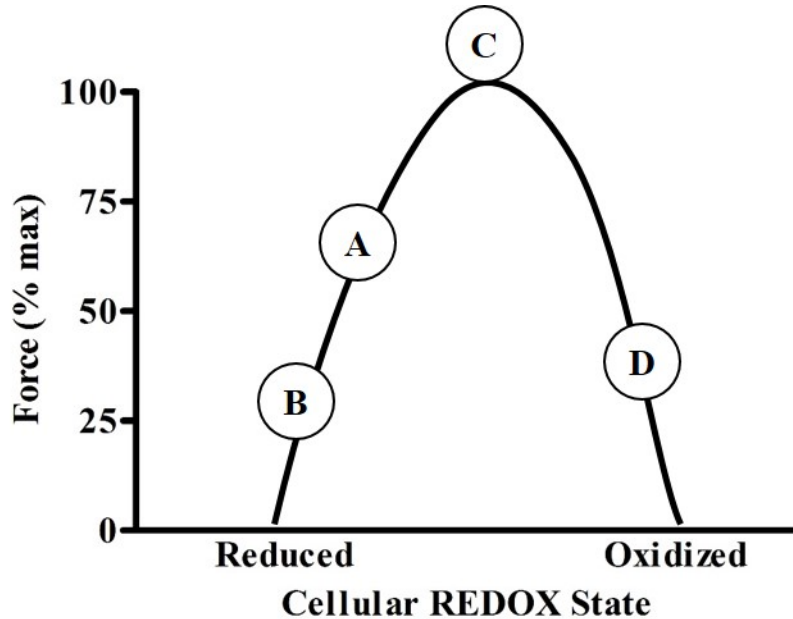
Figure 1.4. A model of the effects of cellular REDOX state on force production. (A) Represents the basal or unfatigued state. (B) Application of a reducing agent or antioxidant to an unfatigued muscle results in a reduction of force. (C) Exposure to mild levels of ROS augments force production. (D) Excessive ROS production or prolonged exposure attenuates force. Adapted from (Reid, 2001).

Evidence of increased ROS production and decreased cardiac function following acute exercise has recently been demonstrated in the myocardium of rats (Wonders et al., 2007; Vitiello et al., 2011; Olah et al., 2015). Indeed, a prolonged bout of swimming in rats has been demonstrated to increase dihydroethidium (DHE) fluorescence (a marker of ROS production) in cross-sections of LV, which accompanied a significant reduction in ejection fraction (Olah et al., 2015). Wonders and colleagues (2007) ran rats at 25 m/min and 5% grade for 60 minutes and observed a significant reduction in LVDP at 24 and 48 hours post-exercise, which recovered 72 hours following the acute bout of exercise. Myocardial lipid peroxidation, as indicated by

malondialdehyde (MDA) and 4-hydroxy-alkenal (4-HAE) content, was increased post-exercise and followed a similar recovery time course as that of LVDP. In another study, rats ran for four hours at 60-65% of their maximal running speed had a significant reduction in LVDP when compared to controls. The exercise-induced cardiac fatigue was associated with a decrease in the ratio of reduced glutathione to oxidized glutathione (GSH:GSSG), a marker of oxidative stress (Vitiello et al., 2011). These studies suggest a possible role for enhanced ROS production and oxidative stress in the development of exercise-induced cardiac fatigue. However, the intracellular protein targets of exercise-induced ROS were not examined in these studies.

Depressed Myocardial and Protein Function in Response to Exogenous ROS

The isolated perfused heart technique is a powerful model that allows researchers to manipulate the constituents of the perfusate and observe the effects on cardiac function in a controlled environment. A study by Chen and co-workers (Chen et al., 2002) demonstrated that addition of conjugated iron-hydroxyquinoline and 50 μM H_2O_2 (generates $\cdot$OH through the Fenton reaction) to the cardiac perfusate resulted in an ~50% reduction in LVDP. Following ROS exposure the activities of lactate dehydrogenase (LDH) and creatine kinase (CK) in the coronary effluent (an indication of sarcolemmal damage to the myocyte) were significantly higher when compared to control. In addition, lipid peroxidation was significantly greater in the oxidative stress condition compared to control hearts (Chen et al., 2002). These data suggest that $\cdot$OH damaged the sarcolemma, which may have contributed to the contractile dysfunction following exposure to iron and H_2O_2. Following exposure of isolated rat hearts to H_2O_2, there is a concentration dependent decrease in LVDP when compared to control hearts (Wang et al., 1999; Matsumoto et al., 2000). The decrease in LVDP was primarily mediated by a rise in end diastolic pressure, which was likely caused by the observed increase in diastolic $[Ca^{2+}]_f$ (Wang

et al., 1999; Matsumoto et al., 2000). A rise in diastolic $[Ca^{2+}]_f$ may be the result of sarcolemmal damage, reduced SERCA2a activity, aberrant Ca^{2+} release or some combination of the three.

To determine the effects of exogenous ROS on intracellular Ca^{2+} handling, the use of isolated cardiomyocytes loaded with Ca^{2+} sensitive fluorescent dyes has been readily utilized. Incubation of rat cardiomyocytes with 100 μM H_2O_2 resulted in a significant reduction in SERCA2a activity and prolonged rate of Ca^{2+} removal from the cytosol (Kennedy et al., 2006). However, the effects of 100 μM H_2O_2 on cell contractile function was not assessed in that study. In another study, rat cardiomyocytes were incubated with 200 μM H_2O_2 and significant impairments in cell shortening and relaxation were observed (Greensmith et al., 2010). The primary mechanism associated with the ROS-induced contractile dysfunction was a reduction in SERCA2a activity, which led to a decreased rate of Ca^{2+} removal, a lower SR Ca^{2+} load and a decrease in the Ca^{2+} transient amplitude (Greensmith et al., 2010). Similarly, Kuster and co-workers (Kuster et al., 2010) exposed rat cardiomyocytes to 100 μM H_2O_2 for 15 minutes and observed a reduction in SERCA2a activity, lower Ca^{2+} transient amplitude and attenuated contractile characteristics. These data suggest that ROS-induced contractile dysfunction is related in part to decreased SERCA2a activity, which leads to lower SR Ca^{2+} load and a decrease in the Ca^{2+} transient.

REDOX Modification of SERCA

The development of mass spectrometry techniques to detect post-translational modifications to proteins has revealed several amino acid residues on SERCA that are sensitive to oxidative modification by ROS. The regulation of SERCA2 by REDOX modification appears to be biphasic in nature. Activation of SERCA2 is mediated by glutathionylation of a specific cysteine residue at position 674 (Adachi et al., 2004; Lancel et al., 2009). A study by Adachi and

colleagues (2004) demonstrated that SERCA2b, the SERCA2 splice variant expressed in vascular smooth muscle, can be S-glutathiolated at Cys674 by $ONOO^-$ (10-50 μM), which increased Ca^{2+} uptake and enhanced relaxation. Importantly, higher concentrations of $ONOO^-$ (50-250 μM) have been shown to cause irreversible oxidation and inactivation of SERCA2b (Grover et al., 2003a; Grover et al., 2003b). A recent study showed an increase in S-glutathiolated SERCA2a and SERCA2a activity in isolated cardiomyocytes following exposure to HNO (Lancel et al., 2009). The importance of the cysteine 674 residue was supported by site directed mutagenesis experiments that substituted Cys674 with a serine residue, which prevented S-glutathionylation and activation of SERCA2a (Lancel et al., 2009).

There is ample evidence from *in vitro* experiments that demonstrate a ROS concentration-dependent reduction in SERCA activity (Table 1.1). Indeed, Knyushko and colleagues (2005) incubated SR vesicles isolated from rat myocardium with $ONOO^-$ and measured tyrosine nitration and cysteine oxidation. As the concentration of $ONOO^-$ was increased, there was a progressive decrease in SERCA2a activity in association with a progressive increases in tyrosine nitration and cysteine oxidation. Analysis of tryptic SERCA2a fragments using mass spectroscopy revealed two tandem tyrosine residues (Tyr294 & Tyr295) that were nitrated by $ONOO^-$. Nitration of these tyrosine residues on SERCA2 have been reported *in vitro* (Knyushko et al., 2005) and *in vivo* as a result of ageing (Viner et al., 1999; Knyushko et al., 2005; Xu et al., 2006) or atherosclerosis (Xu et al., 2006). These tandem tyrosine residues are located on the α-helix M4 of SERCA2, which is located at the SR membrane-lumen interface (Schoneich & Sharov, 2006). Slight alterations to the orientation of M4 induced by nitration may alter SERCA2-Ca^{2+} interaction or the phosphorylation site (Asp351) of SERCA2, which could reduce Ca^{2+} transport and/or ATPase activity (Schoneich & Sharov, 2006). Equally

as important as SERCA2a in the regulation of intracellular Ca^{2+} is the Ca^{2+} release channel, which is also sensitive to the prevailing REDOX state of the cell.

Table 1.1: Effects of ROS on SERCA function.

Isoform	Species	Tissue Prep	ROS	Concentration	Change in Activity (%)	Modification	Reference
SERCA1a; SERCA2a	Rabbit	SR Vesicles	Fenton Reaction	N/A	↓60%	Protein fragmentation	Castilho et al., 1996
SERCA1a	Rabbit	SR Vesicles	ONOO⁻	0.1-1.8 mM	↓17-75%	Cys oxidation	Viner et al., 1996
SERCA2b	HEK-293 cells	Microsomes	H_2O_2	30-1000 μM	↓25-75%	N/A	Grover et al., 1997
SERCA3	HEK-293 cells	Microsomes	H_2O_2	30-1000 μM	↓0-55%	N/A	Grover et al., 1997
SERCA1a	Rabbit	SR Vesicles	HOCl	0.1-3 mM	↓35-100%	Thiol oxidation	Favero et al., 1998
SERCA2a	Rat	SR Vesicles	ONOO⁻	50-200 μM	↓5-45%	Tyrosine nitration	Viner et al., 1999a
SERCA1a	Rabbit	SR Vesicles	ONOO⁻	0.1 mM	Not stated	Oxidation of Cys349	Viner et al., 1999b
SERCA1a	Rabbit	SR Vesicles	NO	0.1 mM	Not stated	Cysteine Oxidation	Viner et al., 2000
SERCA2b	Pig	SR Vesicles	ONOO⁻	25-250 μM	↓10-85%	Protein aggregation	Grover et al., 2003b
SERCA2a	Rat	SR Vesicles	FeSO₄/EDTA	N/A	↓40%	Cysteine oxidation, lipid peroxidation	Kaplan et al., 2003

The table above summarizes the structural and functional effects of incubation of SR samples with several different ROS. Abbreviations: human embryonic kidney cells (HEK), sarco(endo)plasmic reticulum Ca^{2+}-ATPase (SERCA), sarcoplasmic reticulum (SR), not assessed (N/A), hydrogen peroxide (H_2O_2), nitric oxide (NO), peroxynitrite (ONOO⁻), hypochlorus acid (HOCl).

The cardiac ryanodine receptor is the focal point of Ca^{2+} release from the sarcoplasmic reticulum. Indeed, a reduction in Ca^{2+} release would result in a lower Ca^{2+} transient amplitude, which would have a negative impact on force production. Conversely, enhanced Ca^{2+} release from the SR would result in a more forceful contraction. However, if the increased amount of Ca^{2+} released was not sequestered in the SR, but rather extruded from the cell via the NCX, then the SR Ca^{2+} load would decrease. In addition, the total Ca^{2+} load in the SR can be lowered by RyR mediated Ca^{2+} leak coupled to NCX extrusion of Ca^{2+} during diastole. Subsequently, the reduced SR Ca^{2+} load would limit the fraction of Ca^{2+} that could be released during subsequent beats and would thus reduce force. It is evident that there is a fine balance between SR Ca^{2+} release, uptake and leak by the SR.

Ryanodine receptors are sensitive to the REDOX state of the cell. In general, oxidizing agents have a stimulatory effect on RyR2 Ca^{2+} release, whereas reducing agents will inhibit RyR2 Ca^{2+} release (Donoso et al., 2011). Several studies have demonstrated that incubation of reconstituted RyR2 in planar lipid bilayers with ROS (i.e. ·OH, NO or HNO) increased the open probability of the channel, which was likely due to oxidation of sulfhydryl groups since incubation with the reducing agent, dithiothreitol (DTT), restored channel competency (Stoyanovsky et al., 1997; Anzai et al., 1998; Cheong et al., 2005). An increase in the open probability of RyR is associated with increased Ca^{2+} release (Stoyanovsky et al., 1997; Kawakami & Okabe, 1998). Conversely, a study by Zahradnikova and colleagues (1997) found that NO decreased the open probability of RyR in a planar lipid bilayer and decreased Ca^{2+} release. Taken together, there is potentially a biphasic effect of ROS on RyR function.

Table 1.2: Effects of ROS on RyR function.

Species	Tissue Prep	ROS	Concentration	Functional Outcome	Reference
Pig	Planar Bilayer	·OH	N/A	$\uparrow P_o$	Anzai et al., 1998
Rabbit	Planar Bilayer	HNO	N/A	$\uparrow P_o$; $\uparrow$release	Cheong et al., 2005
Rat	Cardiomyocyte	H_2O_2	0.1 or 1.0 mM	$\uparrow$release	Suzuki et al., 1998
Dog	Planar Bilayer	NO donor	N/A	$\uparrow P_o$; $\uparrow$release	Stoyanovsky et al., 1996
Rat	Cardiomyocyte	DTDP	3-100 μM	$\downarrow\uparrow$ spark frequency	Xie & Zhu, 2006
Dog	Planar Bilayer	NO donor	N/A	$\uparrow P_o$	Xu et al., 1998
Rat	Cardiomyocyte	H_2O_2	50 or 200 μM	$\downarrow\uparrow$ spark frequency	Yan et al., 2008
Dog	Planar Bilayer	NO	N/A	$\downarrow P_o$; $\downarrow$release	Zahradnikova et al., 1997

The table above summarizes the functional effects of incubation of cardiomyocytes or SR samples reconstituted in a planar bilayer with different ROS or NO donors. Abbreviations: not assessed (N/A), hydroxyl radical (·OH), nitroxyl (HNO), nitric oxide (NO), hydrogen peroxide (H_2O_2), 4-4'-dithiopyridine (DTDP), open probability (P_o).

The effects of increased oxidant stress on RyR function have been assessed in more intact experimental preparations and show similar findings to the aforementioned planar bilayer studies. Kawakami & Okabe (1998) isolated heavy SR vesicles from canine LV and incubated them with hypoxanthine and xanthine oxidase, a superoxide generating system, and found that Ca^{2+} release was increased. The addition of 0.1 or 1.0 mM H_2O_2 to the media of isolated cardiomyocytes augmented Ca^{2+}-induced Ca^{2+} release (Suzuki et al., 1998). These studies indicate that incubation with oxidants may activate the Ca^{2+} release channel. However, it appears that RyR may respond transiently to ROS in a concentration- and time-dependent manner, where low concentrations of ROS or a brief incubation period results in channel activation and prolonged exposure or higher ROS concentrations results in inactivation of the channel (Xie & Zhu, 2006; Yan et al., 2008).

A shift in the cellular environment to a more oxidative state may result in enhanced leak of Ca^{2+} through RyRs. Several cardiac injury or pathological models have demonstrated that oxidative stress associated with these models resulted in an increased rate of Ca^{2+} leak from the SR. In rat and canine models of heart failure the rate of SR Ca^{2+} leak was elevated in the failing cardiomyocyte, which resulted in a decrease in the SR luminal Ca^{2+} concentration (Terentyev et al., 2008; Gonzalez et al., 2010). It was hypothesized that a reduction in the concentration of Ca^{2+} in the SR would result in a lower Ca^{2+} transient amplitude and thus force, which likely contributed to the decline in cardiac performance observed in heart failure (Terentyev et al., 2008). A hallmark of heart failure is augmented adrenergic output, which attempts to enhance contractile function in the short term, but chronically contributes to the progression of the disease (Rundqvist et al., 1997). A study by Bovo and co-workers (2012) incubated isolated rabbit cardiomyocytes with ISO and observed that following an initial increase in SR Ca^{2+}

concentration, that there was a progressive decline in SR Ca^{2+} load that was due to Ca^{2+} leakage from the SR. Lastly, the rate of Ca^{2+} leak from the SR was exacerbated in cardiomyocytes from aged rabbits when compared to young rabbit cardiomyocytes (Cooper et al., 2013). A common feature of these Ca^{2+} leak studies was that ROS production was elevated in the chronic disease animals when compared to control animals (Terentyev et al., 2008; Gonzalez et al., 2010; Bovo et al., 2012; Cooper et al., 2013). In addition, if the oxidative cellular environment was restored to control levels then Ca^{2+} leak rates were also reversed, which suggests that the modification to RyR is reversible.

Previous studies have demonstrated that altered RyR function can be normalized or partially normalized following incubation with a reducing agent. This suggests that modification to sulfhydryl groups on RyR contribute to ROS-induced changes in function. Indeed, *in vitro* (Anzai et al., 1998; Cheong et al., 2005) and isolated cardiomyocyte experiments (Suzuki et al., 1998; Terentyev et al., 2008) have demonstrated that the stimulatory or inhibitory effects of exogenous ROS are prevented in the presence of reducing agents. Work by Sanchez and co-workers (2005), used tachycardia as a preconditioning stimulus to evaluate changes in REDOX state as well as RyR function. In SR fractions from the preconditioned group there was an elevated rate of Ca^{2+} release, which coincided with a 1.7-fold increase in RyR S-glutathionylation (Sanchez et al., 2005). In a follow up study, dogs ran on a treadmill at 6 km/h for a total of 25 min using a 5 min on, 5 min off pattern and SR vesicles were isolated from myocardium for *in vitro* analysis of RyR function and post-translational modification (Sanchez et al., 2008). Similar to previous findings by this group, exercise augmented S-glutathionylation of RyR and SR Ca^{2+} release. When dogs were administered the NOX inhibitor, APO, prior to exercise, there were no significant differences between the control and exercise groups in terms

of NOX activity, RyR S-glutathionylation content and Ca^{2+} release kinetics. These findings suggest that mild exercise activates NOX in canine myocardium, which, in the presence of glutathione, can augment S-glutathionylation of RyR and increase RyR activity. The effect of exhaustive exercise on RyR activity and NOX derived ROS in the rat myocardium has not been addressed to date. Furthermore, the effect of exhaustive exercise on RyR structure and function is not known

NADPH Oxidase Derived ROS, and Post-Translational Modification of RyR

NADPH Oxidases (NOXs) are a family of multi-subunit enzyme complexes that catalyze the transfer of an electron from NADPH to O_2 and generate superoxide anion ($O_2^{..}$). In adult ventricular cardiomyocytes the primary isoforms expressed are NOX2 and NOX4 (Byrne et al., 2003; Krijnen et al., 2003). The complete complex is comprised of the membrane bound NOX, which is stabilized by the $p22^{phox}$ subunit. Activation of the NOX enzyme occurs following translocation and docking of the cytosolic regulatory proteins $p40^{phox}$, $p47^{phox}$, $p67^{phox}$ and rac (Bedard & Krause, 2007). APO is a NOX inhibitor that acts by preventing the docking of the cytosolic regulatory proteins to the NOX complex (Stefanska & Pawliczak, 2008). APO has been widely used in *in vivo* and *in vitro* experiments that involved skeletal and cardiac muscle (Sanchez et al., 2005; Sanchez et al., 2008; Sun et al., 2011; Vitiello et al., 2011). Recent evidence suggests that the RyR in skeletal muscle (RyR1) is regulated by NOX4, whereby NOX4 derived ROS oxidized cysteine residues on RyR1, which led to enhanced Ca^{2+} release and augmented force production (Sun et al., 2011). In canine myocardium, NOX-dependent ROS caused S-glutathionylation and activation of RyR2 following pacing-induced tachycardia and exercise (Sanchez et al., 2005; Sanchez et al., 2008). In a recent transgenic study, it was demonstrated that cardiac specific overexpression of rac1 (a NOX regulatory protein) was

associated with an increased rate of SR Ca^{2+} leak, reduced Ca^{2+} transient amplitude and lower cell shortening in mouse cardiomyocytes (Oberhofer et al., 2013). These studies suggest that modest activation of NOX can augment RyR activity and that chronic activation of NOX can have deleterious effects on RyR and cardiomyocyte function.

Exercise-Induced Cardiac Fatigue and NOX Inhibition

There is evidence that suggests oxidative stress may play a role in exercise-induced cardiac fatigue (Wonders et al., 2007; Vitiello et al., 2011; Olah et al., 2015). However, only one study has employed an intervention aimed to prevent oxidative stress and preserve cardiac function following prolonged exercise. Vitiello and colleagues (2011) ran rats for four hours and observed a significant reduction in cardiac function when assessed *in vivo* and *ex vivo*. A key finding in this study was that there was no LV fatigue in the hearts of rats that consumed drinking water supplemented with APO for three days prior to the exercise bout. The authors concluded that NOX inhibition prevented oxidative stress and preserved cardiac function. Unfortunately, the intracellular targets of NOX derived superoxide were not examined in the study by Vitiello and co-workers (2011). It is possible that exercise-induced NOX mediated oxidative modification of proteins are associated with cardiac fatigue. However, no study has concurrently examined the relationship between exercise-induced cardiac fatigue and changes in protein structure and function. In addition, no study has attempted to determine the mechanisms by which NOX inhibition can prevent cardiac fatigue.

Thesis Objective

The objectives of this thesis were: 1) to determine if exhaustive exercise could induce cardiac fatigue in the rat heart; 2) to determine if exhaustive exercise reduced β-adrenergic responsiveness of the LV; 3) to determine if reactive oxygen species produced during exhaustive exercise reduced the activities of the Na^+/K^+-ATPase, the Ca^{2+}-ATPase and the Ca^{2+} release channel; and 4) to determine if NADPH oxidase inhibition could prevent exercise-induced cardiac fatigue and restore SR Ca^{2+} leak and calpain activity.

Study 1:

The purpose of Study 1 was to determine if:

1)   Cardiac fatigue can be induced using an exhaustive treadmill exercise protocol;

2)   Cardiac function would remain depressed following a 24 hour recovery period;

3)   Exhaustive exercise reduced left ventricular β-adrenergic responsiveness.

Study 1 Hypotheses:

1)   Exhaustive exercise will result in a significant reduction in LVDP immediately following the exercise bout and 24 hour post-exercise;

2)   The left ventricular β-adrenergic response to ISO will be lower following exercise.

Study 2:

The purpose of Study 2 was to determine if:

1)   Exhaustive exercise resulted in an increase in ROS production;

2)   Exhaustive exercise impaired the Na^+/K^+-ATPase activity;

3)   Exhaustive exercise attenuated Ca^{2+}-ATPase activity and RyR gating;

4)   Impaired protein function (above) was due to post-translational oxidative modification;

5)   Reduced Na^+ and Ca^{2+} regulation would activate calpains.

37

Study 2 Hypotheses:

1) ROS production will be increased immediately following acute, exhaustive exercise;

2) The maximal rate of Na^+/K^+-ATPase activity will be reduced immediately post-exercise;

3) There will be a decrease in Ca^{2+}-ATPase activity and an increase in Ca^{2+} leak through RyR following exhaustive exercise;

4) There will be an increase in markers of oxidative damage on the Na^+/K^+-ATPase, Ca^{2+}-ATPase and RyR;

5) Impaired Na^+ and Ca^+ regulation will result in activation of calpains.

Study 3:

The purpose of Study 3 was to determine if:

1) Inhibition of NADPH oxidase will prevent exercise-induced cardiac fatigue;

2) Inhibition of NOX would reduce the production of ROS immediately following exhaustive exercise;

3) SR Ca^{2+} leak will be reduced following exhaustive exercise when NOX is inhibited;

4) Calpain activation is prevented when NOX is inhibited;

5) *In vitro* activation of NOX will increase ROS production and SR Ca^{2+} leak.

Study 3 Hypotheses:

1) Consumption of apocynin and inhibition of NOX will prevent exercise-induced cardiac fatigue;

2) ROS production will be blunted following exhaustive exercise when NOX is inhibited;

3) SR Ca^{2+} leak will not be affected by exhaustive exercise when NOX is inhibited;

4) Calpain activation will not occur following exhaustive exercise in the presence of NOX inhibition;

5)   Activation of NOX *in vitro* will increase ROS production and SR Ca^{2+} leak, which will be

prevented in the presence of apocynin.

Chapter II: Cardiac fatigue is present in the basal state and during β-adrenergic stimulation in rats following exhaustive exercise

Synopsis

In humans, prolonged or exhaustive exercise has been shown to result in cardiac fatigue and is associated with a reduction in the myocardium's ability to respond to β-adrenergic stimulation. The purpose of this study was to develop an exhaustive treadmill running protocol to induce cardiac fatigue in the rat myocardium and to determine if exhaustive exercise reduced the myocardial response to β-adrenergic stimulation. Male Sprague-Dawley rats (21-23 weeks) were randomly assigned to a CTL group or one of two exercise groups that ran at 20 m/min and 5% grade until exhaustion and were either sacrificed immediately (AC) or were allowed to recover for 24 hours (24H). The hearts were excised and perfused in a retrograde fashion at a constant perfusion pressure (~80 mmHg). In the basal state and during adrenergic stimulation, there was a significant reduction ($p < 0.05$) in the LVDP of hearts from the AC and 24H groups when compared to CTL hearts. Compared to the CTL, there was a trend ($p = 0.076$) for a reduction in the –dP/dt in the AC and 24H groups in the basal state. Similarly, the –dP/dt was reduced ($p < 0.05$) in the AC group during β-adrenergic stimulation. There were no significant differences ($p > 0.05$) in the +dP/dt in the basal state or during β-adrenergic stimulation. The depression in LVDP and contractile kinetics were not due to changes in heart rate, coronary vascular resistance or coronary flow ($p > 0.05$). This study demonstrated that exhaustive exercise reduced the LVDP of the rat myocardium immediately post-exercise and that this depression in LV function persisted for up to 24 hours. The β-adrenergic stimulation findings suggest that, potentially, the ability of the heart to respond to a subsequent bout of exercise would be impaired, which is indicative of cardiac fatigue.

Introduction

There is a growing body of evidence that suggests that some individuals who partake in prolonged endurance competitions experience a decline in cardiac function following the event (Douglas et al., 1987; Douglas et al., 1998; Whyte et al., 2000; Shave et al., 2004; George et al., 2009). Indeed, following a 24 hour endurance race, the ratio of systolic blood pressure to end systolic dimension was significantly reduced, which is suggestive of a reduced contractile state (Niemela et al., 1984). A study by Douglas and colleagues (1987) observed that for a given afterload, the LV fractional shortening was impaired following an Ironman® triathlon. In both of these studies the indices of LV systolic function partially or fully recovered within 1-3 days post-exercise. Given the transient nature of the depressed cardiac function, these studies described their findings as "cardiac fatigue" (Niemela et al., 1984; Douglas et al., 1987). Numerous studies have documented a reduction in diastolic function and preserved systolic function following a relatively shorter distanced marathon (George et al., 2005; George et al., 2004; Hart et al., 2007; Neilan et al., 2006). Thus, there appears to be an interaction between event duration and/or intensity and the degree of diastolic and systolic fatigue.

Evidence of exercise-induced cardiac fatigue has been observed in several models of prolonged aerobic exercise using rats. In one treadmill study where rats exercised on five sequential days and culminated in a final bout to exhaustion, the tetanic force produced in trabecular muscles excised from the LV of animals that ran to exhaustion was reduced by ~50% when compared to control trabeculae (Maher et al., 1972). More recent studies have demonstrated that prolonged swimming (from 3-8 hours) reduced EF and LVDP by 26% and 30-40%, respectively (Venditti et al., 2001; Olah et al., 2015). Vitiello and co-workers (2011) assessed *in vivo* and *ex vivo* LVDP in rats following four hours of submaximal treadmill running

and noted a ~10 and 20% reduction in LVDP, respectively. Even as little as one hour of treadmill running at 25 m/min has been shown to significantly reduce LVDP for up to 48 hours post-exercise (Wonders et al., 2007). Conversely, Seward and colleagues (1995) failed to observe cardiac fatigue in rats following exhaustive treadmill running. In addition, cardiac performance in instrumented dogs was not different at the point of exhaustion when compared to five minutes into the exercise bout (Grimditch et al., 1981). Thus, prolonged or exhaustive exercise in rodents has been shown to induce cardiac fatigue, yet little research has been done using this model to investigate the mechanisms associated with cardiac fatigue.

Research using humans and animals has examined the effects of prolonged and/or exhaustive exercise on the chronotropic and inotropic response of the myocardium to β-adrenergic stimulation. In humans, the chronotropic response to β-adrenergic stimulation is reduced following prolonged exercise (Banks et al., 2010), which seems to be more pronounced in males compared to females (Scott et al., 2007) and is associated with impaired systolic function as opposed to diastolic function (Hart et al., 2006; Welsh et al., 2005). In canines, there is a reduction in the chronotropic response to ISO infusion following one hour of running at 60-80% of maximal heart rate (Friedman et al., 1987). However, changes in the inotropic response to ISO infusion were not examined in that study. The inotropic effect of exogenous NE was blunted in isolated trabeculae from rats that ran to exhaustion when compared to trabeculae from sedentary control hearts (Maher et al., 1972). Conversely, Vitiello and colleagues (2011) found no change in the inotropic response to ISO in the isolated perfused rat heart following four hours of submaximal running. A reduction in the chronotropic response to β-adrenergic stimulation could compromise the contractility of the heart based on the force frequency relationship. If reduced chronotropy was coupled with an attenuation of the inotropic effects of β-adrenergic

stimulation then *in vivo* LV ejection would likely be depressed. Thus, exercise-induced desensitization to β-adrenergic stimulation represents a form of cardiac fatigue such that the heart may not be able to cope with the demands placed upon it by a subsequent bout of exercise.

In this study, the effect of exhaustive aerobic exercise on LV function was investigated *ex vivo* using the isolated perfused rat heart. It was hypothesized that exhaustive exercise would result in left ventricular fatigue and that this fatigue would be present in the basal state and persist during β-adrenergic stimulation. It was imperative to establish an exercise protocol that induced cardiac fatigue so that subsequent studies in this thesis could utilize this exercise protocol to determine the mechanisms associated with cardiac fatigue.

Methods

Animals

Adult male Sprague-Dawley rats (21-23 weeks) were used in this study. The anthropometric data from these animals is presented in Table 2.1. All animals were obtained from the breeding colony at the University of Waterloo. Animals were group housed (4 per cage) on a reverse 12 hour light cycle and had free access to food and water. All procedures were reviewed and approved by the University of Waterloo Animal Care Committee.

Table 2.1: Anthropometric data from animals used in isolated perfused heart experiments

Masses	CTL (n=12)	AC (n=8)	24H (n=8)	p value
Body Mass (g)	459 ± 6	436 ± 9	447 ± 10	0.16
Heart Mass (g)	1.81 ± 0.04	1.77 ± 0.06	1.83 ± 0.05	0.77
Left Ventricle Mass (g)	1.17 ± 0.02	1.13 ± 0.03	1.17 ± 0.03	0.50
Left Ventricle/Body Mass	0.00255 ± 0.00006	0.00258 ± 0.00007	0.00261 ± 0.00005	0.75

The body mass, heart mass, left ventricle mass and the ratio of left ventricle to body mass data are listed for the control group (CTL), the group sacrificed immediately after exercise (AC) and the group sacrificed 24 hours-post exercise (24H). Data are presented as means $\pm$ SE.

Experimental Design

There were three groups in this study; a control group (CTL), an acute exercise group (AC) whereby animals were sacrificed immediately following exhaustive exercise (see protocol below) and a group of animals that were sacrificed 24 hours after exhaustive exercise (24H). Animals in all three groups were acclimated to treadmill running for seven days leading up to the exhaustive exercise bout. For a detailed description of the acclimation protocol refer to Appendix A.

The exhaustive exercise bout consisted of a 10 minute warm-up on a motorized rat treadmill (Columbus Instruments) set at 5° grade and 10 m/min. Subsequently, the speed was

ramped to 20 m/min and the rats ran until exhaustion, which was deemed to occur when the rats could no longer maintain the pace of the treadmill and were in prolonged contact with the electrical grid. Upon exhaustion animals were either immediately anaesthetized (35 mg/kg sodium pentobarbital; intravenous) for isolated perfused heart experiments or they were returned to their cages and allowed to recover for 24 hours. During the exhaustive exercise bouts, animals in the CTL group remained in their cages and were anaesthetized just prior to excision of their hearts.

Isolated Perfused Heart

The chest cavity of anaesthetized animals was exposed, thus permitting the removal of the pericardium and thymus and rapid excision of the heart. Cardioplegia was achieved by placing the heart in ice cold Krebs-Henseleit buffer which contained (in mM): 118 NaCl, 4.7 KCl, 1.2 $MgSO_4 \cdot 7H_2O$, 24 $NaHCO_3$, 1.1 KH_2PO_4, 1.25 $CaCl_2 \cdot 2H_2O$ and 10 glucose, pH 7.4. Hearts were mounted on an aortic cannula, secured via 4.0 silk sutures and perfused at a constant pressure (~80 mmHg) with Krebs-Henseleit buffer warmed to 37°C and bubbled with 95%O_2-5%CO_2. The pressure head was achieved by raising the bubble trap ~1 m (based on 1 cm $H_2O \approx$ 0.735 mmHg) above the tip of the aortic cannula (Figure 2.1). To measure perfusion pressure, a pressure transducer (MLT844, AD Instruments) was connected to the system proximal to the aortic cannula. A similar pressure transducer was connected to a balloon tipped catheter and was used to measure indices of LV function. The balloon was fed through the left atrium into the left ventricle and the volume of the balloon was adjusted to provide a diastolic pressure of ~10 mmHg. An ultrasonic flow probe (2PXL, Transonic Systems) was placed proximal to the aortic cannula, which measured global coronary flow. Following instrumentation, hearts were allowed to equilibrate for 30 minutes at which point baseline data were recorded. Subsequently, an ISO

dose response was performed using a range of ISO concentrations from 10^{-11} to 10^{-7} M. Each dose was infused for 2 minutes at a rate equivalent to 1% of the coronary flow using a syringe pump (Model 74900, Cole Parmer). Following each dose of ISO the LVDP was allowed to return to baseline before the subsequent dose. All data were collected using a Powerlab data acquisition system (4/sp, AD Instruments) and were analyzed using Chart software (Ver. 5, AD Instruments). After the perfusion experiments were completed, the aorta and any remaining fat and connective tissue were removed and the heart was weighed. Subsequently, the atria and right ventricle were removed and the left ventricle (plus septum) were weighed.

Statistics

All data are presented as means ± standard error. A one-way ANOVA was used to analyze basal measures from isolated perfused hearts. A two-way ANOVA (group x ISO concentration) was used to analyze the ISO dose response data. To investigate relationships between variables, linear regression analysis was performed using GraphPad Prism 4 software. The significance level was set at 0.05, and, when appropriate, a Newman-Keuls post-hoc test was used to compare specific means. A trend in the data was considered when the probability was between 0.05 and 0.1.
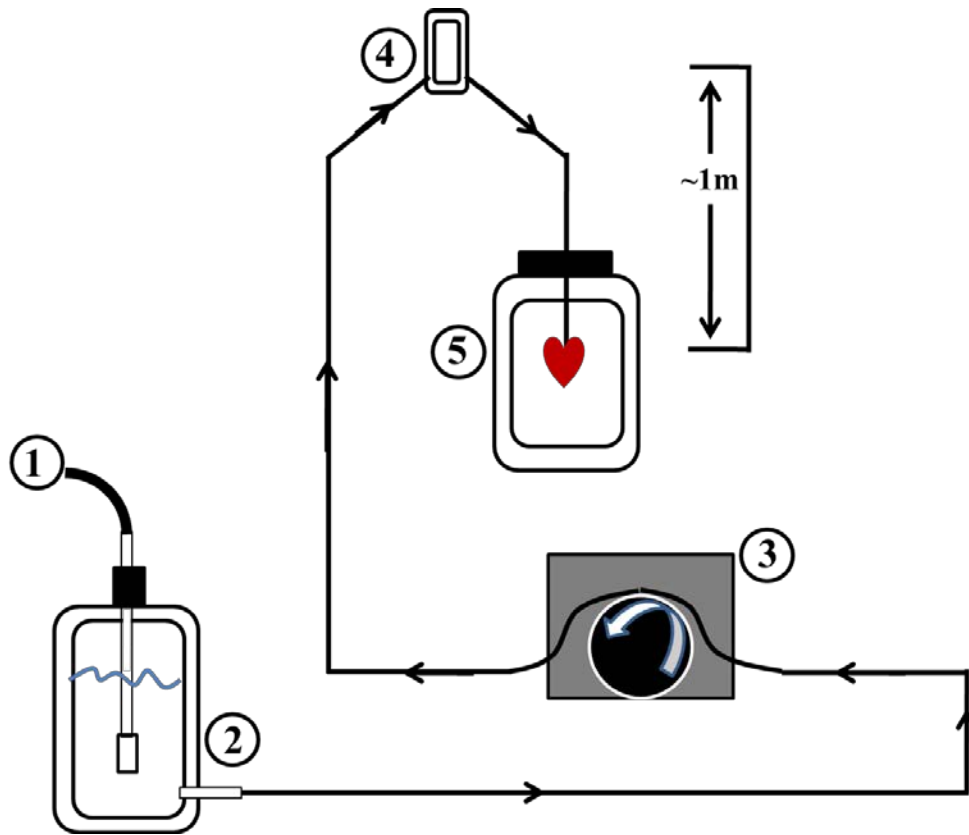
Figure 2.1. A schematic of the constant perfusion pressure setup used to assess cardiac function. (1) Kreb's Henseleit buffer was aerated with 95/5% O_2/CO_2 and (2) warmed to 37°C in a water-jacketed reservoir. (3) The perfusate was pumped at a high rate to the bubble trap (4), which was raised approximately 1 m above the heart such that perfusion pressure was ~80 mmHg. Excess perfusate from the bubble trap was returned to the reservoir for re-oxygenation. (5) The hearts were mounted to a glass cannula and the left ventricle was instrumented with a pressure transducer.

Results

Anthropometric Data and Run Times

The anthropometric data of the three groups in this study are presented in Table 2.1. As expected, there were no significant differences (p>0.05) between the three groups with respect to body mass, heart mass, left ventricle mass and the ratio of left ventricle mass to body mass. The animals in the AC group and 24H group ran for durations of 69 ± 3 minutes and 72 ± 5 minutes, respectively, which did not differ significantly (p>0.05) from each other.

Basal Cardiac Function and Hemodynamics

To examine the effect of acute, exhaustive exercise on cardiac and hemodynamic function in the basal state, the isolated perfused heart technique was utilized. Table 2.2 summarizes the basal cardiac and hemodynamic data. Exhaustive exercise resulted in a 12% reduction (p<0.05) in LVDP in the AC group when compared to the CTL group. This cardiac impairment persisted for up to 24 hours post-exercise as LVDP was 14% lower (p<0.05) in the 24H group than the CTL group. There were no significant differences (p>0.05) observed in +dP/dt or the time to peak pressure between the three groups. However, there was a trend (p=0.076) for a reduction in the –dP/dt in the AC and 24H groups when compared to the CTL group. It is important to note that the impairments in LVDP observed in the AC and 24H groups occurred in the absence of any changes in heart rate.

Table 2.2: Basal cardiac and hemodynamic measures from isolated perfused heart experiments

Cardiovascular Measure	CTL (n=12)	AC (n=8)	24H (n=8)	p value
LVDP (mmHg)	133 ± 4	117 ± 7*	114 ± 5*	0.02
+dP/dt (mmHg/s)	4547 ± 326	3747 ± 354	3995 ± 179	0.32
-dP/dt (mmHg/s)	-2695 ± 102	-2361 ± 139	-2374 ± 103	0.08
Heart Rate (bpm)	270 ± 8	262 ± 12	281 ± 7	0.53
LVeDP (mmHg)	10.08 ± 1.74	9.83 ± 1.69	10.59 ± 2.18	0.98
Time-to-peak Pressure (ms)	66.8 ± 1.7	66.1 ± 1.4	63.1 ± 1.6	0.24
Perfusion Pressure (mmHg)	80.71 ± 0.38	81.45 ± 0.48	80.80 ± 0.52	0.49
Coronary Flow (mL/min)	21.85 ± 2.25	20.82 ± 1.35	18.04 ± 1.29	0.36
Coronary Vascular Resistance (mmHg/mL/min)	4.06 ± 0.33	4.04 ± 0.30	4.67 ± 0.39	0.43

Cardiac and hemodynamic summary data recorded in the basal state. Abbreviations: Left ventricular developed pressure (LVDP); left ventricular end diastolic pressure (LVeDP); maximal rate of pressure development and pressure decline (±dP/dt). The number of animals in each group is indicated beside the group label. Data are presented as means ± SE. There was a trend (p=0.076) for a reduction in -dP/dt in the AC and 24H groups.
* Significantly different (p<0.05) CTL

This study utilized a constant perfusion pressure setup during isolated perfused heart experiments, such that the flow could increase when ATP demand of the heart increased during ISO infusion. The perfusion pressure was equal to ~80 mmHg among all three groups (Table 2.2). Acute exercise did not alter resting levels of global coronary flow nor did exercise alter coronary vascular resistance (CVR) when compared to the CTL group (p>0.05) (Table 2.2). These data suggest that acute exercise did not alter vascular function in the isolated perfused heart model.
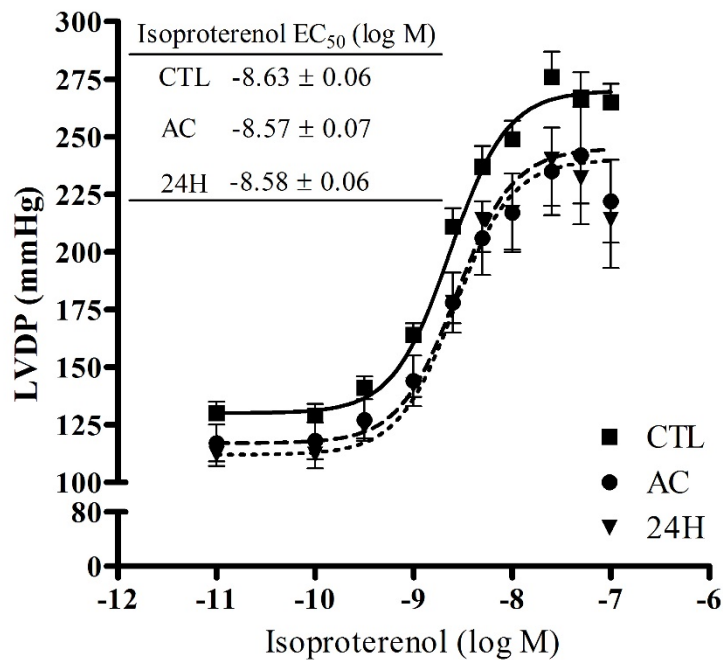
Figure 2.2. Isoproterenol dose response curves from the control group (CTL, solid squares), acute exercise group (AC, solid circles) and 24 hour post-exercise group (24H, solid triangles). The inset indicates the concentration required to increase LVDP by 50% (EC_{50}). Values are means ± SE (CTL n=12; AC & 24H n=8). Main effect of exercise ($p<0.05$), with CTL > AC & 24H. Main effect of isoproterenol dose ($p<0.05$).

Cardiac and Hemodynamic Responses to Isoproterenol

There are conflicting reports regarding the effects of prolonged aerobic exercise and desensitization of cardiac β-adrenergic receptors. To examine the exercise-induced changes in the chronotropic and inotropic response to β-adrenergic stimulation, an ISO dose response was performed. As can be seen in Figure 2.2, the reduced LVDP in the AC and 24H groups observed in the basal state (i.e. absence of ISO) persisted throughout the entire ISO dose response. Accordingly, there was a main effect of exercise such that the AC and 24H groups response to ISO were lower ($p<0.05$) than the CTL group. There were no significant differences ($p>0.05$) in the concentration required to increase LVDP by 50% (EC_{50}) in either exercise group when compared to the CTL group (Figure 2.2 inset). Table 2.3 summarizes the cardiac and

51

hemodynamic effects of the ISO dose response. There were main effects of ISO for each variable examined. The heart rate increased progressively throughout the ISO dose response but did not differ among the CTL, AC and 24H groups ($p > 0.05$). Importantly, the coronary flow was not different between the three groups in the basal state and increased ($p < 0.05$) to the same extent in each group during the ISO dose response (peaked at $10^{-8.3}$ M). Accordingly, the increase in coronary flow resulted from a decrease ($p < 0.05$) in the resistance across the coronary vasculature, which also plateaued at an ISO concentration of $10^{-8.3}$ M. The +dP/dt increased ($p < 0.05$) to similar extents in all three groups during ISO infusion. Progressively increasing the concentration of ISO in the perfusate resulted in faster ($p < 0.05$) –dP/dt in all groups. However, there was a significant main effect of exercise on the –dP/dt, whereby the AC group relaxed at a slower rate ($p < 0.05$) when compared to the CTL and 24H groups during ISO infusion (Table 2.3).

Table 2.3: Cardiac and hemodynamic responses to isoproterenol

| | Negative log M Isoproterenol Dosage | | | | | | | | | | p value |
	-11	-10	-9.5	-9	-8.6	-8.3	-8	-7.6	-7.3	-7	
LVDP (mmHg)											
CTL	130 ± 5	129 ± 5	141 ± 5	164 ± 5	211 ± 8	237 ± 9	249 ± 8	276 ± 11	267 ± 11	265 ± 8	0.047
AC	117 ± 8	118 ± 8	127 ± 9	144 ± 11	178 ± 13	206 ± 16	217 ± 17	235 ± 19	242 ± 21	222 ± 18	
24H	112 ± 5	112 ± 6	124 ± 5	142 ± 5	178 ± 9	214 ± 14	217 ± 16	240 ± 20	232 ± 20	214 ± 21	
+dP/dt (mmHg/s)											
CTL	4429 ± 343	4467 ± 352	5038 ± 415	5759 ± 450	7327 ± 607	8610 ± 682	9151 ± 660	11546 ± 742	11666 ± 886	11551 ± 731	0.14
AC	3827 ± 383	3873 ± 397	4355 ± 496	4861 ± 577	5830 ± 712	6928 ± 966	7507 ± 1055	8387 ± 1073	9393 ± 1413	8844 ± 1339	
24H	3965 ± 197	4021 ± 232	4519 ± 284	5037 ± 318	6130 ± 513	7585 ± 731	7844 ± 802	9535 ± 1173	9946 ± 1098	9144 ± 1305	
-dP/dt (mmHg/s)											
CTL	-2604 ± 114	-2604 ± 122	-2898 ± 139	-3487 ± 145	-4639 ± 262	-5329 ± 294	-5544 ± 359	-6455 ± 344	-6211 ± 289	-6074 ± 214	0.048
AC	-2396 ± 164	-2395 ± 165	-2593 ± 186	-2970 ± 228	-3654 ± 300	-4259 ± 375	-4605 ± 432	-4734 ± 373	-4974 ± 480	-4740 ± 487	
24H	-2313 ± 117	-2332 ± 132	-2659 ± 135	-3162 ± 154	-4267 ± 260	-5183 ± 406	-5288 ± 481	-5718 ± 545	-5389 ± 470	-5218 ± 503	
HR (bpm)											
CTL	268 ± 8	271 ± 8	283 ± 7	289 ± 7	299 ± 7	316 ± 7	321 ± 8	337 ± 7	349 ± 8	355 ± 6	0.35
AC	262 ± 11	262 ± 11	275 ± 12	287 ± 12	299 ± 12	308 ± 11	320 ± 9	327 ± 10	338 ± 12	353 ± 8	
24H	277 ± 7	278 ± 7	285 ± 7	293 ± 7	315 ± 7	321 ± 7	332 ± 10	348 ± 11	364 ± 15	380 ± 14	
Coronary Flow (mL/min)											
CTL	21.8 ± 2.5	21.8 ± 2.6	23.0 ± 2.5	24.5 ± 2.5	27.7 ± 2.5	29.8 ± 2.3	29.7 ± 2.3	29.7 ± 2.3	28.2 ± 2.0	29.6 ± 2.7	0.73
AC	19.8 ± 1.2	19.5 ± 1.3	20.3 ± 1.3	21.4 ± 1.4	24.6 ± 1.2	24.7 ± 1.2	25.8 ± 1.3	25.6 ± 1.3	26.1 ± 1.5	27.1 ± 1.6	
24H	18.0 ± 1.4	18.1 ± 1.4	19.2 ± 1.5	20.6 ± 1.7	24.8 ± 2.7	25.2 ± 2.7	25.8 ± 2.5	26.0 ± 2.4	26.0 ± 2.5	26.6 ± 2.4	
Coronary Vascular Resistance (mmHg/mL/min)											
CTL	4.11 ± 0.34	4.16 ± 0.36	3.85 ± 0.31	3.56 ± 0.28	3.10 ± 0.27	2.79 ± 0.21	2.81 ± 0.23	2.80 ± 0.22	2.92 ± 0.23	2.85 ± 0.23	0.71
AC	4.25 ± 0.27	4.33 ± 0.29	4.15 ± 0.28	3.91 ± 0.25	3.31 ± 0.17	3.31 ± 0.18	3.17 ± 0.19	3.19 ± 0.18	3.14 ± 0.21	3.03 ± 0.22	
24H	4.71 ± 0.41	4.69 ± 0.44	4.42 ± 0.42	4.13 ± 0.44	3.53 ± 0.49	3.45 ± 0.46	3.30 ± 0.39	3.21 ± 0.33	3.25 ± 0.37	3.13 ± 0.33	

Summary of cardiac and hemodynamic response to progressive dosages of isoproterenol. Each negative log molar concentration of isoproterenol is indicated in the first row. The cardiac and hemodynamic variables are indicated in the first column. Abbreviations: left ventricular developed pressure (LVDP); rate of pressure development (+dP/dt); rate of pressure decline (-dP/dt); heart rate (HR). The p value corresponds with the main effect of exercise
There was a main effect of exercise for LVDP: CTL > AC, 24H.
There was a main effect of exercise for -dP/dt: AC < CTL, 24H.
There was a main effect of isoproterenol for all variables.
Data are presented as mean ± SE (AC & 24H n=8; CTL n=12).

Relationships between Cardiac Variables

To explore relationships between cardiac, exercise and anthropometric variables in this study, linear regression analysis was used. There was no significant relationship between run time to exhaustion and body mass (Figure 2.3C). In addition, linear regression analysis of LVDP and heart rate revealed that there was not a significant relationship between these two variables (Figure 2.3A). Interestingly, there was a significant, positive relationship between LVDP and run time to exhaustion, such that hearts from animals that ran longer had a higher LVDP (Figure 2.3B).
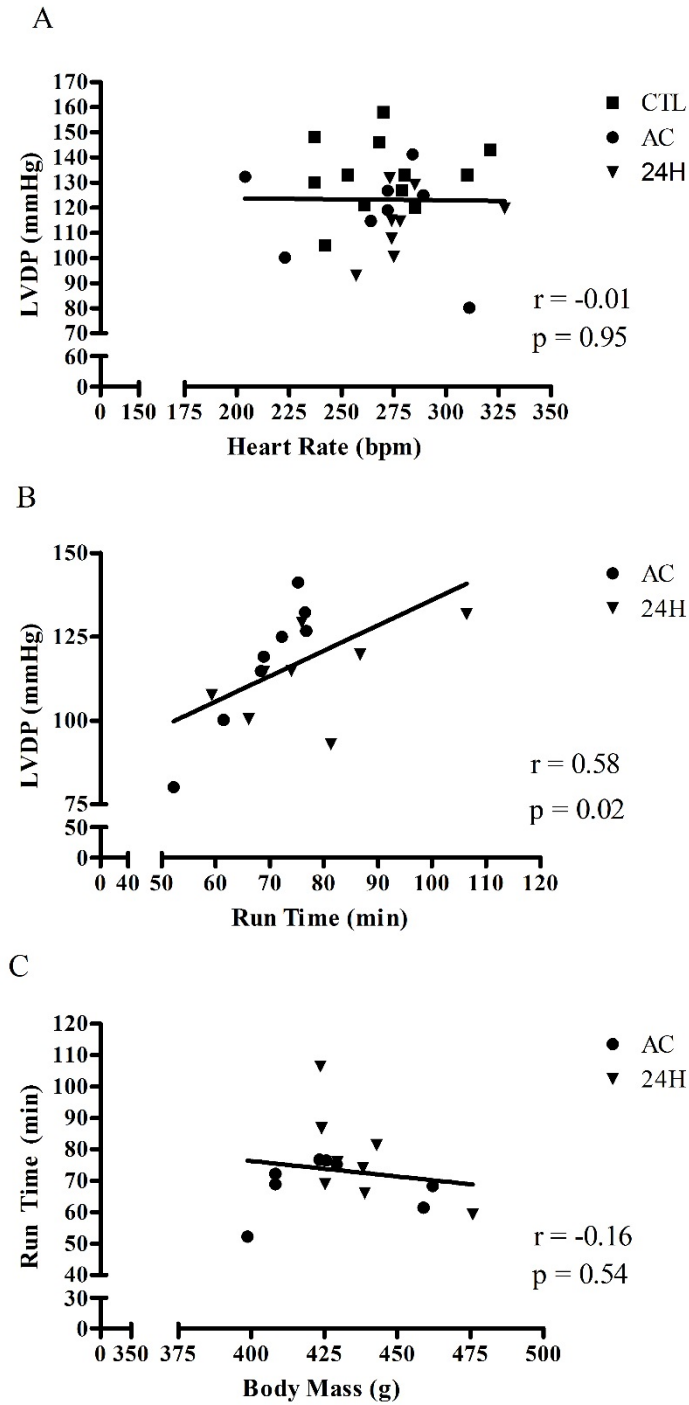
Figure 2.3. Linear regression analysis of cardiac, exercise and anthropometric data. Examination of the relationship between (A) left ventricular developed pressure (LVDP) and heart rate; (B) LVDP and run time and (C) run time and body mass. The strength of each relationship and probability values are indicated within each panel.

Discussion

It is well established that various types of prolonged aerobic exercise in humans can lead to a transient decline in cardiac function (Shave et al., 2008). However, there is minimal and conflicting evidence regarding the effect of exhaustive exercise on the cardiac function of rats and the intracellular mechanisms associated with cardiac fatigue. The aim of this study was to develop a model of cardiac fatigue for the subsequent examination of potential intracellular mechanisms associated with cardiac fatigue. A secondary aim was to determine if exhaustive exercise impaired the ability of the myocardium to respond to β-adrenergic stimulation. To assess cardiac performance, the isolated perfused heart technique was employed, which permitted the measurement of LVDP, contraction/relaxation kinetics and whole heart hemodynamic measures in the basal state and during β-adrenergic stimulation.

A significant finding of this study was that acute, exhaustive exercise resulted in a ~12% reduction in LVDP immediately following the exercise bout. Furthermore, the exercise-induced cardiac fatigue persisted for 24 hours post-exercise. The absolute LVDP observed in the CTL group (133±4 mmHg) is in agreement with the LVDP observed in the study by Vitiello and colleagues (2011). These authors observed a ~19% reduction in LVDP immediately after a four hour submaximal bout of treadmill running, which was greater than the ~12-14% decline in LVDP observed in the current study. Another study observed a ~25% reduction in LVDP following an hour of running at 25 m/min (Wonders et al., 2007). This speed represents an intensity that is 25% greater than that used in the current study. Olah and colleagues (2015) swam rats for three hours and observed a ~25% reduction in EF in rats that swam compared to controls rats. These data suggest that the duration and intensity of activity may influence the magnitude of exercise-induced cardiac fatigue, which has been observed in human studies (Shave et al.,

2008). However, the regression analysis performed on LVDP and run time in the current study suggests the opposite, as there was an increase in LVDP in hearts from animals that ran for a longer duration. The reason for this relationship is not currently clear, but is not due to differences in the pool from which animals were selected as they were littermates and were randomly assigned to either the AC or 24H group. If the reduction in LVDP observed *ex vivo* was present *in vivo*, then it is possible that animals with the lowest LVDP had lower run times due to impaired cardiac output. The reduction in LVDP observed in the basal state was not related to changes in heart rate or coronary flow. This is a key observation given that a decrease in coronary flow (i.e. ischemia) and an increase in the pacing frequency in the isolated perfused rat heart have been demonstrated to reduce LVDP (Simor et al., 1997; Spinder et al., 2004; Dias et al., 2006). Taken together, these findings suggest that exhaustive treadmill exercise can induce cardiac fatigue in the basal state and that exercise-induced cardiac fatigue may be due to intrinsic deficits within the cardiomyocyte.

Despite the significant reductions in LVDP observed in this study in the basal state, there was no significant change in the +dP/dt or time to peak pressure. Similar observations have been made in isolated trabeculae following exhaustive exercise. A study by Maher and colleagues (1972) ran rats to exhaustion and observed a ~50% reduction in the tension produced in isolated trabeculae when compared to control trabeculae, but there were no significant differences in the time to peak tension between the exhaustive exercise group and control group. Conversely, studies have demonstrated an exercise-induced reduction in +dP/dt that coincided with a reduction in LVDP (Wonders et al., 2007; Vitiello et al., 2011). The experiments by Wonder and co-workers (2007) and Vitiello and colleagues (2011) did not address the potential mechanisms that contributed to the attenuated +dP/dt. The divergent findings between LVDP and +dP/dt in

the current study suggest that the ability of the cardiomyocytes to develop tension was compromised but the kinetics of contraction were not altered. Exhaustive exercise has been demonstrated to reduce the sensitivity of the cardiac myofilaments to Ca^{2+} (Belcastro & Sopper, 1984), which may have contributed to the decline in LVDP in the absence of any change in +dP/dt.

There was a trend (p=0.076) for a reduction (~12%) in the –dP/dt in the AC and 24H groups when compared to the CTL group. Similarly, hearts from rats that performed 1-4 hours of treadmill exercise had a significantly depressed –dP/dt (Wonders et al., 2007; Vitiello et al., 2011). It was hypothesized that a reduction in SERCA2a activity may have contributed to the decreased –dP/dt (Wonders et al., 2007). The implication that SERCA2a activity contributed to an exercise-induced reduction in –dP/dt is logical given the role SERCA2a plays in lowering the $[Ca^{2+}]_f$ in the cardiomyocyte. It has been demonstrated that exhaustive swimming exercise resulted in a significant decrease in the rate of SR Ca^{2+} uptake (Pierce et al., 1984). However, a later study did not observe any change in SERCA2a activity following intense, exhaustive treadmill running in rats (Delgado et al., 1999). These studies lacked measurements of cardiac function; therefore, further examination of the effects of exhaustive exercise on Ca^{2+} regulation in conjunction with cardiac function is warranted.

The assessment of the cardiac response to a β-adrenergic receptor agonist may provide further evidence of exercise-induced cardiac fatigue in the rat myocardium. For example, if the chronotropic and inotropic response of the myocardium to β-adrenergic stimulation was blunted then the ability to augment cardiac output may be compromised, which would impair performance during a subsequent exercise bout. Increasing the ISO dose progressively from 10^{-11} M to 10^{-7} M resulted in a sigmoidal LVDP curve, which is consistent with previous findings

(Bilginoglu et al., 2009; Soltysinska et al., 2011; Vitiello et al., 2011). As hypothesized, there was a significant main effect of exercise, such that the LVDP of the AC and 24H groups were lower during the ISO dose response when compared to the CTL group. A study by Vitiello and colleagues (2011) performed a similar ISO dose response on isolated perfused hearts following prolonged exercise and did not observe a significant difference in LVDP between the exercise and control groups. It is important to note that the LVDP data from the ISO dose response was normalized to basal LVDP. It is possible that normalization of LVDP data in the study by Vitiello and colleagues (2011) masked an exercise effect, such as the one observed in the current study. These data demonstrate that under the experimental conditions utilized in this study, the exercise-induced cardiac fatigue present in the basal state cannot be overcome by β-adrenergic stimulation.

The duration of the cardiac cycle is shortened during exercise due to an elevated heart rate. This poses a temporal limitation to filling and ejection of the ventricles, which is overcome by an enhanced rate of contraction and relaxation of the ventricles. To the author's knowledge, this is the first study to examine the effects of progressive ISO concentrations on cardiac +dP/dt and –dP/dt following exhaustive treadmill exercise. The +dP/dt of the LV was not significantly different between the three groups in the basal state. Subsequently, a progressive increase in ISO concentration added to the perfusate resulted in an increase in the +dP/dt that was similar between the CTL, AC and 24H groups. These data suggest that LV contractility during β-adrenergic stimulation was not altered by exhaustive exercise, which is contrary to previous reports in humans (Welch et al., 2005; Scott et al., 2007). Loading conditions are lacking in the isolated perfused heart as the LV end diastolic pressure is artificially adjusted and no volume is actually ejected from the heart (Liao et al., 2012). Thus, it is possible that changes in loading

conditions during β-adrenergic stimulation in human subjects can account for these divergent results (Scott et al., 2007). Interestingly, the –dP/dt in the AC group was significantly lower than the CTL and 24H groups in response to β-adrenergic stimulation. These results suggest that immediately following exhaustive exercise the ability of the heart to relax was compromised. During exercise, augmented cardiomyocyte relaxation is largely dependent on PKA mediated phosphorylation of PLN and TnI, which results in an increase in SERCA2a activity and a decrease in the apparent affinity of TnC for Ca^{2+}, respectively (Odermatt et al., 1996, MacLennan & Kranias, 2003; Rao et al., 2014). From a functional perspective impaired relaxation kinetics *in vivo* could reduce filling of the ventricle during diastole, which would lower EDV and thus lower SV.

The persistent depression in LVDP and –dP/dt observed during progressive ISO doses was not due to differences in heart rate or coronary flow. The LVDP and –dP/dt increased in an ISO-dependent manner and statistically peaked at an ISO concentration of $10^{-8.3}$ M and $10^{-8.0}$ M, respectively. Similarly, the coronary flow rate increased to the same extent in all three groups during progressive ISO doses and reached a statistical plateau at $10^{-8.3}$ M. These data suggest that the reduced LVDP and –dP/dt were not due to coronary flow limitations. It has been demonstrated in some (Eysmann et al., 1996; Douglas et al., 1998; Hart et al., 2006; Scott et al., 2007) but not all human studies (Martin et al., 1991; Banks et al., 2010) that the chronotropic effect of a β-adrenergic agonist (i.e. ISO or dobutamine) is blunted following prolonged aerobic activity. In an animal model, the ISO dose required to increase heart rate by 25 bpm increased 3-fold in dogs that ran for an hour at 60-80% of their maximal heart rate (Friedman et al., 1987). In the current study, there was no difference in heart rate between the three groups in the basal state or at any concentration of ISO, which counters the findings in dogs and the majority of

human studies. This observation is important considering the negative inotropic effect an increase in heart rate can have on the isolated perfused rat heart (Simor et al., 1997; Lankford et al., 1998). Thus, there appears to be experimental (i.e. *in vivo* versus *ex vivo*) and species differences that may explain the divergent results with respect to the chronotropic response to β-adrenergic stimulation following prolonged or exhaustive exercise. Taken together, heart rate and coronary flow did not contribute to the exercise-induced reduction in LVDP and –dP/dt observed during the ISO dose response, which suggests one or more mechanisms intrinsic to the cardiomyocyte may contribute to cardiac fatigue.

Currently, it is not clear as to the mechanisms associated with exercise-induced reductions in LVDP. The decline in cardiac function following exhaustive exercise observed in the current study is reminiscent of myocardial stunning. Myocardial stunning is characterized by an ischemic-induced reduction in cardiac function, which may last for hours to days (Bolli & Marban 1999). Experiments by Heyndrickx and colleagues (1975) were the first to demonstrate that following a brief ischemic period there was a transient decline in cardiac contractile function despite restoration of normal coronary flow. There are two critical features that accompany myocardial stunning; one, is that the ischemic bout did not result in any cardiomyocyte cell death and two, the contractile dysfunction is present despite normal or near-normal coronary flow (Bolli, 1990). It has been suggested that prolonged aerobic exercise resulting in cardiac fatigue may be a form of "pseudo-stunning" brought on by exercise-induced myocardial ischemia (Scott et al., 2008). It is well documented in individuals/animals with coronary artery disease, left ventricular hypertrophy or artificial stenosis, that acute exercise results in ischemia and myocardial stunning (Vatner & Hittinger, 1993; Monnet et al., 2004; Ishii et al., 2009). It is impossible to comment on whether there were coronary flow limitations during the exercise

bouts in the current study. However, during the isolated perfused heart experiments there was no significant difference between the three groups in terms of coronary flow, yet LVDP was reduced for up to 24 hours post-exercise. Thus, the reductions in cardiac function observed after exhaustive exercise appear to share similar traits as myocardial stunning and accordingly may also possess similar mechanisms. Based on the similar physiological features of myocardial stunning models and cardiac fatigue models, it seems logical to identify potential mechanisms associated with exercise-induced cardiac fatigue from the myocardial stunning literature.

In summary, this study developed an exhaustive exercise protocol that effectively induced cardiac fatigue in the basal state and during β-adrenergic stimulation. The contractile response shared similarities to myocardial stunning, such that cardiac contractile function was depressed for up to 24 hours post-exercise, despite normal coronary flow. It can be concluded that cardiac fatigue was not due to changes in hemodynamics or heart rate. Thus, cardiac fatigue is likely due to impaired function of EC coupling proteins within the ventricular myocyte.

Chapter III: Exercise-induced cardiac fatigue is associated with increased ROS production, SR Ca^{2+} leak and calpain activation

Synopsis

In humans, there is extensive research demonstrating that prolonged or exhaustive exercise results in cardiac fatigue. There is a growing body of evidence, which includes observations from Chapter 2, that cardiac fatigue can be induced in rats using various exercise modalities. However, the intracellular mechanisms that contribute to exercise-induced cardiac fatigue in rodents have yet to be determined. Thus, the purpose of this study was to examine the effects of exhaustive exercise on *in vitro* ROS production, Ca^{2+} regulation, Na^+/K^+-ATPase activity and calpain activation. Adult, male Sprague-Dawley rats (21-23 weeks) were randomly assigned to either a CTL, AC or 24H group. Animals in the AC and 24H groups ran at 20 m/min and 5% grade until exhaustion, which occurred after 67 ± 3 and 66 ± 3 minutes, respectively. The hearts were excised and a portion of the LV was frozen and another homogenized for *in vitro* biochemical analyses. Exhaustive exercise did not alter the maximal rates of Ca^{2+}-ATPase activity or Na^+/K^+-ATPase activity ($p > 0.05$). In addition, the rates of SR Ca^{2+} release were not significantly different ($p > 0.05$) between the three groups. A novel finding in this study was that the rate of SR Ca^{2+} leak increased ~40% ($p < 0.05$) in the AC group when compared to the CTL group. Acute exercise resulted in a significant increase in ROS production ($p < 0.05$) and no significant change in lipid peroxidation ($p > 0.05$). To determine if ROS production resulted in post-translational modification of RyR, immunoprecipitation and Western blotting were performed. The degree of glutathionylation, nitration and carbonylation of RyR were not different ($p > 0.05$) between the three groups. Furthermore, phosphorylation of serine 2808 on RyR was not different ($p > 0.05$) between the CTL, AC and 24H groups, despite a significant increase ($p < 0.05$) in the concentration of plasma Epi. Thus, these specific post-translational modifications to RyR were not associated with the increased rate of SR Ca^{2+} leak observed in

this study. The reduction in LVDP observed in the 24H group may be associated with the significant increase ($p<0.05$) in calpain activity that was observed in the AC group. Calpain activation has been shown to degrade EC coupling related proteins, which would require *de novo* protein synthesis. Taken together, an increased rate of SR Ca^{2+} leak and subsequent calpain activation may have contributed mechanistically to the cardiac fatigue observed in the AC and 24H groups via reduced SR Ca^{2+} load and impaired EC coupling, respectively.

Introduction

Chronic aerobic exercise training has numerous health and cardiovascular benefits, which include, but are not limited to, reduced blood pressure, reduced risk of cardiovascular disease and prevention of diabetes, cancer and obesity (Warburton et al., 2006). However, a single bout of prolonged aerobic exercise has been demonstrated to result in exercise-induced cardiac fatigue in humans and other rodent models (Chapter 2 included) when assessed at rest, following the exercise bout (George et al., 2009; Scott et al., 2009; Vitiello et al., 2011; Olah et al., 2015). It has been proposed that this phenomenon displays features similar to the stunned myocardium (Starnes & Bowles, 1995; Siegel et al., 1997; Scott et al., 2008).

Research into the molecular mechanisms responsible for myocardial stunning has provided two primary hypotheses (for a review see Bolli & Marban, 1999). The first theory postulates that ROS production is exacerbated during the ischemic period and the subsequent reperfusion period. Oxidative stress can contribute to impaired cardiomyocyte function as a result of damage to proteins and/or lipids. Indeed, models of myocardial stunning have demonstrated impaired Na^+/K^+-ATPase activity (Kaplan et al., 2005; Kaplan et al., 2008), impaired Ca^{2+} handling (Kim et al., 2001; Kumar et al., 2009), altered protein phosphorylation (Weber et al., 2006) and protein degradation (White et al., 2003). The second theory states that myocardial stunning is due to a reduction in the sensitivity of the contractile apparatus to Ca^{2+}, a reduction in the regulation of Ca^{2+} by the SR and/or Ca^{2+} overload (Bolli and Marban, 1999). Although these two theories first evolved separately, there are undoubtedly common threads between the two. A ROS-induced reduction in Na^+/K^+-ATPase activity would result in Na^+ accumulation within the cardiomyocyte, this would favour reverse mode Na^+/Ca^{2+} exchange and would result in Ca^{2+} overload (Wei et al., 2007). Calcium overload has been demonstrated to

activate calpains, which resulted in myofibrillar protein degradation, a feature associated with the first myocardial stunning hypothesis (Gao et al., 1997). Degradation of myofibrillar proteins would require *de novo* protein synthesis to replace the damaged proteins and may explain the reduced LVDP observed 24 hours post-exercise.

In striated muscle, the production of ROS is exacerbated during contractile activity and is an established mechanism that contributes to the development of fatigue in skeletal muscle (Kobzik et al., 1994; Kolbeck et al., 1997; Lamb & Westerblad, 2011). Previous studies have demonstrated that acute exercise resulted in a marked increase in indices of oxidative stress in the rat myocardium, which were related to the exercise-induced cardiac fatigue (Wonders et al., 2007; Vitiello et al., 2011; Olah et al., 2015). Work by Olah and colleagues (2015) demonstrated that prolonged swimming caused an increase in leukocyte infiltration and superoxide production in the myocardium, which was associated with a significantly lower stroke volume and cardiac output when compared to a control group. Wonders and colleagues (2007) ran rats at 25 m/min and 5% grade for 60 minutes and observed a significant reduction in LVDP at 24 and 48 hours post-exercise, which recovered 72 hours after the acute bout of exercise. Indices of lipid peroxidation, namely MDA and 4-HAE content, were increased post-exercise and followed a similar recovery time course as that of LVDP. Vitiello and co-workers (2011) showed that prolonged treadmill running resulted in a significant decrease in the ratio of reduced glutathione to oxidized glutathione (GSH/GSSG; a marker of oxidative stress), which was associated with cardiac fatigue. Conversely, Seward and co-workers (1995) ran rats until exhaustion and failed to observe any change in cardiac function following exercise despite increased ROS production. Nevertheless, there is a strong possibility that ROS produced during acute exercise contributed

to the cardiac impairment reported in Chapter 2. Thus, further research is warranted to examine the intracellular protein targets of exercise-induced ROS.

Few studies have attempted to elucidate the intracellular mechanisms that contribute to exercise-induced cardiac fatigue. Given the relationship between $[Ca^{2+}]_f$ and force, it would seem logical that a reduction in contractile function in the heart following acute exercise may be related to impaired Ca^{2+} regulation. A study by Delgado and colleagues (1999) examined the effects of exhaustive exercise on maximal Ca^{2+}-ATPase activity. These authors found no significant differences in the rates of maximal Ca^{2+}-ATPase activity between sedentary control rats and rats that ran to exhaustion. Conversely, an abstract from the 1977 proceedings of the American College of Sports Medicine reported that rats run to exhaustion had an approximate 50% reduction in the rate of Ca^{2+} uptake in SR vesicles isolated from the LV (Sembrowich & Gollnick, 1977). Similarly, Pierce and colleagues (1984) isolated SR vesicles from rat LV following an exhaustive bout of swimming and observed a ~40% reduction in the rate of SR Ca^{2+} uptake. A reduction in Ca^{2+} uptake would result in less Ca^{2+} sequestered in the SR after each cardiac cycle. Unfortunately, these studies did not investigate the mechanism associated with the decreased Ca^{2+} uptake, nor were the consequences of decreased Ca^{2+} uptake on cardiac contractile function examined. It is possible that production of ROS during exercise caused the decrease in SERCA2a activity. Indeed, in pathological models in which ROS production is augmented there is a reduction in SERCA2a activity and an increase in SERCA2a nitration (Thomas et al., 2011), cysteine oxidation (Qin et al., 2013) and/or carbonylation (Shao et al., 2011). Taken together, oxidative stress and exhaustive exercise can reduce SERCA2a activity in the heart. However, a possible relationship between oxidative stress, SERCA2a activity and exercise-induced cardiac fatigue has not been examined to date.

The ryanodine receptor in cardiomyocytes is a focal point of Ca^{2+} homeostasis, whereby deficits in RyR function can lead to contractile dysfunction (Bers, 2014). The occurrence of aberrant Ca^{2+} leak during diastole can lead to a reduction in the SR Ca^{2+} content and the amplitude of the Ca^{2+} transient (Sag et al., 2013). This has been demonstrated in heart failure and aging models where the production of ROS is elevated. In a pacing model of canine heart failure, there was significant oxidation of free thiols on RyR, which resulted in an increase in Ca^{2+} leak from Ca^{2+} loaded SR vesicles (Yano et al., 2005; Terentyev et al., 2008). In aged mice and rabbits, diastolic Ca^{2+} leak was elevated in isolated atrial and ventricular myocytes. When DTT was incubated with aged myocytes the diastolic Ca^{2+} leak rate was restored to the level of young control myocytes (Cooper et al., 2013; Guo et al., 2014). These studies suggest that increased production of ROS resulted in oxidative post-translational modification of RyR, which increased Ca^{2+} leak from the SR.

Phosphorylation of RyR is an alternative type of post-translational modification that has been shown to increase SR Ca^{2+} leak. In models of heart failure, PKA mediated hyperphosphorylation of RyR at serine 2808 has been shown to cause the RyR regulatory protein, calstabin2, to dissociate from the RyR tetrameric complex, which resulted in destabilization of the channel and increased Ca^{2+} leak (Marx et al., 2000; Wehrens et al., 2006; Marks, 2013). Taken together, post-translational modification (i.e. oxidation and phosphorylation) of RyR in pathological models resulted in increased leakage of Ca^{2+} from the SR and impaired cardiac contractility. Thus, it is possible that the decreased LVDP observed in Chapter 2 was a result of post-translational modification of RyR, which resulted in an increase in the rate of SR Ca^{2+} leak and consequently a decrease in Ca^{2+} release.

There is minimal work that has investigated the effects of acute exercise on cardiac RyR function. A study by Delgado and colleagues (1999) did not observe any differences in the amount of [^{3}H]ryanodine bound to RyR in SR vesicles isolated from animals that ran to exhaustion when compared to control vesicles. The measure of ryanodine bound to RyR is a surrogate measure of the open probability of the channel as ryanodine will only bind to Ca^{2+} release channels that are in the open conformation in response to activating Ca^{2+} concentrations (Delgado et al., 1999). Sanchez and co-workers (2008) isolated SR vesicles from the LV of dogs following an intermittent running protocol that consisted of 5 repetitions of 5 minutes on and 5 minute off. These authors observed a significant increase in the rate of Ca^{2+} release and a decrease in the rate of SR Ca^{2+} leak, which was associated with S-glutathionylation of the Ca^{2+} release channel. These changes in RyR function would likely augment cardiac function as reduced Ca^{2+} leak during diastole would increase SR Ca^{2+} load and lead to enhanced fractional release during systole (Sanchez et al., 2008). In the studies noted above, the total exercise time was ≤ 25 minutes (Delgado et al., 1999; Sanchez et al., 2008). In skeletal muscle, exhaustive or prolonged aerobic exercise exceeding 60 minutes has been demonstrated to decrease the rate of SR Ca^{2+} release (Favero et al., 1993; Leppik et al., 2004; Duhamel et al., 2005; Chen et al., 2007 Green et al., 2011). Therefore, it is possible that exhaustive exercise of a longer duration may impair cardiac RyR function and contribute to exercise-induced cardiac fatigue.

In Chapter 2, cardiac fatigue persisted for up to 24 hours post-exercise and cardiac fatigue has been shown to last for 48 hours following an acute bout of treadmill exercise in rats (Wonders et al., 2007). The fact that cardiac fatigue is present for an extended period of time post-exercise suggests that the mechanism responsible for the contractile deficit may differ from those associated with cardiac fatigue immediately post-exercise. Impaired Ca^{2+} regulation can result

in an elevation in the intracellular Ca^{2+} concentration (Despa et al., 2014), which would result in the activation of calpains (Matsumura et al., 2001). Studies have demonstrated that acute treadmill exercise activated calpains in the LV of rat (Raj et al., 1998; Tiidus et al., 2002). Activation of calpains has been shown to degrade cardiac Ca^{2+} regulatory proteins (French et al., 2006; Pedrozo et al., 2010; Wanichawan et al., 2014) and sarcomeric proteins (Kositprapa et al., 2000; Ke et al 2008), which may result in contractile dysfunction (van der Laarse, 2002; Ke et al., 2008). Degradation of EC coupling proteins would require *de novo* protein synthesis, which may explain the reduction in cardiac contractility observed 24 hours post-exercise in Chapter 2.

The activity of the Na^+/K^+-ATPase is an important variable to consider when investigating mechanisms associated with exercise-induced cardiac fatigue, as changes in Na^+ regulation can impair Ca^{2+} homeostasis and potentially lead to Ca^{2+} overload in the cardiomyocyte (Wei et al., 2007). There is scant research that has investigated the acute effects of exhaustive exercise on maximal Na^+/K^+-ATPase activity in the heart. A study by Pierce and colleagues (1984) examined the effects of an exhaustive bout of swimming on maximal Na^+/K^+-ATPase activity in sarcolemmal vesicles isolated from the LV of rat. These authors found no significant differences in maximal Na^+/K^+-ATPase activity between sarcolemmal vesicles isolated from animals that swam or remained sedentary (i.e. control). No study has examined Na^+/K^+-ATPase activity 24 hours after an exhaustive exercise bout. In skeletal muscle, there are conflicting results regarding acute exercise and Na^+/K^+-ATPase activity, with some evidence indicating a decrease (Leppik et al., 2004; Petersen et al., 2005), increase (Juel et al., 2013) or no change in Na^+/K^+-ATPase activity (Green et al., 2007; Green et al., 2011). Therefore, further research is warranted to determine the effect of exhaustive exercise on Na^+/K^+-ATPase activity in the LV of rat.

In this study, the effect of exhaustive treadmill exercise on the function of Na^+/K^+-ATPase, SERCA2a and RyR2 were examined in LV homogenates. It was hypothesized that exhaustive exercise would result in an increased production of ROS in the myocardium, which would decrease the function of the Ca^{2+} regulatory proteins SERCA2a and RyR2. It was further hypothesized that exhaustive exercise would impair Na^+/K^+-ATPase activity. The impairment in these Na^+ and Ca^{2+} regulatory proteins would likely result in elevated Ca^{2+} concentration in the cleft region of the cardiomyocyte, which would activate calpains. Therefore, it was hypothesized that activation of calpains may be associated with the reduction in LV contractile function 24 hours post-exercise.

Methods

Animals

This study used male Sprague-Dawley rats (21-23 weeks) that were obtained from the breeding colony at the University of Waterloo. Animals were group housed (4 per cage) on a reverse 12 hour light cycle and had access to food and water *ad libitum*. All procedures were reviewed and approved by the University of Waterloo Animal Care Committee.

Experimental Design

This study contained two cohorts of animals. The first cohort was used solely for collection of tissue and to perform *in vitro* experiments aimed at identifying mechanisms associated with exercise-induced cardiac fatigue. After assessment of Na^+/K^+-ATPase, SERCA2a and RyR2 function, it was determined that an increase in SR Ca^{2+} leak in the AC group was the only significant impairment in *in vitro* protein function. Subsequently, a second cohort of animals were chosen to test whether SR Ca^{2+} leak remained elevated during isolated perfused heart experiments as this would strengthen the observations regarding SR Ca^{2+} leak made in the first cohort (i.e. *in vitro* analysis only). The hearts from animals in the second cohort were excised, instrumented and perfused for 30 minutes prior to collection and homogenization of LV. Groups within in the cohort that were only used for *in vitro* experiments were referred to as the *in vitro groups* and the cohort where hearts were perfused were referred to as the *post-perfusion groups*. Within the *in vitro groups* and the *post-perfusion groups* there was a control group (CTL), an acute exercise group (AC) with animals sacrificed immediately following exhaustive exercise and a group of animals that were sacrificed 24 hours after exhaustive exercise (24H). The anthropometric data from all animals used in this study are presented in

73

Table 3.1. The identical acclimation and exhaustive exercise protocols that were developed in Chapter 2 were employed in this study.

Table 3.1: Anthropometric data for the in vitro and post-perfusion groups

	Masses	CTL	AC	24H	p values
In Vitro	Body Mass (g)	449 ± 13	466 ± 6	468 ± 8	0.32
	Heart Mass (g)	1.43 ± 0.040	1.48 ± 0.029	1.42 ± 0.026	0.43
	Left Ventricle Mass (g)	0.99 ± 0.025	1.03 ± 0.021	1.00 ± 0.024	0.51
	Left Ventricle/Body Mass	0.0022 ± 0.00010	0.0022 ± 0.00005	0.0021 ± 0.00004	0.67
Post-Perfusion	Body Mass (g)	474 ± 11	443 ± 16	464 ± 13	0.29
	Heart Mass (g)	1.86 ± 0.05	1.74 ± 0.075	1.77 ± 0.039	0.31
	Left Ventricle Mass (g)	1.21 ± 0.038	1.15 ± 0.058	1.15 ± 0.031	0.50
	Left Ventricle/Body Mass	0.0026 ± 0.00005	0.0026 ± 0.00008	0.0025 ± 0.00006	0.48

The *in vitro* group was used for all *in vitro* analyses performed to investigate the mechanisms associated with exercise-induced cardiac fatigue. The *post-perfusion* group consisted of hearts that were perfused for 30 minutes and then LV homogenate Data are presented as means ± SE (*post-perfusion* n=7; *in vitro* n=9).

Plasma Collection and Tissue Sampling

Prior to excision of the heart, blood was drawn from the inferior vena cava into a 1 mL syringe containing 25 µL of 0.195 M reduced glutathione and 0.237 M EGTA pH 7.0. Blood was gently inverted several times and was centrifuged at 4500 g for 10 min. The plasma was collected and stored at -80°C until analyses of NE and Epi concentrations.

Hearts from anaesthetized animals were excised and placed in an ice cold homogenizing buffer that contained (in mM) 250 sucrose, 5 HEPES pH 7.5, 0.2 phenylmethanesulfonyl fluoride and 0.2% NaN_3. Next, the aorta was cannulated using a teflon catheter and flushed with 10 mL of ice cold homogenization buffer to remove blood (*in vitro* groups) or perfusate (*post-perfusion* groups) within the coronary vasculature. The hearts were trimmed of atria, the aorta, connective tissue and the right ventricle. A piece of LV was frozen and the remaining LV was diluted

(wt:vol, 1:10) in homogenization buffer and homogenized using a motorized tissue grinder (PT3100, Polytron). The homogenate was aliquoted, frozen in liquid nitrogen and stored along with the whole LV pieces at -80°C.

Ca^{2+}- Dependent Ca^{2+}-ATPase Activity

Measurements of Ca^{2+}-dependent Ca^{2+}-ATPase activity were made at 37°C using a spectrophotometric assay developed by Simonides and Van Hardeveld (Simonides & van Hardeveld, 1990), which has since been adapted as a 96-well plate reader assay (Duhamel *et al.*, 2007). The assay buffer contained (in mM): 20 HEPES pH 7.0, 200 KCl, 15 $MgCl_2$, 1 EGTA, 10 NaN_3, 10 PEP and 5 ATP. For each sample, a cocktail that contained 5 mL assay buffer, 18 U/mL LDH, 18 U/mL PK, 1 µM Ca^{2+} ionophore (A23187, Sigma) and 25 µL LV homogenate was combined in a test tube on ice. The cocktail was subdivided (300 µL) into 16 microcentrifuge tubes with varying concentrations of $CaCl_2$. Next, two 100 µL aliquots from each of the sixteen subdivisions was loaded onto a clear bottom 96-well plate. The final step required addition of ~4 µL of 33 mM NADH to each well. The decrease in NADH absorbance at 340 nm was made using a spectrophotometer (SPECTRAmax Plus, Molecular Devices) and represents total ATPase activity. To distinguish Ca^{2+}-ATPase activity from total ATPase activity, 240 µM of the specific SERCA inhibitor, cyclopiazonic acid (CPA) was used (Seidler *et al.*, 1989). The difference between the total ATPase activity and the basal ATPase activity (activity in the presence of CPA) represents the Ca^{2+}-ATPase activity. The $[Ca^{2+}]_f$ corresponding to each $CaCl_2$ addition was determined separately by use of dual-wavelength spectrofluorometry and the Ca^{2+}-fluorescent dye Indo-1. The range of calcium concentrations translated into a pCa range of ~7.0-5.0.

Ca²⁺ Uptake, Ca²⁺ Leak and Ca²⁺ Release

Ca²⁺ uptake, Ca²⁺ leak and Ca²⁺ release were measured at 37°C in LV homogenates using Indo-1 as previously described (Tupling & Green, 2002). Briefly, a dual-emission wavelength spectrofluorometer (Ratiomaster system, Photon Technology International) was used to perform fluorescence measurements. The assay buffer contained (in mM): pH 7.0, 200 KCl, 20 HEPES, 10 NaN₃, 0.005 N,N,N′,N′-tetrakis(2-pyridylmethyl) ethylenediamine, 5 oxalate, 15 MgCl₂. In a 4-sided clear cuvette, 1.5 μM Indo-1, ~4.5 μL of 10 mM CaCl₂ (corresponded to a $[Ca^{2+}]_f$ of ~3.0-3.5 μM) and ~1.5 mg LV homogenate were brought to a total volume of 2.0 ml with assay buffer. The reaction was initiated with the addition of 40 μL of 250 mM ATP. The measurement of $[Ca^{2+}]_f$ using Indo-1 is based on the difference in the maximal emission wavelengths between the Ca²⁺-bound form of Indo-1 and the Ca²⁺-free form. The excitation wavelength was 355 nm, and the emission maxima were recorded at 485 and 405 nm for the Ca²⁺-free (G) and Ca²⁺-bound (F) forms of Indo-1, respectively. The $[Ca^{2+}]_f$ was calculated using Felix Software (Photon Technology International), which utilized the ratio (R) of F to G and the following equation (Grynkiewicz *et al.*, 1985):

$$[Ca^{2+}]_f = K_d \times \left(\frac{G_{max}}{G_{min}}\right)\left(\frac{R - R_{min}}{R_{max} - R}\right)$$

where K_d is the equilibrium constant for the interaction between Ca²⁺ and Indo-1, R_{min} is the minimum value of R following the addition of 338 μM EGTA, G_{max} is the maximum value of G at the addition of 338 μM EGTA, G_{min} is the minimum value of G at the addition of 1.38 mM CaCl₂, and R_{max} is the maximum value of R at the addition of 1.38 mM CaCl₂. The K_d value for the Ca²⁺-dye complex is 250 nM for muscle homogenates (Grynkiewicz *et al.*, 1985). The rate of Ca²⁺ uptake (μmol·g protein⁻¹·min⁻¹) was determined at a $[Ca^{2+}]_f$ of 2.0, 1.5, 1.0 and 0.5 μM by differentiating the $[Ca^{2+}]_f$ curve. Ca²⁺ release and leak were measured in a similar fashion to

Ca^{2+} uptake. The SR of the LV homogenate was actively loaded with Ca^{2+} using the same method as the uptake assay. Once [Ca^{2+}]$_f$ plateaued, 5 mM 4-CMC was added to the cuvette to induce Ca^{2+} release. It is important to note that 4-CMC directly activates the RyR to induce Ca^{2+} release (Tupling & Green, 2002). To assess SR Ca^{2+} leak, a second aliquot of homogenate was used and Ca^{2+} uptake was performed as outlined above; however, 40 µM CPA was added to the cuvette once Ca^{2+} uptake was complete and [Ca^{2+}]$_f$ plateaued. The maximal rates of Ca^{2+} release and leak were calculated using the initial fast phase of the [Ca^{2+}]$_f$ versus time curve. A graphical representation of Ca^{2+} uptake, release and leak is provided in Figure 3.1.
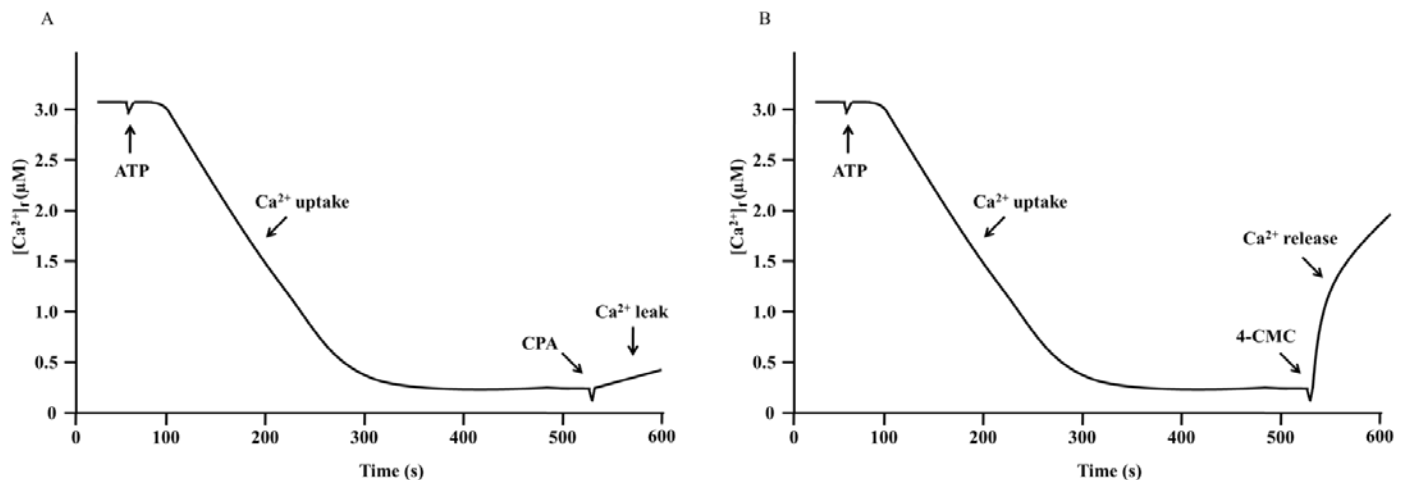
Figure 3.1. An illustration of Ca^{2+} uptake, release and leak. (A) The addition of ATP initiates Ca^{2+} uptake. Once uptake has reached a minimum, cyclopiazonic acid (CPA) was added to the assay. CPA inhibits SERCA2a and permits the assessment of passive Ca^{2+} leak. (B) Once uptake has reached a minimum 4-CMC was added to activate RyR and assess Ca^{2+} release.

Na$^+$-Dependent Na$^+$/K$^+$-ATPase Activity

Measurements of ouabain-sensitive Na$^+$/K$^+$-ATPase activity were made at 37°C using a spectrophotometric assay as previously described (Kutchai & Geddis, 2001; Despa *et al.*, 2005), but with slight modifications. For each sample, 10 µL of LV homogenate was diluted in 5 mL of assay buffer that contained (in mM): pH 7.2, 30 Tris, 20 KCl, 3 MgCl, 1 EDTA, 1.5 PEP, 3

ATP, 40 µM CPA, 4.6 U/mL LDH and 3.3 U/mL PK. Then the buffer was subdivided into 16 microcentrifuge tubes with varying NaCl concentrations (0-120 mM). The decline in NADH absorbance was used to calculate Na^+/K^+-ATPase activity. Background ATPase activity was determined in the presence of 10 mM ouabain and subtracted from total ATPase activity to yield Na^+/K^+-ATPase activity.

Dichlorofluorescein (DCF) Fluorescence and ROS Production

ROS production in whole LV homogenate was determined using 2',7'-dichloro-dihydrofluorescein-diacetate (DCFH-DA) as previously described (Campbell et al., 2015). DCFH-DA is hydrolyzed by cellular esterases to form the minimally fluorescent DCFH. The oxidation of DCFH by ROS creates the highly fluorescent 2',7'-dichlorofluorescein (DCF). Briefly, 20 µL of LV homogenate were incubated at 37°C in the dark with 5 µM DCFH-DA in imidazole buffer (20 mM imidazole pH 7.0, 125 mM KCl 10µM $CaCl_2$). DCF fluorescence was quantified using a SPECTRAmax Gemini XS 96-well plate spectrofluorometer (Molecular Devices) with excitation and emission wavelengths of 490 nm and 525 nm, respectively. The fluorescence intensity was normalized to the total protein in each well and was expressed as arbitrary units per µg protein (AU/µg protein).

Malondialdehyde Content

MDA content is a marker of lipid peroxidation and was assessed as per the methods of Ohkawa and colleagues (1979). Briefly, ~25 mg of frozen LV was homogenized in ten volumes of 1.15% KCl using a glass homogenizer (Kontes). In a glass test tube with a crew cap, 50 µL of homogenate or MDA standard (Cayman Chemical) were combined with a reaction mixture that consisted of: 100 µL 8.1% SDS, 750 µL 20% acetic acid pH 3.5 using NaOH, 750 µL 0.8% thiobarbituric acid (TBA) and 350 µL H_2O. The standards and samples were incubated in a water

bath at 95-100°C for one hour and subsequently cooled for ~10 minutes in an ice-water bath. After cooling, 500 μL of H_2O and 2.5 mL of a mixture of *n*-butanol and pyridine (15:1, v/v) were added and the tubes were vortexed for 30 seconds. Then the samples were centrifuged at 2000 g for 10 minutes, 200 μL of the organic layer from each sample was added to a clear, round bottom 96-well plate and the absorbance was read at 532 nm (SPECTRAmax Plus, Molecular Devices). The concentration of MDA in each sample was calculated using the slope and y-intercept of the MDA standard curve and was normalized to protein content in the homogenate.

Calpain Activity

Calpain activity was assessed using a fluorescent assay as described by McMillan and Quadrilatero (2011). Briefly, LV homogenates were incubated at 37°C with the non-fluorescent calpain substrate, *N*-Succinyl-Leu-Leu-Val-Tyr-7-amino-4-methylcoumarin (Suc-LLVY-AMC) (Enzo Life Sciences) in the presence or absence of the calpain inhibitor, *N*-benzyloxycarbonyl-Leu-leucinal (Z-LL-CHO) (Enzo Life Sciences). Cleavage of the Suc-LLVY-AMC peptide by calpains releases the highly fluorescent AMC molecule. Fluorescence was determined using a SPECTRAmax Gemini XS 96-well plate spectrofluorometer (Molecular Devices) with excitation and emission wavelengths of 380 nm and 460 nm, respectively. The calpain activity was calculated by taking the difference between the fluorescence from homogenate incubated without and with the calpain inhibitor. The fluorescence intensity was normalized to the total protein in each well and was expressed as arbitrary units per μg protein (AU/μg protein).

Western Blotting

The following antibodies were used in this study. The dilution factor of each primary antibody is provided in the parentheses: SERCA2a (1:4000), PLN (1:2000), RyR (1:1000)

(Pierce Antibodies); p-PLN (1:1000) (Cell Signaling); anti-GSH (1:1000) (Virogen); Ser2808 p-RyR (1:1000) (Abcam); anti-DNP (1:1000) (Sigma).

Western blotting was used to determine the relative expression level and oxidative modification of several key cardiac proteins from LV homogenate. Unless described elsewhere, all samples were diluted in 1X Sample Buffer that contained 62.5 mM Tris, pH 6.8, 2% SDS, 5% 2-mercaptoethanol, 10% glycerol and bromophenol blue. Samples were loaded on a polyacrylamide gel and separated using standard electrophoresis techniques (Laemmli, 1970). In the case of PLN, electrophoresis of proteins was performed using a Tris-Tricine procedure developed by Schaggar (2006). The proteins were transferred to a polyvinylidene fluoride (PVDF) membrane (BIO-RAD) and blocked for 1 hour at room temperature with a 5% non-fat milk suspension in Tris-buffered saline plus Tween (TBST; 20 mM Tris, pH 7.5, 150 mM NaCl, 0.1% Tween 20). Following a brief wash in TBST, membranes were incubated with the appropriate primary antibody, washed, incubated with a horse-radish peroxidise (HRP) conjugated secondary antibody and washed a final time. Luminescence was enhanced using either ECL Western Blot Substrate (BioVision) or Luminata™ Forte Western HRP Substrate (Millipore) and captured using the ChemiGenius[2] imaging system and GeneSnap Software (SynGene). Optical density of protein bands was quantified using GeneTools Software (SynGene).

Immunoprecipitation

Immunoprecipitation was used to measure post-translational modification of RyR. Anti-RyR antibody was used to immunoprecipitate RyR2 from 200 µg of LV homogenate. The homogenate was diluted in 0.2 mL of a modified radioimmunoprecipitation assay (RIPA) buffer that contained (in mM): 50 Tris, pH 7.4, 0.9% NaCl, 5.0 NaF, 1.0 Na_3VO_4, 1% Triton X-100 and Roche Complete Protease Inhibitors, and mixed with gentle rotation for 1 hour at 4°C with

1 µg anti-RyR. The immune complexes were incubated with 30 µL of a 50% protein-A sepharose (Sigma) slurry for 1 hour at 4°C. The protein-A sepharose was washed 3 times with RIPA buffer for 5 min and then the immunoprecipitated RyR2 was solubilised by adding 5% SDS. The purified RyR2 was separated using SDS-PAGE and probed for tyrosine nitration and glutathionylation.

To determine the reactive carbonyl content of RyR, the immunoprecipitation procedures outlined above were used with additional steps following the purification of RyR. Briefly, 5 µL of immunoprecipitated RyR was combined with 6 µL of 10 mM 2,4-dinitrophenylhydrazine (DNPH) dissolved in 2 M HCl and incubated for 15 minutes at room temperature with gentle agitation periodically. Subsequently, 7.5 µL of a 2 M Tris and 30% glycerol solution were added to neutralize the mixture followed by the addition of 18 µL 2X Sample Buffer (see *Western Blotting*) and 30 µL 4X Stacking Buffer (0.5 M Tris, pH 6.8 & 0.4% SDS). The samples were then loaded on polyacrylamide gels, separated by electrophoresis and Western blotting was performed as outlined in *Western Blotting*.

Plasma Catecholamine Quantification

The concentration of plasma NE and Epi was determined as per the methods of Weicker and colleagues (1984). Briefly, from 200 µL of plasma catecholamines were adsorbed using 10 mg Al_2O_3. Subequently, the conjugated catecholamine-Al_2O_3 were washed three times with 0.5 mL of buffer that contained 2.0 M Tris and 2% EDTA pH 8.7. Catecholamines were desorbed from Al_2O_3 by adding 0.1 M $HClO_4$ to the samples. The samples (50 µL) were automatically injected into a Waters 2465 HPLC. The samples were separated at a flow rate of 1.2 mL/min using a Supelcosil 15cmx4.6mm 5 µm column (58230-U) and a mobile phase that consisted of 50 mM sodium acetate, 20 mM citric acid, 2 mM sodium octane sulfate, 1 mM di-*n*-butylamine,

100 µM EDTA dissolved in 96:4 volumes of water:methanol pH 3.5. Samples were compared to freshly made NE (A9512) and Epi (Sigma; E4375) standards.

Isolated Perfused Heart

In the *post-perfusion* group of animals (n=7/group), the chest cavity was exposed, thus permitting the removal of the pericardium and thymus and rapid excision of the heart. The heart was placed in ice cold Krebs-Henseleit buffer which contained (in mM): pH 7.4, 118 NaCl, 4.7 KCl, 1.2 $MgSO_4 \cdot 7H_2O$, 24 $NaHCO_3$, 1.1 KH_2PO_4, 1.25 $CaCl_2 \cdot 2H_2O$ and 10 glucose. Hearts were secured to an aortic cannula via 4.0 silk sutures and perfused at a constant pressure (~80 mmHg) with Krebs-Henseleit buffer warmed to 37°C and bubbled with $95\%O_2$-$5\%CO_2$. To measure perfusion pressure a pressure transducer (MLT844, AD Instruments) was connected to the system proximal to the aortic cannula. A second pressure transducer was connected to a balloon tipped catheter and measured indices of LV contractile function. The balloon was fed through the left atria into the left ventricle and the volume of the balloon was adjusted to provide a diastolic pressure of ~10 mmHg. An ultrasonic flow probe (2PXL, Transonic Systems) was placed proximal to the aortic cannula, which measured global coronary flow. Following instrumentation, hearts were allowed to equilibrate for 30 minutes at which point baseline data were recorded. All data were collected using a Powerlab data acquisition system (4/sp, AD Instruments) and were analyzed using Chart software (Ver. 5, AD Instruments). After the 30 minute equilibration period hearts were removed from the perfusion apparatus and homogenized as per the methods in *Blood Collection and Tissue Sampling*. These homogenate samples were used to confirm if any *in vitro* changes in protein structure and function persisted throughout the perfusion period.

Statistics

All data are presented as means ± standard error. A one-way ANOVA was used to compare group means of the variables outlined above. To investigate relationships between two variables, linear regression analysis was performed using GraphPad Prism 4 software. Power analysis was performed using G*Power software, which was developed by Heinrich Heine University in Dusseldorf, Germany. The significance level was set at 0.05, and, when appropriate, a Newman-Keuls post hoc test was used to compare specific means. A trend in the data was deemed when the probability was less than or equal to 0.1 and greater than 0.05. In some analytical measures there was a high degree of inter-animal variability. Accordingly, if a value was greater than 2 standard deviations from the mean that outlying value was removed from the data set.

Results

Anthropometric Data and Run Times

   The anthropometric data of the two cohorts in this study are presented in Table 3.1. In the animals used for *in vitro* analysis and the *post-perfusion* animals, there were no significant differences ($p>0.05$) between the CTL, AC and 24H groups with respect to body mass, heart mass, left ventricle mass and the ratio of left ventricle mass to body mass. The *in vitro* animals in the AC group and 24H group ran for durations of 67 ± 3 and 66 ± 3 minutes, respectively, which did not differ from each other ($p>0.05$). Similarly, there were no significant differences ($p>0.05$) in run times (AC 72 ± 6 min vs. 24H 70 ± 7 min) between the *post-perfusion* AC and 24H groups.
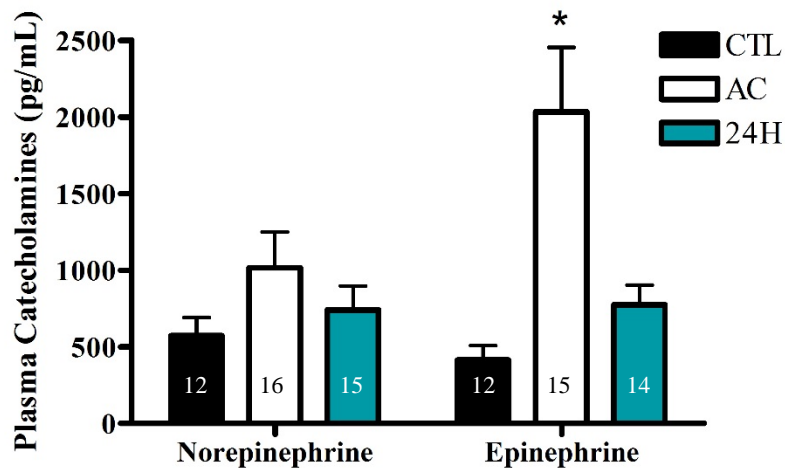
Figure 3.2. The plasma concentration of norepinephrine and epinephrine (pg/mL) in the plasma from CTL, AC and 24H groups. Catecholamine data in the *in vitro* and *post-perfusion* groups were pooled and are presented as means ± SE. The number in each bar represents the number of samples used for statistical analysis as several outliers were removed. *Significantly different ($p<0.05$) than CTL and 24H.

Catecholamines

Since all of the animals in the *in vitro* and *post-perfusion* groups were handled identically up until plasma collection, the catecholamine data were pooled. Immediately following exhaustive exercise there was a significant ~5-fold increase ($p<0.05$) in plasma Epi concentration when compared to the CTL group (Figure 3.2). However, there were no significant differences ($p>0.05$) in the concentration of NE in the plasma after the acute exercise bout. The Epi and NE concentrations in the 24H group were not different than the CTL group ($p>0.05$).

Reactive Oxygen Species Production and Lipid Peroxidation

To assess the production of reactive oxygen species, LV homogenate from the *in vitro* group were incubated with DCFH-DA. The fluorescence of DCF was 15% higher ($p<0.05$) in the AC group when compared to the CTL (Figure 3.3A). Lipid peroxidation was determined by measuring the concentration of MDA in LV homogenate. There was a ~30% difference in the MDA concentration between the AC group and the CTL group; however, the difference between groups failed to reach statistical significance ($p>0.05$) (Figure 3.3B). Power analysis revealed that an additional ten animals per group would be required to achieve a statistically significant increase in lipid peroxidation in the AC group.

A

B
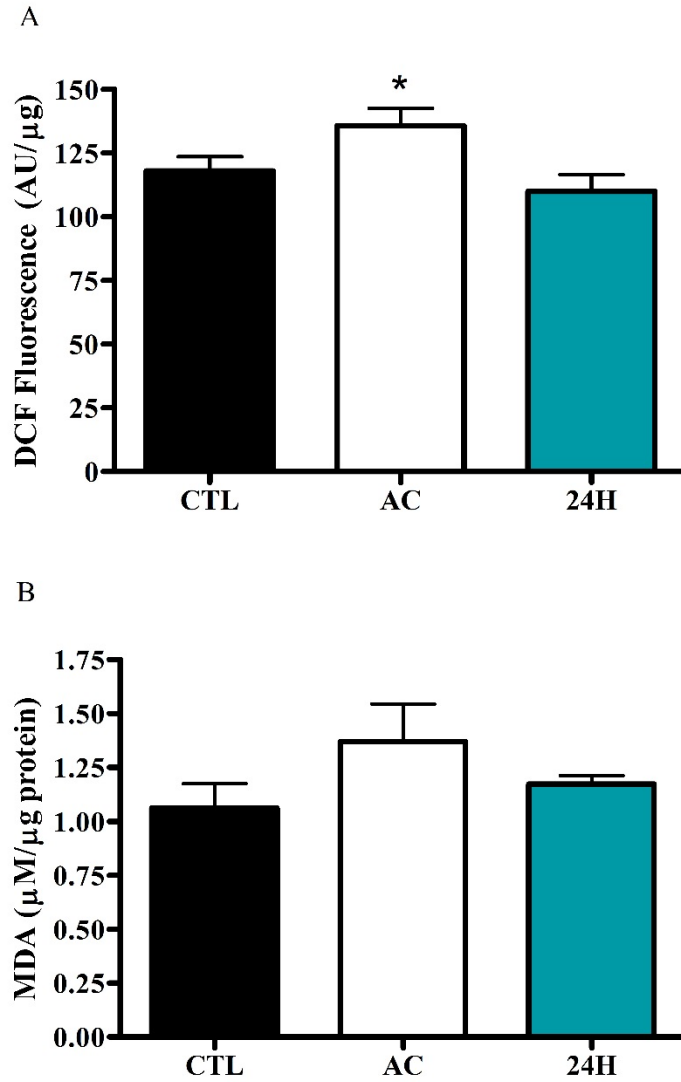
Figure 3.3. ROS production and lipid peroxidation. (A) The production of ROS was assessed by measuring DCF fluorescence in LV homogenate (n=6). (B) Lipid peroxidation was determined by measuring the concentration of malondialdehyde (MDA) in LV homogenates (n=8). All values were normalized to total protein and are means ± SE. *Significantly different ($p < 0.05$) than CTL and 24H.

Maximal Na$^+$/K$^+$-ATPase Activity

Ouabain-sensitive, maximal Na$^+$/K$^+$-ATPase activity was determined in LV homogenate in the *in vitro* group using a spectrophotometric assay (Kutchai & Geddis, 2001; Despa et al., 2005). Contrary to what was hypothesized, there were no differences in maximal Na$^+$/K$^+$-ATPase activity between CTL, AC and 24H groups (Figure 3.4).
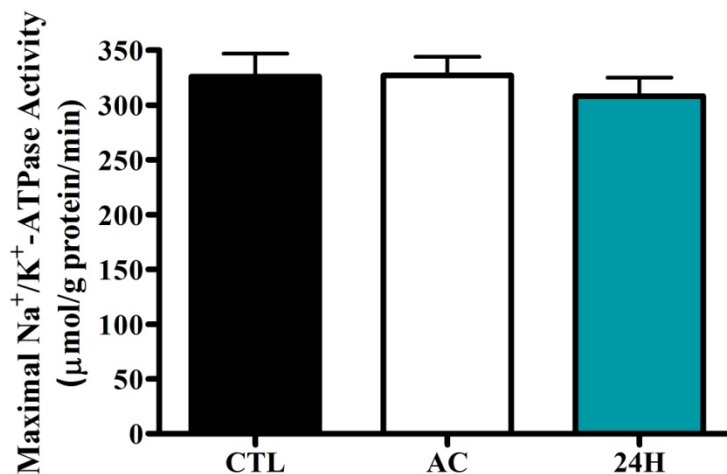
Figure 3.4. The ouabain sensitive, maximal rate of Na$^+$/K$^+$-ATPase activity was assessed in LV homogenates from CTL, AC and 24H groups using a spectrophotometric assay that measured the rate of disappearance of NADH. Values are means $\pm$ SE (n=9).

Calcium Regulation

To determine if exercise-induced cardiac fatigue was associated with impaired regulation of intracellular Ca^{2+}, SERCA2a and RyR2 function were assessed in the *in vitro* groups. The rates of Ca^{2+}-dependent Ca^{2+}-ATPase activity were determined across a ~10^{-7}-10^{-5} M range of [Ca^{2+}]$_f$ and the response to increasing [Ca^{2+}]$_f$ was sigmoidal in nature (Figure 3.5A). The [Ca^{2+}]$_f$ required to increase Ca^{2+}-ATPase activity by 50% (pCa$_{50}$), which represents the apparent Ca^{2+} affinity of SERCA2a, was not significantly different (p>0.05) between the three groups (inset Figure 3.5A). The highest Ca^{2+}-ATPase rate that occurred in a *p*Ca range of 5.26 to 4.92 was

deemed the maximal Ca^{2+}-ATPase activity. As illustrated in Figure 3.5B, there were no significant differences ($p>0.05$) in maximal Ca^{2+}-ATPase activity between the CTL, AC and 24H groups. Across all $[Ca^{2+}]_f$ examined, there was a non-significant (2.0 µM p=0.24, 1.5 µM p=0.25, 1.0 µM p=0.12, 0.5 µM p=0.16) depression in Ca^{2+} uptake of ~20% in the AC group relative to CTL and 24H groups (Figure 3.5C). Since Ca^{2+}-dependent Ca^{2+}-ATPase activity was unaltered, the reduction (albeit non-significant) in Ca^{2+} uptake could reflect a reduced efficiency or Ca^{2+}/ATP coupling ratio of SERCA2a or may be due to increases in SR Ca^{2+} leak.

The function of RyR was assessed in two ways. The first was via 4-CMC-induced opening of the Ca^{2+} release channel. The rate of Ca^{2+} release was not altered ($p>0.05$) by exhaustive exercise when compared to the CTL group (Figure 3.6A). The second assessment of RyR function was achieved by adding CPA, a SERCA2a inhibitor, to the assay after the SR was loaded with Ca^{2+}. Interestingly, there was a ~40% increase ($p<0.05$) in the rate of SR Ca^{2+} leak immediately following exhaustive exercise when compared to the CTL group (Figure 3.6B). During the 24 hour recovery period SR Ca^{2+} leak normalized and was not significantly different ($p>0.05$) than CTL values.
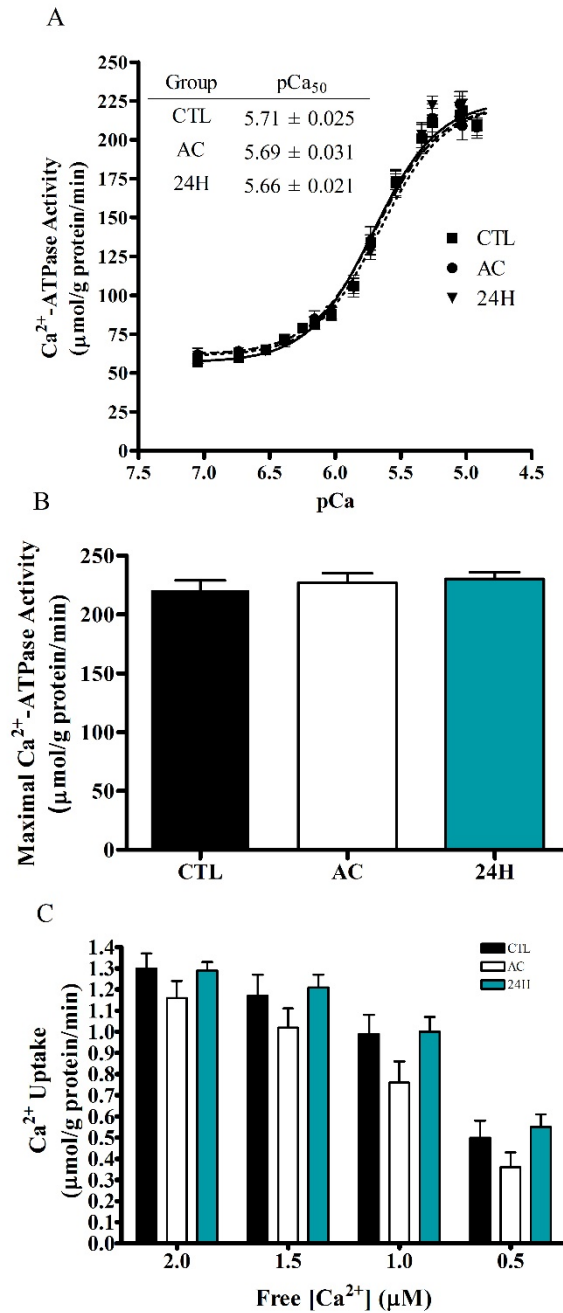
Figure 3.5. Determination of *in vitro* SERCA2a function. (A) The rate of Ca^{2+}-dependent Ca^{2+}-ATPase activity was assessed in LV homogenate from CTL (solid squares), AC (solid circles) and 24H groups (solid triangle), over a negative log molar range of ~7-5. The pCa_{50} for Ca^{2+}-ATPase activity is displayed in the inset. (B) The maximal rate of Ca^{2+}-ATPase activity. (C) The rate of oxalate supported Ca^{2+} uptake was assessed using Indo-1 and dual emission spectrofluorometry. The slope of the Ca^{2+} uptake curve was determined by differentiating the curve at four different free Ca^{2+} concentrations. Values are means ± SE (n=9).
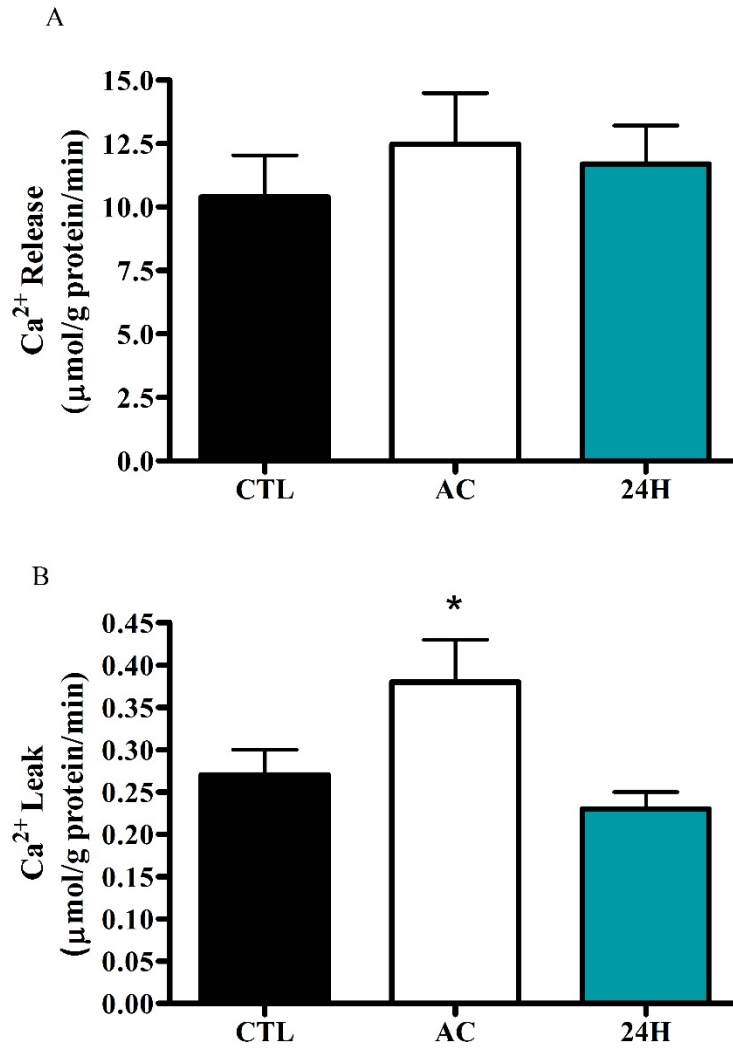
Figure 3.6. Determination of *in vitro* RyR2 function. (A) The rate of 4-CMC-induced Ca^{2+} release. (B) The rate of Ca^{2+} leak out of the SR was assessed following the addition of CPA to the assay once Ca^{2+} uptake had reached a minimum (see *Methods*). Values are means $\pm$ SE (n=9). *Significantly different (p<0.05) than CTL and 24H groups.

SR Protein Content and Phosphorylation Status of SR Proteins

To examine any potential exercise-induced changes in protein content or phosphorylation state of SR proteins, semiquantitative Western blotting was performed. Exhaustive exercise did not alter ($p > 0.05$) the protein content of SERCA2a, PLN and the ratio of phosphorylated PLN (pPLN) to PLN (Figure 3.7). PKA phosphorylation of serine 2808 on RyR was assessed and normalized to total RyR content. Acute exercise did not alter ($p > 0.05$) the phosphorylation status of RyR nor did it alter the total RyR content ($p > 0.05$) in LV homogenate from the CTL, AC or 24H groups (Figure 3.8).

Since phosphorylated RyR content was not altered by acute exercise and given the fact that exercise caused an increase in ROS production, it is possible that oxidative modification of RyR caused an increase in Ca^{2+} leak from the SR. To assess oxidative modifications to RyR, RyR was immunoprecipitated from LV homogenates and Western blotting was performed on purified RyR. The formation of an aldehyde or ketone on an amino acid residue is referred to as carbonylation and is a marker of oxidative stress (Dalle-Donne et al., 2003). Protein carbonylation was assessed by reacting the immunoprecipitated RyR with 2,4-dinitrophenylhydrazine, which creates 2,4-dinitrophenylhydrazone adducts on carbonylated RyR. There was no significant difference ($p > 0.05$) in carbonyl content on RyR in the AC and 24H groups when compared to the CTL group (Figure 3.9A). The addition of a $-NO_2$ group to tyrosine residues results in the formation of nitrotyrosine and is a marker of oxidative stress (Viner et al., 1999; Xu et a., 2006). Western blot analysis demonstrated that exhaustive exercise did not alter ($p > 0.05$) the nitrotyrosine content on RyR (Figure 3.9B). Similarly, there were no significant differences ($p > 0.05$) in the glutathionylation of RyR between the CTL, AC and 24H groups (Figure 3.9C).
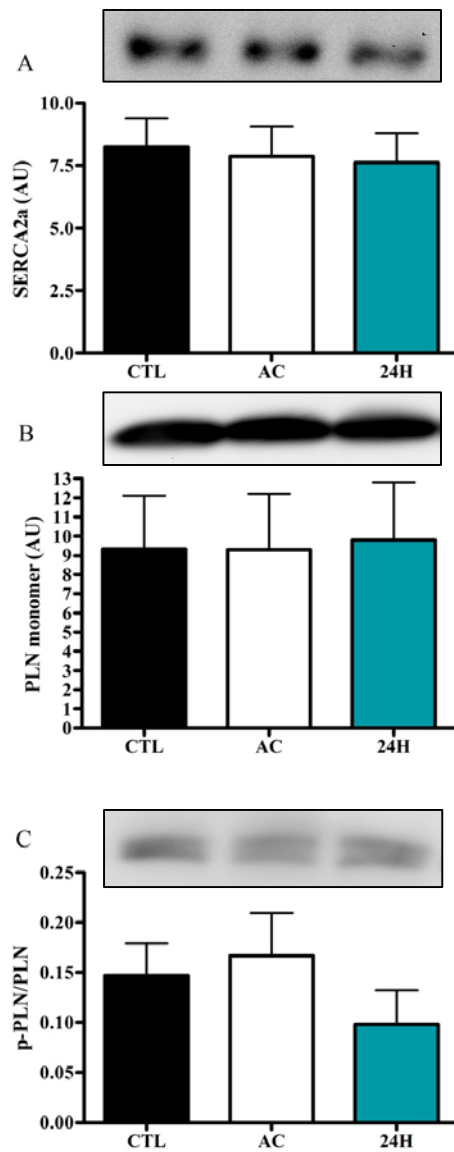
Figure 3.7. Western blot analysis of SR Ca^{2+} regulatory proteins from CTL, AC and 24H LV homogenate. (A) SERCA2a content, (B) PLN monomer content and (C) the ratio of phosphorylated monomeric PLN to monomeric PLN. Equal amounts of protein were loaded in each well. A representative blot is displayed in the inset above each graph. The optical densities of bands were measured using GeneTools and are presented as means ± SE (n=9).
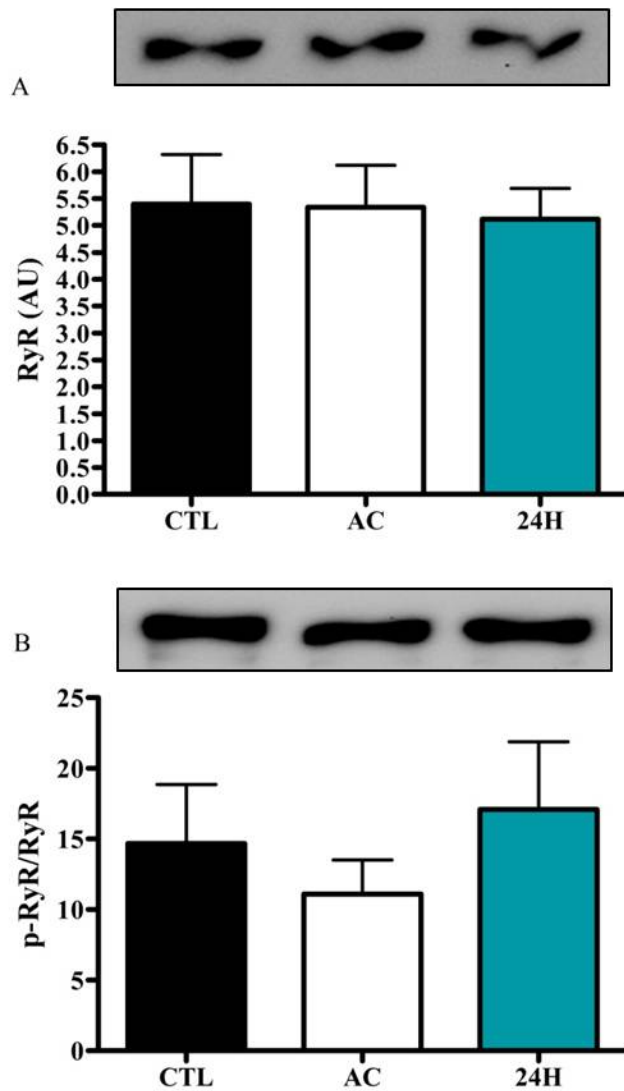
Figure 3.8. Western blot analysis of RyR and phosphorylated RyR from CTL, AC and 24H LV homogenate. (A) Total RyR content and (B) the ratio of phosphorylated RyR to RyR. Equal amounts of protein were loaded in each well. A representative blot is displayed in the inset above each graph. Values are presented as means $\pm$ SE (n=8).
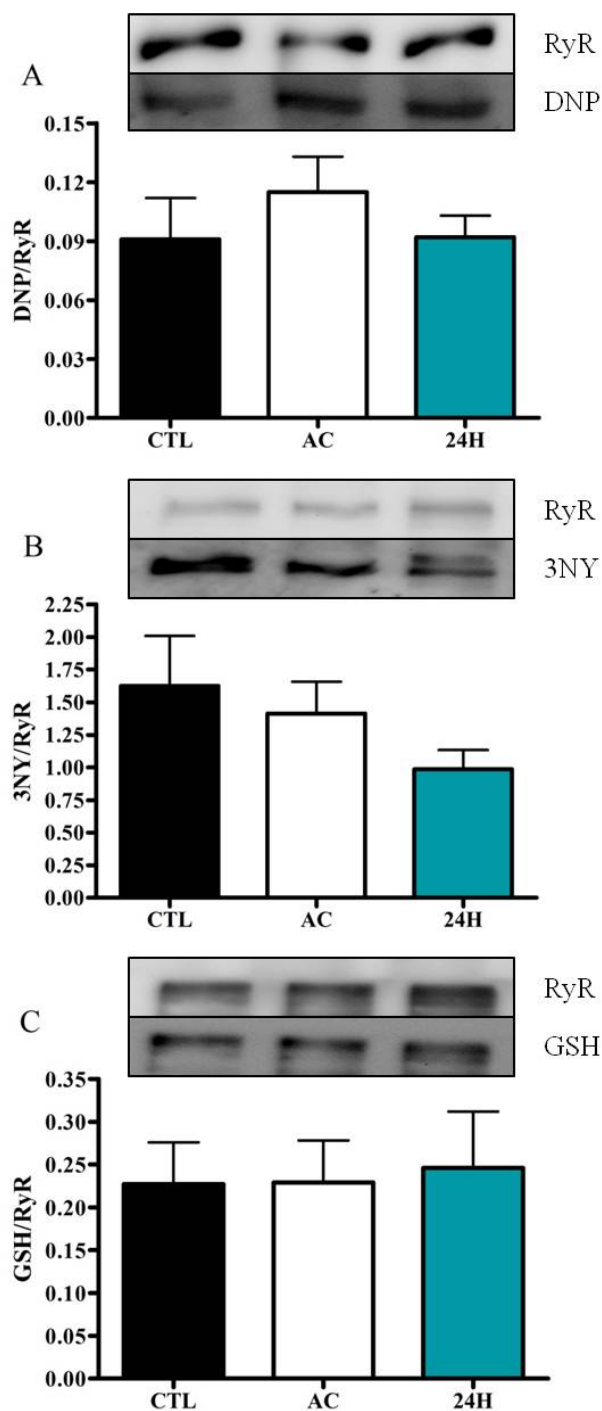
Figure 3.9. Oxidative post-translational modifications to RyR2. Immunoprecipitated RyR was separated via SDS-PAGE and Western blotting was performed to assess oxidative modifications to RyR using antibodies specific for (A) carbonyl content (anti-dinitrophenyl), (B) 3-nitrotyrosine content and (C) glutathionylation. Representative blots of the RyR pull down via immunoprecipitation and the post-translational modification to RyR are provided in each panel. Data are ratios of modified RyR to total RyR and are presented as means ± SE (n=8).

Calpain Activity

The augmented SR Ca^{2+} leak observed at the AC time point may have contributed to the decline in LVDP in the 24H group via activation of calpains due to a rise in the cleft Ca^{2+} concentration. Calpains are cysteine proteases that are activated by elevated cytosolic Ca^{2+} concentrations. Calpain activity was measured in LV homogenates using a minimally fluorescent peptide substrate that becomes highly fluorescent once cleaved by calpains. There was a significant increase ($p<0.05$) in calpain activity in the AC group when compared to the CTL group (Figure 3.10).
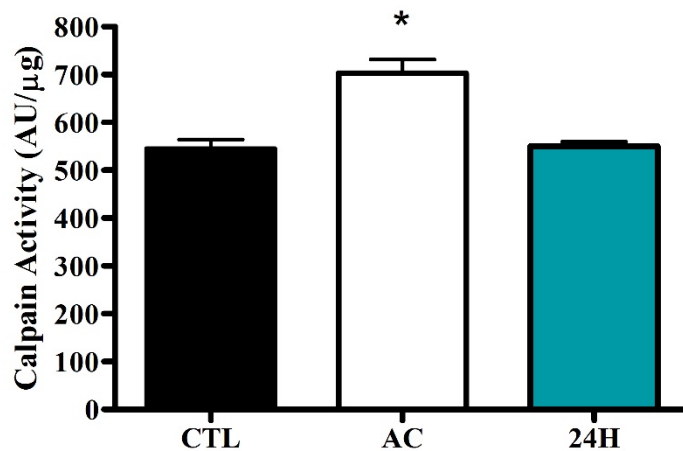
Figure 3.10. Calpain activity in LV homogenates were determined by measuring the fluorescence of AMC (7-amino-4-methylcoumarin), the cleavage product of Suc-LLVY-AMC. Calpain activity was calculated as the difference between AMC fluorescence in the absence or presence of a calpain inhibitor (Z-LL-CHO) normalized to total protein. Values are means ± SE (n=5). *Significantly different ($p<0.05$) than CTL and 24H.

Isolated Perfused Heart Function and Post-Perfusion SR Ca^{2+} Leak

To determine if there was an association between enhanced SR Ca^{2+} leak and reduced LVDP, which were observed in the AC groups in the current study and in Chapter 2, respectively, LV homogenate was collected from hearts after they were perfused for 30 minutes. Similar to

the findings in Chapter 2, there was a significant reduction ($p<0.05$) in basal LVDP in the AC and 24H groups when compared to the CTL group in *post-perfusion* cohort (Figure 3.11A). In addition, there were no significant differences ($p>0.05$) in $\pm dP/dt$ in the basal state from any of the three groups (Figures 3.11 B&C). Similar to the *in vitro* groups, in the *post-perfusion* AC group the rate of SR Ca^{2+} leak increased ($p<0.05$) by ~54% when compared to the *post-perfusion* CTL and *post-perfusion* 24H groups (Figure 3.12). The relationship between LVDP and SR Ca^{2+} leak was assessed using linear regression analysis. When all three groups were included in the analysis there was no significant relationship ($p>0.05$) between LVDP and SR Ca^{2+} leak. However, examination of CTL and AC data resulted in a trend ($p=0.09$) for an inverse relationship between LVDP and SR Ca^{2+} leak such that as the rate of SR Ca^{2+} leak increased the LVDP decreased (Figure 3.13B). These data suggest that increased SR Ca^{2+} leak was associated with the decline in LVDP observed in the AC group.
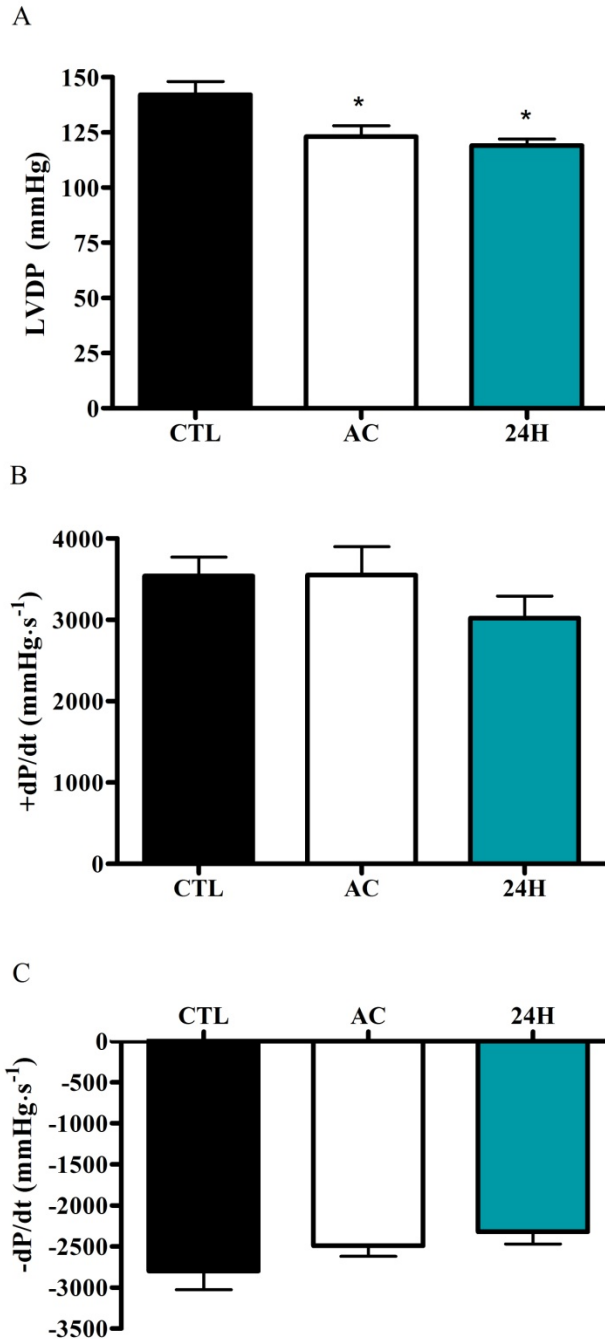
Figure 3.11. Indices of LV contractility from isolated perfused hearts in the *post-perfusion* group. (A) Left ventricular developed pressure (LVDP) from the CTL, AC and 24H groups. (B) The maximal rate of left ventricular pressure development (+dP/dt) and (C) the maximal rate of left ventricular pressure decline (-dP/dt). Values are means ± SE (n=7). *Significantly different (p<0.05) than CTL.
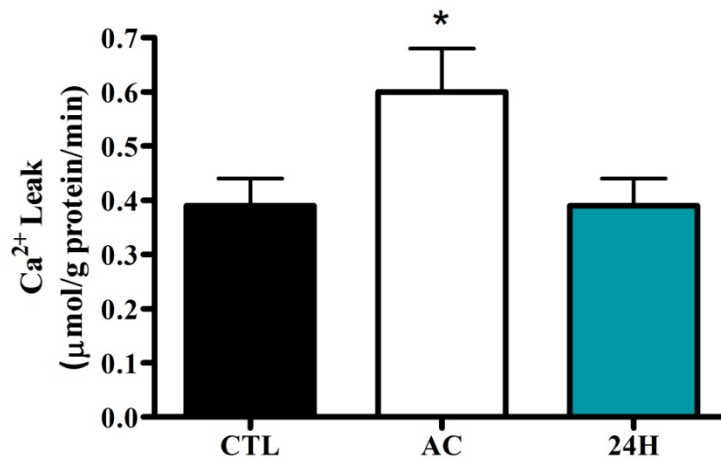
Figure 3.12. Assessment of SR Ca^{2+} leak following perfusion of isolated hearts. SR Ca^{2+} leak was assessed in LV homogenates from the CTL, AC and 24H groups in the *post-perfusion* groups of animals. Values are means ± SE (n=7). *Significantly different (p<0.05) than CTL and 24H.

Discussion

Research involving humans and animals has demonstrated the existence of cardiac fatigue in the basal state following an acute bout of prolonged or exhaustive exercise. Several rat studies have shown that aerobic activity resulted in elevated ROS production (Liu et al., 2000; Lin et al., 2006; Wonders et al., 2007). There are surprisingly few animal studies that have attempted to elucidate the intracellular mechanisms associated with exercise-induced cardiac fatigue, beyond elevated ROS production. The aim of this chapter was to examine the effect of exhaustive exercise on ROS production, maximal Ca^{2+}-ATPase and Na^+/K^+-ATPase activity, Ca^{2+} uptake, Ca^{2+} release, Ca^{2+} leak and respective protein modifications when warranted.

A hallmark of acute aerobic exercise is an increase in circulating plasma NE and Epi (Chin & Evonuk, 1971; LeBlanc et al., 1982; Cox et al., 1985; Scheurink et al., 1989). In this study, the average run time to exhaustion in the *in vitro* AC group and the *post-perfusion* AC group were 67 and 72 minutes, respectively. Immediately following exhaustive exercise, there was a ~5-fold increase in plasma Epi in the pooled AC group when compared to the CTL group (414 ± 93 pg/mL). This resting plasma Epi concentration is in close agreement with some (Blizard et al., 1980; Conlee et al., 1991), but not all studies (LeBlance et al., 1982; Cox et al., 1985). Handling of animals prior to and during administration of anesthesia may explain the discrepancy among studies in terms of resting plasma Epi concentration. The magnitude of change in plasma Epi in the current study is within what appears to be a broad range (0.5-fold to 10-fold) that depends on the type (i.e. treadmill versus swimming) and duration of exercise (LeBlanc et al., 1982; Cox et al., 1985; Scheurink et al., 1989; Conlee et al., 1991). The resting concentration of plasma NE was slightly above values previously reported in the literature (LeBlanc et al., 1982; Cox et al., 1985; Scheurink et al., 1989; Conlee et al., 1991). Contrary to

previous work, and despite a near doubling of plasma NE in the pooled AC group, there were no significant differences in NE concentrations between the AC group and the CTL group. It is possible that variability between animals masked an exercise effect. The coefficient of variation for the CTL group was ~72% compared to a range of ~34-45% in previously reported control groups (Cox et al., 1985; Scheurink et al., 1989; Conlee et al., 1991). The Epi data suggest that there was enhanced adrenergic drive during the exhaustive exercise, which may have implications for PKA mediated phosphorylation and protein function (to be discussed below).

Striated muscle produces detectable amounts of ROS in the basal state, which is augmented during exercise and contributes to the genesis of fatigue (Reid, 2001; Allen et al., 2008; Lamb & Westerblad, 2011). Unfortunately, it was not logistically possible to assess ROS production *in vivo* during the exhaustive exercise bout. However, markers of ROS production, namely DCF fluorescence and lipid peroxidation, were assessed in LV homogenates and represent post-hoc indicators of exercise-induced ROS production. In the AC *in vitro* group, animals that ran to exhaustion had increased ROS production (i.e. DCF fluorescence) when compared to the CTL and 24H groups. The elevated ROS in the AC group is in agreement with previous studies that have observed increased markers of an oxidative cellular environment following acute exercise of various lengths and modalities (Vitiello et al., 2011; Olah et al., 2015). However, a study reported that following exhaustive treadmill exercise, DCF fluorescence in LV homogenate was not significantly different than the sedentary control group (Bejma et al., 2000). The amount of lipid peroxidation in the current study was not significantly different between the three groups. Similarly, several studies have reported that the amount of lipid peroxidation was not altered by exhaustive exercise in whole LV homogenate (Bejma et al., 2000; Liu et al., 2000) and post-nuclear homogenate (Gul et al., 2006). Conversely, studies

by Wonders and colleagues (2007) and Lin and colleagues (2006) observed a significant increase in lipid peroxidation of ~60% and ~40%, respectively, following an acute bout of treadmill running. The magnitude of increased lipid peroxidation in those studies is comparable to the non-significant 30% increase in lipid peroxidation observed in the current study. Power analysis of the lipid peroxidation data revealed that to reach significance, an additional ten animals would be required in each to group. Taken together, these data suggest that exhaustive treadmill exercise increased ROS production, which may be associated with the exercise-induced cardiac fatigue observed in Chapter 2 and the current study.

The increased ROS production observed in this study lends support to the hypothesis that cardiac fatigue may share similar mechanisms as myocardial stunning. Another mechanism that has been demonstrated to contribute to myocardial stunning is a ROS mediated reduction in Na^+/K^+-ATPase activity (Kaplan et al., 2005). In the current study, maximal Na^+/K^+-ATPase activity was assessed using a spectrophotometric assay in LV homogenate collected from the CTL, AC and 24H *in vitro* groups. When compared to the control group, exhaustive exercise did not have an effect on maximal Na^+/K^+-ATPase activity acutely, or 24 hours post-exercise. To the author's knowledge, only one other study has examined the effects of exhaustive exercise on maximal Na^+/K^+-ATPase activity in the rat myocardium. In the study by Pierce and colleagues (1984), sarcolemmal membrane fractions were isolated from the LV of rats that swam with 2% of their body weight attached to their tail to the point of exhaustion (~38 minutes). In that study, the maximal Na^+/K^+-ATPase activities were not significantly different between the control group and the group that swam to exhaustion (Pierce et al., 1984). These authors did not examine the LV function to determine if the exhaustive swim protocol induced cardiac fatigue. Thus, it

appears that cardiac fatigue observed in this study was not associated with altered maximal Na^+/K^+-ATPase activity.

In cardiomyocytes, SERCA2a is a key regulator of SR Ca^{2+} content and subsequently cardiac contractility (Bers, 2002). Thus, it is possible that reduced SERCA2a function may have contributed to the decline in LVDP following acute exercise. The function of SERCA2a was assessed by measuring the rate of Ca^{2+} transport across the SR membrane (i.e. Ca^{2+} uptake) and the maximal Ca^{2+}-ATPase activity. Contrary to what was hypothesized, the rate of Ca^{2+} uptake was not different between the CTL, AC and 24H *in vitro* groups. When SR Ca^{2+} uptake was calculated at a $[Ca^{2+}]_f$ of 1.0 µM, the probability of the AC groups being statistically different than the CTL and 24H groups was 0.12. Of the four different $[Ca^{2+}]_f$ that were chosen to assess the rate of SR Ca^{2+} uptake, this was the comparison that was closest to achieving significance. The rate of SR Ca^{2+} uptake reported is equal to the total Ca^{2+} uptake minus Ca^{2+} leak from the SR. As will be discussed below, the rate of Ca^{2+} leak was increased following exhaustive exercise and can account for the apparent decline in Ca^{2+} uptake in the AC group. Similar to the Ca^{2+} uptake data, the rate of maximal Ca^{2+}-ATPase activity was not significantly different between the three groups. Not surprisingly, there were no significant differences in SERCA2a or PLN content between the three groups. In support of the Ca^{2+}-ATPase data in the current study, Delgado and co-workers (1999) ran rats to exhaustion and found that the rates of maximal Ca^{2+}-ATPase activity were not significantly different between a control group, a group that completed exhaustive exercise and a group that was sacrificed 24 hours post-exercise. In another study, it was demonstrated that the rates of Ca^{2+} uptake were reduced by 40% in isolated SR membrane fractions from rats that swam until exhaustion when compared to a control group (Pierce et al., 1984). The 40% reduction in Ca^{2+} uptake observed by Pierce and colleagues (1984) is similar in

magnitude to the reduction in Ca^{2+} uptake observed in myocardial stunning (O'Brien et al., 1991; Kumar et al., 2009) and would have likely resulted in depressed LV contractility. However, the study by Pierce and colleagues (1984) did not assess cardiac function following exhaustive exercise. Taken together, this model of exhaustive exercise caused cardiac fatigue, which was not associated with any alterations to *in vitro* SERCA2a function. SERCA2a is only one part of the Ca^{2+} regulatory system in the cardiomyocyte. Thus, regulation of Ca^{2+} may have been altered due to depressed RyR function.

The ryanodine receptor is a key regulator of cardiomyocyte function in both health and disease (Dulhunty et al., 2012). Accordingly, a reduction in Ca^{2+} release or increased Ca^{2+} leak would result in a decline in the Ca^{2+} transient amplitude and attenuated force production. The rate of Ca^{2+} release was assessed *in vitro* using the specific RyR agonist, 4-CMC (Herrmann-Frank et al., 1996; Tupling & Green, 2002). The maximal rate of 4-CMC stimulated Ca^{2+} release was not significantly different immediately after exhaustive exercise or 24 hours post-exercise when compared to the CTL group. It has been demonstrated in canine LV that the rate of Ca^{2+} release was increased following 25 minutes of intermittent exercise (Sanchez et al., 2008). These authors demonstrated that the augmentation of Ca^{2+} release was dependent on NOX activity and glutathionylation of the release channel. It is possible that low to moderate amounts of exercise can augment Ca^{2+} release, whereas exhaustive exercise may result in modifications to RyR that nullify the positive effect of brief exercise. Further studies would be required to confirm this hypothesis.

In addition to SR Ca^{2+} release, the rate of SR Ca^{2+} leak through the Ca^{2+} release channel was assessed *in vitro* as described in the methods. When compared to the CTL group, the rates of SR Ca^{2+} leak were significantly increased by ~40% in the AC group. In the 24 hour period

103

following the exhaustive exercise bout the rates of SR Ca^{2+} leak normalized and were not different than the CTL group. Few studies have attempted to examine the effects of acute exercise on SR Ca^{2+} leak in healthy animals. The increased rate of SR Ca^{2+} leak observed in the current study conflicts with previous research that demonstrated a decrease in SR Ca^{2+} leak following 25 minutes of intermittent exercise (Sanchez et al., 2008). These data suggest that brief intermittent aerobic activity reduced SR Ca^{2+} leak, which may augment cardiac function, whereas, exhaustive exercise caused an increase in SR Ca^{2+} leak, which may have impaired LVDP.

To further demonstrate the importance of increased SR Ca^{2+} leak on LVDP, hearts from a second cohort of animals (i.e. *post-perfusion* groups) were isolated and perfused for 30 minutes and then LV homogenates were collected. The rationale for including the *post-perfusion* experiments were to develop an association between exercise-induced impairments in SR Ca^{2+} leak and reduced LVDP. If the increased rate of Ca^{2+} leak observed in the *in vitro* AC group was indeed associated with reduced LVDP then it would be expected that following isolated heart experiments that SR Ca^{2+} leak would also be increased. Similar to Chapter 2, exhaustive exercise resulted in a significant reduction in LVDP in the AC and 24H groups when compared to the CTL group. Importantly, there was a significant increase in SR Ca^{2+} leak in the *post-perfusion* AC group when compared to the *post-perfusion* CTL group. Regression analysis using the *post-perfusion* CTL and AC data revealed a trend (p=0.09) towards an inverse relationship between LVDP and the rate of SR Ca^{2+} leak, such that as the SR Ca^{2+} leak rate increased, the LVDP decreased. As this is the first study to demonstrate this relationship following exhaustive exercise, insight into the mechanisms associated with increased SR Ca^{2+} leak and impaired cardiac contractile function may be drawn from chronic disease models.

A link between aberrant SR Ca^{2+} leak and depressed cardiac function has been demonstrated in studies using models of heart failure (Terentyev et al., 2008; Gonzalez et al., 2010; Bers, 2014). Research by Andrew Marks' group from Columbia University has resulted in the development of a RyR Ca^{2+} leak model of heart failure (for review see Marks, 2013). The model states that heart failure results in chronically elevated circulating catecholamines (i.e. NE and Epi), which leads to augmented PKA activity. The enhanced PKA activity results in hyperphosphorylation of RyR, which causes the accessory protein, calstabin2 to dissociate from RyR. Under normal conditions calstabin2 stabilizes the RyR macromolecular complex, but upon dissociation, the RyR complex destabilizes and becomes "leaky". Persistent leakage of Ca^{2+} from the SR results in a decline in the total SR Ca^{2+} content, a reduction in the amplitude of subsequent Ca^{2+} transients and a decline in force production. It is possible that elevated catecholamines, specifically Epi, observed in the current study resulted in PKA activation and phosphorylation of RyR, which subsequently augmented SR Ca^{2+} leak. However, contrary to observations in heart failure studies, acute exercise did not alter the ratio of phosphorylated RyR to RyR in any of the three groups. Acute exercise has been demonstrated to increase phosphorylation of RyR1 and RyR2 (Bellinger et al., 2008; Gehlert et al., 2012; Wehrens et al., 2003). The discrepancy between the current study and previous exercise studies in terms of RyR phosphorylation may be related to the temporal effects of LV collection and homogenization. These steps were performed as quickly as possible, but several minutes elapsed from the time of exercise cessation to LV homogenization, which may have resulted in dephosphorylation of RyR. Indeed, in order to observe increased RyR phosphorylation in the isolated perfused heart following ISO infusion (i.e. simulated exercise), a mild protein phosphatase inhibitor was required in the perfusate (Reiken et al., 2003). Thus, it is possible that high phosphatase activity post-exercise limited the

ability to detect changes in phosphorylated RyR in the current study. In addition, studies have challenged the Marks group model regarding the functional consequences of RyR phosphorylation in the healthy and failing myocardium (MacDonnell et al., 2008; Zhang et al., 2012). Taken together, the increased SR Ca^{2+} leak through the RyR observed in the current chapter may not be related to changes in phosphorylation state, which suggests that alternative RyR post-translational modification may have occurred during acute exercise.

Acute exercise and disease models can alter the function of RyRs via ROS dependent post-translational modification (Sanchez et al., 2008; Bellinger et al., 2009; Andersson et al., 2011a). To determine if oxidative modification of RyR contributed to the increased rate of SR Ca^{2+} leak observed in the current study, RyR was immunoprecipitated and Western blot analyses were performed to probe for oxidative modifications to purified RyR. Exhaustive exercise did not alter the carbonyl content on RyR acutely or 24 hours post-exercise. Acute exercise has been shown to increase carbonyl content in whole LV homogenate and in post-nuclear homogenate (Perez et al., 2003; Aydin et al., 2007). In support of the current findings, Liu and co-workers (2000) did not observe a change in carbonyl content in LV homogenate from rats run to exhaustion. Unfortunately assessment of carbonylation using any type of homogenate preparation does not provide an indication of specific proteins that were carbonylated. In chronic disease models such as diabetes, muscular dystrophy and aging, immunoprecipitation of RyR has been used to demonstrate that RyR specific carbonylation and Ca^{2+} leak is increased in these models when compared to healthy control groups (Andersson et al., 2011a; Andersson et al., 2011b; Shao et al., 2012). In the current study we demonstrated a rise in ROS production, increased SR Ca^{2+} leak and no change in carbonylation in the AC group. These data suggest that carbonylation of RyR did not contribute to the increased rate of SR Ca^{2+} leak following

exhaustive exercise or that the techniques employed were not sensitive enough to detect differences in carbonylation. It is possible that alternative redox modifications to RyR may have taken place during exhaustive exercise, which contributed to the increased rate of Ca^{2+} leak.

The production of nitric oxide (NO) and superoxide results in increased nitration of cardiac proteins in models such as aging and cardiovascular disease (Viner et al., 1999; Xu et a., 2006). The accumulation of nitrotyrosine residues on SR proteins has been demonstrated to have a negative impact on the protein function (Viner et al., 1999; Knyushko et al., 2005; Lokuta et al., 2005; Tang et al., 2010). Given that NO and superoxide production is augmented during exercise in the heart (Bo et al., 2008; Roof et al., 2013), it is possible that the increased SR Ca^{2+} leak was a result of tyrosine nitration of RyR. Surprisingly, Western blot analysis failed to detect differences in nitrotyrosine content between the three groups. However, several studies have demonstrated in disease models where ROS production is chronically augmented, that there is an increase in nitration of RyR (Kanski et al., 2005; Jain et al., 2014; Yamada et al., 2014). These data suggest that perhaps chronic exposure to elevated ROS is required to nitrate RyR and alter channel function, compared to the acute period of increased ROS production observed in the current study.

The addition of glutathione (GSH) to a free thiol (-SH) containing cysteine residue on a protein is referred to as S-glutathionylation and is an important physiological regulator of protein function in both health and disease (Ghezzi, 2013). To determine if S-glutathionylation of RyR contributed to the increase in SR Ca^{2+} leak, S-glutathionylation content was assessed via Western blotting of immunoprecipitated RyR from the CTL, AC and 24H groups. Exhaustive exercise did not alter S-glutathione content on RyR. These findings are at odds with a previous study that found acute exercise increased S-glutathione content on RyR, which resulted in an increase in

SR Ca^{2+} release and an attenuation of SR Ca^{2+} leak (Sanchez et al., 2008). The exercise protocol employed by Sanchez and colleagues (2008) was brief in duration and of a moderate intensity, thus the exhaustive nature of the exercise protocol used in the current study may have prevented or reversed any S-glutathionylation of RyR. Indeed, under more extreme models of cardiac stress, namely ischemia and reperfusion, the amount of S-glutathionylated RyR was reduced, which was associated with attenuated SR Ca^{2+} release (Tang et al., 2010; Wang et al., 2013). These previous studies demonstrate that RyR function can be regulated via S-glutathionylation. However, it appears likely that S-glutathionylation of RyR did not contribute to the increased leak through the Ca^{2+} release channel observed in the present study.

The increased rate of Ca^{2+} leak from the SR may have contributed to the reduced LVDP observed in the AC group and it may also explain the reduction in LVDP observed 24 hours post-exercise. An elevated rate of SR Ca^{2+} leak would likely increase the Ca^{2+} concentration in the cleft region of the cardiomyocyte. Calpains are Ca^{2+} activated cysteine proteases, which are activated by nM to µM concentrations of Ca^{2+} (Matsumura et al., 2001). Acute exercise increased the calpain activity immediately after exercise when compared to the CTL and 24H groups. These findings are similar to previous studies that ran rats for one hour at 25 m/min and 8% grade or 21 m/min and 12% grade and found that calpain activity in the LV was increased by 46% and ~1.8-fold, respectively (Raj et al., 1998; Tiidus et al., 2002). Activation of calpains has been demonstrated to participate in myocardial stunning (Matsumura et al., 1993; Matsumura et al., 1996). In addition, calpains have been demonstrated to cleave Na^+/K^+-ATPase, troponins, NCX and RyR (Zeitz et al., 2002; Inserte et al., 2005; Pedrozo et al., 2010; Wanichawan et al., 2014). Thus it is possible that activation of calpains and degradation of one or more of these proteins may have impaired EC coupling and contributed to the cardiac fatigue observed in the

24H group. Unfortunately, assessment of EC coupling cannot be performed by an *in vitro* assay. Therefore, further research is warranted to examine this hypothesis.

This study demonstrated that exhaustive exercise resulted in an increased rate of SR Ca^{2+} leak, which was observed in the *in vitro* and *post-perfusion* groups. These data suggest that the cardiac fatigue observed in the AC groups in Chapter 2 and the current study were associated with increased SR Ca^{2+} leak. Exhaustive exercise resulted in an increase in ROS production and a robust increase in plasma Epi concentration. However, our results indicate that carbonylation, nitration, glutathionylation and phosphorylation of RyR do not appear to be linked mechanistically to the observed increase in SR Ca^{2+} leak. It is possible that the Western blot techniques employed in this study were not sensitive enough to detect exercise-induced post-translational modifications to RyR. Acute exercise activated the protease, calpain, which has been implicated in myocardial stunning. Calpain activation may explain the prolonged (up to 24 hours) depression in LVDP observed in the current study as cleavage of EC coupling proteins would require *de novo* protein synthesis. Thus, an increase in SR Ca^{2+} leak resulted in cardiac fatigue acutely and 24 hours post-exercise, likely via changes in SR Ca^{2+} load and calpain mediated impairment of EC coupling.

Chapter IV: Inhibition of NADPH oxidase prevents exercise-induced cardiac fatigue by preventing SR Ca^{2+} leak and calpain activation

Synopsis

Previous studies and the findings from Chapter 3 suggest that ROS production is augmented following prolonged or exhaustive exercise, which may be associated with cardiac fatigue. However, only one study has utilized an intervention to reduce ROS production and prevent cardiac fatigue. Thus, the purpose of this study was to determine if NOX inhibition would prevent cardiac fatigue and to determine the mechanisms associated with preservation of cardiac contractility. Three groups of adult, male Sprague-Dawley rats (21-23 weeks) were provided 1.5 mM APO in their drinking water for three days and assigned to a control group (APO CTL), a group that was sacrificed following the exhaustive exercise bout (APO AC) or a group that was sacrificed 24 hours post-exercise (APO 24H). One cohort of animals were used for isolated perfused heart experiments while another was used for *in vitro* experiments. The LVDP and ±dP/dt were not significantly different between the three APO groups in the basal state or during β-adrenergic stimulation, which suggests that inhibition of NOX prevented exercise-induced cardiac fatigue. There were no significant differences in ROS production or lipid peroxidation between the APO treated groups. Additionally, the level of ROS production was significantly lower in the APO treated groups when compared to the non-APO treated groups in Chapter 3. The rates of SR Ca^{2+} leak were not significantly different between the APO treated groups. Furthermore, APO treated groups had reduced rates of SR Ca^{2+} leak when compared to non-APO treated groups in Chapter 3. NOX inhibition further augmented RyR function in terms of Ca^{2+} release, whereby Ca^{2+} release was higher in APO treated groups when compared to non-APO treated groups. Within the APO treated groups there were no significant differences in RyR nitration, carbonylation, glutathionylation or phosphorylation, which suggests that these post-translational modifications were not associated with the reduction in SR

111

Ca^{2+} leak in the APO AC group. The maximal Ca^{2+}-ATPase activities were not different between the three APO treated groups. There was a main effect of NOX inhibition such that maximal Ca^{2+}-ATPase activity was lower in APO treated groups when compared to non-APO treated groups. Consequently, there was a significant increase in the coupling ratio (Ca^{2+} uptake/Ca^{2+}-ATPase activity) in the APO treated groups, which was due in part to the reduction in SR Ca^{2+} leak. NOX inhibition resulted in a significant increase in the apparent Ca^{2+} affinity of SERCA2a in APO treated groups, which was likely due to increased phosphorylation of PLN. These data suggest that the function of SERCA2a and RyR were augmented when NOX was inhibited, which mechanistically may explain the prevention of cardiac fatigue observed in APO AC and APO 24H groups. Lastly, there were no significant differences in calpain activity in the APO treated groups and overall calpain activity was lower in these groups when compared to non-APO treated groups. Taken together, NOX inhibition prevented cardiac fatigue and the associated mechanisms were a reduction in ROS production, improved Ca^{2+} regulation and an attenuation in calpain activity.

Introduction

Several studies have observed cardiac fatigue in rats following one to four hours of aerobic exercise, which was associated with an increase in ROS production (Wonders et al., 2007; Vitiello et al., 2011; Olah et al., 2015). In the previous chapter it was observed that exhaustive exercise resulted in a significant increase in ROS production as measured in LV homogenates. Interestingly, a study by Vitiello and colleagues (2011) found that animals provided with the NADPH oxidase inhibitor, apocynin, prior to the acute exercise bout did not experience cardiac fatigue or oxidative stress. Their results suggest that activation of NADPH oxidases during exercise resulted in increased ROS production, which contributed to cardiac fatigue. However, the downstream effects of NOX activation were not investigated in that study.

NADPH oxidases (NOXs) are a multi-subunit enzyme complex that catalyzes the following reaction:

$$NADPH + 2O_2 \xrightarrow{\text{NADPH oxidase}} 2O_2^- + NADP^+ + H^+$$
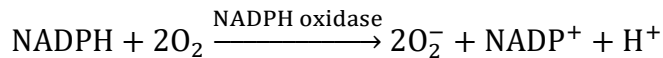
The activation of NOXs are important under physiological and pathological conditions (Bedard & Krause, 2007). There are five NOX isoforms (NOX1-5), with NOX2 and NOX4 being the two predominant isoforms expressed in the myocardium (Bendall et al., 2002; Li et al., 2006; Akki et al., 2009). NOXs are transmembrane proteins that require interaction with one or more regulatory proteins to confer activity. In cardiomyocytes, NOX2 and NOX4 associate with the regulatory protein, p22^{phox}, which acts to stabilize the enzyme. Activation of NOX2 requires translocation of the cytosolic proteins p40^{phox}, p47^{phox}, p67^{phox} and rac to the nascent NOX2 and p22^{phox} complex. NOX4 only requires p22^{phox} in order to be activated, and thus is constitutively active at a low level in the basal state (Matsushima et al., 2014).

In Chapter 3 it was demonstrated that exhaustive exercise resulted in an increase in ROS production, which was associated with a ~40% increase in the rate of SR Ca^{2+} leak and reduced cardiac contractility. Currently it is not clear what the source of ROS production was in Chapter 3. It is possible that the increased rate of SR Ca^{2+} leak was mediated by NOX dependent ROS production. Acute activation of NOX has been shown to regulate RyR1 and RyR2 function via ROS-induced post-translational modification (Sanchez et al., 2008; Sun et al., 2011). An *in vitro* study incubated skeletal muscle SR membrane fractions under varying partial pressures of oxygen (1, 5 and 20% PO_2) and observed a progressive increase in ROS production as PO_2 increased (Sun et al., 2011). It was determined that NOX4 dependent ROS production oxidized a small number of cysteine residues on RyR1 and increased the open probability of the Ca^{2+} channel. Another study incubated triads (a t-tubule flanked by two SR terminal cisternae) isolated from skeletal muscle with NADPH in order to activate NOX, and observed an increase in the open probability and S-glutathionylation of RyR (Hidalgo et al., 2006). An increase in the open probability of RyR results in an increase in the leak rate through the channel (Williams et al., 2011; Wang et al., 2014). Conversely, a study by Sanchez and co-workers (2008) ran dogs intermittently for 25 minutes, which resulted in S-glutathionylation of RyR2 and a decrease in the rate of Ca^{2+} leak. Interestingly, inhibition of NOX with APO prevented structural and functional modifications to RyR, in these previous studies. The SR Ca^{2+} leak data from the study by Sanchez and colleagues (2008) is opposite to the SR Ca^{2+} leak data from Chapter 3 and may be related to the exhaustive nature of the exercise protocol used in the current thesis. Perhaps the effects of exhaustive exercise on NOX activation and SR Ca^{2+} leak in association with cardiac fatigue are more analogous to models of severe stress rather than brief, low intensity exercise.

In pathological models such as heart failure, diabetes and atherosclerosis there is an increase in NOX dependent ROS production (Liu et al., 2010; Maalouf et al., 2012; Kinkade et al., 2013). When NOX was inhibited in these disease models the progression and/or severity of the disease was reduced (Liu et al., 2010; Roe et al., 2011; Kinkade et al., 2013). The improvement in health of these animals when NOX was inhibited may have been due to improved Ca^{2+} regulation. Indeed, in a mouse model of dystrophic cardiomyopathy, it was demonstrated that dystrophic hearts had a 5-fold increase in NOX2 expression and a decrease in contractility, which was associated with an increased rate of SR Ca^{2+} leak (Gonzalez et al., 2014). Incubation of cardiomyocytes with APO partially restored contractility and fully restored SR Ca^{2+} regulation. In a transgenic mouse line that expressed constitutively active Rac1 it was demonstrated that RyR2 function was impaired as indicated by a significant reduction in the fractional release of Ca^{2+} from the SR and an increase in the rate of SR Ca^{2+} leak (Oberhofer et al., 2013). Taken together, chronic activation of NOX is associated with increased SR Ca^{2+} leak, which may contribute to impaired contractile function. Thus, it is possible that the exhaustive exercise protocol employed in Chapter 3 resulted in activation of NOX and ROS production, which contributed to the genesis of cardiac fatigue.

There appears to be a link between activation of NOX and calpains in the myocardium in response to physiological stress. In isolated cardiomyocytes, incubation with NE significantly increased NOX activity and activated calpains, which lead to apoptosis of cardiomyocytes (Li et al., 2009a). Induction of cardiomyocyte apoptosis was prevented when cells were treated with APO prior to application of NE. In a separate study, rat cardiomyocytes were incubated with high concentrations of glucose, which resulted in calpain activation and subsequently lead to cell death (Li et al., 2009b). The effects of hyperglycemic stress were prevented when a NOX

inhibitor or a RyR antagonist were incubated with the cardiomyocytes. These data suggest that there may be an interaction between activation of NOX, altered RyR function and calpain activation.

In Chapter 2 and Chapter 3, exhaustive exercise caused a reduction in LVDP, which persisted for 24 hours post-exercise. It has been hypothesized that exercise-induced cardiac fatigue is a form of pseudo-myocardial stunning (Starnes & Bowles, 1995; Siegel et al., 1997; Scott et al., 2008) and perhaps may share common mechanisms. It has been demonstrated that exposure of skinned trabeculae to calpains recapitulated the decreased myofilament sensitivity to Ca^{2+} and decreased maximal Ca^{2+} activated force present in trabeculae from stunned myocardium (Gao et al., 1996). Furthermore, myocardial stunning was prevented in hearts that were provided leupeptin, a calpain inhibitor, prior to ischemia and reperfusion (Matsumura et al., 1993; Matsumura et al., 1996). Activation of calpains in cardiomyocytes has been shown to cleave troponins, NCX, RyR, desmin, actin, myosin and junctophilin (Zeitz et al., 2002; Blunt et al., 2007; Ke et al., 2008; Pedrozo et al., 2010; Celes et al., 2013; Murphy et al., 2013; Wanichawan et al., 2014). In Chapter 3, there was an increase in calpain activity immediately after exhaustive exercise. Therefore, it is possible that activation of calpains resulted in degradation of one or more EC coupling related proteins, which impaired EC coupling and contributed to the cardiac fatigue observed 24 hours post-exercise.

Inhibition of NOX has been shown to prevent exercise-induced cardiac fatigue (Vitiello et al., 2011). It is possible that the increased rate of SR Ca^{2+} leak observed in Chapter 3 was mediated by NOX activation and contributed to the development of cardiac fatigue via two distinct mechanisms. The first mechanism would be a reduction in the amount of stored Ca^{2+} in the SR due to increased Ca^{2+} leak, which would lower the fractional release of Ca^{2+} and the

developed tension in cardiomyocytes. The second mechanism is related to augmented SR Ca^{2+} leak and an elevation in the intracellular Ca^{2+} concentration, which likely activated calpains. Accordingly, the purpose of this study was to supplement rats with APO prior to an exhaustive exercise bout to examine the hypotheses that NOX inhibition would prevent the exercise-induced cardiac fatigue by preventing ROS production, increased SR Ca^{2+} leak and activation of calpains.

Methods

Animals

Adult male Sprague-Dawley rats (21-23 weeks) were used in this study. All animals were obtained from the breeding colony at the University of Waterloo. Animals were housed four per cage, were placed on a reverse 12 hour light cycle and had free access to food and water. All procedures were reviewed and approved by the University of Waterloo Animal Care Committee.

Experimental Design

A pharmacological intervention was employed in this study in an attempt to prevent exercise-induced cardiac fatigue. Rats were provided drinking water supplemented with 1.5 mM APO for 3 days prior to the exhaustive exercise bout. Pilot studies demonstrated that there were no significant differences in the amount of water consumed in the absence or presence of APO and that daily consumption of APO averaged ~19 mg/kg body wt/day. The concentration of APO in the drinking water and consumption rate are well within previously reported concentrations (1.5-12 mM) and consumption rates (4-100 mg/kg/day) (Sanchez et al., 2008; Roe et al., 2011; Vitiello et al., 2011; Castro et al., 2012; Dal-Ros et al., 2012; El-Sawalhi & Ahmed, 2014; Winiarska et al., 2014). The APO supplementation regime used in the current study was selected based off of work by Vitiello and colleagues (2011), who demonstrated that this concentration prevented exercise-induced cardiac fatigue.

Two cohorts of animals were used in this study, the first was used solely for isolated perfused heart experiments and the second was used for *in vitro* experiments (described below). There were three groups in each cohort; a control group (APO CTL), an acute exercise group (APO AC) that was sacrificed immediately following exhaustive exercise and a group that was sacrificed 24 hours after exhaustive exercise (APO 24H). The anthropometric data for all of these

groups are presented in Table 4.1. Animals in all groups were acclimated to treadmill running for 7 days prior to the exhaustive exercise bout. The exhaustive exercise bout utilized was identical to that described in Chapters 2 and 3.

Table 4.1: Anthropometric data from the APO treated in vitro and isolated perfused heart groups

	Masses	APO CTL (n=8)	APO AC (n=8)	APO 24H (n=8)	p values
In Vitro	Body Mass (g)	471 ± 14	464 ± 8	466 ± 7	0.89
	Heart Mass (g)	1.53 ± 0.031	1.51 ± 0.038	1.50 ± 0.060	0.87
	Left Ventricle Mass (g)	1.07 ± 0.026	1.03 ± 0.018	1.04 ± 0.039	0.62
	Left Ventricle/Body Mass	0.00229 ± 0.00010	0.00222 ± 0.00005	0.00223 ± 0.00006	0.81
		APO CTL (n=17)	APO AC (n=12)	APO 24H (n=11)	
Perfused Heart	Body Mass (g)	473 ± 9	484 ± 10	474 ± 12	0.73
	Heart Mass (g)	1.73 ± 0.030	1.83 ± 0.029	1.76 ± 0.044	0.11
	Left Ventricle Mass (g)	1.14 ± 0.021	1.21 ± 0.019 #	1.18 ± 0.027	0.04
	Left Ventricle/Body Mass	0.0024 ± 0.00002*	0.00251 ± 0.00003	0.0025 ± 0.00003	0.01

Anthropometric data from apocynin supplemented animals that were used for isolated perfused heart experiments and *in vitro* experiments. The number of animals in each group is indicated beside the group label. Data are presented as means ± SE.
\# Significantly different (p<0.05) than CTL
* Significantly different (p<0.05) AC & 24H

Isolated Perfused Heart

A detailed description of the isolated perfused heart experiments were presented in Chapters 2 and 3. Briefly, animals were anesthetized via a tail vein injection of sodium pentobarbital (35 mg/kg) prior to excision of the heart. Hearts were mounted to an aortic cannula and perfused in a retrograde fashion at a constant pressure (~80 mmHg) with Krebs-Henseleit buffer warmed to 37°C and bubbled with 95%O_2-5%CO_2. The LV was instrumented with a balloon tipped catheter and the volume of the balloon was adjusted to provide a diastolic pressure of ~10 mmHg. Pressure transducers (MLT844, AD Instruments) were connected to the system proximal to the aortic cannula and to the balloon tipped catheter for determination of perfusion pressure and LV pressure, respectively. An ultrasonic flow probe (2PXL, Transonic Systems)

was placed proximal to the aortic cannula, which measured global coronary flow. Following instrumentation, hearts were allowed to equilibrate for 30 minutes at which point baseline data were recorded. On a subset of hearts (n=6/group) an ISO dose response was performed using a range of ISO concentrations from 10^{-11} to 10^{-7} M. All data were collected using a Powerlab data acquisition system (4/sp, AD Instruments) and were analyzed using Chart software (Ver. 5, AD Instruments).

Plasma Collection and Tissue Sampling

Prior to excision of the heart, blood was drawn from the inferior vena cava into a 1 mL syringe containing 25 µL of 0.195 M reduced glutathione and 0.237 M EGTA pH 7.0. Blood was gently inverted several times and was centrifuged at 4500 g for 10 min. The plasma was collected and stored at -80°C until analysis of NE and Epi concentrations.

In the cohort of animals used for *in vitro* experiments, the hearts from anaesthetized animals (n=8/group) were excised and placed in ice cold homogenizing buffer. Subsequently, the aorta was cannulated using a teflon catheter and flushed with 10 mL of ice cold homogenization buffer to remove blood from the coronary vasculature. The heart was trimmed of atria, the aorta, connective tissue and the right ventricle. A piece of LV was frozen and the remaining LV was diluted (wt:vol, 1:10) in homogenization buffer and homogenized using a motorized tissue grinder (PT3100, Polytron). The piece of LV and homogenate were frozen and stored at -80°C.

DCF fluorescence and ROS Production

ROS production in LV homogenate was determined using DCFH-DA as previously described (Campbell et al., 2014). Briefly, LV homogenates were incubated at 37°C in the dark with 5 µM DCFH-DA in imidazole buffer and DCF fluorescence was quantified using a 96-well

plate spectrofluorometer (SPECTRAmax Gemini XS, Molecular Devices) with excitation and emission wavelengths of 490 nm and 525 nm, respectively. The fluorescence intensity was normalized to the total protein in each well and was expressed as arbitrary units per μg protein (AU/μg protein).

Malondialdehyde Content

MDA content was assessed in fresh LV homogenate following the methods of Ohkawa and colleagues (1979). Briefly, ~25 mg of frozen LV was homogenized in ten volumes of 1.15% KCl using a glass homogenizer (Kontes). LV homogenate samples and MDA standards were reacted with acidic TBA for an hour at 95-100°C and subsequently cooled. After cooling, 500 μL of H_2O and 2.5 mL of a mixture of *n*-butanol and pyridine (15:1, v/v) were added and the samples were vortexed for 30 seconds. Then the samples were centrifuged at 2000 g for 10 minutes, 200 μL of the organic layer from each sample was added to a clear, round bottom 96-well plate and the absorbance was read at 532 nm (SPECTRAmax Plus, Molecular Devices). The MDA concentration in each sample was calculated using the slope and y-intercept of the MDA standard curve and was normalized to protein content in the homogenate.

Ca^{2+}- Dependent Ca^{2+}-ATPase Activity

The assay used to measure Ca^{2+}-dependent Ca^{2+}-ATPase activity was described in detail in Chapter 3 and was adapted from a cuvette based spectrophotometric assay to a 96-well plate reader assay (Simonides & van Hardeveld, 1990; Duhamel et al., 2007). Each LV homogenate sample was added to a cocktail that contained 5 mL assay buffer, 18 U/mL LDH, 18 U/mL PK and 1 μM Ca^{2+} ionophore (A23187, Sigma). Subsequently, the cocktail was subdivided into 16 microcentrifuge tubes with varying concentrations of $CaCl_2$. Next, two aliquots from each of the sixteen subdivisions was loaded onto a clear bottom 96-well plate and then NADH was added to

each well. The decrease in NADH absorbance at 340 nm represents total ATPase activity (SPECTRAmax Plus, Molecular Devices). The difference between the total ATPase activity and the basal ATPase activity (i.e. activity in the presence of CPA) represents the Ca^{2+}-ATPase activity.

Ca^{2+} Uptake, Ca^{2+} Leak and Ca^{2+} Release

Ca^{2+} uptake, Ca^{2+} leak and Ca^{2+} release were measured at 37°C in LV homogenates using Indo-1 as previously described in Chapter 3 and by Tupling & Green (2002). The assay buffer contained (in mM): 200 KCl, 20 HEPES pH7.0, 10 NaN$_3$, 0.005 N,N,N′,N′-tetrakis(2-pyridylmethyl) ethylenediamine, 5 oxalate, 15 MgCl$_2$. In a 4-sided clear cuvette, 1.5 µM Indo-1, ~4.5 µL of 10 mM CaCl$_2$ and ~1.5 mg LV homogenate were brought to a total volume of 2.0 mL with assay buffer. The reaction was initiated with the addition of 40 µL of 250 mM ATP. The rate of Ca^{2+} uptake (µmol·g protein^{-1}·min^{-1}) was determined at a $[Ca^{2+}]_f$ of 2.0, 1.5, 1.0 and 0.5 µM by differentiating the $[Ca^{2+}]_f$ versus time curve. Ca^{2+} release and Ca^{2+} leak were induced using 4-CMC and CPA, respectively, once Ca^{2+} uptake reached a minimum.

In Vitro Activation of NOX, ROS Production and Ca^{2+} Leak

In the previous chapter, it was demonstrated that exhaustive exercise increased ROS production, which was associated with increased SR Ca^{2+} leak and cardiac fatigue. In this study, it was hypothesized that *in vivo* inhibition of NOX would ameliorate exercise-induced ROS production and SR Ca^{2+} leak, which would prevent cardiac fatigue. In an attempt to further confirm this hypothesis several *in vitro* experiments were performed. Previous *in vitro* studies demonstrated that PO$_2$ manipulation or exogenous NADPH activated NOX, which augmented ROS production and increased RyR open probability (Hidalgo et al., 2006; Sun et al., 2011). Therefore, the aim of the first experiment was to determine if endogenous NOX in LV

homogenate could be activated using exogenous NADPH as a substrate. ROS production, as indicated by DCF fluorescence, was assessed in LV homogenate alone, LV homogenate plus 1 mM NADPH and in LV homogenate with 1 mM NADPH and 30 μM APO. Once, it was established that exogenous NADPH could activate NOX and increase ROS production, these incubation conditions (i.e. LV incubation in the presence and absence of APO and NADPH) were performed in LV homogenate subsequent to measurement of SR Ca^{2+} leak.

Calpain Activity

Calpain activity was assessed using a fluorescent assay as described by (McMillan and a, 2011). Briefly, LV homogenates were incubated at 37°C with the non-fluorescent calpain substrate, Suc-LLVY-AMC (Enzo Life Sciences) in the presence or absence of the calpain inhibitor, Z-LL-CHO (Enzo Life Sciences). Calpain activity was calculated as the difference between AMC fluorescence from LV homogenate incubated with and without the calpain inhibitor. The fluorescence intensity was normalized to the total protein in each well and was expressed as arbitrary units per μg protein (AU/μg protein).

Western Blotting

The following antibodies were used in this study. The dilution factor of each primary antibody is provided in the parentheses: SERCA2a (1:4000), PLN (1:2000), RyR (1:1000), NOX4 (1:1000) (Pierce Antibodies); p-PLN (1:1000) (Cell Signaling); anti-GSH (1:1000) (Virogen); Ser2808 p-RyR (1:1000) (Abcam); anti-DNP (1:1000) (Sigma).

The Western blotting protocol used in this study was described in further detail in Chapter 3. Unless described elsewhere, all samples were diluted in 1X Sample Buffer under reducing conditions. Samples were loaded on a polyacrylamide gel and separated using standard electrophoresis techniques (Laemmli, 1970), or in the case of PLN, proteins were separated using

a Tris-Tricine gel (Schaggar, 2006). Once proteins were transferred to a PVDF membrane, the membrane was blocked for 1 hour at room temperature using 5% non-fat milk in TBST. Membranes were washed with TBST and then incubated with the appropriate primary antibody. The membranes were then washed, incubated with secondary antibody and washed a final time. Signals were detected using enhanced chemiluminescence and the ChemiGenius[2] imaging system and GeneSnap Software (SynGene). The optical density of protein bands were quantified using GeneTools Software (SynGene).

Immunoprecipitation

Immunoprecipitation was used to measure post-translational modification of RyR. Anti-RyR antibody was used to immunoprecipitate RyR2 from 200 µg of LV homogenate. The homogenate was diluted in 0.2 mL of a modified radioimmunoprecipitation assay (RIPA) buffer that contained (in mM): 50 Tris pH 7.4, 0.9% NaCl, 5.0 NaF, 1.0 Na_3VO_4, 1% Triton X-100 and Roche Complete Protease Inhibitors and mixed with gentle rotation for 1 hour at 4°C with 1 µg anti-RyR. The immune complexes were incubated with 30 µL of a 50% protein-A sepharose (Sigma) slurry for 1 hour at 4°C. The protein-A sepharose was washed 3 times with RIPA buffer for 5 min and then the immunoprecipitated RyR2 was solubilised by adding 5% SDS. The purified RyR2 was separated using SDS-PAGE and probed for nitration and glutathionylation.

To determine the reactive carbonyl content of RyR the immunoprecipitation procedures outlined above were used with additional steps following the purification of RyR. Briefly, immunoprecipitated RyR was derivatized for 15 minutes at room temperature with 10 mM 2,4-DNPH dissolved in 2 M HCl. Subsequently, the samples were neutralized, loaded on polyacrylamide gels, separated by electrophoresis and Western blotting was performed as outlined in *Western Blotting*.

Plasma Catecholamine Quantification

The concentration of plasma NE and Epi was determined as described in Chapter 3 and by Weicker and colleagues (1984) using high-performance liquid chromatography and electrochemical detection.

Statistics

All data are presented as means ± standard error. A one-way ANOVA was used to compare group means of the variables outlined above. A two-way ANOVA was used to compare group by ISO data. A two-way ANOVA was also used to make comparisons between results from this study and previous chapters. To investigate key relationships, linear regression analysis was performed using GraphPad Prism 4 software. The significance level was set at 0.05, and, when appropriate, a Newman-Keuls post hoc test was used to compare specific means. If a value was greater than 2 standard deviations from the mean that outlying value was removed from the data set.

Results

Anthropometric Data and Run Times

The anthropometric data from the animals used in isolated perfused heart and *in vitro* experiments are presented in Table 4.1. There were no significant differences ($p>0.05$) in any anthropometric measures between the *in vitro* APO CTL, APO AC and APO 24H groups. Similarly, body mass and heart mass were not significantly different ($p>0.05$) in the groups used for isolated perfused heart experiments. However, the LV mass from perfused hearts in the APO AC group was significantly larger ($p<0.05$) than the APO CTL group. In addition, the LV/body mass ratio was significantly lower ($p<0.05$) in the perfused heart APO CTL group compared to the APO AC and APO 24H groups.

Cardiovascular Indices in the Basal State

The results of the isolated perfused heart experiments from animals that were supplemented with 1.5 mM APO in their drinking water are presented in Table 4.2. As hypothesized, APO treatment prevented exercise-induced cardiac fatigue in the basal state, such that there were no significant differences ($p>0.05$) in LVDP between any of the groups (Table 4.2). The LVDP was similar between the three groups, despite the fact that heart rate in the APO AC and APO 24H groups increased ($p<0.05$) by 7.4% and 10.7%, respectively. Importantly, the regression analysis between LVDP and HR did not reveal a significant relationship ($p>0.05$) between these two variables in the current study (Appendix B). In addition to LVDP, the time-to-peak pressure and $\pm dP/dt$ were not different between the APO treated groups ($p>0.05$). In the basal state, there was a trend for increased perfusion pressure in the APO AC. Importantly, there were no significant differences ($p>0.05$) in coronary flow or CVR between the APO CTL, APO AC and APO 24H groups. However, the coronary flow and CVR means in the APO treated

126

groups appeared to differ from the coronary flow and CVR means in the non-APO treated animals from Chapter 2 (See Table 2.2). Therefore, a two-way ANOVA was performed to examine a potential main effect of APO treatment on variables assessed in this Chapter. Unfortunately, a non-APO CTL group was not run concurrently with the APO treated groups, which is major limitation to this study and as such these comparisons and subsequent discussions must be taken with a degree of caution. Interestingly, there were main effects of APO treatment with respect to coronary flow and CVR, such that hearts from animals treated with APO had lower coronary flow and higher CVR ($p < 0.05$).

Table 4.2: Basal cardiac and hemodynamic measures in APO groups

Cardiac Measure	APO CTL (n=17)	APO AC (n=12)	APO 24H (n=11)	p values
LVDP (mmHg)	135 ± 2.7	135 ± 4.1	126 ± 2.4	0.19
LVeDP (mmHg)	8.0 ± 1.20	8.3 ± 1.74	10.1 ± 1.61	0.59
+dP/dt (mmHg/s)	4122 ± 236	4396 ± 235	3943 ± 245	0.47
-dP/dt (mmHg/s)	-2525 ± 91	-2796 ± 157	-2415 ± 96	0.11
Time-to-peak Pressure (ms)	69.2 ± 2.1	67.9 ± 2.5	65.1 ± 2.3	0.46
Heart Rate (bpm)	272 ± 3.5	292 ± 7.8*	301 ± 8.6*	0.01
Perfusion Pressure (mmHg)	79.8 ± 0.25	80.8 ± 0.28	80.0 ± 0.37	0.06
Coronary Flow (mL/min)	16.97 ± 0.81	16.47 ± 0.37	17.57 ± 1.22	0.70
Coronary Vascular Resistance (mmHg/mL/min)	4.86 ± 0.21	4.93 ± 0.11	4.79 ± 0.35	0.93

Summary cardiac and hemodynamic data in the basal state. Abbreviations: Left ventricular developed pressure (LVDP); left ventricular end diastolic pressure (LVeDP); maximal rate of pressure development and pressure decline (±dP/dt). The number of animals in each group is indicated beside the group label. Data are presented as means ± SE.
* Significantly different ($p < 0.05$) CTL

Cardiovascular Indices During β-Adrenergic Stimulation

The cardiac and hemodynamic responses to progressive doses of ISO were assessed on a subset of APO CTL, APO AC and APO 24H hearts and the data are presented in Table 4.3.

There were significant main effects of ISO for all recorded variables. Progressively increasing the concentration of ISO (10^{-11} – 10^{-7} M) infused into the perfusate resulted in an increase in LVDP, $\pm$dP/dt, HR and coronary flow and a decrease in perfusion pressure and CVR (Table 4.3). There were no significant differences ($p>0.05$) in the ISO concentration required to increase LVDP by 50% (in log M: APO CTL -8.59 $\pm$ 0.05 vs. APO AC -8.70 $\pm$ 0.11 vs. APO 24H -8.56 $\pm$ 0.05). In addition, there was no significant effect ($p>0.05$) of exhaustive exercise with respect to any cardiovascular variable.

Table 4.3: Cardiac and hemodynamic responses to isoproterenol

| | Negative log M Isoproterenol Dosage | | | | | | | | | | p values |
	-11	-10	-9.5	-9	-8.6	-8.3	-8	-7.6	-7.3	-7	
LVDP (mmHg)											
CTL	128 ± 4	129 ± 4	137 ± 4	154 ± 6	194 ± 11	212 ± 20	230 ± 13	246 ± 22	265 ± 41	244 ± 15	0.83
AC	130 ± 4	130 ± 4	144 ± 6	160 ± 8	212 ± 11	215 ± 28	234 ± 12	240 ± 19	264 ± 16	250 ± 10	
24H	134 ± 6	134 ± 6	145 ± 6	164 ± 7	203 ± 16	227 ± 33	244 ± 19	269 ± 22	265 ± 37	234 ± 20	
+dP/dt (mmHg/s)											
CTL	4181 ± 252	4253 ± 278	4609 ± 340	5275 ± 478	6646 ± 670	7246 ± 1165	8292 ± 757	9631 ± 1390	11715 ± 2357	10239 ± 1084	0.85
AC	4419 ± 167	4388 ± 183	4743 ± 299	5124 ± 363	6640 ± 538	7122 ± 1271	8098 ± 495	8570 ± 1242	10109 ± 1511	8976 ± 842	
24H	4453 ± 281	4482 ± 301	4929 ± 388	5497 ± 509	6701 ± 912	7610 ± 1782	8337 ± 878	9846 ± 1331	10396 ± 1759	8985 ± 1179	
-dP/dt (mmHg/s)											
CTL	-2702 ± 64	-2714 ± 76	-2946 ± 139	-3421 ± 201	-4462 ± 339	-4776 ± 418	-5367 ± 269	-5542 ± 403	-5838 ± 162	-5516 ± 302	0.93
AC	-2652 ± 89	-2665 ± 110	-3002 ± 160	-3506 ± 244	-4725 ± 386	-5229 ± 739	-5559 ± 462	-6130 ± 579	-5838 ± 834	-5604 ± 402	
24H	-2862 ± 152	-2865 ± 170	-3098 ± 201	-3605 ± 238	-4593 ± 456	-5000 ± 922	-5622 ± 491	-6101 ± 570	-5709 ± 679	-5223 ± 431	
HR (bpm)											
CTL	275 ± 16	276 ± 16	285 ± 15	296 ± 15	309 ± 14	313 ± 23	320 ± 9	335 ± 16	316 ± 20	332 ± 19	0.90
AC	265 ± 8	266 ± 9	276 ± 10	290 ± 9	304 ± 12	305 ± 10	317 ± 14	341 ± 22	320 ± 21	349 ± 22	
24H	277 ± 7	278 ± 7	281 ± 6	283 ± 7	294 ± 8	296 ± 9	308 ± 3	321 ± 7	338 ± 10	352 ± 14	
Coronary Flow (mL/min)											
CTL	18.0 ± 1.5	17.9 ± 1.5	18.8 ± 1.6	20.4 ± 1.4	24.2 ± 1.5	23.7 ± 2.4	22.7 ± 1.5	23.2 ± 2.0	23.7 ± 4.3	24.9 ± 1.9	0.43
AC	15.2 ± 1.4	15.4 ± 1.5	16.6 ± 1.5	18.3 ± 1.6	23.1 ± 1.6	22.6 ± 1.1	25.4 ± 0.9	24.6 ± 3.4	24.8 ± 1.5	22.6 ± 1.9	
24H	18.7 ± 2.0	18.7 ± 2.0	19.8 ± 2.1	20.8 ± 2.1	25.2 ± 2.4	26.5 ± 3.0	27.5 ± 1.6	26.0 ± 2.0	27.6 ± 1.5	26.2 ± 1.9	
Coronary Vascular Resistance (mmHg/mL/min)											
CTL	4.60 ± 0.40	4.63 ± 0.41	4.39 ± 0.38	3.96 ± 0.28	3.27 ± 0.21	3.40 ± 0.46	3.52 ± 0.25	3.47 ± 0.34	3.46 ± 0.67	3.22 ± 0.30	0.51
AC	5.56 ± 0.53	5.56 ± 0.56	5.10 ± 0.49	4.58 ± 0.43	3.49 ± 0.28	3.53 ± 0.20	3.07 ± 0.12	3.37 ± 0.58	3.15 ± 0.17	3.57 ± 0.34	
24H	4.59 ± 0.55	4.58 ± 0.53	4.32 ± 0.51	4.06 ± 0.44	3.26 ± 0.33	3.10 ± 0.38	2.86 ± 0.16	3.11 ± 0.27	2.85 ± 0.19	3.08 ± 0.32	

Summary of cardiac and hemodynamic response to progressive dosages of isoproterenol. Each negative log molar concentration of isoproterenol is indicated in the first row. The cardiac and hemodynamic variables are indicated in the first column. Abbreviations: left ventricular developed pressure (LVDP); rate of pressure development (+dP/dt); rate of pressure decline (-dP/dt); heart rate (HR). The p value corresponds with the main effect of exercise.

Data are presented as mean ± SE (n=6).

There were no interaction effects for any variable analyzed.

There was a main effect of isoproterenol for all variables.

Catecholamines

The concentration of plasma Epi and NE were assessed using HPLC. Similar to Chapter 3, there were no significant differences ($p>0.05$) in plasma NE concentration among the three APO treated groups. Interestingly, there were no differences ($p>0.05$) in the concentration of Epi between the APO groups (Figure 4.1). Comparison of these data to the Epi and NE data from Chapter 3 revealed a main effect of APO, whereby plasma Epi concentration was lower ($p<0.05$) in APO treated animals when compared to the non-APO treated groups. There was no main effect of APO treatment on plasma NE concentration ($p>0.05$).
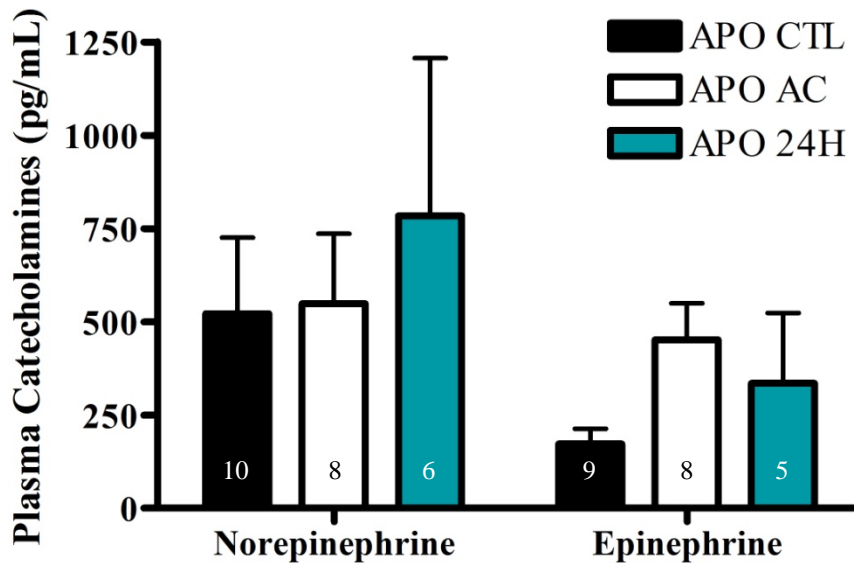
Figure 4.1. The concentration of norepinephrine and epinephrine (pg/mL) in the plasma from the APO CTL, APO AC and APO 24H groups. The number in each bar represents the number of samples used for statistical analysis as several outliers were removed. Values are means ± SE.

Reactive Oxygen Species Production and Lipid Peroxidation

Homogenates isolated from the LV of animals treated with APO were incubated with DCFH-DA to measure the production of ROS. As hypothesized, there were no significant differences (p>0.05) in fluorescent intensity of DCF between the three APO treated groups (Figure 4.2A). Furthermore, when compared to the DCF fluorescence data from Chapter 3, the ROS production in the APO treated groups were lower (p<0.05) than the non-APO treated groups. The MDA concentration (i.e. lipid peroxidation) in LV homogenates from the APO treated groups were not significantly different from each other (p>0.05) (Figure 4.2B). Furthermore, there was no main effect (p>0.05) of APO treatment on lipid peroxidation.
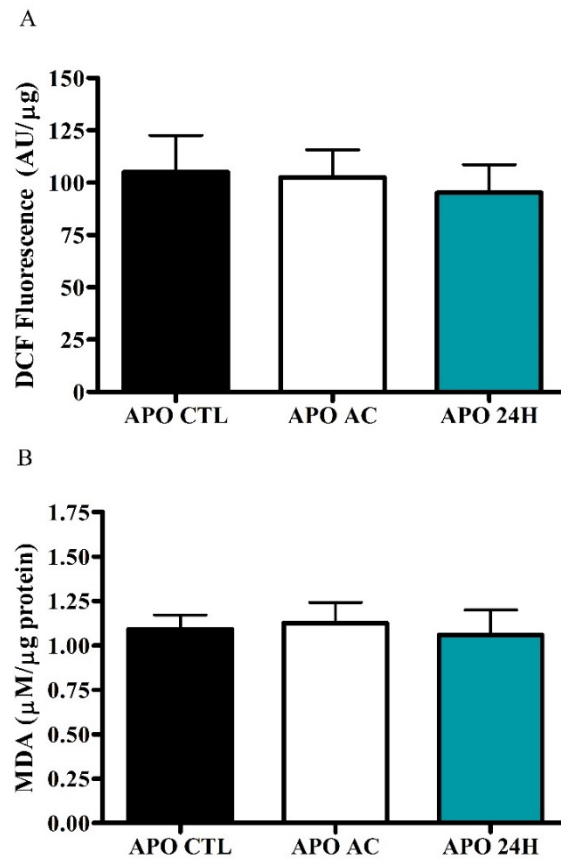
Figure 4.2. ROS production and lipid peroxidation in APO treated groups. (A) The production of ROS was assessed by measuring DCF fluorescence in LV homogenate (n=6). (B) Lipid peroxidation was determined by measuring the concentration malondialdehyde (MDA) in LV homogenate (n=8). All values were normalized to total protein and are presented as means ± SE.

131

SERCA2a Function

The maximal rate of Ca^{2+}-ATPase activity and the rate of Ca^{2+} uptake were not different between the three APO treated groups in this study (Figure 4.3B & C). However, several main effects of APO treatment have revealed some interesting findings regarding SERCA2a function. On average, the apparent Ca^{2+} affinity of SERCA2a (i.e. pCa_{50}) was greater ($p<0.05$) in the APO treated groups when compared to the non-APO treated groups. This can be illustrated by examining the Ca^{2+}-dependent Ca^{2+}-ATPase activity of the CTL and APO CTL groups (Figure 4.4A). Additionally, there were main effects of APO on maximal Ca^{2+}-ATPase activity and Ca^{2+} uptake, such that Ca^{2+}-ATPase activity was lower and Ca^{2+} uptake was higher in the APO treated groups ($p<0.05$). This observation lead to an examination of the coupling ratio, which provides a measure of the transport efficiency of SERCA2a (i.e. the moles of Ca^{2+} transport per mole ATP hydrolyzed) and is calculated by dividing the rate of Ca^{2+} uptake at 2.0 µM by the maximal Ca^{2+}-ATPase activity. The coupling ratios were significantly higher ($p<0.05$) across groups that were provided APO in their drinking water when compared to non-APO treated groups (Figure 4.4B).
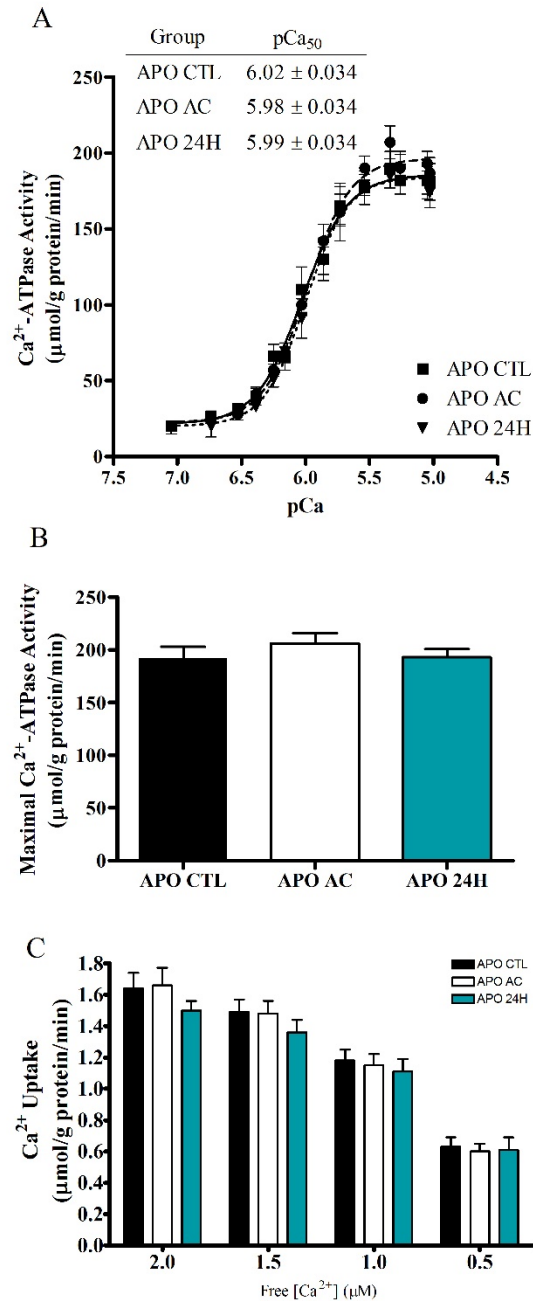
Figure 4.3. SERCA2a function in APO treated groups. (A) The rate of Ca^{2+}-dependent Ca^{2+}-ATPase activity was assessed in left ventricle homogenate from APO CTL (solid squares), APO AC (solid circles) and APO 24H groups (solid triangle), over a negative log molar range of ~7-5. The pCa_{50} for Ca^{2+}-ATPase activity is displayed in the inset. (B) The maximal rate of Ca^{2+}-dependent Ca^{2+}-ATPase activity. (C) The rate of oxalate supported Ca^{2+} uptake was assessed in LV homogenates using Indo-1 and dual emission spectrofluorometry. The slope of the Ca^{2+} uptake curve was determined by differentiating the curve at four different free Ca^{2+} concentrations. Values are means ± SE (n=8).
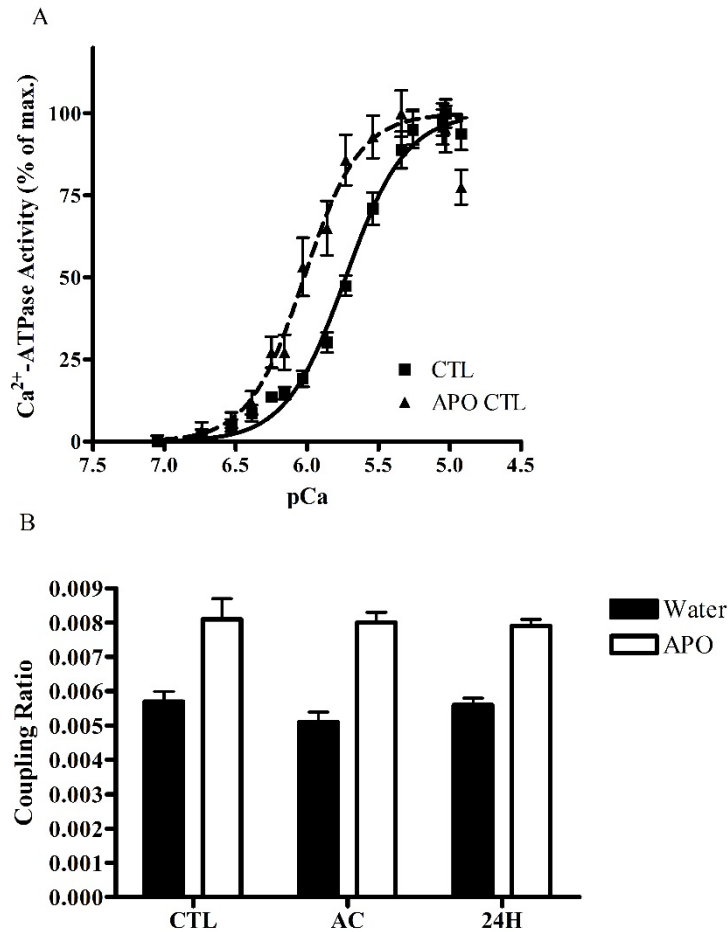
Figure 4.4. Comparison of the coupling ratios and Ca^{2+}-dependent Ca^{2+}-ATPase activity between Chapter 3 and Chapter 4. (A) The rate of Ca^{2+}-dependent Ca^{2+}-ATPase activity normalized to the maximal Ca^{2+}-ATPase activity in the CTL group from Chapter 3 (solid squares) and the APO CTL group from the current study (solid triangles). (B) The coupling ratio was calculated by dividing the rate of Ca^{2+} uptake at 2.0 μM by the maximal Ca^{2+}-ATPase activity. Solid bars represent the coupling ratios from Chapter 3 and open bars are the coupling ratios from the current study. Values are means ± SE. There were a main effects of APO such that pCa_{50} and coupling ratios were higher in APO treated groups.

RyR Function

      The function of the Ca^{2+} release channel was assessed by determining the rates of SR Ca^{2+} release and the rates of SR Ca^{2+} leak. The rates of 4-CMC-induced Ca^{2+} release were not significantly different ($p>0.05$) between the three APO groups (Figure 4.5A). However, there was a main effect of APO treatment on the rates of Ca^{2+} release whereby the APO treated groups had higher ($p<0.05$) rates of Ca^{2+} release when compared to the non-APO treated groups. As hypothesized, APO treatment preserved SR Ca^{2+} leak, such that leak was not significantly different ($p>0.05$) between the APO CTL, APO AC and APO 24H groups (Figure 4.5B). In addition, a main effect of APO was observed between groups in Chapter 3 and the current study, with SR Ca^{2+} leak being lower ($p<0.05$) in the APO treated animals.
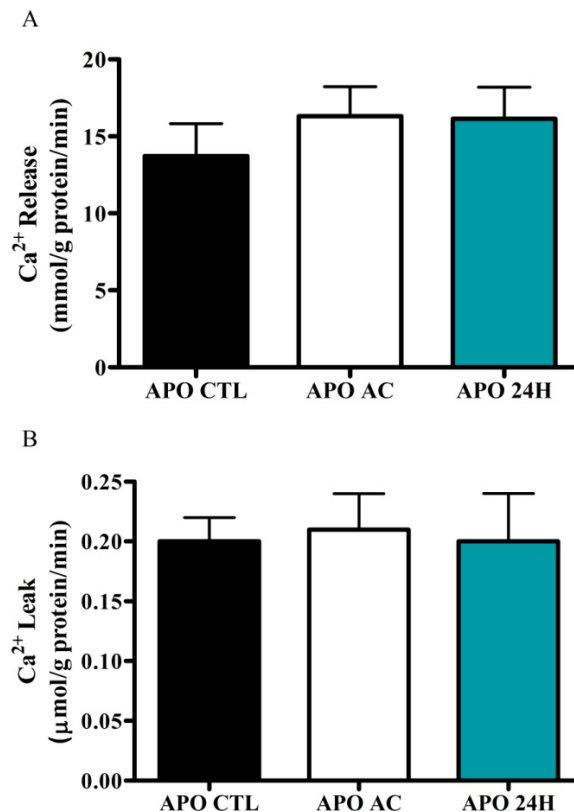
Figure 4.5. RyR function in APO treated groups. (A) The rates of 4-CMC-induced Ca^{2+} release in the APO treated groups. (B) The rates of Ca^{2+} leak out of the SR was assessed following the addition of CPA to the assay once Ca^{2+} uptake reached a minimum (see *Methods*). Values are means ± SE (n=8).

Calpain Activity

The calpain activity was assessed by incubating LV homogenate with the minimally fluorescent calpain substrate, Suc-LLVY-AMC, and monitoring the fluorescence in the presence or absence of Z-LL-CHO, a calpain inhibitor. It was hypothesized that NOX inhibition would prevent calpain activation following exhaustive exercise. As illustrated in Figure 4.6, calpain activity was not altered by exhaustive exercise in animals that were given APO (p>0.05).
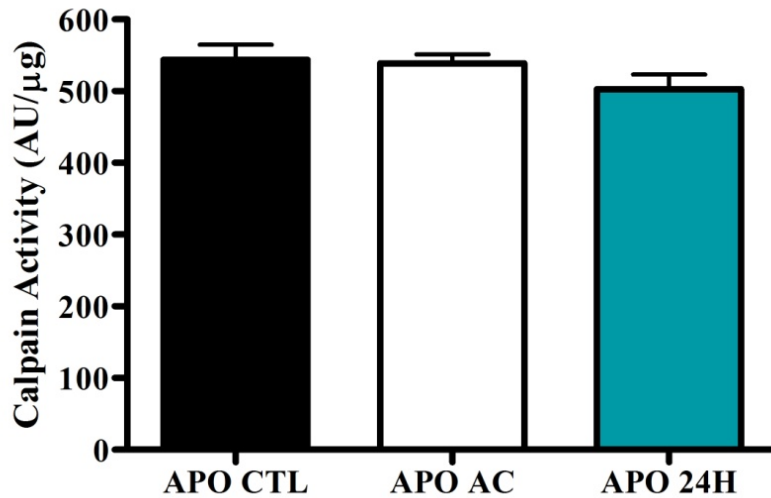
Figure 4.6. Calpain activity in APO treated groups. Calpain activity was determined in LV homogenates by measuring the fluorescence of AMC (7-amino-4-methylcoumarin), the cleavage product of Suc-LLVY-AMC. Calpain activity was calculated as the difference between AMC fluorescence in the absence or presence of a calpain inhibitor (Z-LL-CHO) normalized to total protein. Values are means ± SE (n=5).

Western Blotting

Western blotting was performed to determine the content of proteins and their phosphorylation status. Three days of APO consumption did not alter (p>0.05) the expression of NOX4 in the LV of rats from the APO CTL, APO AC and APO 24H groups (Figure 4.7C). There were no differences (p>0.05) between the three APO treated groups in relation to SERCA2a content, PLN content or phosphorylation of PLN (Figure 4.7). In addition, there were no

significant differences (p>0.05) in total RyR or the ratio of pRyR to RyR between the three APO

treated groups (Figure 4.8). Interestingly, the pRyR to RyR ratio was higher (p<0.05) in APO

treated animals when compared to non-APO treated counterparts. Consistent with the findings

from Chapter 3, there were no significant (p>0.05) oxidative modifications to RyR in the APO

AC and APO 24H groups when compared to the APO CTL group (Figure 4.9).
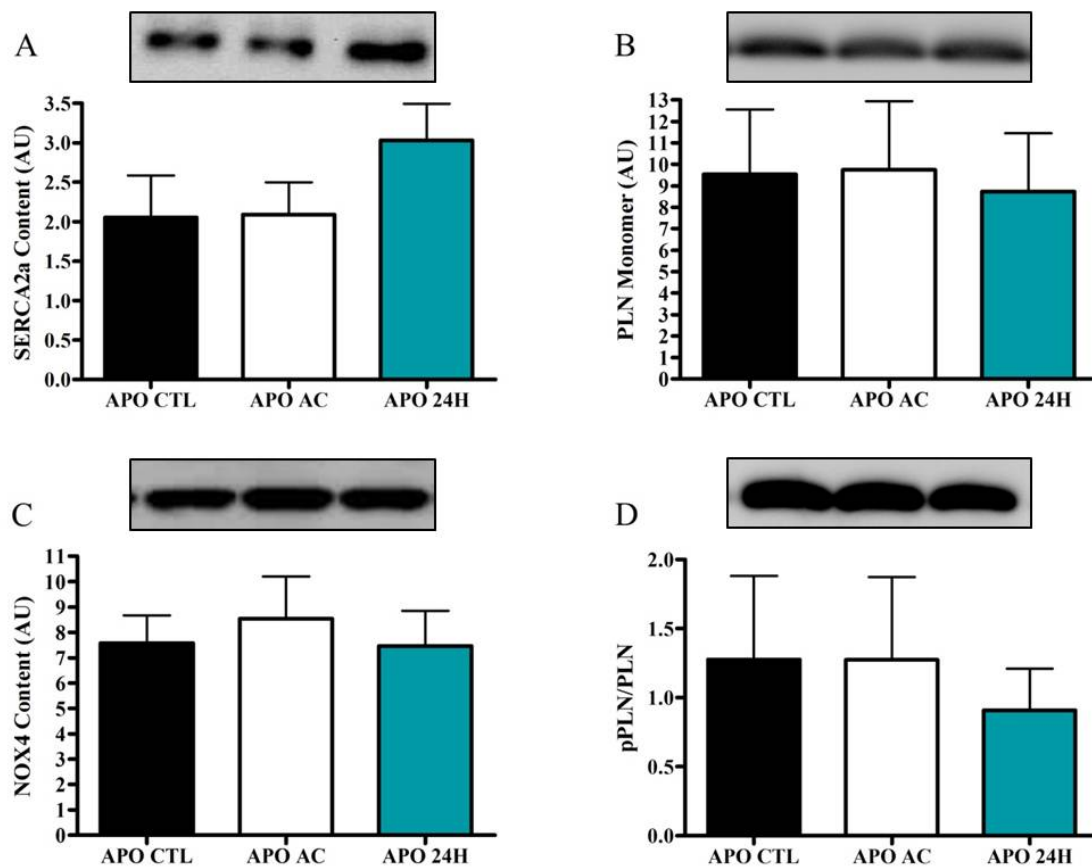
Figure 4.7. Western blot analysis of whole LV homogenates from APO treated groups. The inset in each panel is a representative blot, which was loaded in the same sequence as displayed on the bar graphs. (A) SERCA2a protein content. (B) Protein content of the PLN monomer. (C) NOX4 content. (D) The ratio of phosphorylated monomeric PLN to monomeric PLN; the inset blot is pPLN. Values are means ± SE (n=8).
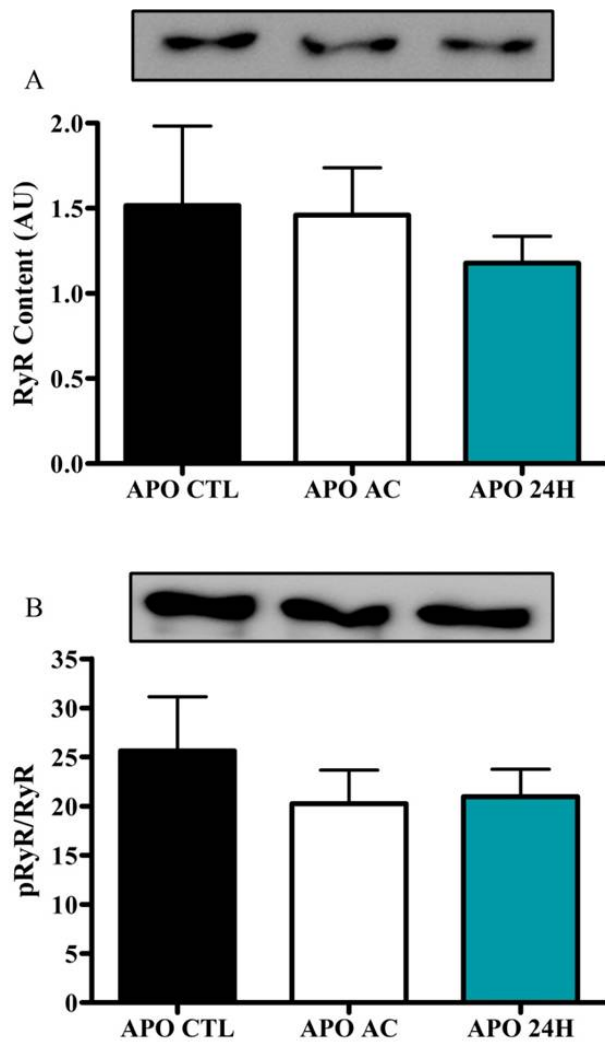
Figure 4.8. Western blot analysis of RyR2 from APO treated groups. The inset in each panel is a representative blot, which was loaded in the same sequence as the data displayed on the bar graphs. (A) Total RyR protein content. (B) The ratio of phosphorylated RyR to RyR; the inset blot is pRyR. Values are means ± SE (n=8).
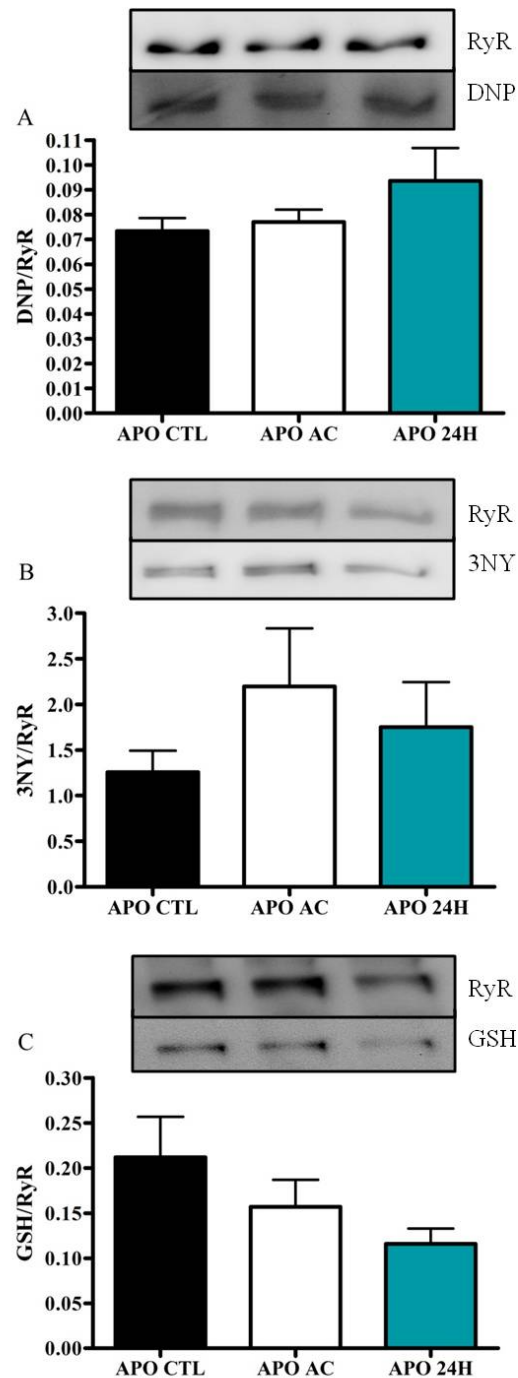
Figure 4.9. Oxidative modification of RyR was assessed using immunoprecipitation and Western blotting techniques. RyR was probed for (A) carbonyl content as indicated using anti-DNP antibody, (B) 3-nitrotyrosine and (C) glutathionylation. Representative blots of the RyR pull down via immunoprecipitation and the post-translational modification to RyR are provided in each panel. Samples were loaded in the same order as the data presented in the bar graphs. Data are ratios of modified RyR to total RyR and are presented as means ± SE (n=8).

In Vitro Activation of NOX, ROS Production and SR Ca^{2+} Leak

To support the hypotheses that exercise-induced NOX activation increased SR Ca^{2+} leak and that NOX inhibition contributed to the reduction of SR Ca^{2+} leak observed in the current study, *in vitro* experiments were performed to activate NOX and assess ROS production and SR Ca^{2+} leak. Incubation of LV homogenates with 1 mM NADPH increased ($p < 0.05$) ROS production by ~30% when compared to LV homogenates alone (Figure 4.10A). The addition of 30 µM APO to LV homogenates incubated with 1 mM NADPH prevented the increase in ROS production. These experiments were repeated, but instead of measuring ROS production, samples were assayed for SR Ca^{2+} leak. In the presence of 1 mM NADPH there was a significant increase ($p < 0.05$) in SR Ca^{2+} leak, which was prevented in the presence of APO (Figure 4.10B).
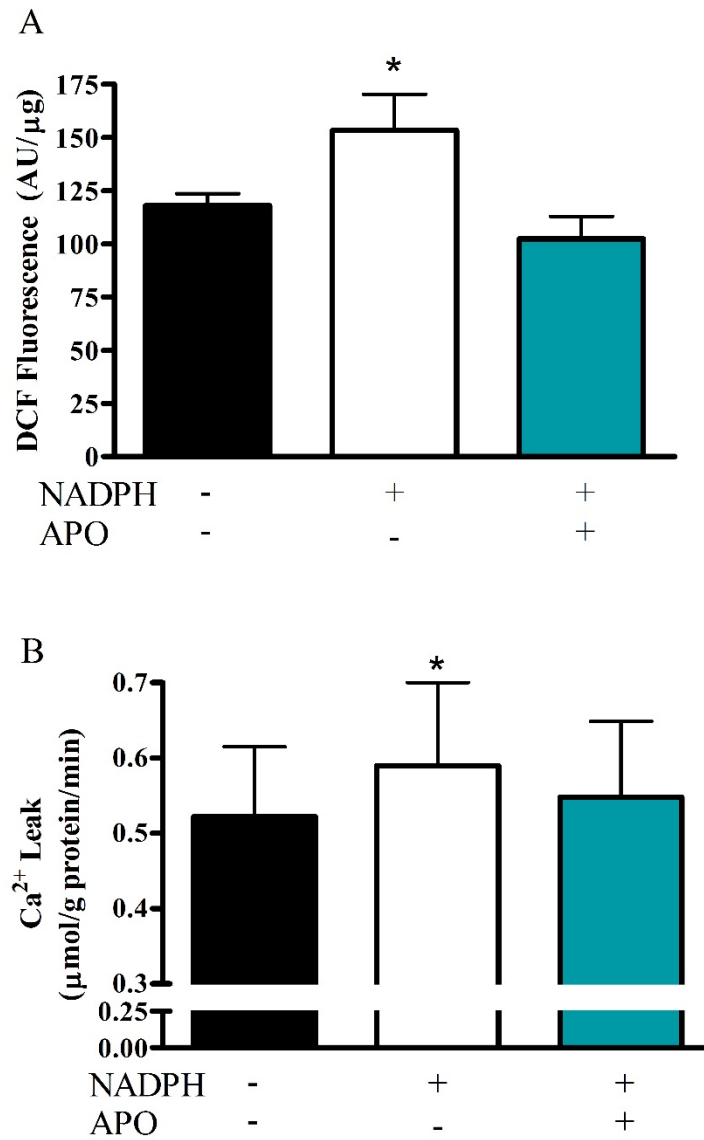
Figure 4.10. *In vitro* activation of NOX and assessment of ROS production and SR Ca^{2+} leak. (A) ROS production assessed by measuring DCF fluorescence. LV homogenates were incubated with 1 mM NADPH to activate NOX and in some experiments 30 μM APO were added to inhibit NOX. The presence or absence of a chemical is indicated by a "+" or "-", respectively. (B) LV homogenates were exposed to the same concentrations of NADPH or APO and SR Ca^{2+} leak was assessed using Indo-1 and dual emission fluorometry. Values are means $\pm$ SE (n=8). * Significantly different (p<0.05) than the other groups.

Discussion

This study produced several novel findings regarding acute exercise and cardiac function. The first was that APO supplementation and inhibition of NOX prior to exhaustive exercise prevented exercise-induced cardiac fatigue. The second was that NOX inhibition resulted in improved Ca^{2+} regulation in the form of a reduction in SR Ca^{2+} leak, an increase in the coupling ratio and an increase in the apparent Ca^{2+} affinity of SERCA2a. The third exciting finding was that NOX inhibition prevented activation of calpains immediately following exhaustive exercise. Lastly, it was demonstrated that activation of NOX *in vitro* in LV homogenates can regulate RyR2 function, which resulted in an increase in the rate of SR Ca^{2+} leak.

A key finding in this study was that NOX inhibition prevented exercise-induced cardiac fatigue in the basal state. This is primarily evident in the LVDP data, which demonstrated that NOX inhibition prevented an exercise-induced decline in LVDP. These findings are in support of a previous study that inhibited NOX using APO prior to a prolonged, submaximal exercise bout (Vitiello et al., 2011). In that study, acute exercise resulted in a significant decline in LVDP in the absence of NOX inhibition. However, inhibition of NOX maintained LVDP following the prolonged exercise bout (Vitiello et al., 2011). In the current study, the ±dP/dt were not significant different between the APO CTL, APO AC and APO 24H groups. Similarly, the study by Vitiello and colleagues (2011) found that ±dP/dt was not different between control and exercise groups that consumed APO. These data suggest that by inhibiting NOX activity, the contractile function of the myocardium is maintained following exhaustive exercise.

The protective effects of NOX inhibition observed in the basal state carried forward during β-adrenergic stimulation of the isolated perfused hearts. A novel finding in this study was that LVDP was not significantly different between the three APO groups during infusion of

progressively higher concentrations of ISO. This is in contrast to the results of Chapter 2, which demonstrated that cardiac fatigue (i.e. depressed LVDP) persisted throughout the ISO dose response. In addition, there were no significant differences in the $\pm$dP/dt of isolated perfused hearts when NOX was inhibited. Unfortunately, the $\pm$dP/dt during β-adrenergic stimulation were not reported by Vitiello and co-workers (2011). In Chapter 2, there was a significant reduction in the $-$dP/dt during β-adrenergic stimulation in the AC group. It is possible that improved Ca^{2+} regulation, namely decreased SR Ca^{2+} leak, increased apparent affinity of SERCA2a for Ca^{2+} and the coupling ratios (discussed below), contributed to the maintenance of $-$dP/dt in the APO AC group in the current study. These data suggest that the mechanism responsible for the cardiac fatigue present during β-adrenergic stimulation in Chapter 2 was mitigated by NOX inhibition.

The basal LVDP in the APO AC and APO 24H groups were similar to the LVDP in the APO CTL group despite a significant 7.4% and 10.7% increase in heart rate in the APO AC and APO 24H groups, respectively. Linear regression analysis of LVDP and heart rate produced a negative, non-significant correlation coefficient, which suggests that an increase in heart rate was not related to a decrease in LVDP. However, the force frequency relationship in isolated perfused rodent hearts has been shown to be negative (Simor et al., 1997; Lankford et al., 1998; Dias et al., 2006). In the isolated perfused mouse heart, an increase in the stimulation frequency from 300 to 600 bpm resulted in a progressive reduction in LVDP (Dias et al., 2006). Another study perfused rat hearts at a constant pressure and paced the hearts from 250 to 500 bpm and monitored changes in LVDP (Simor et al., 1997). When the stimulation frequency was increased from 250 to 300 bpm the LVDP declined by ~33%. A similar study observed a modest reduction of ~8% in LVDP when stimulation frequency was increased from 250 to 300 bpm (Lankford et al., 1998). The increase in heart rate between the APO AC group and APO CTL group was 20

bpm and between the APO 24H group and APO CTL group was 29 bpm. If the changes in heart rate in the current study were extrapolated to the trends observed in the studies by Simor and co-workers (1997) and Lankford and colleagues (1998), it would be expected that the increased heart rate could have resulted in a ~4-16% reduction in LVDP. These data suggest that, the LVDP in the APO AC and APO 24H groups could possibly have been higher, had heart rate not been elevated in these groups.

Coronary flow was not affected by the combination of NOX inhibition and exhaustive exercise, suggesting that changes in coronary flow were not responsible for the preserved LVDP observed in the current study. However, APO treatment resulted in significantly lower coronary flow across all three APO groups when compared to the coronary flow data from Chapter 2. Attenuated delivery of oxygen (i.e. ischemia) would result in a reduction in LVDP (Hamilton et al., 2003; Cai et al., 2003). APO has been shown to have no effect on basal coronary flow in the isolated perfused mouse heart and the conscious instrumented dog (Zhang et al., 2009; El-Awady et al., 2013). In aortic rings, APO has been shown to have vasodilatory effects in healthy animals and in animals with endothelial dysfunction (i.e. hypertension, genetic knockouts) (Oelze et al., 2006; Baumer et al., 2007; Unger & Patil, 2009; Senejoux et al., 2011). These findings would suggest that consumption of APO would have resulted in vasodilation and increased coronary flow. However, this hypothesis was not supported when the CVR and coronary flow data from the current study were compared to the hemodynamic data from Chapter 2. Thus, the mechanism responsible for the reduced coronary flow in the current study may not reside in the coronary vasculature, but rather the ventricular myocyte. A major determinant of coronary flow is the metabolic demand of the myocardium (Duncker & Bache, 2008). The metabolic demand in the myocardium may have been reduced in APO treated animals. The coupling ratio was

significantly higher in APO treated animals, which means that the ATP cost to transport a given amount of Ca^{2+} across the SR membrane was reduced. Furthermore, the rate of SR Ca^{2+} leak across the three APO treated groups was lower than the non-APO treated groups. Lower Ca^{2+} leak would lead to less Ca^{2+}-ATPase activity during diastole, which would potentially lower ATP demand even further. Although speculative, this improved Ca^{2+} transport efficiency and lower Ca^{2+} leak may have lowered ATP demand in the LV and thus lowered LV oxygen demand, which resulted in reduced coronary flow.

The intracellular mechanisms associated with NOX inhibition and prevention of cardiac fatigue were evaluated using LV homogenates from a second cohort of animals treated with APO. Several studies have demonstrated an increased production of ROS and increased lipid peroxidation in LV from animals that exhibited exercise-induced cardiac fatigue (Wonders et al., 2007; Vitiello et al., 2011; Olah et al., 2015). In Chapter 3, it was demonstrated that exhaustive exercise resulted in a significant increase in ROS production, which was associated with a reduction in LVDP. To determine if ROS generated during exhaustive exercise were due to activation of NOX, 1.5 mM APO was supplemented in the drinking water of rats for three days prior to the exercise bout. In the current study, inhibition of NOX prevented the increase in ROS production in LV homogenates collected immediately after the exhaustive exercise bout. Furthermore, there was significantly lower ROS production in each group in the presence of NOX inhibition (i.e. the current study) when compared to groups in the absence of NOX inhibition (i.e. Chapter 3). These findings are supported by a study by Vitiello and colleagues (2011), who provided APO in the drinking water of rats and subjected them to prolonged treadmill running. Following prolonged exercise the ratios of GSH to GSSH were not significantly different between the APO treated group and the control group (Vitiello et al.,

2011). In the current study, the concentrations of MDA in LV homogenates were not significantly different between the APO treated groups. Visually, when the lipid peroxidation data from Chapter 3 and the current study were compared there appeared to be an effect of acute exercise on non-APO treated animals. However, analysis of both these data sets did not reveal a significant interaction or main effect of APO treatment. These findings suggest that lipid peroxidation may not factor into the development of cardiac fatigue, which is opposite to a previous study (Wonders et al., 2007). By inhibiting NOX, ROS production was blunted, which suggests that NOX is activated during acute exercise and is likely a main source of ROS production in the rat myocardium during exercise.

The reduced ROS production observed in the present study may have been mediated in part by the reduction in plasma Epi concentration following acute exercise. It has been demonstrated that stimulation of β-adrenergic receptors results in elevated ROS production within cardiomyocytes (Zhang et al., 2005; Andersson et al., 2011a; Bovo et al., 2012). Indeed, incubation of isolated rat cardiomyocytes with Epi has been demonstrated to increase production of ROS (Costa et al., 2009). A novel finding in this study was that the concentration of plasma Epi in the APO AC group was not significantly different than the APO CTL and APO 24H groups. As a result, the plasma Epi concentration was lower in APO treated groups when compared to non-APO treated groups. The mechanism by which NOX inhibition prevented the rise in circulating Epi is not immediately clear in this study. Epi is secreted from chromaffin cells in the adrenal medulla. One study demonstrated that intermittent hypoxia augmented Epi secretion from chromaffin cells. If cells were incubated with inhibitors of NOX or RyR prior to hypoxia, then Epi secretion was reduced (Souvannakitti et al., 2010). Perhaps APO prevented

activation of NOX in the adrenal medulla during exhaustive exercise, which reduced the secretion of Epi.

The prevention of exercise-induced cardiac fatigue may have been mediated by changes in SERCA2a Ca^{2+} transport efficiency. When compared to the APO CTL group, exhaustive exercise did not alter the maximal Ca^{2+}-ATPase activity or the rate of Ca^{2+} uptake in the APO AC or APO 24H groups. However, maximal Ca^{2+}-ATPase activity and Ca^{2+} uptake were lower and higher, respectively, in all APO treated groups when compared to the non-APO treated groups in Chapter 3. These differences in Ca^{2+}-ATPase activity and Ca^{2+} uptake resulted in a significantly higher coupling ratio in APO treated groups. An increased coupling ratio indicates that there is greater net Ca^{2+} accumulation in the SR for a given amount of ATP hydrolysis (de Meis, 2002). The increased coupling ratio was likely mediated by an increase in the apparent Ca^{2+} affinity of SERCA2a and lower rates of SR Ca^{2+} leak in the APO treated groups (Chamberlain et al., 1984; Beeler & Gable, 1994; Frank et al., 2000). In the current study, there were no significant differences in the expression of SERCA2a or the phosphorylation status of PLN between the APO treated groups. However, the ratio of pPLN to PLN was greater in APO treated groups compared to non-APO treated groups, which would have increased the apparent Ca^{2+} affinity of SERCA2a. A study by Frank and colleagues (2000) observed a leftward shift in the Ca^{2+}-dependent Ca^{2+}-ATPase curve and an increase in the coupling ratio in the LV of PLN knockout mice. These findings were replicated in LV of wild type mice when PLN was phosphorylated via the addition of active PKA, which is in support of the observations in the current study. The increased phosphorylation of PLN observed in the current study cannot be accounted for by the NE and Epi data. Indeed, there was a main effect of Epi, such that the plasma concentrations were lower in the APO treated groups. Intuitively, this would result in a

147

reduction in PLN phosphorylation. It is possible that NOX inhibition contributed to the enhanced phosphorylation of PLN. However, there are conflicting reports in the literature regarding activation and inhibition of NOX and the phosphorylation status of PLN. In a MDX model of cardiomyopathy, inhibition of NOX resulted in a significant increase in pPLN. However, NOX inhibition had no effect on pPLN content in cardiomyocytes from wild type mice (Gonzalez et al., 2014). In another study, perfusion of isolated rat hearts with APO alone had no effect on pPLN content, but when APO and dobutamine were combined there was greater pPLN content compared to dobutamine alone (Kubin et al., 2011). Lastly, studies using isolated cardiomyocytes have demonstrated that activation of NOX via angiotensin II augmented pPLN content (Jin et al., 2012; Zhang et al., 2015). Thus, the mechanism by which NOX inhibition increased pPLN content in the current study is not clear. Regardless, the functional consequence of increased pPLN content, coupling ratio and the apparent affinity of SERCA2a for Ca^{2+} would result in enhanced Ca^{2+} sequestration at low $[Ca^{2+}]_f$ (i.e. during diastole) (Frank et al., 2000). This would increase SR Ca^{2+} load and augment the fractional release of Ca^{2+}, which would result in a more forceful contraction. This may account for the protection against exercise-induced cardiac fatigue afforded by NOX inhibition.

Another novel finding regarding Ca^{2+} regulation was that NOX inhibition enhanced RyR function when assessed *in vitro*. The rates of SR Ca^{2+} leak were not significantly different in the APO AC group when compared to the APO CTL group. In addition, the rate of SR Ca^{2+} leak in Chapter 3 was significantly elevated in the AC group, which was associated with a reduction in LVDP. On average, the rates of SR Ca^{2+} leak were lower in the APO treated groups when compared to the non-APO treated groups. These data suggest that NOX inhibition prevented aberrant SR Ca^{2+} leak and may have contributed to the prevention of exercise-induced cardiac

fatigue. These findings are opposite to a study by Sanchez and co-workers (2008), who demonstrated that NOX activation and augmented RyR glutathionylation decreased the rate of SR Ca^{2+} leak following a brief bout of aerobic exercise. Unfortunately, these authors did not investigate the effects of NOX inhibition on SR Ca^{2+} leak following acute exercise. In the current study there was a main effect of APO for RyR glutathionylation, such that APO treated groups had lower glutathionylated RyR content when compared to non-APO treated groups. Given the observations by Sanchez and colleagues (2008), a reduction in glutathionylated RyR would be expected to increase SR Ca^2 leak. Similarly, there was significantly greater pRyR content in APO treated groups when compared to non-APO groups, which would be expected to increase SR Ca^{2+} leak (Wehrens et al., 2007). Thus, the mechanisms associated with the protective effects of NOX inhibition on SR Ca^{2+} leak remain to be determined.

The function of RyR was also determined by measuring the rate of 4-CMC-induced Ca^{2+} release. In the current study, there were no significant differences in the rates of Ca^{2+} release between the APO CTL, APO AC and APO 24H groups. However, the rate of Ca^{2+} release was significantly higher in the APO treated groups when compared to the non-APO treated groups. These findings are paradoxical as activation of NOX has been demonstrated to increase Ca^{2+} release in skeletal and cardiac muscle preparations (Hidalgo et al., 2006; Sanchez et al., 2008; Donoso et al., 2014). Therefore, inactivation of NOX would be expected to reduce the rate of SR Ca^{2+} release. In addition, exogenous ROS have been demonstrated to increase the rate of SR Ca^{2+} release (Stoyanovsky et al., 1997; Cheong et al., 2005). ROS production was lower in the APO treated groups, which would be expected to cause a reduction in SR Ca^{2+} release. The reduction in SR Ca^{2+} leak and the leftward shift in the Ca^{2+}-ATPase activity curve in the current

study would result in augmented SR Ca^{2+} load and greater fractional Ca^{2+} release *in vivo*. These factors may have contributed to the greater rate of Ca^{2+} release in the APO treated animals.

To demonstrate that NOX can regulate RyR, *in vitro* experiments were employed in an attempt to activate NOX and subsequently assess SR Ca^{2+} leak. Incubation of LV homogenates with exogenous NADPH significantly increased NOX dependent ROS production, which was prevented when APO was incubated in combination with NADPH. When LV homogenates were incubated with NADPH there was an increase in the rate of SR Ca^{2+} leak, which was prevented by the addition of APO to the assay. Similar *in vitro* findings have been observed using skeletal muscle samples. Sun and co-workers (2011) incubated SR vesicles isolated from rabbit hindlimb muscles with 1 mM NADPH and observed a significant increase in NOX mediated ROS production and an increase in the open probability of RyR1. A similar study reported that 0.1-0.5 mM NADPH incubated with isolated triads caused an increase in the open probability of RyR1 (Hidalgo et al., 2006). Taken together, these studies and the current study demonstrate that *in vitro* activation of NOX can regulate RyR function. This is an important finding as it supports the hypothesis that exhaustive exercise activated NOX *in vivo*, which was associated with an increased rate of SR Ca^{2+} leak and cardiac fatigue.

In Chapter 3 it was observed that calpain activity was increased in the AC group when compared to the CTL group. In this study, inhibition of NOX prevented exercise-induced activation of calpains as there were no significant differences between the APO treated groups. Activation of calpains in isolated cardiomyocytes has been shown using high glucose or NE as a stressor, which resulted in apoptosis (Li et al., 2009a; Li et al., 2009b). Cell death and calpain activation were prevented when cardiomyocytes were incubated with either a NOX or RyR inhibitor prior to the lethal stress. The fact that calpains were not activated during exhaustive

exercise may have contributed to the preservation of LVDP in the APO 24H group. Once activated, calpains can degrade a host of EC coupling related proteins, which include, but are not limited to troponins, NCX, RyR, desmin, actin, myosin and junctophilin (Zeitz et al., 2002; Blunt et al., 2007; Ke et al., 2008; Pedrozo et al., 2010; Celes et al., 2013; Murphy et al., 2013; Wanichawan et al., 2014). These studies suggest that there is a potential interaction between NOX activation, RyR dysfunction, increased cytosolic Ca^{2+} concentration, activation of calpains and excitation-contraction uncoupling. Inhibition of this pathway may explain the protective effects of APO on LVDP observed in the current study.

To summarize, this study used a pharmacological intervention, namely APO treatment for 3 days, to inhibit NADPH oxidase. It was demonstrated that NOX inhibition prevented exercise-induced cardiac fatigue observed immediately following and 24 hours after the exercise bout. In addition, the production of ROS in the APO AC group was not different than the APO CTL group and on average, the APO treated groups had lower ROS production than the non-APO treated groups. The mechanisms responsible for the APO mediated preservation of LVDP in hearts from animals that ran to exhaustion appear to be due to improved Ca^{2+} regulation, which was associated with preserved calpain activity. In Chapter 3 it was demonstrated that acute, exhaustive exercise increased SR Ca^{2+} leak and calpain activity. Inhibition of NOX maintained the rate of SR Ca^{2+} leak in the APO AC group, such that it was not different than the APO CTL group. The altered RyR function was not mediated by phosphorylation or post-translational oxidative modification. To confirm the relationship between NOX and RyR, NOX was activated *in vitro*, which increased ROS production and resulted in RyR mediated SR Ca^{2+} leak. When these *in vitro* experiments were repeated in the presence of APO, ROS production and SR Ca^{2+} leak were blunted. The reduction in SR Ca^{2+} leak observed immediately following exhaustive

151

exercise likely contributed to the prevention of calpain activation. Calpains can target and degrade EC coupling proteins and by preventing calpain activation, NOX inhibition may have prevented sarcomeric damage and cardiac fatigue in the APO 24H group. These findings suggest a possible connection between exercise-induced activation of NOX and the subsequent increase in SR Ca^{2+} leak, which may have two functional consequences. The first being that Ca^{2+} leakage from the SR reduces the SR Ca^{2+}load and results in a lower Ca^{2+} transient amplitude and thus force production. The second is that SR Ca^{2+} leak in the cleft region may raise cleft Ca^{2+} concentration sufficiently to activate calpains, which may contribute to prolonged cardiac fatigue due to EC coupling failure.

Chapter V: General discussion, conclusions, perspective and future directions

General Discussion

The purpose of this thesis was to develop an exhaustive exercise model that induced cardiac fatigue and to determine the mechanisms associated with exercise-induced cardiac fatigue. The literature suggests that exhaustive exercise increases ROS production in the LV and that ROS production is associated with cardiac fatigue. These observations were replicated in the current thesis and it was further demonstrated that by inhibiting NOX activity during exhaustive exercise, ROS production was blunted and cardiac fatigue was abolished. A major finding in this thesis was that SR Ca^{2+} leak was increased following exhaustive exercise in the absence of NOX inhibition, but that inhibition of NOX prior to exhaustive exercise prevented exercise-induced SR Ca^{2+} leak. Evidence for an interaction between NOX activation and RyR2 was further demonstrated by assessing ROS production and SR Ca^{2+} leak in the presence and absence of APO. These findings provide clear support for the hypothesis that impaired Ca^{2+} regulation would be mechanistically associated with cardiac fatigue. The fact that ROS production and SR Ca^{2+} leak returned to control levels 24 hours post-exercise suggests that alternate mechanism(s) are responsible for cardiac fatigue present 24 hours post-exercise. The activation of calpains was a likely consequence of increased SR Ca^{2+} leak following exhaustive exercise and may have contributed to EC uncoupling and cardiac fatigue 24 hours after the exercise bout. An important observation was that by inhibiting NOX and preserving Ca^{2+} regulation, calpains were not activated following exhaustive exercise and cardiac fatigue was not observed 24 hour post-exercise.

For these collective studies to be successful, it was necessary to develop an exhaustive exercise protocol that could be used to induce cardiac fatigue. Evidence from several studies

performed on rats suggest that exhaustive or prolonged aerobic exercise results in cardiac fatigue. Therefore, it was hypothesized that the exhaustive exercise protocol used in this thesis would result in a reduction in LVDP, which was confirmed in Chapter 2. Seward and co-workers (1995) did not detect cardiac fatigue in rat hearts following an exhaustive exercise protocol (18 m/min, 0% grade) that was very similar to the protocol used in this thesis. The discrepancy between this thesis and the results of Seward and colleagues (1995) may be due to the fact that the Langendorff technique was employed in this thesis whereas, the working heart technique was utilized in the previous study. The working heart technique more closely mimics the *in situ* effects of preload and afterload on pump function of the heart (i.e. perfusate is pumped from the left atria into the left ventricle and from there out the aorta). The Langendorff technique lacks preload and afterload and there is no fluid ejected from the heart. However, there is evidence that cardiac fatigue is present *in vivo* under conditions where preload and afterload would influence cardiac function (Vitiello et al., 2011; Olah et al., 2015). Taken together, the isolated perfused heart technique is a suitable method for the investigation of cardiac fatigue in rat.

A novel observation in this thesis was that cardiac fatigue was present during periods of β-adrenergic stimulation. This was evident as the LVDP was significantly lower in the AC and 24H groups during progressive doses of ISO. These findings differ from a previous study that performed an ISO dose response on isolated perfused hearts and did not observe any differences in LVDP between a control group and a group that performed prolonged exercise (Vitiello et al., 2011). The data presented in the study by Vitiello and colleagues (2011) was normalized, such that the maximal response was set at 100%, which makes comparison to the current study difficult as the maximal LVDP responses to ISO were lower in the AC and 24H groups when compared to the CTL group. It is possible that the maximal LVDP observed in the study by

154

Vitiello and co-workers (2011) were not different between the control and exercise groups. An important observation in this thesis, was that cardiac fatigue in the basal state and during β-adrenergic stimulation were not due to differences in heart rate or coronary flow. It is possible that metabolite accumulation occurred in the cardiomyocyte during exhaustive exercise, which contributed to cardiac fatigue. However, the contractile function of hearts were assessed under optimal *ex vivo* conditions (i.e. pH, electrolyte concentration, temperature) following 30 minutes of perfusion, which should have been ample time to restore metabolite concentrations (Humphrey et al., 1985). These data suggest that cardiac fatigue is due to a deficit within the cardiomyocyte and reinforces the importance of the *in vitro* findings within this thesis.

The production of ROS is a well-defined mechanism associated with myocardial stunning and skeletal muscle fatigue (Reid et al., 1992; Kolbeck et al., 1997; Kaplan et al., 2002; Kaplan et al., 2005; Moopanar and Allen, 2005; Tatarkova et al., 2005; Moopanar and Allen, 2006; Zweier & Talukder, 2006; Bruton et al., 2008). The exhaustive exercise protocol utilized in this thesis resulted in a significant increase in ROS production and cardiac fatigue in the AC group. These data are consistent with the study by Olah and co-workers (2015), who used the ROS sensitive dye, DHE to demonstrate that ROS production was elevated following three hours of swimming. In this thesis, there were no significant differences in lipid peroxidation in LV homogenates despite there being a mean difference of 30% between the CTL and AC groups. These data are opposite of several studies that reported increased lipid peroxidation following exhaustive or prolonged exercise (Lin et al., 2006; Aydin et al., 2007; Wonders et al., 2007; Huang et al., 2008). Although speculative, it may be possible that ROS produced during acute exercise caused lipid peroxidation in certain membrane fractions (i.e. the SR membrane) and not others (i.e. the sarcolemma), which may have been masked by measuring lipid peroxidation in

155

whole homogenate. Indeed, a study exposed hearts to ischemia-reperfusion and assessed MDA content in various subcellular fractions and observed an increase of ~50% in homogenate, a near doubling in mitochondrial membranes and no change in the microsomal or cytosolic fractions (Ambrosio et al., 1991). Such varied subcellular distributions of lipid peroxidation have been demonstrated in other tissues and models of stress (Aguilar-Delfin et al., 1996; Oztezcan et al., 2000; Luna-Moreno et al., 2007). In Chapter 4, inhibition of NOX prevented the exercise-induced increase in ROS production that was observed in Chapter 3. Furthermore, there was no evidence of cardiac fatigue in hearts in the presence of NOX inhibition. Taken together, cardiac fatigue is associated with NOX-dependent production of ROS.

There is evidence suggesting that exogenous and endogenous ROS has deleterious effects on the maximal Na^+/K^+-ATPase activity in LV homogenate and LV sarcolemmal vesicles (Vinnikova et al., 1992; Kaplan et al., 2005; Kaplan et al., 2008; Singh et al., 2012). To determine if production of ROS during exhaustive exercise impaired Na^+/K^+ pump function, maximal Na^+/K^+-ATPase activity was assessed using a spectrophotometric assay in LV homogenates. When compared to the CTL group, exhaustive exercise did not affect maximal Na^+/K^+-ATPase activity in the AC or 24H groups. This is the first study to examine the effects of exhaustive exercise on maximal rates of Na^+/K^+-ATPase activity in a 24 hour post-exercise group. Pierce and colleagues (1984) swam rats to exhaustion and isolated sarcolemmal membrane fractions from the LV immediately following the exercise bout. In that study, there were no significant differences in maximal Na^+/K^+-ATPase activities between the exercise group and the control group. The *in vitro* analyses of Na^+/K^+-ATPase activity in this thesis were performed under optimal conditions, which means that a reduction in maximal Na^+/K^+-ATPase activity would be indicative of structural damage to the pump. Exhaustive exercise has be shown to reduce

156

glycogen content in the LV (Pierce et al., 1984; Seward et al., 1995). Furthermore, glycogen has been demonstrated to be the preferential source of glucose for glycolytic ATP provision for the Na^+/K^+-ATPase (James et al., 1999; Dutka & Lamb, 2007). Therefore, metabolic inhibition of Na^+/K^+-ATPase activity may have occurred *in vivo*; however, our *in vitro* analyses are not able to determine whether that occurred or not. Taken together, exhaustive exercise did not alter the structure or function of the Na^+/K^+-ATPase.

In the myocardium SERCA2a and RyR2 are the main regulators of intracellular Ca^{2+}, SR Ca^{2+} load and the Ca^{2+} transient. The increased production of ROS during exhaustive exercise may have altered the structure and function of SERCA2a and contributed to cardiac fatigue. Thus, it was hypothesized that exhaustive exercise would result in a reduction in maximal Ca^{2+}-ATPase activity and Ca^{2+} uptake. Contrary to these hypotheses, the rates of maximal Ca^{2+}-ATPase activity and Ca^{2+} uptake were not significantly different between the CTL, AC and 24H groups. These data suggest that the structure of SERCA2a was not altered by exhaustive exercise, as these analyses were performed under optimal *in vitro* conditions. However, it is possible that metabolic inhibition of SERCA2a occurred *in vivo*, which contributed to Ca^{2+} overload and activation of calpains. Indeed, exhaustive exercise results in a reduction in the concentration of ATP and accumulation of AMP and ADP in rat myocardium (Weicker et al., 1990). Furthermore, studies have reported that by increasing the concentration of inorganic phosphate that the decay phase of the Ca^{2+} transient was prolonged and Ca^{2+} loading of the SR was impaired (i.e. reduced SERCA2a function) (Smith & Steele, 1992; Xiang & Kentish, 1995; Yang & Steele, 2002). The Ca^{2+} uptake data in this thesis differs from two previously reported studies that found a reduction in Ca^{2+} uptake following exhaustive exercise (Sembrowich & Gollinick, 1977; Pierce et al., 1984). These disparate results may be related to the sample preparation and assays used to assess

157

Ca^{2+} uptake. In the current study, whole homogenate and the Ca^{2+} sensitive dye, Indo-1 were used to measure Ca^{2+} uptake. The studies by Sembrowich & Gollinick (1977) and Pierce and co-workers (1984) performed Ca^{2+} uptake analyses using purified SR vesicles. The SR yield using differential centrifugation is reduced compared to whole homogenate (Chin & Green, 1996) and thus may not accurately represent the function of the entire population of Ca^{2+} pumps. In addition, exercise has been shown to differentially alter Ca^{2+} uptake when assessed in skeletal muscle homogenate and SR vesicles (Byrd et al., 1989). Sembrowich & Gollinick (1977) and Pierce and co-workers (1984) assessed Ca^{2+} uptake using a ^{45}Ca^{2+} assay, which contained 50 µM ^{45}Ca^{2+} and 5 mM oxalate in the assay medium. These conditions make it difficult to determine the free Ca^{2+} concentration in the assay. The use of Indo-1 and dual emission fluorometry in the current thesis allowed for precise control of the free Ca^{2+} concentration in the assay medium. However, a limitation to the Indo-1 Ca^{2+} uptake assay is that the free Ca^{2+} concentration in the assay medium was not maximal (i.e. ~10 µM) and thus maximal Ca^{2+} uptake could not be assessed. If the free Ca^{2+} concentration was indeed maximal in the studies by Sembrowich & Gollinick (1977) and Pierce and co-workers (1984), then it is difficult to compare Ca^{2+} uptake data in these studies to data in this thesis. In the studies by Sembrowich & Gollinick (1977) and Pierce and co-workers (1984), Ca^{2+} uptake was reduced by ~40-50%, which is comparable to the relative reduction in Ca^{2+} uptake in patients and animals with heart failure (i.e. models with pronounced LV contractile deficits) (O'Brien et al., 1991; Schwinger et al., 1995; Shao et al., 2005). Unfortunately, the former studies did not assess LV contractile properties following exhaustive exercise, and thus, it is not clear if the reduction in Ca^{2+} uptake had any effect on LV contractility. Taken together, exhaustive exercise did not alter the structure and function of SERCA2a as determined by the *in vitro* analyses used in this thesis. However, it cannot be ruled

out that maximal Ca^{2+} uptake was altered by exhaustive exercise or that metabolic inhibition of SERCA2a occurred *in vivo*.

The ryanodine receptor is emerging as a key regulator of cardiomyocyte function in both health and disease (Dulhunty et al., 2012). Accordingly, a reduction in SR Ca^{2+} release or increased SR Ca^{2+} leak would result in a decline in the Ca^{2+} transient and attenuated force production. In Chapter 3, the rates of maximal SR Ca^{2+} release were not significantly different between the CTL, AC and 24H groups. To the author's knowledge only one study has assessed the rate of SR Ca^{2+} release in the LV following an acute bout of aerobic exercise. In that study, dogs were subjected to an intermittent exercise protocol, which consisted of five bouts of running at 6 km/h for five minutes followed by five minutes of rest. It was found that intermittent exercise resulted in an increase in the rates of Ca^{2+}-induced Ca^{2+} release, which was associated with NOX-dependent ROS production and glutathionylation of RyR (Sanchez et al., 2008). These divergent results may stem from species and methodological differences in the two studies. It has been shown that there are ultrastructural, functional and Ca^{2+}-induced Ca^{2+} release differences between rats and dogs (Fabiato and Fabiato, 1978; Fabiato, 1982; Schaper et al., 1985; Bouchard and Bose, 1989). The exercise protocol employed in this thesis was continuous and exhaustive in nature, whereas the protocol used by Sanchez and colleagues (2008) was intermittent and did not result in exhaustion. Perhaps there is a relationship between SR Ca^{2+} release and the duration or intensity of exercise, such that brief periods of exercise can augment RyR function, which results in optimal SR Ca^{2+} release and exhaustive exercise results in a progressive decline in the rate of Ca^{2+} release. This hypothesis is analogous to the inverted "U" model of muscle force versus cellular REDOX state (refer to Figure 1.4 and Ried, 2001). A more likely explanation is derived from the method employed to induce Ca^{2+} release. In the current

thesis, 4-CMC was used to induced Ca^{2+} release, which directly binds to and activates RyR (Jacobson et al., 2006), whereas, the study by Sanchez and colleagues (2008) utilized a buffered solution with a free Ca^{2+} concentration of 1 μM to induce Ca^{2+} release. Previous studies have shown that maximal Ca^{2+} release or RyR open probability occurred at a free Ca^{2+} concentration of ~10 μM (Rousseau et al., 1986; Meissner and Henderson, 1987; Copello et al., 1997). It is possible that the Ca^{2+} release conditions utilized in the study by Sanchez and co-workers (2008) were submaximal and represent an exercise-induced increase in the affinity of RyR to submaximal trigger Ca^{2+} as opposed to an increase in the maximal rate of Ca^{2+} release. Currently, it is not clear what affect exhaustive exercise had on Ca^{2+}-induced Ca^{2+} release. However, it can be concluded that exhaustive exercise did not alter 4-CMC-induced conductance of Ca^{2+} through the Ca^{2+} release channel.

The rate of Ca^{2+} leak from the SR is equally as important as the rate of SR Ca^{2+} release with respect to cardiomyocyte function. In aging and heart failure there is increased oxidative stress in the cardiomyocyte, which is associated with an increased rate of SR Ca^{2+} leak and impaired contractile function (Cooper et al., 2013; Umanskaya et al., 2014; Kobayashi et al., 2015). In this thesis, the rate of SR Ca^{2+} leak was increased by ~40% immediately following exhaustive exercise when compared to the CTL and 24H groups. Few studies have examined the effects of acute exercise on SR Ca^{2+} leak in healthy myocardium. One study found a decrease in SR Ca^{2+} leak following 25 minutes of intermittent exercise (Sanchez et al., 2008). The assessment of SR Ca^{2+} leak in this thesis and the study by Sanchez and colleagues (2008) were performed in a similar manner. Ca^{2+} uptake was monitored using fluorescence spectroscopy and when Ca^{2+} uptake had reached a minimum a SERCA inhibitor (CPA in the current thesis and thapsigargin in Sanchez et al., 2008) was added to the assay and passive Ca^{2+} efflux was

160

recorded. Despite these similarities, there were differences in assay temperature (37°C versus 30°C), sample preparation (homogenate versus SR membrane isolation), exercise protocols and species that may account for the divergent results with respect to SR Ca^{2+} leak. Regardless of the methodological differences between these studies, these data can be interpreted that brief intermittent aerobic activity reduced SR Ca^{2+} leak, which would likely augment cardiac function, whereas, exhaustive exercise caused an increase in SR Ca^{2+} leak, which was associated with a reduction in LVDP.

The putative post-translational modifications to RyR that are associated with increased SR Ca^{2+} leak are elevated PKA mediated phosphorylation and oxidative modification to the channel (Marx et al., 2000; Wehrens et al., 2006; Bellinger et al., 2008; Bellinger et al., 2009; Andersson et al., 2011b). Despite a significant increase in circulating Epi in the AC group, PKA mediated phosphorylation of RyR was not altered in this group. These findings conflict with previous studies that found increased pRyR content following acute exercise (Wehrens et al., 2003; Gelhert et al., 2012). The discrepancy in pRyR2 from LV following acute exercise may be related to tissue collection and processing. The study by Wehrens and co-workers (2003) flash froze the LV immediately after exercise ceased. In this thesis, the collection and homogenization of LV was performed as quickly as possible, but it is possible that dephosphorylation of RyR occurred in the time period from exercise cessation to freezing of LV homogenates. The significance of PKA mediated phosphorylation of RyR2 and the subsequent impact on cardiac function has been challenged (MacDonnell et al., 2008; Zhang et al., 2012). The results from this thesis indicate that exercise-induced SR Ca^{2+} leak was not associated with changes in PKA mediated phosphorylation of RyR, which suggests a different mechanism was responsible for increasing SR Ca^{2+} leak.

To determine if oxidative post-translational modification of RyR contributed to the increase in SR Ca^{2+} leak, nitration, carbonylation and glutathionylation of RyR were assessed using immunoprecipitation and Western blotting techniques. Despite an increase in ROS production following exhaustive exercise, there were no significant differences between the CTL, AC and 24H groups with respect to glutathionylation, nitration or carbonylation of RyR. Using immunohistochemistry it has been demonstrated that acute exercise increased the nitrotyrosine content of cardiac cross-sections (Olah et al., 2015). Unfortunately, the immunohistochemistry technique does not permit the evaluation of specific proteins that are nitrated. To the author's knowledge, this thesis is the first study to assess nitration of RyR2 following an acute bout of exhaustive exercise. Taken together nitration of proteins may increase in the LV following acute exercise (Olah et al., 2015); however, RyR does not appear to be the target of tyrosine nitration. The protocol that was used to measure carbonylation of RyR was very similar to previous studies that demonstrated group differences in RyR carbonylation (Andersson et al., 2011a; Andersson et al., 2012; Umanskaya et al., 2014). Those studies used chronic models of oxidative stress compared to the acute increase in ROS production observed in this thesis. Perhaps a persistent increase in ROS production, as seen in aging and muscular dystrophy, is required to carbonylate RyR and have functional effects. The interaction of ROS with amino acids is quite complex and can result in a wide range of oxidative modifications to amino acids (Stadtman & Levine, 2003). It is possible that the ROS produced during exercise modified RyR2 in a manner not assessed in this thesis. For example RyR2 can be S-nitrosylated (the addition of NO to the thiol moiety of cysteine) in exercise, aging and disease models (Bellinger et al., 2008; Bellinger et al., 2009; Andersson et al., 2011a). An alternate explanation is that the immunoprecipitation and Western blot techniques utilized in this thesis were not

162

sensitive enough to detect differences between groups or that specific amino acids were modified, which cannot be determined using these techniques. Indeed, mass spectroscopy studies indicate that tyrosine nitration of RyR from skeletal muscle and the cerebellum is increased with aging (Kanski et al., 2005; Gokulrangan et al., 2007). Furthermore, mass spectroscopy analysis revealed that of the 100 cysteine residues on RyR1, 13 or fewer cysteine residues are sensitive to redox regulation (Voss et al., 2004; Aracena-Parks et al., 2006). Taken together, exhaustive exercise did not alter the post-translational oxidative modifications assessed in this thesis; however, it is possible that different modifications to RyR occurred or more sensitive methods were required to detect structural modifications to RyR.

An interesting finding in his thesis was that LVDP remained depressed 24 hours post-exercise despite the fact that ROS production and SR Ca^{2+} leak had normalized, which suggests an alternate mechanism was responsible for the cardiac fatigue present in the 24H group. It was hypothesized that the increased SR Ca^{2+} leak observed *in vitro* resulted in an increase in cytosolic $[Ca^{2+}]_f$ *in vivo*, which activated calpains. Indeed, calpain activity was significantly increased immediately following exhaustive exercise, which is consistent with previous reports (Raj et al., 1998; Tiidus et al., 2002). Activation of calpains has been demonstrated to degrade a host of EC coupling proteins (Matsumura et al., 1993; Matsumura et al., 1996; Zeitz et al., 2002; Inserte et al., 2005; Pedrozo et al., 2010; Wanichawan et al., 2014). Degradation of EC coupling proteins would result in EC uncoupling and would require *de novo* synthesis of proteins in order to replace the degraded proteins. It can be concluded that calpains did not target Na^+/K^+-ATPase, SERCA2a or RyR2 since the assay conditions used to determine the function of these proteins were optimal and thus, degradation would have resulted in a decrease in activity measured *in vitro*. Therefore, calpain mediated degradation of proteins such as NCX, TnI, TnT, desmin, α-

163

actinin, spectrin or junctophilin may have occurred, which contributed to EC uncoupling in the 24H group (Matsumura et al., 1996; Goa et al., 1997; Zeitz et al., 2002; Murphy et al., 2013; Wanichawan et al., 2014). Toxicological and disease models have implicated activation of calpains as a contributing factor to impaired cardiac contractile function (French et al., 2006; Campos et al., 2011; Celes et al., 2013). Interestingly, when animals were provided a RyR antagonist prior to toxicological stress, there was a reduction in calpain activity and cardiac contractile function was preserved (Campos et al., 2011; Celes et al., 2013). These data support the hypothesis that exhaustive exercise increased ROS production, which resulted in an increased rate of SR Ca^{2+} leak and activation of calpains. The latter two mechanisms likely contributed to the depression in LVDP in the AC and 24H groups via a reduction in SR Ca^{2+} load and EC uncoupling, respectively.

Once potential mechanisms associated with exercise-induced cardiac fatigue were determined, a pharmacological intervention was sought in an attempt to prevent cardiac fatigue. The NADPH oxidase inhibitor, apocynin was supplemented in the drinking water of rats for three days leading up to the exhaustive exercise bout. Inhibition of NOX prevented exercise-induced cardiac fatigue, as there were no significant differences in LVDP and ±dP/dt between the APO treated groups in the basal state. These findings are in agreement with a work by Vitiello and colleagues (2011), who demonstrated that NOX inhibition blunted exercise-induced oxidative stress, which was associated with prevention of exercise-induced cardiac fatigue. Therefore, it was hypothesized that NOX inhibition would reduce ROS production following exhaustive exercise. Indeed, NOX inhibition blunted ROS production, such that there were no significant differences in DCF fluorescence between the three APO treated groups. There are two approaches that can be used to mitigate the effects of ROS. The first is the prevention of

164

ROS production and the second is the scavenging of ROS by antioxidants. It is well defined in human and animal skeletal muscle that treatment with antioxidants prior to exercise or tetanic stimulation can delay time to fatigue or reduce the magnitude of fatigue (Shindoh et al., 1990; Ried et al., 1994; Medved et al., 2004; Moopanar & Allen, 2005). These studies provide causal evidence that ROS produced during exercise or tetanic contractions contribute to fatigue in skeletal muscle. By inhibiting NOX and preventing ROS production and cardiac fatigue it can be stated with confidence that ROS production contributed to the development of exercise-induced cardiac fatigue.

A novel finding in this thesis was that NOX inhibition prevented cardiac during β-adrenergic stimulation. The study by Vitiello and colleagues (2011) did not report the effects of NOX inhibition on the LVDP response to progressive concentrations of ISO. In this thesis, there were no significant differences between the APO treated groups with respect to heart rate or coronary flow during the ISO dose response, which suggests that these variables were not associated with the preserved LV function following exhaustive exercise. These data suggest that the protective effects of NOX inhibition on LV contractility following exhaustive exercise were due to reduced ROS production and improved protein function within cardiomyocytes (discussed below). In this thesis it was impossible to determine if cardiac output was impaired in rats during the exhaustive exercise bout when compared to APO treated animals. Since LVDP was preserved in the basal state and during β-adrenergic stimulation in APO treated groups, it could be hypothesized that APO treated animals had preserved cardiac function *in vivo* and thus, should have been able to run for longer periods of time. However, this was not the case, as there were no significant differences between the run times of animals in the non-APO and APO treated groups. A study by Grimditch and co-workers (1981) utilized instrumented dogs to

demonstrate that upon exhaustion cardiac output and stroke volume were not significantly different than values recorded within the first 5-10 minutes of exercise. It is possible that cardiac fatigue only manifests after the completion of the exercise bout and is a protective mechanism such that it would potentially limit exercise capacity during a subsequent bout, which would prevent further substrate depletion (i.e. glycogen) or muscle damage.

It is well established that acute exercise results in an increase in circulating Epi and NE (Chin et al., 1971; Cox et al., 1985; Scheurink et al., 1989; Conlee et al., 1991). A novel finding in this study was that NOX inhibition blunted the catecholamine response to exercise, such that the concentration of plasma Epi in the APO AC group was not significantly different than the APO CTL and APO 24H groups. This is the first study demonstrating that NOX inhibition can reduce Epi secretion. The mechanism by which NOX inhibition prevented the rise in circulating Epi following exhaustive exercise is not immediately clear. It has been demonstrated that intermittent hypoxia augmented Epi secretion from chromaffin cells. If cells were incubated with inhibitors of NOX or RyR prior to hypoxia, then Epi secretion was attenuated (Souvannakitti et al., 2010). The fact that either a NOX or RyR inhibitor was effective at reducing Epi secretion in that study is intriguing as evidence from this thesis suggests that activation of NOX can regulate RyR function. Perhaps an interaction between NOX and RyR is a conserved mechanism across cell types that regulates intracellular Ca^{2+}. Psychological stress has been shown to increase the concentration of Epi in the plasma (Dimsdale & Moss, 1980; Gerra et al., 2001). The likelihood that the reduction in Epi in the APO AC group was due to a reduction in stress placed on the animals is minimal. All of the rats in this thesis were handled in a similar manner and the average time to exhaustion (i.e. stress of the exercise protocol) were not significantly different

between the groups. Therefore, it is possible that APO prevented activation of NOX in the adrenal medulla during exhaustive exercise, which reduced the secretion of Epi.

A novel observation this thesis was that inhibition of NOX resulted in a reduction in coronary flow when APO treated groups were compared to non-APO treated groups. Previous studies using the isolated perfused mouse heart and the conscious instrumented dog have demonstrated that NOX inhibition using APO had no effect on coronary flow when compared to non-APO groups (Zhang et al., 2009; El-Awady et al., 2013). The conflicting results between these studies and this thesis may be methodological in nature. In this thesis, animals were provided APO over a three day period, whereas, the former studies perfused APO directly into the coronary circulation. A common feature of endothelial dysfunction is a reduction in nitric oxide (NO) bioavailability due to the reaction of NO with superoxide, which produces peroxynitrite (Levy et al., 2009). In the current thesis, inhibition of NOX decreased ROS production (i.e. decreased superoxide production), which would be expected to increase NO bioavailability, decrease CVR and increase coronary flow. However, the opposite results were observed; CVR was greater and coronary flow was reduced in APO treated groups when compared to non-APO treated groups. Thus, the mechanism responsible for the reduced coronary flow in the current study may not be related to ROS production and NO bioavailability in the coronary vasculature, but may be related to metabolic demand in the ventricular myocyte. The increased coupling ratio observed in APO treated animals would be expected to reduce the amount of ATP required to transport a given amount of Ca^{2+} across the SR membrane. Furthermore, lower SR Ca^{2+} leak would lead to less Ca^{2+}-ATPase cycling during diastole, which would reduce ATP demand even further. Although speculative, the improved Ca^{2+} transport

167

efficiency and lower SR Ca^{2+} leak may have lowered ATP demand (i.e. lower oxygen demand), which resulted in a reduction in coronary flow.

Inhibition of NOX resulted in several improvements in Ca^{2+} regulation. It was hypothesized that NOX inhibition would prevent the exercise-induced increase in SR Ca^{2+} leak that was observed in Chapter 3. As postulated, there were no significant differences in the rates of SR Ca^{2+} leak in the APO treated groups. In addition, there was a main effect of NOX inhibition on SR Ca^{2+} leak, such that leak was lower in APO treated groups when compared to non-APO treated groups. Evidence to support these novel findings comes from a model of dystrophic cardiomyopathy. Gonzalez and colleagues (2014) demonstrated that in cardiomyocytes from dystrophic hearts ROS production was augmented, which was associated with increased SR Ca^{2+} leak, a reduction in SR Ca^{2+} content and depressed contractile function. Incubation of dystrophic cardiomyocytes with APO restored SR Ca^{2+} leak and SR Ca^{2+} load, which improved cell shortening (Gonzalez et al., 2014). These data suggest that RyR is a downstream target of NOX dependent ROS production and the activation of NOX can regulate RyR function, which can impact contractile function. To further demonstrate that NOX can regulate RyR, an *in vitro* experiment was designed, whereby NADPH was added to LV homogenates, which activated NOX and increased ROS production and SR Ca^{2+} leak. When these *in vitro* experiments were repeated in the presence of APO, ROS production was blunted and SR Ca^{2+} leak was equal to control values. These results are similar to studies that utilized skeletal muscle preparations and demonstrated that exogenous NADPH activated NOX, increased ROS production and increased the open probability of RyR (Hidalgo et al., 2006; Sun et al., 2011). Taken together, exercise or NADPH-induced activation of NOX resulted in increased ROS production and increased SR Ca^{2+} leak through RyR2, which was prevented when NOX was inhibited by APO.

The inhibition of NOX resulted in augmented SERCA2a function (i.e. increased Ca^{2+} transport efficiency and apparent affinity to Ca^{2+}), which may have contributed to the prevention of exercise-induced cardiac fatigue. The maximal Ca^{2+}-ATPase activities were lower and the rates of Ca^{2+} uptake were higher in the APO treated groups when compared to the non-APO treated groups. Consequently, there were significantly higher coupling ratios in the APO treated groups. The increase in the coupling ratio was likely mediated by the increased apparent affinity of SERCA2a for Ca^{2+} and the lower rate of SR Ca^{2+} leak in the APO treated groups (Chamberlain et al., 1984; Beeler & Gable, 1994; Frank et al., 2000). Studies have shown a leftward shift in the Ca^{2+}-dependent Ca^{2+}-ATPase curve in the LV of PLN knockout mice (Luo et al., 1994; Frank et al., 2000). These findings have been replicated in LV samples from non-transgenic mice and rabbits when PLN was phosphorylated or when PLN antibody was added to the Ca^{2+}-ATPase assay to mimic PLN phosphorylation (Kranias et al., 1985; Xu & Narayanan, 1999; Mahaney et al., 2000). In this thesis, the ratio of pPLN to PLN was greater in the APO treated groups when compared the non-APO treated groups, which would explain the increased apparent affinity of SERCA2a for Ca^{2+}. The mechanism responsible for the increased pPLN to PLN ratio following NOX inhibition was not associated with plasma Epi concentrations. PLN is phosphorylated by CaMKII at threonine 17. However, activation of CaMKII does not seem to be a likely mechanism, as this kinase is activated by elevated Ca^{2+} and ROS (Couchonnal & Anderson, 2008), both of which were reduced in APO treated groups. Furthermore, activation of NOX has been shown to attenuate phosphatase activity (Lee et al., 2007; Shinohara et al., 2007; Jiang et al., 2011). Therefore, by inhibiting NOX it would be expected that phosphatase activity was elevated, which would have the opposite effect on pPLN compared to what was observed in this thesis. The functional consequence of increased coupling ratios and the apparent affinity of

SERCA2a for Ca^{2+} would be enhanced Ca^{2+} sequestration at low $[Ca^{2+}]_f$ (i.e. during diastole) (Frank et al., 2000). This would increase SR Ca^{2+} load and augment the fractional release of Ca^{2+}, which would result in a more forceful contraction. This may account for the protection against exercise-induced cardiac fatigue afforded by NOX inhibition.

The results from this thesis suggest that exercise-induced cardiac fatigue was associated with increased ROS production, increased SR Ca^{2+} leak and activation of calpains. Due to technical limitations, measurements of the $[Ca^{2+}]_f$ during exercise or in isolated perfused hearts were not performed in this thesis. However, based on the results from *in vitro* experiments, it is reasonable to speculate that the concentration of Ca^{2+} in the cytosol rose sufficiently to activate calpains. Thus far, this thesis has demonstrated that inhibition of NOX blunted ROS production and reduced SR Ca^{2+} leak. Therefore, the final postulate examined in this thesis stated that inhibition of NOX would prevent activation of calpains immediately following exhaustive exercise. As hypothesized there were no significant differences in calpain activity between the APO CTL, APO AC and APO 24H groups. These data are in agreement with previous studies that demonstrated that NOX inhibition using APO prevented ROS production and calpain activation following chemical and mechanical stress (Li et al., 2009a; McClung et al., 2009). Brief exposure of skeletal and cardiac muscle to elevated Ca^{2+} concentrations activates calpains and may result in EC uncoupling (Verburg et al., 2005; Verburg et al., 2009; Murphy et al., 2013). Furthermore, there is evidence to suggest that by inhibiting calpain activity, EC coupling and thus force production is preserved in skeletal muscle fibres (Verburg et al., 2005; Zhang et al., 2008; Verburg et al., 2009). These data suggest that the reduction in calpain activity observed in this thesis likely prevented degradation of EC coupling proteins, which maintained EC coupling and thus LVDP in the APO 24H group.

Conclusion

The results from the studies that comprise this thesis demonstrate that exhaustive exercise decreased LVDP immediately following the exercise bout and that the depression in LVDP persisted for up to 24 hours post-exercise. *In vitro* analyses revealed that exhaustive exercise increased ROS production and SR Ca^{2+} leak in LV homogenates. The increased SR Ca^{2+} leak may explain the acute depression in LVDP, which is likely mediated through a decrease in the SR Ca^{2+} load and a decrease in the Ca^{2+} transient amplitude. However, ROS production and SR Ca^{2+} leak were equal to control values 24 hour post-exercise, yet LVDP remained depressed. Activation of calpains, possibly due to increased SR Ca^{2+} leak, may have contributed to the persistent decrease in LVDP observed 24 hours post-exercise via EC uncoupling. The exercise-induced deficits in LV observed in this thesis share features of myocardial stunning at the whole organ and biochemical level. Thus, exhaustive exercise confers a pseudo-stunned phenotype on the rat myocardium.

The reduction in myocardial function, and biochemical changes following exhaustive exercise were prevented in animals that consumed APO, a NOX inhibitor. A potential pathway of biochemical events is illustrated in Figure 5.1. During exhaustive exercise NOXs were activated, which increased ROS production. This caused an increase in SR Ca^{2+} leak, which contributed to the acute depression of LVDP and activation of calpains. The increase in calpain activity contributed to the depression in LVDP that persisted for 24 hours. The activation of a NOX-RyR pathway (Souvannakitti et al., 2010) or NOX-RyR-calpain pathway (Li et al., 2009b) has been demonstrated in the myocardium and other tissues. Interestingly, by inhibiting upstream steps in the pathway (i.e. NOX and RyR) calpain activation and apoptosis of cardiomyocytes was prevented (Li et al., 2009b). By inhibiting NOXs with APO in this thesis, the downstream

biochemical processes in the pathway proposed in Figure 5.1 were preserved, and thus, cardiac fatigue did not occur. Overall, this thesis has proposed that acute, exhaustive exercise places the myocardium in a pseudo-stunned state and determined a potential pathway that explains some of the mechanisms that contribute to exercise-induced cardiac fatigue.
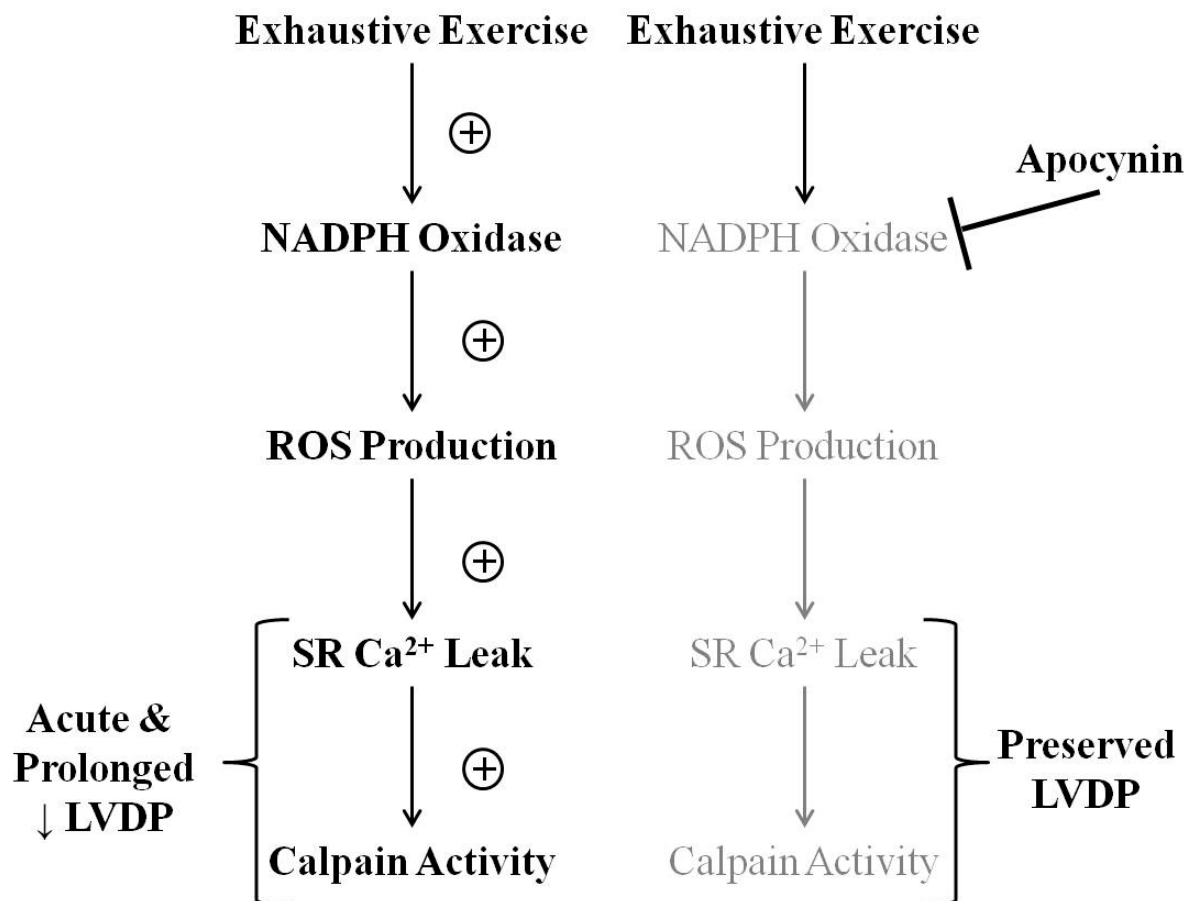
Figure 5.1. Proposed pathway linking the mechanisms that contribute to exercise-induced cardiac fatigue. The (+) sign represents activation or increased activity. Exhaustive exercise activates NADPH oxidase, which increases ROS production. That leads to increased SR Ca^{2+} leak and activation of calpains. These later events contribute to the acute and persistent depression in cardiac contractile function. Apocynin blunts exercise-induced activation of NADPH oxidase, which prevents downstream processes from occurring (greyed out to indicate no change in activity).

Perspective

The aim of this thesis was not to cast aerobic exercise in a negative light. Participation in a regular aerobic exercise regime results in weight loss, increased peak oxygen uptake, improved insulin sensitivity, reduction in serum triglycerides and cholesterol, improved glucose metabolism, reduction in blood pressure and an improved mental health (King et al., 1989; Dengel et al., 1998; Andersen et al., 1999; Ross et al., 2000). These positive effects of exercise far outweigh the transient decline in cardiac function following a prolonged or exhaustive bout of exercise. The fact that this is a transient phenomenon indicates that this may be a normal physiological process (discussed below). Thus, the goal of this thesis was to answer the basic question, what are the mechanisms that underlie exercise-induced cardiac fatigue? Since the rats used in this thesis were sedentary, perhaps the functional and biochemical deficits observed in this thesis are a normal processes that are required for physiological adaptation in the myocardium to the stress of regular aerobic exercise. Similar to cycles of damage, repair and growth in skeletal muscle in response to aerobic or resistance exercise, the activation of the pathway proposed in Figure 5.1 may lead to short-term deficits in cardiac function but the subsequent adaptation (i.e. *de novo* protein synthesis) following a finite recovery period may lead to overall improved cardiomyocyte function with repeated periods of exhaustive exercise and recovery (i.e. endurance training). This thesis demonstrated that inhibition of NOX prevented cardiac fatigue by blocking the activation of a proposed ROS-SR Ca^{2+} leak-calpain pathway. This observation was very beneficial from a basic understanding of exercise-induced cardiac fatigue mechanisms. However, scavenging of ROS produced during exercise has been shown to limit the cellular adaptations to aerobic exercise in skeletal muscle (Gomez-Cabrera et al., 2005; Paulsen et al., 2014). It could be hypothesized that, similar to skeletal muscle, ROS

produced in the LV during exhaustive exercise contributes to the development of cardiac fatigue and is an important signalling step in physiological adaptation.

Limitations

This thesis contained several cohorts of animals that were randomly assigned to either CTL, AC or 24H groups. Certain cohorts of animals were used for isolated perfused heart studies and other cohorts for *in vitro* experiments. It is difficult to say with certainty that the mechanisms associated with cardiac fatigue identified using *in vitro* assays were present during isolated perfused heart experiments. However, it was demonstrated that a key finding in the *in vitro* experiments, namely increased SR Ca^{2+} leak, was present in LV homogenates collected following 30 minutes of perfusion using the Langendorff technique. It is possible to assess ROS production and Ca^{2+} transients in actively beating isolated perfused hearts (Del Nido et al., 1998; Du et al., 2001; Kevin et al., 2003; Napankangas et a., 2012). Unfortunately, our laboratory is not equipped to make such measurements. The evaluation of ROS production and Ca^{2+} transients following exhaustive exercise in the isolated heart would greatly enhance the cardiac fatigue literature. Nonetheless, it was possible to detect increased ROS production in LV homogenates following exhaustive exercise and by activating NOX using NADPH.

The training status of the rats used in this thesis may be a potential limitation. Similar to previously reported studies that have examined cardiac fatigue, the rats used in this thesis were sedentary. It is possible that the effects of exhaustive exercise are magnified in sedentary rats as these animals were not accustomed to such a stress to the cardiovascular system. No study has examined the influence of training status on the development of cardiac fatigue in rats (see Future Directions). Perhaps cardiac fatigue is absent following exhaustive exercise in trained rats. Accordingly, these collective studies offer novel insight as to the mechanism associated with cardiac fatigue and may serve as a starting point for training studies that investigate cardiac fatigue.

The aim of this study was to investigate the mechanisms associated with cardiac fatigue. Unfortunately, it is problematic to extrapolate these findings to the human literature as there are several species differences between rats and humans, which include but are not limited to action potential duration, resting heart rate, contractile protein isoform expression and the relative amount of Ca^{2+} released and sequestered by the SR (i.e. ~90% in rats and ~70% in humans) (Milani-Nejad & Janssen, 2014). Thus, the altered SR function observed in this thesis may not be associated with functional deficits in the LV of humans following exhaustive exercise. Logistically, it is impossible to carry out such analyses on human LV, but the findings in this thesis may direct future studies in larger mammals (i.e. dog, sheep or pig) that have a myocardium that more closely resembles humans in terms of structure and biochemical function.

The isolated perfused heart technique is a powerful tool insofar as it allows careful manipulation of the constituents of the perfusate, pH, metabolic substrates and the hearts are devoid of neurohumoral influences. However, these factors may be a limitation in this thesis, as it is not known what effect exhaustive exercise had on *in vivo* cardiac function. The exercise-induced reduction in LVDP may not translate into a reduction in cardiac output as neurohumoral factors and loading conditions can influence heart rate and stroke volume in order to maintain cardiac output *in vivo*. In the basal state there were no significant difference in heart rate in the CTL, AC and 24H groups. Studies have utilized pressure sensitive catheters and echocardiography to demonstrate that LVDP and ejection fraction measured *in vivo* were lower following exhaustive exercise (Vitiello et al., 2011; Olah et al., 2015). Furthermore, the study by Olah and colleagues (2015) observed a reduced stroke volume and cardiac output in animals that swam to exhaustion despite loading conditions and heart rates being equal to a sedentary control group. These data suggest that the cardiac fatigue observed in this thesis likely existed *in vivo*

and that the isolated perfused heart technique is a valid approach to assessment of cardiac fatigue in rat.

As mentioned in Chapter 4, a comparison of *in vitro* results from groups that were treated with APO and groups that were not treated with APO revealed some interesting main effects of APO treatment. There was a temporal gap between the isolation of homogenates from non-APO treated animals and APO treated animals. In addition, there were no homogenates collected from a non-APO treated control group at the same time as all of the APO treated groups, which is a major limitation of this study. Several of the main effects of APO treatment may partially explain the mechanisms by which NOX inhibition prevented cardiac fatigue, however, these discussions and interpretation must be taken with a degree of caution.

Future Directions

The collection of studies in this thesis demonstrated that exhaustive exercise resulted in depressed cardiac contractile function that persisted for up to 24 hours post-exercise. A similar study observed a reduction in LVDP for up to 48 hours following an acute bout of exercise. Expanding on the hypothesis developed in the *Perspective* section, it would be of interest to examine the effects of repeated bouts of the same exercise stress over an extended period of time. One study would have rats perform exhaustive exercise such that cardiac fatigue was induced and present 24 hours post-exercise. At that time point one group of rats would perform an exercise protocol to determine if cardiac fatigue translated into impaired exercise capacity/performance. A second group of rats would perform the exhaustive exercise protocol that induced cardiac fatigue to determine if there is a negative effect of a second exhaustive exercise bout on LVDP. A second study would track the effects of 1, 3, 5, 10, 21, etc. bouts of exhaustive exercise on functional and biochemical changes in the LV (i.e. the transition from a sedentary to trained animal). If the hypothesis that the cellular deficits associated with cardiac fatigue will eventually lead to positive LV adaptations is correct, then by the xth bout of exhaustive exercise the magnitude of cardiac fatigue should be blunted or cardiac fatigue should not be present.

The studies in this thesis and those in the literature have used healthy, but cage sedentary rats to investigate the effects of acute exercise on cardiac function. Evidence in humans suggests that transient reductions in cardiac function occur in the post-exercise period even in highly trained individuals who compete in high level athletic events (i.e. marathon, Ironman triathlon). An ideal study would utilize sedentary, moderately trained and highly trained rats to investigate

178

the influence of training status on the development of exercise-induced cardiac fatigue. This has not been examined in an animal model to date.

A study designed to confirm the pathway presented in Figure 5.1, would utilize permeabilized cardiomyocytes incubated with NADPH to activate NOX in order to induce SR Ca^{2+} leak and activate calpains. Cell shortening and lengthening would be used to assess the effects of NOX activation on contraction and relaxation properties. Subsequent experiments would activate NOX in the presence of antioxidants, specific inhibitors of RyR (i.e. dantrolene) or specific inhibitors of calpains (i.e. leupeptin), which should in theory prevent downstream events from occurring based on what step in the pathway is being inhibited. For example, activation of NOX should increase ROS production but incubation with dantrolene would prevent SR Ca^{2+} leak through RyR, which should prevent activation of calpains.

An exciting study would incorporate direct measurement of Ca^{2+} transients and ROS production in isolated perfused rat hearts following exhaustive exercise. In the discussion throughout this thesis it was hypothesized that an increase rate in SR Ca^{2+} leak may lower SR Ca^{2+} load and reduce the Ca^{2+} transient amplitude. By monitoring the Ca^{2+} transient *ex vivo* and by measuring SR Ca^{2+} leak *in vitro*, this hypothesis could be substantiated.

References

Adachi T, Weisbrod RM, Pimentel DR, Ying J, Sharov VS, Schoneich C & Cohen RA. (2004). S-Glutathiolation by peroxynitrite activates SERCA during arterial relaxation by nitric oxide. *Nat Med* **10,** 1200-1207.

Aguilar-Delfin I, Lopez-Barrera F & Hernandez-Munoz R. (1996). Selective enhancement of lipid peroxidation in plasma membrane in two experimental models of liver regeneration: partial hepatectomy and acute CC14 administration. *Hepatology* **24,** 657-662.

Akki A, Zhang M, Murdoch C, Brewer A & Shah AM. (2009). NADPH oxidase signaling and cardiac myocyte function. *J Mol Cell Cardiol* **47,** 15-22.

Allen DG & Blinks JR. (1978). Calcium transients in aequorin-injected frog cardiac muscle. *Nature* **273,** 509-513.

Allen DG, Lamb GD & Westerblad H. (2008). Skeletal muscle fatigue: cellular mechanisms. *Physiol Rev* **88,** 287-332.

Ambrosio G, Flaherty JT, Duilio C, Tritto I, Santoro G, Elia PP, Condorelli M & Chiariello M. (1991). Oxygen radicals generated at reflow induce peroxidation of membrane lipids in reperfused hearts. *J Clin Invest* **87,** 2056-2066.

Andersen RE, Wadden TA, Bartlett SJ, Zemel B, Verde TJ & Franckowiak SC. (1999). Effects of lifestyle activity vs structured aerobic exercise in obese women: a randomized trial. *JAMA* **281,** 335-340.

Andersson DC, Betzenhauser MJ, Reiken S, Meli AC, Umanskaya A, Xie W, Shiomi T, Zalk R, Lacampagne A & Marks AR. (2011a). Ryanodine receptor oxidation causes intracellular calcium leak and muscle weakness in aging. *Cell Metab* **14,** 196-207.

Andersson DC, Fauconnier J, Yamada T, Lacampagne A, Zhang SJ, Katz A & Westerblad H. (2011b). Mitochondrial production of reactive oxygen species contributes to the beta-adrenergic stimulation of mouse cardiomycytes. *J Physiol* **589,** 1791-1801.

Anzai K, Ogawa K, Kuniyasu A, Ozawa T, Yamamoto H & Nakayama H. (1998). Effects of hydroxyl radical and sulfhydryl reagents on the open probability of the purified cardiac ryanodine receptor channel incorporated into planar lipid bilayers. *Biochem Biophys Res Commun* **249,** 938-942.

Aracena-Parks P, Goonasekera SA, Gilman CP, Dirksen RT, Hidalgo C & Hamilton SL. (2006). Identification of cysteines involved in S-nitrosylation, S-glutathionylation, and oxidation to disulfides in ryanodine receptor type 1. *J Biol Chem* **281,** 40354-40368.

Aydin C, Ince E, Koparan S, Cangul IT, Naziroglu M & Ak F. (2007). Protective effects of long term dietary restriction on swimming exercise-induced oxidative stress in the liver, heart and kidney of rat. *Cell Biochem Funct* **25,** 129-137.

Backx PH, Gao WD, Azan-Backx MD & Marban E. (1995). The relationship between contractile force and intracellular [Ca2+] in intact rat cardiac trabeculae. *J Gen Physiol* **105,** 1-19.

Banks L, Sasson Z, Busato M & Goodman JM. (2010). Impaired left and right ventricular function following prolonged exercise in young athletes: influence of exercise intensity and responses to dobutamine stress. *J Appl Physiol (1985)* **108,** 112-119.

Bannister RA & Ohrtman JD. (2009). Reassessing the molecular mechanism of beta-adrenergic stimulation of cardiac L-type Ca2+ current. *Channels (Austin)* **3,** 146-148.

Baumer AT, Kruger CA, Falkenberg J, Freyhaus HT, Rosen R, Fink K & Rosenkranz S. (2007). The NAD(P)H oxidase inhibitor apocynin improves endothelial NO/superoxide balance and lowers effectively blood pressure in spontaneously hypertensive rats: comparison to calcium channel blockade. *Clin Exp Hypertens* **29,** 287-299.

Bedard K & Krause KH. (2007). The NOX family of ROS-generating NADPH oxidases: physiology and pathophysiology. *Physiol Rev* **87,** 245-313.

Beeler TJ & Gable KS. (1994). Phosphate, nitrendipine and valinomycin increase the Ca2+/ATP coupling ratio of rat skeletal muscle sarcoplasmic reticulum Ca(2+)-ATPase. *Biochim Biophys Acta* **1189,** 189-194.

Bejma J, Ramires P & Ji LL. (2000). Free radical generation and oxidative stress with ageing and exercise: differential effects in the myocardium and liver. *Acta Physiol Scand* **169,** 343-351.

Belcastro AN & Sopper MM. (1984). Calcium requirements of cardiac myofibril ATPase activity following exhaustive exercise. *Int J Biochem* **16,** 93-98.

Bellinger AM, Reiken S, Carlson C, Mongillo M, Liu X, Rothman L, Matecki S, Lacampagne A & Marks AR. (2009). Hypernitrosylated ryanodine receptor calcium release channels are leaky in dystrophic muscle. *Nat Med* **15,** 325-330.

Bellinger AM, Reiken S, Dura M, Murphy PW, Deng SX, Landry DW, Nieman D, Lehnart SE, Samaru M, LaCampagne A & Marks AR. (2008). Remodeling of ryanodine receptor complex causes "leaky" channels: a molecular mechanism for decreased exercise capacity. *Proc Natl Acad Sci U S A* **105,** 2198-2202.

Bendall JK, Cave AC, Heymes C, Gall N & Shah AM. (2002). Pivotal role of a gp91(phox)-containing NADPH oxidase in angiotensin II-induced cardiac hypertrophy in mice. *Circulation* **105,** 293-296.

Bers DM. (2002). Cardiac excitation-contraction coupling. *Nature* **415,** 198-205.

Bers DM. (2008). Calcium cycling and signaling in cardiac myocytes. *Annu Rev Physiol* **70,** 23-49.

Bers DM. (2014). Cardiac sarcoplasmic reticulum calcium leak: basis and roles in cardiac dysfunction. *Annu Rev Physiol* **76,** 107-127.

Bers DM, Barry WH & Despa S. (2003). Intracellular Na+ regulation in cardiac myocytes. *Cardiovasc Res* **57,** 897-912.

Bilginoglu A, Seymen A, Tuncay E, Zeydanli E, Aydemir-Koksoy A & Turan B. (2009). Antioxidants but not doxycycline treatments restore depressed beta-adrenergic responses of the heart in diabetic rats. *Cardiovasc Toxicol* **9,** 21-29.

Blizard DA, Liang B & Emmel DK. (1980). Blood pressure, heart rate, and plasma catecholamines under resting conditions in rat strains selectively bred for differences in response to stress. *Behav Neural Biol* **29,** 487-492.

Bluhm WF, Kranias EG, Dillmann WH & Meyer M. (2000). Phospholamban: a major determinant of the cardiac force-frequency relationship. *Am J Physiol Heart Circ Physiol* **278,** H249-255.

Blunt BC, Creek AT, Henderson DC & Hofmann PA. (2007). H2O2 activation of HSP25/27 protects desmin from calpain proteolysis in rat ventricular myocytes. *Am J Physiol Heart Circ Physiol* **293,** H1518-1525.

Bo H, Jiang N, Ma G, Qu J, Zhang G, Cao D, Wen L, Liu S, Ji LL & Zhang Y. (2008). Regulation of mitochondrial uncoupling respiration during exercise in rat heart: role of reactive oxygen species (ROS) and uncoupling protein 2. *Free Radic Biol Med* **44,** 1373-1381.

Bodi I, Mikala G, Koch SE, Akhter SA & Schwartz A. (2005). The L-type calcium channel in the heart: the beat goes on. *J Clin Invest* **115,** 3306-3317.

Bolli R. (1990). Mechanism of myocardial "stunning". *Circulation* **82,** 723-738.

Bolli R & Marban E. (1999). Molecular and cellular mechanisms of myocardial stunning. *Physiol Rev* **79,** 609-634.

Bossuyt J, Ai X, Moorman JR, Pogwizd SM & Bers DM. (2005). Expression and phosphorylation of the na-pump regulatory subunit phospholemman in heart failure. *Circ Res* **97,** 558-565.

Bossuyt J, Despa S, Han F, Hou Z, Robia SL, Lingrel JB & Bers DM. (2009). Isoform specificity of the Na/K-ATPase association and regulation by phospholemman. *J Biol Chem* **284,** 26749-26757.

Bouchard RA & Bose D. (1989). Analysis of the interval-force relationship in rat and canine ventricular myocardium. *Am J Physiol* **257,** H2036-2047.

Bovo E, Lipsius SL & Zima AV. (2012). Reactive oxygen species contribute to the development of arrhythmogenic Ca(2)(+) waves during beta-adrenergic receptor stimulation in rabbit cardiomyocytes. *J Physiol* **590,** 3291-3304.

Bridge JH & Bassingthwaighte JB. (1983). Uphill sodium transport driven by an inward calcium gradient in heart muscle. *Science* **219,** 178-180.

Brillantes AB, Ondrias K, Scott A, Kobrinsky E, Ondriasova E, Moschella MC, Jayaraman T, Landers M, Ehrlich BE & Marks AR. (1994). Stabilization of calcium release channel (ryanodine receptor) function by FK506-binding protein. *Cell* **77,** 513-523.

Brittsan AG, Kiss E, Edes I, Grupp IL, Grupp G & Kranias EG. (1999). The effect of isoproterenol on phospholamban-deficient mouse hearts with altered thyroid conditions. *J Mol Cell Cardiol* **31,** 1725-1737.

Bruton JD, Place N, Yamada T, Silva JP, Andrade FH, Dahlstedt AJ, Zhang SJ, Katz A, Larsson NG & Westerblad H. (2008). Reactive oxygen species and fatigue-induced prolonged low-frequency force depression in skeletal muscle fibres of rats, mice and SOD2 overexpressing mice. *J Physiol* **586,** 175-184.

Buckberg G, Hoffman JI, Nanda NC, Coghlan C, Saleh S & Athanasuleas C. (2011). Ventricular torsion and untwisting: further insights into mechanics and timing interdependence: a viewpoint. *Echocardiography* **28,** 782-804.

Byrd SK, Bode AK & Klug GA. (1989). Effects of exercise of varying duration on sarcoplasmic reticulum function. *J Appl Physiol (1985)* **66,** 1383-1389.

Byrne JA, Grieve DJ, Bendall JK, Li JM, Gove C, Lambeth JD, Cave AC & Shah AM. (2003). Contrasting roles of NADPH oxidase isoforms in pressure-overload versus angiotensin II-induced cardiac hypertrophy. *Circ Res* **93,** 802-805.

Cai Z, Manalo DJ, Wei G, Rodriguez ER, Fox-Talbot K, Lu H, Zweier JL & Semenza GL. (2003). Hearts from rodents exposed to intermittent hypoxia or erythropoietin are protected against ischemia-reperfusion injury. *Circulation* **108,** 79-85.

Campbell TL, Mitchell AS, McMillan EM, Bloemberg D, Pavlov D, Messa I, Mielke JG & Quadrilatero J. (2015). High-fat feeding does not induce an autophagic or apoptotic phenotype in female rat skeletal muscle. *Exp Biol Med (Maywood)* **240,** 657-668.

Campos EC, O'Connell JL, Malvestio LM, Romano MM, Ramos SG, Celes MR, Prado CM, Simoes MV & Rossi MA. (2011). Calpain-mediated dystrophin disruption may be a potential structural culprit behind chronic doxorubicin-induced cardiomyopathy. *Eur J Pharmacol* **670,** 541-553.

Cantilina T, Sagara Y, Inesi G & Jones LR. (1993). Comparative studies of cardiac and skeletal sarcoplasmic reticulum ATPases. Effect of a phospholamban antibody on enzyme activation by Ca2+. *J Biol Chem* **268,** 17018-17025.

Castilho RF, Carvalho-Alves PC, Vercesi AE & Ferreira ST. (1996). Oxidative damage to sarcoplasmic reticulum Ca(2+)-pump induced by Fe2+/H2O2/ascorbate is not mediated by lipid peroxidation or thiol oxidation and leads to protein fragmentation. *Mol Cell Biochem* **159,** 105-114.

Castro MC, Francini F, Schinella G, Caldiz CI, Zubiria MG, Gagliardino JJ & Massa ML. (2012). Apocynin administration prevents the changes induced by a fructose-rich diet on rat liver metabolism and the antioxidant system. *Clin Sci (Lond)* **123,** 681-692.

Cazorla O, Wu Y, Irving TC & Granzier H. (2001). Titin-based modulation of calcium sensitivity of active tension in mouse skinned cardiac myocytes. *Circ Res* **88,** 1028-1035.

Celes MR, Malvestio LM, Suadicani SO, Prado CM, Figueiredo MJ, Campos EC, Freitas AC, Spray DC, Tanowitz HB, da Silva JS & Rossi MA. (2013). Disruption of calcium homeostasis in cardiomyocytes underlies cardiac structural and functional changes in severe sepsis. *PLoS One* **8,** e68809.

Chamberlain BK, Volpe P & Fleischer S. (1984). Calcium-induced calcium release from purified cardiac sarcoplasmic reticulum vesicles. General characteristics. *J Biol Chem* **259,** 7540-7546.

Chan-Dewar F, Oxborough D, Shave R, Gregson W, Whyte G, Noakes T & George K. (2010). Evidence of increased electro-mechanical delay in the left and right ventricle after prolonged exercise. *Eur J Appl Physiol* **108,** 581-587.

Chen W, Ruell PA, Ghoddusi M, Kee A, Hardeman EC, Hoffman KM & Thompson MW. (2007). Ultrastructural changes and sarcoplasmic reticulum Ca2+ regulation in red vastus muscle following eccentric exercise in the rat. *Exp Physiol* **92,** 437-447.

Chen YY, Ho KP, Xia Q & Qian ZM. (2002). Hydrogen peroxide enhances iron-induced injury in isolated heart and ventricular cardiomyocyte in rats. *Mol Cell Biochem* **231,** 61-68.

Cheung JY, Zhang XQ, Song J, Gao E, Rabinowitz JE, Chan TO & Wang J. (2010). Phospholemman: a novel cardiac stress protein. *Clin Transl Sci* **3,** 189-196.

Chin AK & Evonuk E. (1971). Changes in plasma catecholamine and corticosterone levels after muscular exercise. *J Appl Physiol* **30,** 205-207.

Chin ER & Green HJ. (1996). Effects of tissue fractionation on exercise-induced alterations in SR function in rat gastrocnemius muscle. *J Appl Physiol (1985)* **80,** 940-948.

Claflin DR, Morgan DL & Julian FJ. (1998). The effect of length on the relationship between tension and intracellular [Ca2+] in intact frog skeletal muscle fibres. *J Physiol* **508 (Pt 1),** 179-186.

Colson BA, Locher MR, Bekyarova T, Patel JR, Fitzsimons DP, Irving TC & Moss RL. (2010). Differential roles of regulatory light chain and myosin binding protein-C phosphorylations in the modulation of cardiac force development. *J Physiol* **588,** 981-993.

Conlee RK, Barnett DW, Kelly KP & Han DH. (1991). Effects of cocaine, exercise, and resting conditions on plasma corticosterone and catecholamine concentrations in the rat. *Metabolism* **40,** 1043-1047.

Cooper LL, Li W, Lu Y, Centracchio J, Terentyeva R, Koren G & Terentyev D. (2013). Redox modification of ryanodine receptors by mitochondria-derived reactive oxygen species contributes to aberrant Ca2+ handling in ageing rabbit hearts. *J Physiol* **591,** 5895-5911.

Copello JA, Barg S, Onoue H & Fleischer S. (1997). Heterogeneity of Ca2+ gating of skeletal muscle and cardiac ryanodine receptors. *Biophys J* **73,** 141-156.

Copello JA, Barg S, Sonnleitner A, Porta M, Diaz-Sylvester P, Fill M, Schindler H & Fleischer S. (2002). Differential activation by Ca2+, ATP and caffeine of cardiac and skeletal muscle ryanodine receptors after block by Mg2+. *J Membr Biol* **187,** 51-64.

Costa VM, Silva R, Ferreira R, Amado F, Carvalho F, de Lourdes Bastos M, Carvalho RA, Carvalho M & Remiao F. (2009). Adrenaline in pro-oxidant conditions elicits intracellular survival pathways in isolated rat cardiomyocytes. *Toxicology* **257,** 70-79.

Couchonnal LF & Anderson ME. (2008). The role of calmodulin kinase II in myocardial physiology and disease. *Physiology (Bethesda)* **23,** 151-159.

Cox RH, Hubbard JW, Lawler JE, Sanders BJ & Mitchell VP. (1985). Cardiovascular and sympathoadrenal responses to stress in swim-trained rats. *J Appl Physiol (1985)* **58,** 1207-1214.

Curtis BM & Catterall WA. (1984). Purification of the calcium antagonist receptor of the voltage-sensitive calcium channel from skeletal muscle transverse tubules. *Biochemistry* **23,** 2113-2118.

Dal-Ros S, Bronner C, Auger C & Schini-Kerth VB. (2012). Red wine polyphenols improve an established aging-related endothelial dysfunction in the mesenteric artery of middle-aged rats: role of oxidative stress. *Biochem Biophys Res Commun* **419,** 381-387.

Dalle-Donne I, Giustarini D, Colombo R, Rossi R & Milzani A. (2003). Protein carbonylation in human diseases. *Trends Mol Med* **9,** 169-176.

Davies KJ, Quintanilha AT, Brooks GA & Packer L. (1982). Free radicals and tissue damage produced by exercise. *Biochem Biophys Res Commun* **107,** 1198-1205.

Dawson EA, Shave R, George K, Whyte G, Ball D, Gaze D & Collinson P. (2005). Cardiac drift during prolonged exercise with echocardiographic evidence of reduced diastolic function of the heart. *Eur J Appl Physiol* **94,** 305-309.

Dawson EA, Shave R, Whyte G, Ball D, Selmer C, Jans O, Secher NH & George KP. (2007). Preload maintenance and the left ventricular response to prolonged exercise in men. *Exp Physiol* **92,** 383-390.

De Jongh KS, Murphy BJ, Colvin AA, Hell JW, Takahashi M & Catterall WA. (1996). Specific phosphorylation of a site in the full-length form of the alpha 1 subunit of the cardiac L-type calcium channel by adenosine 3',5'-cyclic monophosphate-dependent protein kinase. *Biochemistry* **35,** 10392-10402.

de Meis L. (2002). Ca2+-ATPases (SERCA): energy transduction and heat production in transport ATPases. *J Membr Biol* **188,** 1-9.

de Tombe PP, Mateja RD, Tachampa K, Ait Mou Y, Farman GP & Irving TC. (2010). Myofilament length dependent activation. *J Mol Cell Cardiol* **48,** 851-858.

Del Nido PJ, Glynn P, Buenaventura P, Salama G & Koretsky AP. (1998). Fluorescence measurement of calcium transients in perfused rabbit heart using rhod 2. *Am J Physiol* **274,** H728-741.

Delgado J, Saborido A, Moran M & Megias A. (1999). Chronic and acute exercise do not alter Ca2+ regulatory systems and ectonucleotidase activities in rat heart. *J Appl Physiol (1985)* **87,** 152-160.

Dengel DR, Hagberg JM, Pratley RE, Rogus EM & Goldberg AP. (1998). Improvements in blood pressure, glucose metabolism, and lipoprotein lipids after aerobic exercise plus weight loss in obese, hypertensive middle-aged men. *Metabolism* **47,** 1075-1082.

DeSantiago J, Maier LS & Bers DM. (2002). Frequency-dependent acceleration of relaxation in the heart depends on CaMKII, but not phospholamban. *J Mol Cell Cardiol* **34,** 975-984.

Despa S, Bossuyt J, Han F, Ginsburg KS, Jia LG, Kutchai H, Tucker AL & Bers DM. (2005). Phospholemman-phosphorylation mediates the beta-adrenergic effects on Na/K pump function in cardiac myocytes. *Circ Res* **97,** 252-259.

Despa S, Shui B, Bossuyt J, Lang D, Kotlikoff MI & Bers DM. (2014). Junctional cleft [Ca(2)(+)]i measurements using novel cleft-targeted Ca(2)(+) sensors. *Circ Res* **115,** 339-347.

Dias FA, Walker LA, Arteaga GM, Walker JS, Vijayan K, Pena JR, Ke Y, Fogaca RT, Sanbe A, Robbins J & Wolska BM. (2006). The effect of myosin regulatory light chain

phosphorylation on the frequency-dependent regulation of cardiac function. *J Mol Cell Cardiol* **41,** 330-339.

Diaz PT, She ZW, Davis WB & Clanton TL. (1993). Hydroxylation of salicylate by the in vitro diaphragm: evidence for hydroxyl radical production during fatigue. *J Appl Physiol (1985)* **75,** 540-545.

Dimsdale JE & Moss J. (1980). Plasma catecholamines in stress and exercise. *JAMA* **243,** 340-342.

Dobesh DP, Konhilas JP & de Tombe PP. (2002). Cooperative activation in cardiac muscle: impact of sarcomere length. *Am J Physiol Heart Circ Physiol* **282,** H1055-1062.

Donoso P, Finkelstein JP, Montecinos L, Said M, Sanchez G, Vittone L & Bull R. (2014). Stimulation of NOX2 in isolated hearts reversibly sensitizes RyR2 channels to activation by cytoplasmic calcium. *J Mol Cell Cardiol* **68,** 38-46.

Donoso P, Sanchez G, Bull R & Hidalgo C. (2011). Modulation of cardiac ryanodine receptor activity by ROS and RNS. *Front Biosci (Landmark Ed)* **16,** 553-567.

Douglas PS, O'Toole ML, Hiller WD, Hackney K & Reichek N. (1987). Cardiac fatigue after prolonged exercise. *Circulation* **76,** 1206-1213.

Douglas PS, O'Toole ML & Katz SE. (1998). Prolonged exercise alters cardiac chronotropic responsiveness in endurance athletes. *J Sports Med Phys Fitness* **38,** 158-163.

Du C, MacGowan GA, Farkas DL & Koretsky AP. (2001). Calcium measurements in perfused mouse heart: quantitating fluorescence and absorbance of Rhod-2 by application of photon migration theory. *Biophys J* **80,** 549-561.

Duhamel TA, Green HJ, Perco JG & Ouyang J. (2005). Metabolic and sarcoplasmic reticulum Ca2+ cycling responses in human muscle 4 days following prolonged exercise. *Can J Physiol Pharmacol* **83,** 643-655.

Duhamel TA, Stewart RD, Tupling AR, Ouyang J & Green HJ. (2007). Muscle sarcoplasmic reticulum calcium regulation in humans during consecutive days of exercise and recovery. *J Appl Physiol (1985)* **103,** 1212-1220.

Dulhunty AF, Beard NA & Hanna AD. (2012). Regulation and dysregulation of cardiac ryanodine receptor (RyR2) open probability during diastole in health and disease. *J Gen Physiol* **140,** 87-92.

Duncker DJ & Bache RJ. (2008). Regulation of coronary blood flow during exercise. *Physiol Rev* **88,** 1009-1086.

Dutka TL & Lamb GD. (2007). Na+-K+ pumps in the transverse tubular system of skeletal muscle fibers preferentially use ATP from glycolysis. *Am J Physiol Cell Physiol* **293,** C967-977.

El-Awady MS, Rajamani U, Teng B, Tilley SL & Mustafa SJ. (2013). Evidence for the involvement of NADPH oxidase in adenosine receptors-mediated control of coronary flow using A and A knockout mice. *Physiol Rep* **1,** e00070.

El-Sawalhi MM & Ahmed LA. (2014). Exploring the protective role of apocynin, a specific NADPH oxidase inhibitor, in cisplatin-induced cardiotoxicity in rats. *Chem Biol Interact* **207,** 58-66.

Eysmann SB, Gervino E, Vatner DE, Katz SE, Decker L & Douglas PS. (1996). Prolonged exercise alters beta-adrenergic responsiveness in healthy sedentary humans. *J Appl Physiol (1985)* **80,** 616-622.

Fabiato A. (1982). Calcium release in skinned cardiac cells: variations with species, tissues, and development. *Fed Proc* **41,** 2238-2244.

Fabiato A & Fabiato F. (1975a). Contractions induced by a calcium-triggered release of calcium from the sarcoplasmic reticulum of single skinned cardiac cells. *J Physiol* **249,** 469-495.

Fabiato A & Fabiato F. (1975b). Dependence of the contractile activation of skinned cardiac cells on the sarcomere length. *Nature* **256,** 54-56.

Fabiato A & Fabiato F. (1978). Calcium-induced release of calcium from the sarcoplasmic reticulum of skinned cells from adult human, dog, cat, rabbit, rat, and frog hearts and from fetal and new-born rat ventricles. *Ann N Y Acad Sci* **307,** 491-522.

Favero TG, Colter D, Hooper PF & Abramson JJ. (1998). Hypochlorous acid inhibits Ca(2+)-ATPase from skeletal muscle sarcoplasmic reticulum. *J Appl Physiol (1985)* **84,** 425-430.

Favero TG, Pessah IN & Klug GA. (1993). Prolonged exercise reduces Ca2+ release in rat skeletal muscle sarcoplasmic reticulum. *Pflugers Arch* **422,** 472-475.

Frank K, Tilgmann C, Shannon TR, Bers DM & Kranias EG. (2000). Regulatory role of phospholamban in the efficiency of cardiac sarcoplasmic reticulum Ca2+ transport. *Biochemistry* **39,** 14176-14182.

French JP, Quindry JC, Falk DJ, Staib JL, Lee Y, Wang KK & Powers SK. (2006). Ischemia-reperfusion-induced calpain activation and SERCA2a degradation are attenuated by exercise training and calpain inhibition. *Am J Physiol Heart Circ Physiol* **290,** H128-136.

Friedman DB, Ordway GA & Williams RS. (1987). Exercise-induced functional desensitization of canine cardiac beta-adrenergic receptors. *J Appl Physiol (1985)* **62,** 1721-1723.

Fruen BR, Bardy JM, Byrem TM, Strasburg GM & Louis CF. (2000). Differential Ca(2+) sensitivity of skeletal and cardiac muscle ryanodine receptors in the presence of calmodulin. *Am J Physiol Cell Physiol* **279,** C724-733.

Fuchs F & Smith SH. (2001). Calcium, cross-bridges, and the Frank-Starling relationship. *News Physiol Sci* **16,** 5-10.

Gao WD, Atar D, Liu Y, Perez NG, Murphy AM & Marban E. (1997). Role of troponin I proteolysis in the pathogenesis of stunned myocardium. *Circ Res* **80,** 393-399.

Gao WD, Backx PH, Azan-Backx M & Marban E. (1994). Myofilament Ca2+ sensitivity in intact versus skinned rat ventricular muscle. *Circ Res* **74,** 408-415.

Gao WD, Liu Y, Mellgren R & Marban E. (1996). Intrinsic myofilament alterations underlying the decreased contractility of stunned myocardium. A consequence of Ca2+-dependent proteolysis? *Circ Res* **78,** 455-465.

Gehlert S, Bungartz G, Willkomm L, Korkmaz Y, Pfannkuche K, Schiffer T, Bloch W & Suhr F. (2012). Intense resistance exercise induces early and transient increases in ryanodine receptor 1 phosphorylation in human skeletal muscle. *PLoS One* **7,** e49326.

George K, Oxborough D, Forster J, Whyte G, Shave R, Dawson E, Stephenson C, Dugdill L, Edwards B & Gaze D. (2005). Mitral annular myocardial velocity assessment of segmental left ventricular diastolic function after prolonged exercise in humans. *J Physiol* **569,** 305-313.

George K, Shave R, Oxborough D, Cable T, Dawson E, Artis N, Gaze D, Hew-Butler T, Sharwood K & Noakes T. (2009). Left ventricular wall segment motion after ultra-endurance exercise in humans assessed by myocardial speckle tracking. *Eur J Echocardiogr* **10,** 238-243.

George K, Whyte G, Stephenson C, Shave R, Dawson E, Edwards B, Gaze D & Collinson P. (2004). Postexercise left ventricular function and cTnT in recreational marathon runners. *Med Sci Sports Exerc* **36,** 1709-1715.

Gerra G, Zaimovic A, Mascetti GG, Gardini S, Zambelli U, Timpano M, Raggi MA & Brambilla F. (2001). Neuroendocrine responses to experimentally-induced psychological stress in healthy humans. *Psychoneuroendocrinology* **26,** 91-107.

Ghezzi P. (2013). Protein glutathionylation in health and disease. *Biochim Biophys Acta* **1830,** 3165-3172.

Ginsburg KS & Bers DM. (2004). Modulation of excitation-contraction coupling by isoproterenol in cardiomyocytes with controlled SR Ca2+ load and Ca2+ current trigger. *J Physiol* **556,** 463-480.

Ginsburg KS & Bers DM. (2005). Isoproterenol does not enhance Ca-dependent Na/Ca exchange current in intact rabbit ventricular myocytes. *J Mol Cell Cardiol* **39,** 972-981.

Gokulrangan G, Zaidi A, Michaelis ML & Schoneich C. (2007). Proteomic analysis of protein nitration in rat cerebellum: effect of biological aging. *J Neurochem* **100,** 1494-1504.

Gomez-Cabrera MC, Borras C, Pallardo FV, Sastre J, Ji LL & Vina J. (2005). Decreasing xanthine oxidase-mediated oxidative stress prevents useful cellular adaptations to exercise in rats. *J Physiol* **567,** 113-120.

Gonzalez DR, Treuer AV, Castellanos J, Dulce RA & Hare JM. (2010). Impaired S-nitrosylation of the ryanodine receptor caused by xanthine oxidase activity contributes to calcium leak in heart failure. *J Biol Chem* **285,** 28938-28945.

Gonzalez DR, Treuer AV, Lamirault G, Mayo V, Cao Y, Dulce RA & Hare JM. (2014). NADPH oxidase-2 inhibition restores contractility and intracellular calcium handling and reduces arrhythmogenicity in dystrophic cardiomyopathy. *Am J Physiol Heart Circ Physiol* **307,** H710-721.

Goodman JM, McLaughlin PR & Liu PP. (2001). Left ventricular performance during prolonged exercise: absence of systolic dysfunction. *Clin Sci (Lond)* **100,** 529-537.

Gorcsan J, 3rd & Tanaka H. (2011). Echocardiographic assessment of myocardial strain. *J Am Coll Cardiol* **58,** 1401-1413.

Green HJ, Duhamel TA, Foley KP, Ouyang J, Smith IC & Stewart RD. (2007). Glucose supplements increase human muscle in vitro Na+-K+-ATPase activity during prolonged exercise. *Am J Physiol Regul Integr Comp Physiol* **293,** R354-362.

Green HJ, Duhamel TA, Smith IC, Rich SM, Thomas MM, Ouyang J & Yau JE. (2011a). Muscle fatigue and excitation-contraction coupling responses following a session of prolonged cycling. *Acta Physiol (Oxf)* **203,** 441-455.

Green HJ, Duhamel TA, Smith IC, Rich SM, Thomas MM, Ouyang J & Yau JE. (2011b). Muscle metabolic, enzymatic and transporter responses to a session of prolonged cycling. *Eur J Appl Physiol* **111,** 827-837.

Greensmith DJ, Eisner DA & Nirmalan M. (2010). The effects of hydrogen peroxide on intracellular calcium handling and contractility in the rat ventricular myocyte. *Cell Calcium* **48,** 341-351.

Grimditch GK, Barnard RJ & Duncan HW. (1981). Effect of exhaustive exercise on myocardial performance. *J Appl Physiol Respir Environ Exerc Physiol* **51,** 1098-1102.

Grover AK, Kwan CY & Samson SE. (2003a). Effects of peroxynitrite on sarco/endoplasmic reticulum Ca2+ pump isoforms SERCA2b and SERCA3a. *Am J Physiol Cell Physiol* **285,** C1537-1543.

Grover AK, Samson SE & Misquitta CM. (1997). Sarco(endo)plasmic reticulum Ca2+ pump isoform SERCA3 is more resistant than SERCA2b to peroxide. *Am J Physiol* **273,** C420-425.

Grover AK, Samson SE, Robinson S & Kwan CY. (2003b). Effects of peroxynitrite on sarcoplasmic reticulum Ca2+ pump in pig coronary artery smooth muscle. *Am J Physiol Cell Physiol* **284,** C294-301.

Grynkiewicz G, Poenie M & Tsien RY. (1985). A new generation of Ca2+ indicators with greatly improved fluorescence properties. *J Biol Chem* **260,** 3440-3450.

Gul M, Demircan B, Taysi S, Oztasan N, Gumustekin K, Siktar E, Polat MF, Akar S, Akcay F & Dane S. (2006). Effects of endurance training and acute exhaustive exercise on

antioxidant defense mechanisms in rat heart. *Comp Biochem Physiol A Mol Integr Physiol* **143,** 239-245.

Guo X, Yuan S, Liu Z & Fang Q. (2014). Oxidation- and CaMKII-mediated sarcoplasmic reticulum Ca(2+) leak triggers atrial fibrillation in aging. *J Cardiovasc Electrophysiol* **25,** 645-652.

Gwathmey JK, Slawsky MT, Hajjar RJ, Briggs GM & Morgan JP. (1990). Role of intracellular calcium handling in force-interval relationships of human ventricular myocardium. *J Clin Invest* **85,** 1599-1613.

Hain J, Onoue H, Mayrleitner M, Fleischer S & Schindler H. (1995). Phosphorylation modulates the function of the calcium release channel of sarcoplasmic reticulum from cardiac muscle. *J Biol Chem* **270,** 2074-2081.

Hamilton KL, Staib JL, Phillips T, Hess A, Lennon SL & Powers SK. (2003). Exercise, antioxidants, and HSP72: protection against myocardial ischemia/reperfusion. *Free Radic Biol Med* **34,** 800-809.

Han F, Tucker AL, Lingrel JB, Despa S & Bers DM. (2009). Extracellular potassium dependence of the Na+-K+-ATPase in cardiac myocytes: isoform specificity and effect of phospholemman. *Am J Physiol Cell Physiol* **297,** C699-705.

Hart E, Dawson E, Rasmussen P, George K, Secher NH, Whyte G & Shave R. (2006). Beta-adrenergic receptor desensitization in man: insight into post-exercise attenuation of cardiac function. *J Physiol* **577,** 717-725.

Hart E, Shave R, Middleton N, George K, Whyte G & Oxborough D. (2007). Effect of preload augmentation on pulsed wave and tissue Doppler echocardiographic indices of diastolic function after a marathon. *J Am Soc Echocardiogr* **20,** 1393-1399.

Hassan MY, Noakes TD, Berlyn P, Shave R & George K. (2006). Preload maintenance protects against a depression in left ventricular systolic, but not diastolic, function immediately after ultraendurance exercise. *Br J Sports Med* **40,** 536-540; discussion 540.

Hawkins C, Xu A & Narayanan N. (1994). Sarcoplasmic reticulum calcium pump in cardiac and slow twitch skeletal muscle but not fast twitch skeletal muscle undergoes phosphorylation by endogenous and exogenous Ca2+/calmodulin-dependent protein kinase. Characterization of optimal conditions for calcium pump phosphorylation. *J Biol Chem* **269,** 31198-31206.

Herrmann-Frank A, Richter M, Sarkozi S, Mohr U & Lehmann-Horn F. (1996). 4-Chloro-m-cresol, a potent and specific activator of the skeletal muscle ryanodine receptor. *Biochim Biophys Acta* **1289,** 31-40.

Heyndrickx GR, Millard RW, McRitchie RJ, Maroko PR & Vatner SF. (1975). Regional myocardial functional and electrophysiological alterations after brief coronary artery occlusion in conscious dogs. *J Clin Invest* **56,** 978-985.

Hibberd MG & Jewell BR. (1982). Calcium- and length-dependent force production in rat ventricular muscle. *J Physiol* **329,** 527-540.

Hidalgo C, Sanchez G, Barrientos G & Aracena-Parks P. (2006). A transverse tubule NADPH oxidase activity stimulates calcium release from isolated triads via ryanodine receptor type 1 S -glutathionylation. *J Biol Chem* **281,** 26473-26482.

Hosey MM, Barhanin J, Schmid A, Vandaele S, Ptasienski J, O'Callahan C, Cooper C & Lazdunski M. (1987). Photoaffinity labelling and phosphorylation of a 165 kilodalton peptide associated with dihydropyridine and phenylalkylamine-sensitive calcium channels. *Biochem Biophys Res Commun* **147,** 1137-1145.

Huang CC, Tsai SC & Lin WT. (2008). Potential ergogenic effects of L-arginine against oxidative and inflammatory stress induced by acute exercise in aging rats. *Exp Gerontol* **43,** 571-577.

Hulme JT, Westenbroek RE, Scheuer T & Catterall WA. (2006). Phosphorylation of serine 1928 in the distal C-terminal domain of cardiac CaV1.2 channels during beta1-adrenergic regulation. *Proc Natl Acad Sci U S A* **103,** 16574-16579.

Humphrey SM, Holliss DG & Seelye RN. (1985). Myocardial adenine pool depletion and recovery of mechanical function following ischemia. *Am J Physiol* **248,** H644-651.

Inesi G, Millman M & Eletr S. (1973). Temperature-induced transitions of function and structure in sarcoplasmic reticulum membranes. *J Mol Biol* **81,** 483-504.

Inserte J, Garcia-Dorado D, Hernando V & Soler-Soler J. (2005). Calpain-mediated impairment of Na+/K+-ATPase activity during early reperfusion contributes to cell death after myocardial ischemia. *Circ Res* **97,** 465-473.

Irving TC, Konhilas J, Perry D, Fischetti R & de Tombe PP. (2000). Myofilament lattice spacing as a function of sarcomere length in isolated rat myocardium. *Am J Physiol Heart Circ Physiol* **279,** H2568-2573.

Jackson MJ, Edwards RH & Symons MC. (1985). Electron spin resonance studies of intact mammalian skeletal muscle. *Biochim Biophys Acta* **847,** 185-190.

Jacobson AR, Moe ST, Allen PD & Fessenden JD. (2006). Structural determinants of 4-chlorom-cresol required for activation of ryanodine receptor type 1. *Mol Pharmacol* **70,** 259-266.

Jain SS, Paglialunga S, Vigna C, Ludzki A, Herbst EA, Lally JS, Schrauwen P, Hoeks J, Tupling AR, Bonen A & Holloway GP. (2014). High-Fat Diet-Induced Mitochondrial Biogenesis Is Regulated by Mitochondrial-Derived Reactive Oxygen Species Activation of CaMKII. *Diabetes* **63,** 1907-1913.

James JH, Wagner KR, King JK, Leffler RE, Upputuri RK, Balasubramaniam A, Friend LA, Shelly DA, Paul RJ & Fischer JE. (1999). Stimulation of both aerobic glycolysis and Na(+)-K(+)-ATPase activity in skeletal muscle by epinephrine or amylin. *Am J Physiol* **277,** E176-186.

James P, Inui M, Tada M, Chiesi M & Carafoli E. (1989). Nature and site of phospholamban regulation of the Ca2+ pump of sarcoplasmic reticulum. *Nature* **342,** 90-92.

Janssen PM. (2010). Kinetics of cardiac muscle contraction and relaxation are linked and determined by properties of the cardiac sarcomere. *Am J Physiol Heart Circ Physiol* **299,** H1092-1099.

Janssen PM & Periasamy M. (2007). Determinants of frequency-dependent contraction and relaxation of mammalian myocardium. *J Mol Cell Cardiol* **43,** 523-531.

Jiang F, Zhang Y & Dusting GJ. (2011). NADPH oxidase-mediated redox signaling: roles in cellular stress response, stress tolerance, and tissue repair. *Pharmacol Rev* **63,** 218-242.

Jin CZ, Jang JH, Wang Y, Kim JG, Bae YM, Shi J, Che CR, Kim SJ & Zhang YH. (2012). Neuronal nitric oxide synthase is up-regulated by angiotensin II and attenuates NADPH oxidase activity and facilitates relaxation in murine left ventricular myocytes. *J Mol Cell Cardiol* **52,** 1274-1281.

Josephson IR, Sanchez-Chapula J & Brown AM. (1984). Early outward current in rat single ventricular cells. *Circ Res* **54,** 157-162.

Juel C, Nordsborg NB & Bangsbo J. (2013). Exercise-induced increase in maximal in vitro Na-K-ATPase activity in human skeletal muscle. *Am J Physiol Regul Integr Comp Physiol* **304,** R1161-1165.

Kanski J, Hong SJ & Schoneich C. (2005). Proteomic analysis of protein nitration in aging skeletal muscle and identification of nitrotyrosine-containing sequences in vivo by nanoelectrospray ionization tandem mass spectrometry. *J Biol Chem* **280,** 24261-24266.

Kaplan P, Babusikova E, Lehotsky J & Dobrota D. (2003). Free radical-induced protein modification and inhibition of Ca2+-ATPase of cardiac sarcoplasmic reticulum. *Mol Cell Biochem* **248,** 41-47.

Kaplan P, Matejovicova M, Herijgers P & Flameng W. (2005). Effect of free radical scavengers on myocardial function and Na+, K+-ATPase activity in stunned rabbit myocardium. *Scand Cardiovasc J* **39,** 213-219.

Kaplan P, Matejovicova M, Herijgers P & Flameng W. (2008). Lack of the effect of superoxide dismutase and catalase on Na+,K+-ATPase activity in stunned rabbit hearts. *Physiol Res* **57 Suppl 2,** S61-66.

Kaplan P, Matejovicova M, Lehotsky J & Flameng W. (2002). Effect of myocardial stunning on thiol status, myofibrillar ATPase and troponin I proteolysis. *Mol Cell Biochem* **233,** 145-152.

Ke L, Qi XY, Dijkhuis AJ, Chartier D, Nattel S, Henning RH, Kampinga HH & Brundel BJ. (2008). Calpain mediates cardiac troponin degradation and contractile dysfunction in atrial fibrillation. *J Mol Cell Cardiol* **45,** 685-693.

Kennedy DJ, Vetteth S, Xie M, Periyasamy SM, Xie Z, Han C, Basrur V, Mutgi K, Fedorov V, Malhotra D & Shapiro JI. (2006). Ouabain decreases sarco(endo)plasmic reticulum calcium ATPase activity in rat hearts by a process involving protein oxidation. *Am J Physiol Heart Circ Physiol* **291,** H3003-3011.

Kentish JC, McCloskey DT, Layland J, Palmer S, Leiden JM, Martin AF & Solaro RJ. (2001). Phosphorylation of troponin I by protein kinase A accelerates relaxation and crossbridge cycle kinetics in mouse ventricular muscle. *Circ Res* **88,** 1059-1065.

Kevin LG, Camara AK, Riess ML, Novalija E & Stowe DF. (2003). Ischemic preconditioning alters real-time measure of O2 radicals in intact hearts with ischemia and reperfusion. *Am J Physiol Heart Circ Physiol* **284,** H566-574.

Kim SJ, Kudej RK, Yatani A, Kim YK, Takagi G, Honda R, Colantonio DA, Van Eyk JE, Vatner DE, Rasmusson RL & Vatner SF. (2001). A novel mechanism for myocardial stunning involving impaired Ca(2+) handling. *Circ Res* **89,** 831-837.

King LM, Boucher F & Opie LH. (1995). Coronary flow and glucose delivery as determinants of contracture in the ischemic myocardium. *J Mol Cell Cardiol* **27,** 701-720.

Kinkade K, Streeter J & Miller FJ. (2013). Inhibition of NADPH oxidase by apocynin attenuates progression of atherosclerosis. *Int J Mol Sci* **14,** 17017-17028.

Knyushko TV, Sharov VS, Williams TD, Schoneich C & Bigelow DJ. (2005). 3-Nitrotyrosine modification of SERCA2a in the aging heart: a distinct signature of the cellular redox environment. *Biochemistry* **44,** 13071-13081.

Kobayashi S, Susa T, Ishiguchi H, Myoren T, Murakami W, Kato T, Fukuda M, Hino A, Suetomi T, Ono M, Uchinoumi H, Tateishi H, Mochizuki M, Oda T, Okuda S, Doi M, Yamamoto T & Yano M. (2015). A low-dose beta1-blocker in combination with milrinone improves intracellular Ca2+ handling in failing cardiomyocytes by inhibition of milrinone-induced diastolic Ca2+ leakage from the sarcoplasmic reticulum. *PLoS One* **10,** e0114314.

Kobayashi T, Jin L & de Tombe PP. (2008). Cardiac thin filament regulation. *Pflugers Arch* **457,** 37-46.

Kobzik L, Reid MB, Bredt DS & Stamler JS. (1994). Nitric oxide in skeletal muscle. *Nature* **372,** 546-548.

Kolbeck RC, She ZW, Callahan LA & Nosek TM. (1997). Increased superoxide production during fatigue in the perfused rat diaphragm. *Am J Respir Crit Care Med* **156,** 140-145.

Konhilas JP, Irving TC & de Tombe PP. (2002). Myofilament calcium sensitivity in skinned rat cardiac trabeculae: role of interfilament spacing. *Circ Res* **90,** 59-65.

Konhilas JP, Irving TC, Wolska BM, Jweied EE, Martin AF, Solaro RJ & de Tombe PP. (2003). Troponin I in the murine myocardium: influence on length-dependent activation and interfilament spacing. *J Physiol* **547,** 951-961.

Kositprapa C, Zhang B, Berger S, Canty JM, Jr. & Lee TC. (2000). Calpain-mediated proteolytic cleavage of troponin I induced by hypoxia or metabolic inhibition in cultured neonatal cardiomyocytes. *Mol Cell Biochem* **214,** 47-55.

Kranias EG & Bers DM. (2007). Calcium and cardiomyopathies. *Subcell Biochem* **45,** 523-537.

Kranias EG, Garvey JL, Srivastava RD & Solaro RJ. (1985). Phosphorylation and functional modifications of sarcoplasmic reticulum and myofibrils in isolated rabbit hearts stimulated with isoprenaline. *Biochem J* **226,** 113-121.

Krijnen PA, Meischl C, Visser CA, Hack CE, Niessen HW & Roos D. (2003). NAD(P)H oxidase in the failing human heart. *J Am Coll Cardiol* **42,** 2170-2171; author reply 2171-2172.

Kubin AM, Skoumal R, Tavi P, Konyi A, Perjes A, Leskinen H, Ruskoaho H & Szokodi I. (2011). Role of reactive oxygen species in the regulation of cardiac contractility. *J Mol Cell Cardiol* **50,** 884-893.

Kumar S, Hall RJ, Mani AR, Moore KP, Camici PG, Rimoldi OE, Williams AJ & Macleod KT. (2009). Myocardial stunning is associated with impaired calcium uptake by sarcoplasmic reticulum. *Biochem Biophys Res Commun* **387,** 77-82.

Kutchai H & Geddis LM. (2001). Inhibition of the Na,K-ATPase of canine renal medulla by several local anesthetics. *Pharmacol Res* **43,** 399-403.

Laemmli UK. (1970). Cleavage of structural proteins during the assembly of the head of bacteriophage T4. *Nature* **227,** 680-685.

Lai FA, Misra M, Xu L, Smith HA & Meissner G. (1989). The ryanodine receptor-Ca2+ release channel complex of skeletal muscle sarcoplasmic reticulum. Evidence for a cooperatively coupled, negatively charged homotetramer. *J Biol Chem* **264,** 16776-16785.

Lamb GD & Westerblad H. (2011). Acute effects of reactive oxygen and nitrogen species on the contractile function of skeletal muscle. *J Physiol* **589,** 2119-2127.

Lancel S, Zhang J, Evangelista A, Trucillo MP, Tong X, Siwik DA, Cohen RA & Colucci WS. (2009). Nitroxyl activates SERCA in cardiac myocytes via glutathiolation of cysteine 674. *Circ Res* **104,** 720-723.

Lankford EB, Korzick DH, Palmer BM, Stauffer BL, Cheung JY & Moore RL. (1998). Endurance exercise alters the contractile responsiveness of rat heart to extracellular Na+ and Ca2+. *Med Sci Sports Exerc* **30,** 1502-1509.

Lattanzio FA, Jr. & Pressman BC. (1986). Alterations in intracellular calcium activity and contractility of isolated perfused rabbit hearts by ionophores and adrenergic agents. *Biochem Biophys Res Commun* **139,** 816-821.

Layland J & Kentish JC. (1999). Positive force- and [Ca2+]i-frequency relationships in rat ventricular trabeculae at physiological frequencies. *Am J Physiol* **276,** H9-H18.

LeBlanc J, Labrie A, Lupien D & Richard D. (1982). Catecholamines and triiodothyronine variations and the calorigenic response to norepinephrine in cold-adapted and exercise-trained rats. *Can J Physiol Pharmacol* **60,** 783-787.

Lee JK, Edderkaoui M, Truong P, Ohno I, Jang KT, Berti A, Pandol SJ & Gukovskaya AS. (2007). NADPH oxidase promotes pancreatic cancer cell survival via inhibiting JAK2 dephosphorylation by tyrosine phosphatases. *Gastroenterology* **133,** 1637-1648.

Lehman W, Rosol M, Tobacman LS & Craig R. (2001). Troponin organization on relaxed and activated thin filaments revealed by electron microscopy and three-dimensional reconstruction. *J Mol Biol* **307,** 739-744.

Lehnart SE, Wehrens XH, Kushnir A & Marks AR. (2004a). Cardiac ryanodine receptor function and regulation in heart disease. *Ann N Y Acad Sci* **1015,** 144-159.

Lehnart SE, Wehrens XH & Marks AR. (2004b). Calstabin deficiency, ryanodine receptors, and sudden cardiac death. *Biochem Biophys Res Commun* **322,** 1267-1279.

Leppik JA, Aughey RJ, Medved I, Fairweather I, Carey MF & McKenna MJ. (2004). Prolonged exercise to fatigue in humans impairs skeletal muscle Na+-K+-ATPase activity, sarcoplasmic reticulum Ca2+ release, and Ca2+ uptake. *J Appl Physiol (1985)* **97,** 1414-1423.

Levy AS, Chung JC, Kroetsch JT & Rush JW. (2009). Nitric oxide and coronary vascular endothelium adaptations in hypertension. *Vasc Health Risk Manag* **5,** 1075-1087.

Lew WY. (1989). Evaluation of left ventricular diastolic function. *Circulation* **79,** 1393-1397.

Li J, Stouffs M, Serrander L, Banfi B, Bettiol E, Charnay Y, Steger K, Krause KH & Jaconi ME. (2006). The NADPH oxidase NOX4 drives cardiac differentiation: Role in regulating cardiac transcription factors and MAP kinase activation. *Mol Biol Cell* **17,** 3978-3988.

Li Y, Arnold JM, Pampillo M, Babwah AV & Peng T. (2009a). Taurine prevents cardiomyocyte death by inhibiting NADPH oxidase-mediated calpain activation. *Free Radic Biol Med* **46,** 51-61.

Li Y, Li Y, Feng Q, Arnold M & Peng T. (2009b). Calpain activation contributes to hyperglycaemia-induced apoptosis in cardiomyocytes. *Cardiovasc Res* **84,** 100-110.

Liao R, Podesser BK & Lim CC. (2012). The continuing evolution of the Langendorff and ejecting murine heart: new advances in cardiac phenotyping. *Am J Physiol Heart Circ Physiol* **303,** H156-167.

Lin WT, Yang SC, Tsai SC, Huang CC & Lee NY. (2006). L-Arginine attenuates xanthine oxidase and myeloperoxidase activities in hearts of rats during exhaustive exercise. *Br J Nutr* **95,** 67-75.

Lindemann JP, Jones LR, Hathaway DR, Henry BG & Watanabe AM. (1983). beta-Adrenergic stimulation of phospholamban phosphorylation and Ca2+-ATPase activity in guinea pig ventricles. *J Biol Chem* **258,** 464-471.

Liu J, Yeo HC, Overvik-Douki E, Hagen T, Doniger SJ, Chyu DW, Brooks GA & Ames BN. (2000). Chronically and acutely exercised rats: biomarkers of oxidative stress and endogenous antioxidants. *J Appl Physiol (1985)* **89,** 21-28.

Lokuta AJ, Maertz NA, Meethal SV, Potter KT, Kamp TJ, Valdivia HH & Haworth RA. (2005). Increased nitration of sarcoplasmic reticulum Ca2+-ATPase in human heart failure. *Circulation* **111,** 988-995.

Ludtke SJ, Serysheva, II, Hamilton SL & Chiu W. (2005). The pore structure of the closed RyR1 channel. *Structure* **13,** 1203-1211.

Luna-Moreno D, Vazquez-Martinez O, Baez-Ruiz A, Ramirez J & Diaz-Munoz M. (2007). Food restricted schedules promote differential lipoperoxidative activity in rat hepatic subcellular fractions. *Comp Biochem Physiol A Mol Integr Physiol* **146,** 632-643.

Luo W, Grupp IL, Harrer J, Ponniah S, Grupp G, Duffy JJ, Doetschman T & Kranias EG. (1994). Targeted ablation of the phospholamban gene is associated with markedly enhanced myocardial contractility and loss of beta-agonist stimulation. *Circ Res* **75,** 401-409.

Maalouf RM, Eid AA, Gorin YC, Block K, Escobar GP, Bailey S & Abboud HE. (2012). Nox4-derived reactive oxygen species mediate cardiomyocyte injury in early type 1 diabetes. *Am J Physiol Cell Physiol* **302,** C597-604.

MacDonnell SM, Garcia-Rivas G, Scherman JA, Kubo H, Chen X, Valdivia H & Houser SR. (2008). Adrenergic regulation of cardiac contractility does not involve phosphorylation of the cardiac ryanodine receptor at serine 2808. *Circ Res* **102,** e65-72.

MacLennan DH & Kranias EG. (2003). Phospholamban: a crucial regulator of cardiac contractility. *Nat Rev Mol Cell Biol* **4,** 566-577.

Mahaney JE, Autry JM & Jones LR. (2000). Kinetics studies of the cardiac Ca-ATPase expressed in Sf21 cells: new insights on Ca-ATPase regulation by phospholamban. *Biophys J* **78,** 1306-1323.

Maher JT, Goodman AL, Francesconi R, Bowers WD, Hartley LH & Angelakos ET. (1972). Responses of rat myocardium to exhaustive exercise. *Am J Physiol* **222,** 207-212.

Marban E, Kitakaze M, Kusuoka H, Porterfield JK, Yue DT & Chacko VP. (1987). Intracellular free calcium concentration measured with 19F NMR spectroscopy in intact ferret hearts. *Proc Natl Acad Sci U S A* **84,** 6005-6009.

Marengo JJ, Hidalgo C & Bull R. (1998). Sulfhydryl oxidation modifies the calcium dependence of ryanodine-sensitive calcium channels of excitable cells. *Biophys J* **74,** 1263-1277.

Marks AR. (2013). Calcium cycling proteins and heart failure: mechanisms and therapeutics. *J Clin Invest* **123,** 46-52.

Martin WH, 3rd, Spina RJ, Korte E & Ogawa T. (1991). Effects of chronic and acute exercise on cardiovascular beta-adrenergic responses. *J Appl Physiol (1985)* **71,** 1523-1528.

Marx SO, Gaburjakova J, Gaburjakova M, Henrikson C, Ondrias K & Marks AR. (2001). Coupled gating between cardiac calcium release channels (ryanodine receptors). *Circ Res* **88,** 1151-1158.

Marx SO, Reiken S, Hisamatsu Y, Jayaraman T, Burkhoff D, Rosemblit N & Marks AR. (2000). PKA phosphorylation dissociates FKBP12.6 from the calcium release channel (ryanodine receptor): defective regulation in failing hearts. *Cell* **101,** 365-376.

Matsumoto Y, Kaneko M, Iimuro M, Fujise Y & Hayashi H. (2000). Role of high-energy phosphate metabolism in hydrogen peroxide-induced cardiac dysfunction. *Mol Cell Biochem* **204,** 97-106.

Matsumura Y, Kusuoka H, Inoue M, Hori M & Kamada T. (1993). Protective effect of the protease inhibitor leupeptin against myocardial stunning. *J Cardiovasc Pharmacol* **22,** 135-142.

Matsumura Y, Saeki E, Inoue M, Hori M, Kamada T & Kusuoka H. (1996). Inhomogeneous disappearance of myofilament-related cytoskeletal proteins in stunned myocardium of guinea pig. *Circ Res* **79,** 447-454.

Matsumura Y, Saeki E, Otsu K, Morita T, Takeda H, Kuzuya T, Hori M & Kusuoka H. (2001). Intracellular calcium level required for calpain activation in a single myocardial cell. *J Mol Cell Cardiol* **33,** 1133-1142.

Matsuoka S & Hilgemann DW. (1992). Steady-state and dynamic properties of cardiac sodium-calcium exchange. Ion and voltage dependencies of the transport cycle. *J Gen Physiol* **100,** 963-1001.

Matsushima S, Tsutsui H & Sadoshima J. (2014). Physiological and pathological functions of NADPH oxidases during myocardial ischemia-reperfusion. *Trends Cardiovasc Med* **24,** 202-205.

Matsuura H, Ehara T & Imoto Y. (1987). An analysis of the delayed outward current in single ventricular cells of the guinea-pig. *Pflugers Arch* **410,** 596-603.

McClung JM, Van Gammeren D, Whidden MA, Falk DJ, Kavazis AN, Hudson MB, Gayan-Ramirez G, Decramer M, DeRuisseau KC & Powers SK. (2009). Apocynin attenuates diaphragm oxidative stress and protease activation during prolonged mechanical ventilation. *Crit Care Med* **37,** 1373-1379.

McKillop DF & Geeves MA. (1993). Regulation of the interaction between actin and myosin subfragment 1: evidence for three states of the thin filament. *Biophys J* **65,** 693-701.

McMillan EM & Quadrilatero J. (2011). Differential apoptosis-related protein expression, mitochondrial properties, proteolytic enzyme activity, and DNA fragmentation between skeletal muscles. *Am J Physiol Regul Integr Comp Physiol* **300,** R531-543.

Medved I, Brown MJ, Bjorksten AR, Murphy KT, Petersen AC, Sostaric S, Gong X & McKenna MJ. (2004). N-acetylcysteine enhances muscle cysteine and glutathione availability and attenuates fatigue during prolonged exercise in endurance-trained individuals. *J Appl Physiol (1985)* **97,** 1477-1485.

Meissner G & Henderson JS. (1987). Rapid calcium release from cardiac sarcoplasmic reticulum vesicles is dependent on Ca2+ and is modulated by Mg2+, adenine nucleotide, and calmodulin. *J Biol Chem* **262,** 3065-3073.

Milani-Nejad N & Janssen PM. (2014). Small and large animal models in cardiac contraction research: advantages and disadvantages. *Pharmacol Ther* **141,** 235-249.

Miyamoto S, Ozaki H, Hori M, Endoh M & Karaki H. (1999). Tight coupling between the rate of rise of Ca2+ transient and peak twitch contraction in guinea-pig papillary muscle. *Eur J Pharmacol* **377,** 199-207.

Monasky MM & Janssen PM. (2009). The positive force-frequency relationship is maintained in absence of sarcoplasmic reticulum function in rabbit, but not in rat myocardium. *J Comp Physiol B* **179,** 469-479.

Moopanar TR & Allen DG. (2005). Reactive oxygen species reduce myofibrillar Ca2+ sensitivity in fatiguing mouse skeletal muscle at 37 degrees C. *J Physiol* **564,** 189-199.

Moopanar TR & Allen DG. (2006). The activity-induced reduction of myofibrillar Ca2+ sensitivity in mouse skeletal muscle is reversed by dithiothreitol. *J Physiol* **571,** 191-200.

Mope L, McClellan GB & Winegrad S. (1980). Calcium sensitivity of the contractile system and phosphorylation of troponin in hyperpermeable cardiac cells. *J Gen Physiol* **75,** 271-282.

Murphy RM, Dutka TL, Horvath D, Bell JR, Delbridge LM & Lamb GD. (2013). Ca2+-dependent proteolysis of junctophilin-1 and junctophilin-2 in skeletal and cardiac muscle. *J Physiol* **591,** 719-729.

Napankangas JP, Liimatta EV, Joensuu P, Bergmann U, Ylitalo K & Hassinen IE. (2012). Superoxide production during ischemia-reperfusion in the perfused rat heart: a comparison of two methods of measurement. *J Mol Cell Cardiol* **53,** 906-915.

Neilan TG, Januzzi JL, Lee-Lewandrowski E, Ton-Nu TT, Yoerger DM, Jassal DS, Lewandrowski KB, Siegel AJ, Marshall JE, Douglas PS, Lawlor D, Picard MH & Wood MJ. (2006). Myocardial injury and ventricular dysfunction related to training levels among nonelite participants in the Boston marathon. *Circulation* **114,** 2325-2333.

Nerbonne JM & Kass RS. (2005). Molecular physiology of cardiac repolarization. *Physiol Rev* **85,** 1205-1253.

Niemela KO, Palatsi IJ, Ikaheimo MJ, Takkunen JT & Vuori JJ. (1984). Evidence of impaired left ventricular performance after an uninterrupted competitive 24 hour run. *Circulation* **70,** 350-356.

Nottin S, Doucende G, Schuster I, Tanguy S, Dauzat M & Obert P. (2009). Alteration in left ventricular strains and torsional mechanics after ultralong duration exercise in athletes. *Circ Cardiovasc Imaging* **2,** 323-330.

Nottin S, Menetrier A, Rupp T, Boussuges A & Tordi N. (2012). Role of left ventricular untwisting in diastolic dysfunction after long duration exercise. *Eur J Appl Physiol* **112,** 525-533.

O'Brien PJ, Shen H, Weiler J, Ianuzzo CD, Wittnich C, Moe GW & Armstrong PW. (1991). Cardiac and muscle fatigue due to relative functional overload induced by excessive stimulation, hypersensitive excitation-contraction coupling, or diminished performance capacity correlates with sarcoplasmic reticulum failure. *Can J Physiol Pharmacol* **69,** 262-268.

Oberhofer M, Tian Q, Ruppenthal S, Wegener S, Reil JC, Korbel C, Hammer K, Menger M, Neuberger HR, Kaestner L & Lipp P. (2013). Calcium dysregulation in ventricular myocytes from mice expressing constitutively active Rac1. *Cell Calcium* **54,** 26-36.

Odermatt A, Kurzydlowski K & MacLennan DH. (1996). The vmax of the Ca2+-ATPase of cardiac sarcoplasmic reticulum (SERCA2a) is not altered by Ca2+/calmodulin-dependent phosphorylation or by interaction with phospholamban. *J Biol Chem* **271,** 14206-14213.

Oelze M, Warnholtz A, Faulhaber J, Wenzel P, Kleschyov AL, Coldewey M, Hink U, Pongs O, Fleming I, Wassmann S, Meinertz T, Ehmke H, Daiber A & Munzel T. (2006). NADPH oxidase accounts for enhanced superoxide production and impaired endothelium-dependent smooth muscle relaxation in BKbeta1-/- mice. *Arterioscler Thromb Vasc Biol* **26,** 1753-1759.

Ohkawa H, Ohishi N & Yagi K. (1979). Assay for lipid peroxides in animal tissues by thiobarbituric acid reaction. *Anal Biochem* **95,** 351-358.

Olah A, Nemeth BT, Matyas C, Horvath EM, Hidi L, Birtalan E, Kellermayer D, Ruppert M, Merkely G, Szabo G, Merkely B & Radovits T. (2015). Cardiac effects of acute exhaustive exercise in a rat model. *Int J Cardiol* **182,** 258-266.

Oosthuyse T, Avidon I, Likuwa I & Woodiwiss AJ. (2012). Progression of changes in left ventricular function during four days of simulated multi-stage cycling. *Eur J Appl Physiol* **112,** 2243-2255.

Oxborough D, Birch K, Shave R & George K. (2010a). "Exercise-induced cardiac fatigue"--a review of the echocardiographic literature. *Echocardiography* **27,** 1130-1140.

Oxborough D, Whyte G, Wilson M, O'Hanlon R, Birch K, Shave R, Smith G, Godfrey R, Prasad S & George K. (2010b). A depression in left ventricular diastolic filling following prolonged strenuous exercise is associated with changes in left atrial mechanics. *J Am Soc Echocardiogr* **23,** 968-976.

Oztezcan S, Dogru-Abbasoglu S, Mutlu-Turkoglu U, Calay Z, Aykac-Toker G & Uysal M. (2000). The role of stimulated lipid peroxidation and impaired calcium sequestration in the enhancement of cocaine induced hepatotoxicity by ethanol. *Drug Alcohol Depend* **58,** 77-83.

Paulsen G, Cumming KT, Holden G, Hallen J, Ronnestad BR, Sveen O, Skaug A, Paur I, Bastani NE, Ostgaard HN, Buer C, Midttun M, Freuchen F, Wiig H, Ulseth ET, Garthe I, Blomhoff R, Benestad HB & Raastad T. (2014). Vitamin C and E supplementation hampers cellular adaptation to endurance training in humans: a double-blind, randomised, controlled trial. *J Physiol* **592,** 1887-1901.

Pedrozo Z, Sanchez G, Torrealba N, Valenzuela R, Fernandez C, Hidalgo C, Lavandero S & Donoso P. (2010). Calpains and proteasomes mediate degradation of ryanodine receptors in a model of cardiac ischemic reperfusion. *Biochim Biophys Acta* **1802,** 356-362.

Perchenet L, Hinde AK, Patel KC, Hancox JC & Levi AJ. (2000). Stimulation of Na/Ca exchange by the beta-adrenergic/protein kinase A pathway in guinea-pig ventricular myocytes at 37 degrees C. *Pflugers Arch* **439,** 822-828.

Perez AC, Cabral de Oliveira AC, Estevez E, Molina AJ, Prieto JG & Alvarez AI. (2003). Mitochondrial, sarcoplasmic membrane integrity and protein degradation in heart and skeletal muscle in exercised rats. *Comp Biochem Physiol C Toxicol Pharmacol* **134,** 199-206.

Petersen AC, Murphy KT, Snow RJ, Leppik JA, Aughey RJ, Garnham AP, Cameron-Smith D & McKenna MJ. (2005). Depressed Na+-K+-ATPase activity in skeletal muscle at fatigue is correlated with increased Na+-K+-ATPase mRNA expression following intense exercise. *Am J Physiol Regul Integr Comp Physiol* **289,** R266-274.

Pierce GN, Kutryk MJ, Dhalla KS, Beamish RE & Dhalla NS. (1984). Biochemical alterations in heart after exhaustive swimming in rats. *J Appl Physiol Respir Environ Exerc Physiol* **57,** 326-331.

Qin F, Siwik DA, Lancel S, Zhang J, Kuster GM, Luptak I, Wang L, Tong X, Kang YJ, Cohen RA & Colucci WS. (2013). Hydrogen peroxide-mediated SERCA cysteine 674 oxidation contributes to impaired cardiac myocyte relaxation in senescent mouse heart. *J Am Heart Assoc* **2,** e000184.

Raj DA, Booker TS & Belcastro AN. (1998). Striated muscle calcium-stimulated cysteine protease (calpain-like) activity promotes myeloperoxidase activity with exercise. *Pflugers Arch* **435,** 804-809.

Rao V, Cheng Y, Lindert S, Wang D, Oxenford L, McCulloch AD, McCammon JA & Regnier M. (2014). PKA phosphorylation of cardiac troponin I modulates activation and relaxation kinetics of ventricular myofibrils. *Biophys J* **107,** 1196-1204.

Reid MB. (2001). Invited Review: redox modulation of skeletal muscle contraction: what we know and what we don't. *J Appl Physiol (1985)* **90,** 724-731.

Reid MB, Haack KE, Franchek KM, Valberg PA, Kobzik L & West MS. (1992). Reactive oxygen in skeletal muscle. I. Intracellular oxidant kinetics and fatigue in vitro. *J Appl Physiol (1985)* **73,** 1797-1804.

Reiken S, Gaburjakova M, Guatimosim S, Gomez AM, D'Armiento J, Burkhoff D, Wang J, Vassort G, Lederer WJ & Marks AR. (2003). Protein kinase A phosphorylation of the cardiac calcium release channel (ryanodine receptor) in normal and failing hearts. Role of phosphatases and response to isoproterenol. *J Biol Chem* **278,** 444-453.

Reuter H, Cachelin AB, De Peyer JE & Kokubun S. (1983). Modulation of calcium channels in cultured cardiac cells by isoproterenol and 8-bromo-cAMP. *Cold Spring Harb Symp Quant Biol* **48 Pt 1,** 193-200.

Rodriguez P, Jackson WA & Colyer J. (2004). Critical evaluation of cardiac Ca2+-ATPase phosphorylation on serine 38 using a phosphorylation site-specific antibody. *J Biol Chem* **279,** 17111-17119.

Roe ND, Thomas DP & Ren J. (2011). Inhibition of NADPH oxidase alleviates experimental diabetes-induced myocardial contractile dysfunction. *Diabetes Obes Metab* **13,** 465-473.

Roof SR, Tang L, Ostler JE, Periasamy M, Gyorke S, Billman GE & Ziolo MT. (2013). Neuronal nitric oxide synthase is indispensable for the cardiac adaptive effects of exercise. *Basic Res Cardiol* **108,** 332.

Ross R, Dagnone D, Jones PJ, Smith H, Paddags A, Hudson R & Janssen I. (2000). Reduction in obesity and related comorbid conditions after diet-induced weight loss or exercise-induced weight loss in men. A randomized, controlled trial. *Ann Intern Med* **133,** 92-103.

Rousseau E, Smith JS, Henderson JS & Meissner G. (1986). Single channel and 45Ca2+ flux measurements of the cardiac sarcoplasmic reticulum calcium channel. *Biophys J* **50,** 1009-1014.

Rundqvist B, Elam M, Bergmann-Sverrisdottir Y, Eisenhofer G & Friberg P. (1997). Increased cardiac adrenergic drive precedes generalized sympathetic activation in human heart failure. *Circulation* **95,** 169-175.

Sag CM, Wagner S & Maier LS. (2013). Role of oxidants on calcium and sodium movement in healthy and diseased cardiac myocytes. *Free Radic Biol Med* **63,** 338-349.

Sahlen A, Rubulis A, Winter R, Jacobsen PH, Stahlberg M, Tornvall P, Bergfeldt L & Braunschweig F. (2009). Cardiac fatigue in long-distance runners is associated with ventricular repolarization abnormalities. *Heart Rhythm* **6,** 512-519.

Saltin B & Stenberg J. (1964). Circulatory Response to Prolonged Severe Exercise. *J Appl Physiol* **19,** 833-838.

Sanchez G, Escobar M, Pedrozo Z, Macho P, Domenech R, Hartel S, Hidalgo C & Donoso P. (2008). Exercise and tachycardia increase NADPH oxidase and ryanodine receptor-2 activity: possible role in cardioprotection. *Cardiovasc Res* **77,** 380-386.

Sanchez G, Pedrozo Z, Domenech RJ, Hidalgo C & Donoso P. (2005). Tachycardia increases NADPH oxidase activity and RyR2 S-glutathionylation in ventricular muscle. *J Mol Cell Cardiol* **39,** 982-991.

Schagger H. (2006). Tricine-SDS-PAGE. *Nat Protoc* **1,** 16-22.

Schaper J, Meiser E & Stammler G. (1985). Ultrastructural morphometric analysis of myocardium from dogs, rats, hamsters, mice, and from human hearts. *Circ Res* **56,** 377-391.

Scheurink AJ, Steffens AB, Bouritius H, Dreteler GH, Bruntink R, Remie R & Zaagsma J. (1989). Adrenal and sympathetic catecholamines in exercising rats. *Am J Physiol* **256,** R155-160.

Schoneich C & Sharov VS. (2006). Mass spectrometry of protein modifications by reactive oxygen and nitrogen species. *Free Radic Biol Med* **41,** 1507-1520.

Schwinger RH, Bohm M, Schmidt U, Karczewski P, Bavendiek U, Flesch M, Krause EG & Erdmann E. (1995). Unchanged protein levels of SERCA II and phospholamban but reduced Ca2+ uptake and Ca(2+)-ATPase activity of cardiac sarcoplasmic reticulum from dilated cardiomyopathy patients compared with patients with nonfailing hearts. *Circulation* **92,** 3220-3228.

Scott JM, Esch BT, Haykowsky MJ, Isserow S, Koehle MS, Hughes BG, Zbogar D, Bredin SS, McKenzie DC & Warburton DE. (2007). Sex differences in left ventricular function and beta-receptor responsiveness following prolonged strenuous exercise. *J Appl Physiol (1985)* **102,** 681-687.

Scott JM, Esch BT, Shave R, Warburton DE, Gaze D & George K. (2009). Cardiovascular consequences of completing a 160-km ultramarathon. *Med Sci Sports Exerc* **41,** 26-34.

Scott JM & Warburton DE. (2008). Mechanisms underpinning exercise-induced changes in left ventricular function. *Med Sci Sports Exerc* **40,** 1400-1407.

Seidler NW, Jona I, Vegh M & Martonosi A. (1989). Cyclopiazonic acid is a specific inhibitor of the Ca2+-ATPase of sarcoplasmic reticulum. *J Biol Chem* **264,** 17816-17823.

Senejoux F, Girard-Thernier C, Berthelot A, Bevalot F & Demougeot C. (2013). New insights into the mechanisms of the vasorelaxant effects of apocynin in rat thoracic aorta. *Fundam Clin Pharmacol* **27,** 262-270.

Serysheva, II, Schatz M, van Heel M, Chiu W & Hamilton SL. (1999). Structure of the skeletal muscle calcium release channel activated with Ca2+ and AMP-PCP. *Biophys J* **77,** 1936-1944.

Seward SW, Seiler KS & Starnes JW. (1995). Intrinsic myocardial function and oxidative stress after exhaustive exercise. *J Appl Physiol (1985)* **79,** 251-255.

Shan J, Kushnir A, Betzenhauser MJ, Reiken S, Li J, Lehnart SE, Lindegger N, Mongillo M, Mohler PJ & Marks AR. (2010). Phosphorylation of the ryanodine receptor mediates the cardiac fight or flight response in mice. *J Clin Invest* **120,** 4388-4398.

Shao CH, Capek HL, Patel KP, Wang M, Tang K, DeSouza C, Nagai R, Mayhan W, Periasamy M & Bidasee KR. (2011). Carbonylation contributes to SERCA2a activity loss and diastolic dysfunction in a rat model of type 1 diabetes. *Diabetes* **60,** 947-959.

Shao Q, Ren B, Saini HK, Netticadan T, Takeda N & Dhalla NS. (2005). Sarcoplasmic reticulum Ca2+ transport and gene expression in congestive heart failure are modified by imidapril treatment. *Am J Physiol Heart Circ Physiol* **288,** H1674-1682.

Shave R, Dawson E, Whyte G, George K, Gaze D & Collinson P. (2004). Altered cardiac function and minimal cardiac damage during prolonged exercise. *Med Sci Sports Exerc* **36,** 1098-1103.

Shave R, George K, Whyte G, Hart E & Middleton N. (2008). Postexercise changes in left ventricular function: the evidence so far. *Med Sci Sports Exerc* **40,** 1393-1399.

Shave R & Oxborough D. (2012). Exercise-induced cardiac injury: evidence from novel imaging techniques and highly sensitive cardiac troponin assays. *Prog Cardiovasc Dis* **54,** 407-415.

Shindoh C, DiMarco A, Thomas A, Manubay P & Supinski G. (1990). Effect of N-acetylcysteine on diaphragm fatigue. *J Appl Physiol (1985)* **68,** 2107-2113.

Shinohara M, Shang WH, Kubodera M, Harada S, Mitsushita J, Kato M, Miyazaki H, Sumimoto H & Kamata T. (2007). Nox1 redox signaling mediates oncogenic Ras-induced disruption of stress fibers and focal adhesions by down-regulating Rho. *J Biol Chem* **282,** 17640-17648.

Siegel AJ, Sholar M, Yang J, Dhanak E & Lewandrowski KB. (1997). Elevated serum cardiac markers in asymptomatic marathon runners after competition: is the myocardium stunned? *Cardiology* **88,** 487-491.

Silverman B, Fuller W, Eaton P, Deng J, Moorman JR, Cheung JY, James AF & Shattock MJ. (2005). Serine 68 phosphorylation of phospholemman: acute isoform-specific activation of cardiac Na/K ATPase. *Cardiovasc Res* **65,** 93-103.

Simmerman HK, Collins JH, Theibert JL, Wegener AD & Jones LR. (1986). Sequence analysis of phospholamban. Identification of phosphorylation sites and two major structural domains. *J Biol Chem* **261,** 13333-13341.

Simonides WS & van Hardeveld C. (1990). An assay for sarcoplasmic reticulum Ca2(+)-ATPase activity in muscle homogenates. *Anal Biochem* **191,** 321-331.

Simor T, Lorand T, Gaszner B & Elgavish GA. (1997). The modulation of pacing-induced changes in intracellular sodium levels by extracellular Ca2+ in isolated perfused rat hearts. *J Mol Cell Cardiol* **29,** 1225-1235.

Singh RB, Hryshko L, Freed D & Dhalla NS. (2012). Activation of proteolytic enzymes and depression of the sarcolemmal Na+/K+-ATPase in ischemia-reperfused heart may be mediated through oxidative stress. *Can J Physiol Pharmacol* **90,** 249-260.

Smith GL & Steele DS. (1992). Inorganic phosphate decreases the Ca2+ content of the sarcoplasmic reticulum in saponin-treated rat cardiac trabeculae. *J Physiol* **458,** 457-473.

Soltysinska E, Thiele S, Olesen SP & Osadchii OE. (2011). Chronic sympathetic activation promotes downregulation of beta-adrenoceptor-mediated effects in the guinea pig heart independently of structural remodeling and systolic dysfunction. *Pflugers Arch* **462,** 529-543.

Souvannakitti D, Nanduri J, Yuan G, Kumar GK, Fox AP & Prabhakar NR. (2010). NADPH oxidase-dependent regulation of T-type Ca2+ channels and ryanodine receptors mediate the augmented exocytosis of catecholamines from intermittent hypoxia-treated neonatal rat chromaffin cells. *J Neurosci* **30,** 10763-10772.

Stadtman ER & Levine RL. (2003). Free radical-mediated oxidation of free amino acids and amino acid residues in proteins. *Amino Acids* **25,** 207-218.

Starnes JW & Bowles DK. (1995). Role of exercise in the cause and prevention of cardiac dysfunction. *Exerc Sport Sci Rev* **23,** 349-373.

Stefanska J & Pawliczak R. (2008). Apocynin: molecular aptitudes. *Mediators Inflamm* **2008,** 106507.

Stelzer JE, Patel JR, Walker JW & Moss RL. (2007). Differential roles of cardiac myosin-binding protein C and cardiac troponin I in the myofibrillar force responses to protein kinase A phosphorylation. *Circ Res* **101,** 503-511.

Stoyanovsky D, Murphy T, Anno PR, Kim YM & Salama G. (1997). Nitric oxide activates skeletal and cardiac ryanodine receptors. *Cell Calcium* **21,** 19-29.

Sun QA, Hess DT, Nogueira L, Yong S, Bowles DE, Eu J, Laurita KR, Meissner G & Stamler JS. (2011). Oxygen-coupled redox regulation of the skeletal muscle ryanodine receptor-Ca2+ release channel by NADPH oxidase 4. *Proc Natl Acad Sci U S A* **108,** 16098-16103.

Suzuki YJ, Cleemann L, Abernethy DR & Morad M. (1998). Glutathione is a cofactor for H2O2-mediated stimulation of Ca2+-induced Ca2+ release in cardiac myocytes. *Free Radic Biol Med* **24,** 318-325.

Swiderek K, Jaquet K, Meyer HE, Schachtele C, Hofmann F & Heilmeyer LM, Jr. (1990). Sites phosphorylated in bovine cardiac troponin T and I. Characterization by 31P-NMR spectroscopy and phosphorylation by protein kinases. *Eur J Biochem* **190,** 575-582.

Tachampa K, Wang H, Farman GP & de Tombe PP. (2007). Cardiac troponin I threonine 144: role in myofilament length dependent activation. *Circ Res* **101,** 1081-1083.

Tang WH, Cheng WT, Kravtsov GM, Tong XY, Hou XY, Chung SK & Chung SS. (2010). Cardiac contractile dysfunction during acute hyperglycemia due to impairment of SERCA by polyol pathway-mediated oxidative stress. *Am J Physiol Cell Physiol* **299,** C643-653.

Terentyev D, Gyorke I, Belevych AE, Terentyeva R, Sridhar A, Nishijima Y, de Blanco EC, Khanna S, Sen CK, Cardounel AJ, Carnes CA & Gyorke S. (2008). Redox modification of ryanodine receptors contributes to sarcoplasmic reticulum Ca2+ leak in chronic heart failure. *Circ Res* **103,** 1466-1472.

Thomas MM, Vigna C, Betik AC, Tupling AR & Hepple RT. (2011). Cardiac calcium pump inactivation and nitrosylation in senescent rat myocardium are not attenuated by long-term treadmill training. *Exp Gerontol* **46,** 803-810.

Tiidus PM, Zajchowski S, Enns D, Holden D, Bombardier E & Belcastro AN. (2002). Differential effect of oestrogen on post-exercise cardiac muscle myeloperoxidase and calpain activities in female rats. *Acta Physiol Scand* **174,** 131-136.

Timerman AP, Jayaraman T, Wiederrecht G, Onoue H, Marks AR & Fleischer S. (1994). The ryanodine receptor from canine heart sarcoplasmic reticulum is associated with a novel FK-506 binding protein. *Biochem Biophys Res Commun* **198,** 701-706.

Tong CW, Gaffin RD, Zawieja DC & Muthuchamy M. (2004). Roles of phosphorylation of myosin binding protein-C and troponin I in mouse cardiac muscle twitch dynamics. *J Physiol* **558,** 927-941.

211

Tsien RW, Bean BP, Hess P, Lansman JB, Nilius B & Nowycky MC. (1986). Mechanisms of calcium channel modulation by beta-adrenergic agents and dihydropyridine calcium agonists. *J Mol Cell Cardiol* **18,** 691-710.

Tupling R & Green H. (2002). Silver ions induce Ca2+ release from the SR in vitro by acting on the Ca2+ release channel and the Ca2+ pump. *J Appl Physiol (1985)* **92,** 1603-1610.

Umanskaya A, Santulli G, Xie W, Andersson DC, Reiken SR & Marks AR. (2014). Genetically enhancing mitochondrial antioxidant activity improves muscle function in aging. *Proc Natl Acad Sci U S A* **111,** 15250-15255.

Unger BS & Patil BM. (2009). Apocynin improves endothelial function and prevents the development of hypertension in fructose fed rat. *Indian J Pharmacol* **41,** 208-212.

van der Laarse A. (2002). Hypothesis: troponin degradation is one of the factors responsible for deterioration of left ventricular function in heart failure. *Cardiovasc Res* **56,** 8-14.

van Noord C, Eijgelsheim M & Stricker BH. (2010). Drug- and non-drug-associated QT interval prolongation. *Br J Clin Pharmacol* **70,** 16-23.

Varian KD & Janssen PM. (2007). Frequency-dependent acceleration of relaxation involves decreased myofilament calcium sensitivity. *Am J Physiol Heart Circ Physiol* **292,** H2212-2219.

Vatner SF & Hittinger L. (1993). Myocardial perfusion dependent and independent mechanisms of regional myocardial dysfunction in hypertrophy. *Basic Res Cardiol* **88 Suppl 1,** 81-95.

Verburg E, Murphy RM, Richard I & Lamb GD. (2009). Involvement of calpains in Ca2+-induced disruption of excitation-contraction coupling in mammalian skeletal muscle fibers. *Am J Physiol Cell Physiol* **296,** C1115-1122.

Verburg E, Murphy RM, Stephenson DG & Lamb GD. (2005). Disruption of excitation-contraction coupling and titin by endogenous Ca2+-activated proteases in toad muscle fibres. *J Physiol* **564,** 775-790.

Viner RI, Ferrington DA, Williams TD, Bigelow DJ & Schoneich C. (1999a). Protein modification during biological aging: selective tyrosine nitration of the SERCA2a isoform of the sarcoplasmic reticulum Ca2+-ATPase in skeletal muscle. *Biochem J* **340 (Pt 3),** 657-669.

Viner RI, Huhmer AF, Bigelow DJ & Schoneich C. (1996). The oxidative inactivation of sarcoplasmic reticulum Ca(2+)-ATPase by peroxynitrite. *Free Radic Res* **24,** 243-259.

Viner RI, Williams TD & Schoneich C. (1999b). Peroxynitrite modification of protein thiols: oxidation, nitrosylation, and S-glutathiolation of functionally important cysteine residue(s) in the sarcoplasmic reticulum Ca-ATPase. *Biochemistry* **38,** 12408-12415.

Viner RI, Williams TD & Schoneich C. (2000). Nitric oxide-dependent modification of the sarcoplasmic reticulum Ca-ATPase: localization of cysteine target sites. *Free Radic Biol Med* **29,** 489-496.

Vinnikova AK, Kukreja RC & Hess ML. (1992). Singlet oxygen-induced inhibition of cardiac sarcolemmal Na+K(+)-ATPase. *J Mol Cell Cardiol* **24,** 465-470.

Vitiello D, Boissiere J, Doucende G, Gayrard S, Polge A, Faure P, Goux A, Tanguy S, Obert P, Reboul C & Nottin S. (2011). beta-Adrenergic receptors desensitization is not involved in exercise-induced cardiac fatigue: NADPH oxidase-induced oxidative stress as a new trigger. *J Appl Physiol (1985)* **111,** 1242-1248.

Voss AA, Lango J, Ernst-Russell M, Morin D & Pessah IN. (2004). Identification of hyperreactive cysteines within ryanodine receptor type 1 by mass spectrometry. *J Biol Chem* **279,** 34514-34520.

Wang C, Liu N, Luan R, Li Y, Wang D, Zou W, Xing Y, Tao L, Cao F & Wang H. (2013). Apelin protects sarcoplasmic reticulum function and cardiac performance in ischaemia-reperfusion by attenuating oxidation of sarcoplasmic reticulum Ca2+-ATPase and ryanodine receptor. *Cardiovasc Res* **100,** 114-124.

Wang W, Landstrom AP, Wang Q, Munro ML, Beavers D, Ackerman MJ, Soeller C & Wehrens XH. (2014). Reduced junctional Na+/Ca2+-exchanger activity contributes to sarcoplasmic reticulum Ca2+ leak in junctophilin-2-deficient mice. *Am J Physiol Heart Circ Physiol* **307,** H1317-1326.

Wang X, Takeda S, Mochizuki S, Jindal R & Dhalla NS. (1999). Mechanisms of Hydrogen Peroxide-Induced Increase in Intracellular Calcium in Cardiomyocytes. *J Cardiovasc Pharmacol Ther* **4,** 41-48.

Wanichawan P, Hafver TL, Hodne K, Aronsen JM, Lunde IG, Dalhus B, Lunde M, Kvaloy H, Louch WE, Tonnessen T, Sjaastad I, Sejersted OM & Carlson CR. (2014). Molecular

basis of calpain cleavage and inactivation of the sodium-calcium exchanger 1 in heart failure. *J Biol Chem* **289,** 33984-33998.

Warburton DE, Nicol CW & Bredin SS. (2006). Health benefits of physical activity: the evidence. *CMAJ* **174,** 801-809.

Weber T, Neumann J, Meissner A, Grosse Hartlage M, Van Aken H, Hanske G, Schmitz W & Boknik P. (2006). Reduced serine-16 and threonine-17 phospholamban phosphorylation in stunning of conscious dogs: no evidence for any involvement of protein kinase A or protein phosphatases. *Basic Res Cardiol* **101,** 253-260.

Wegener AD, Simmerman HK, Lindemann JP & Jones LR. (1989). Phospholamban phosphorylation in intact ventricles. Phosphorylation of serine 16 and threonine 17 in response to beta-adrenergic stimulation. *J Biol Chem* **264,** 11468-11474.

Wehrens XH, Lehnart SE, Huang F, Vest JA, Reiken SR, Mohler PJ, Sun J, Guatimosim S, Song LS, Rosemblit N, D'Armiento JM, Napolitano C, Memmi M, Priori SG, Lederer WJ & Marks AR. (2003). FKBP12.6 deficiency and defective calcium release channel (ryanodine receptor) function linked to exercise-induced sudden cardiac death. *Cell* **113,** 829-840.

Wehrens XH, Lehnart SE, Reiken S, Vest JA, Wronska A & Marks AR. (2006). Ryanodine receptor/calcium release channel PKA phosphorylation: a critical mediator of heart failure progression. *Proc Natl Acad Sci U S A* **103,** 511-518.

Wehrens XH & Marks AR. (2004). Molecular determinants of altered contractility in heart failure. *Ann Med* **36 Suppl 1,** 70-80.

Wei GZ, Zhou JJ, Wang B, Wu F, Bi H, Wang YM, Yi DH, Yu SQ & Pei JM. (2007). Diastolic Ca2+ overload caused by Na+/Ca2+ exchanger during the first minutes of reperfusion results in continued myocardial stunning. *Eur J Pharmacol* **572,** 1-11.

Wei SK, Ruknudin A, Hanlon SU, McCurley JM, Schulze DH & Haigney MC. (2003). Protein kinase A hyperphosphorylation increases basal current but decreases beta-adrenergic responsiveness of the sarcolemmal Na+-Ca2+ exchanger in failing pig myocytes. *Circ Res* **92,** 897-903.

Weicker H, Feraudi M, Hagele H & Pluto R. (1984). Electrochemical detection of catecholamines in urine and plasma after separation with HPLC. *Clin Chim Acta* **141,** 17-25.

Weicker H, Hageloch W, Luo J, Muller D, Werle E & Sehling KM. (1990). Purine nucleotides and AMP deamination during maximal and endurance swimming exercise in heart and skeletal muscle of rats. *Int J Sports Med* **11 Suppl 2,** S68-77.

Welsh RC, Warburton DE, Humen DP, Taylor DA, McGavock J & Haykowsky MJ. (2005). Prolonged strenuous exercise alters the cardiovascular response to dobutamine stimulation in male athletes. *J Physiol* **569,** 325-330.

White MY, Cordwell SJ, McCarron HC, Tchen AS, Hambly BD & Jeremy RW. (2003). Modifications of myosin-regulatory light chain correlate with function of stunned myocardium. *J Mol Cell Cardiol* **35,** 833-840.

Whyte GP, George K, Sharma S, Lumley S, Gates P, Prasad K & McKenna WJ. (2000). Cardiac fatigue following prolonged endurance exercise of differing distances. *Med Sci Sports Exerc* **32,** 1067-1072.

Williams GS, Chikando AC, Tuan HT, Sobie EA, Lederer WJ & Jafri MS. (2011). Dynamics of calcium sparks and calcium leak in the heart. *Biophys J* **101,** 1287-1296.

Winiarska K, Focht D, Sierakowski B, Lewandowski K, Orlowska M & Usarek M. (2014). NADPH oxidase inhibitor, apocynin, improves renal glutathione status in Zucker diabetic fatty rats: a comparison with melatonin. *Chem Biol Interact* **218,** 12-19.

Wonders KY, Hydock DS & Hayward R. (2007). Time-course of changes in cardiac function during recovery after acute exercise. *Appl Physiol Nutr Metab* **32,** 1164-1169.

Wu Y, Luczak ED, Lee EJ, Hidalgo C, Yang J, Gao Z, Li J, Wehrens XH, Granzier H & Anderson ME. (2012). CaMKII effects on inotropic but not lusitropic force frequency responses require phospholamban. *J Mol Cell Cardiol* **53,** 429-436.

Xiang JZ & Kentish JC. (1995). Effects of inorganic phosphate and ADP on calcium handling by the sarcoplasmic reticulum in rat skinned cardiac muscles. *Cardiovasc Res* **29,** 391-400.

Xie H & Zhu PH. (2006). Biphasic modulation of ryanodine receptors by sulfhydryl oxidation in rat ventricular myocytes. *Biophys J* **91,** 2882-2891.

Xu A & Narayanan N. (1999). Ca2+/calmodulin-dependent phosphorylation of the Ca2+-ATPase, uncoupled from phospholamban, stimulates Ca2+-pumping in native cardiac sarcoplasmic reticulum. *Biochem Biophys Res Commun* **258,** 66-72.

Xu A, Netticadan T, Jones DL & Narayanan N. (1999). Serine phosphorylation of the sarcoplasmic reticulum Ca(2+)-ATPase in the intact beating rabbit heart. *Biochem Biophys Res Commun* **264,** 241-246.

Xu L, Eu JP, Meissner G & Stamler JS. (1998). Activation of the cardiac calcium release channel (ryanodine receptor) by poly-S-nitrosylation. *Science* **279,** 234-237.

Xu S, Ying J, Jiang B, Guo W, Adachi T, Sharov V, Lazar H, Menzoian J, Knyushko TV, Bigelow D, Schoneich C & Cohen RA. (2006). Detection of sequence-specific tyrosine nitration of manganese SOD and SERCA in cardiovascular disease and aging. *Am J Physiol Heart Circ Physiol* **290,** H2220-2227.

Yan Y, Liu J, Wei C, Li K, Xie W, Wang Y & Cheng H. (2008). Bidirectional regulation of Ca2+ sparks by mitochondria-derived reactive oxygen species in cardiac myocytes. *Cardiovasc Res* **77,** 432-441.

Yang Z & Steele DS. (2002). Effects of phosphocreatine on SR Ca(2+) regulation in isolated saponin-permeabilized rat cardiac myocytes. *J Physiol* **539,** 767-777.

Yano M, Okuda S, Oda T, Tokuhisa T, Tateishi H, Mochizuki M, Noma T, Doi M, Kobayashi S, Yamamoto T, Ikeda Y, Ohkusa T, Ikemoto N & Matsuzaki M. (2005). Correction of defective interdomain interaction within ryanodine receptor by antioxidant is a new therapeutic strategy against heart failure. *Circulation* **112,** 3633-3643.

Yue DT, Marban E & Wier WG. (1986). Relationship between force and intracellular [Ca2+] in tetanized mammalian heart muscle. *J Gen Physiol* **87,** 223-242.

Zahradnikova A, Minarovic I, Venema RC & Meszaros LG. (1997). Inactivation of the cardiac ryanodine receptor calcium release channel by nitric oxide. *Cell Calcium* **22,** 447-454.

Zeitz O, Maass AE, Van Nguyen P, Hensmann G, Kogler H, Moller K, Hasenfuss G & Janssen PM. (2002). Hydroxyl radical-induced acute diastolic dysfunction is due to calcium overload via reverse-mode Na(+)-Ca(2+) exchange. *Circ Res* **90,** 988-995.

Zhang BT, Yeung SS, Allen DG, Qin L & Yeung EW. (2008). Role of the calcium-calpain pathway in cytoskeletal damage after eccentric contractions. *J Appl Physiol (1985)* **105,** 352-357.

Zhang GX, Kimura S, Nishiyama A, Shokoji T, Rahman M, Yao L, Nagai Y, Fujisawa Y, Miyatake A & Abe Y. (2005). Cardiac oxidative stress in acute and chronic isoproterenol-infused rats. *Cardiovasc Res* **65,** 230-238.

Zhang H, Makarewich CA, Kubo H, Wang W, Duran JM, Li Y, Berretta RM, Koch WJ, Chen X, Gao E, Valdivia HH & Houser SR. (2012). Hyperphosphorylation of the cardiac ryanodine receptor at serine 2808 is not involved in cardiac dysfunction after myocardial infarction. *Circ Res* **110,** 831-840.

Zhang M, Prosser BL, Bamboye MA, Gondim AN, Santos CX, Martin D, Ghigo A, Perino A, Brewer AC, Ward CW, Hirsch E, Lederer WJ & Shah AM. (2015). Contractile Function During Angiotensin-II Activation: Increased Nox2 Activity Modulates Cardiac Calcium Handling via Phospholamban Phosphorylation. *J Am Coll Cardiol* **66,** 261-272.

Zhang P, Hou M, Li Y, Xu X, Barsoum M, Chen Y & Bache RJ. (2009). NADPH oxidase contributes to coronary endothelial dysfunction in the failing heart. *Am J Physiol Heart Circ Physiol* **296,** H840-846.

Zhang YH & Hancox JC. (2009). Regulation of cardiac Na+-Ca2+ exchanger activity by protein kinase phosphorylation--still a paradox? *Cell Calcium* **45,** 1-10.

Zhou W, Benharash P, Ho J, Ko Y, Patel NA & Mahajan A. (2013). Left ventricular twist and untwist rate provide reliable measures of ventricular function in myocardial ischemia and a wide range of hemodynamic states. *Physiol Rep* **1,** e00110.

Zweier JL & Talukder MA. (2006). The role of oxidants and free radicals in reperfusion injury. *Cardiovasc Res* **70,** 181-190.

Appendix A - Treadmill Acclimation Protocol

Time (min)	Day 1	Day 2	Day 3	Day 4	Day 5	Day 6	Day 7
0-0.5	10 m/min	10	10	10	10	10	10
0.5-1	.	.	.	.	.	.	.
1-1.5	.	.	.	.	.	.	.
1.5-2	.	.	.	.	.	10	10
2-2.5	.	.	.	.	.	11	11
2.5-3	.	.	.	.	10	12	12
3-3.5	.	.	.	.	11	13	13
3.5-4	.	.	10	10	12	14	14
4-4.5	.	.	11	11	13	15	15
4.5-5	.	10	12	12	14	16	16
5-5.5	.	11	13	13	15	17	17
5.5-6	.	12	14	14	16	18	18
6-6.5	.	13	15	15	17	19	19
6.5-7	.	14	.	15	18	20	20
7-7.5	.	15	.	16	19	.	.
7.5-8	.	.	15	17	20	.	.
8-8.5	.	.	16	18	.	.	.
8.5-9	.	.	17	19	.	.	.
9-9.5	.	.	18	20	.	.	.
9.5-10	10	15	19	20	20	20	20

The treadmill acclimation was performed for 7 days leading up to the exhaustive exercise bout. Rats began each session at 10 m/min and the speed was progressively ramped on each subsequent day. The time is indicated in the first column. A "." indicates that the speed was not changed at the time point.
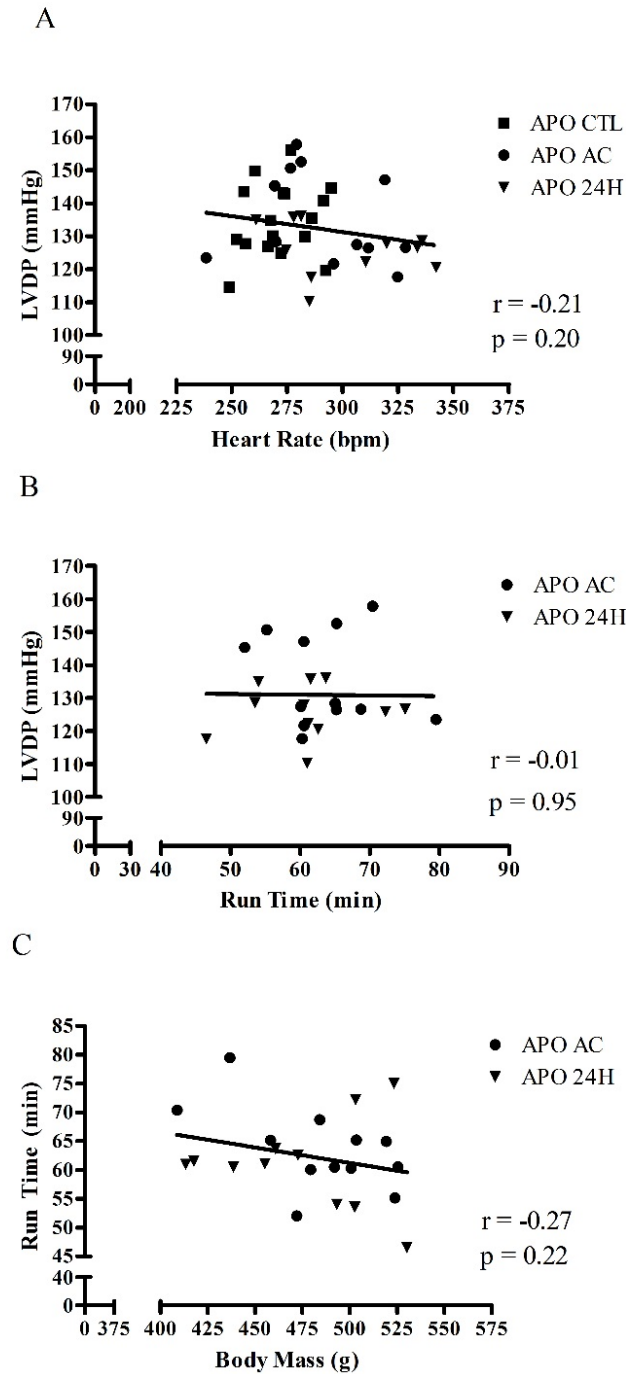
Figure B.1. Linear regression analysis from Chapter 4 was performed to examine the relationships between (A) left ventricular developed pressure (LVDP) and heart rate; (B) left ventricular developed pressure and run time and (C) run time and body mass. The strength of each relationship and probability values are indicated within each panel.